The Hashemite Kingdom of Jordan | Scientific Research Support Fund | The Hashemite University

JJEES

Jordan Journal of Earth and Environmental Sciences

Volume (12) Number (3)

Cover photo © Prof. Dr. Franz Fürsich

JJEES is an International Peer-Reviewed Research Journal

ISSN 1995-6681 jjees.hu.edu.jo September 2021

Jordan Journal of Earth and Environmental Sciences (JJEES)

JJEES is an International Peer-Reviewed Research Journal, Issued by Deanship of Scientific Research, The Hashemite University, in corporation with, the Jordanian Scientific Research Support Fund, the Ministry of Higher Education and Scientific Research.

Editorial Board:

Associate Editorial Board: (Arranged Alphabetically)

International Advisory Board: (Arranged Alphabetically)

Editorial Board Support Team:

Submission address:

Manuscripts should be submitted electronically to the following e-mail:

jjees@hu.edu.jo

For more information and previous issues:

www.jjees.hu.edu.jo

Hashemite Kingdom of Jordan

Scientific Research Support Fund

Hashemite University

Jordan Journal of Earth and Environmental Sciences

JJEES

An International Peer-Reviewed Scientific Journal

Financed by the Scientific Research Support Fund

Volume 12 Number (3)

http:// jjees.hu.edu.jo/

ISSN 1995-6681

Shell bed composed of the bivalve Isognomon rugosus in grwoth position. Kimmeridgian at Santa Cruz, Lusitanian Basin, Portugal.
Photographed by Prof. Dr. Franz Fürsich

JJEES
Jordan Journal of Earth and Environmental Sciences

JJEES

JJEES (2021) 12 (3): 187-197
ISSN 1995-6681

Jordan Journal of Earth and Environmental Sciences

Assessment of groundwater quality in the area surrounding Al-Zaatari Camp, Jordan, using cluster analysis and water quality index (WQI)

Mutawakil Obeidat*[1] and Muheeb Awawdeh[2]

[1]Faculty of Science and Arts, Jordan University of Science and Technology, Jordan.
[2]Department of Earth and Environment Sciences, Laboratory of Applied Geoinformatics, Yarmouk University, Irbid, Jordan.

Received 24 October 2020, Accepted 8 December 2020

Abstract

Groundwater forms the main freshwater supply in arid and semi-arid areas. However, this precious resource has been subjected to depletion, as a direct result of over-pumping and climate change, and to contamination by different types of pollutants, as a result of growing human activities. Assessment of groundwater quality suitability for domestic uses, particularly for drinking, is essential for human health protection, as well as for effective resource management. The overall objective of this study is an assessment of the groundwater quality in the area surrounding Al-Zaatari camp in Jordan using water quality index (WQI) for drinking, using the major cations and anions that potentially have adverse impacts on human health. Moreover, groundwater quality was assessed using multivariate statistical analysis (k-means cluster analysis), and conventional hydrochemical tools. About 95% of the samples were classified as freshwater, and about 67% were classified as hard to very hard. The groundwater in the study area showed two main hydrochemical facies: mixed Ca-Mg-Cl and Na-Cl. Groundwater chemistry in the study area is influenced by the processes of ion exchange of both types (reverse ion exchange and base ion exchange) and rock weathering as it was deduced from Gibbs diagram. K-means cluster analysis resulted in two main clusters that can be differentiated by the distinct ionic concentration. Water quality index (WQI) calculations revealed three categories of the groundwater: 1) Excellent and involved 46% of the sampled wells, 2) Good, and involved 50% of the sampled wells, and 3) Poor that involved only two sampled wells. Overall, it can be stated that about 96% of the sampled wells under study can be described as good-excellent, authenticating the suitability for drinking.

Keywords: Al-Zaatari camp, groundwater, water quality index, cluster analysis

1. Introduction

Groundwater forms the main source of fresh water supply for the different uses, especially in arid and semi-arid areas. Groundwater is particularly important especially in regions having large population and intense human activities, where it is used for domestic, agricultural and industrial purposes (Wang et al., 2020; Li et al., 2016). However, this priceless natural resource has been undergoing overexploitation in water-scarce communities, which caused depletion and drastic drawdowns, as well as deterioration of water quality making it unfit for domestic uses (Zhang et al., 2019; Wu et al., 2019). The issue is further complicated by the aridity of these areas, represented by a low amount of precipitation, high amount of evapotranspiration, slow and low recharge rates (Ahmed et al., 2019). Conservation of groundwater resources is pivotal in groundwater sustainable management (Liu et al., 2019). Therefore, achieving true sustainability of groundwater resources necessitates an assessment of natural as well as human factors/processes that impact groundwater quality (Wang et al., 2020).

Groundwater quality is strongly influenced by human activities and many natural factors/processes such as the quality of recharge water, rock-water interaction, mixing of groundwater along flow paths, and residence time of the groundwater (Abanyie et al., 2020; Gopinath et al., 2019; Zango et al., 2019; Aghazadeh et al., 2017; Qin et al. 2013; Hem, 1985). Agricultural activities, domestic wastewater leakage, industrial influents, and leachate seepage from landfills can raise pollutants' concentrations in groundwater hundreds times higher than the natural backgrounds (Gibrilla et al., 2020; Lermi and Ertan, 2019; Obeidat et al. (2012), Wakida and Lerner, 2005). Groundwater chemistry is modified by many processes, such as dissolution/ precipitation of carbonate and evaporate minerals, and ion exchange (Ahmed et al., 2019; Tiwari et al., 2019; Ayadi et al., 2018; Argamasilla et al., 2017; Han et al., 2015;). Geochemical processes are responsible for the spatiotemporal variation in groundwater chemistry (Kumar et al., 2006).

Multivariate statistical analysis has been extensively used to characterize water quality and to identify sources of contamination (natural and anthropogenic) by analyzing similarities/dissimilarities among the sampled sites (Andrade et al., 2008; Obeidat et al. 2013). It offers a robust method for reliable management of water resources and swift solution of water pollution (Bodrud-Doza et al., 2016). It is a data-reduction technique that can be used to handle and reduce a large number of water quality data (Obeidat et al., 2013). The most common methods are cluster analysis and

* Corresponding author e-mail: mobeidat@just.edu.jo

principal component analysis (factor analysis). The principal component analysis is a data dimension reduction method that explains the variability in surface and groundwater data (Rashid et al., 2019). On the other hand, cluster analysis is used to classify the data into different groups based on similarity and dissimilarity among data (Hegeu and Kshetrimayum, 2019).

Water quality index (WQI) is a powerful method that has been commonly used to assess the overall water quality, and to manage water resources (Fang et al., 2020; Gaiwad et al., 2020; Abbasnia et al., 2019; Adimalla and Qian, 2019; Machiwal et al., 2019). WQI integrates a large number of hydrochemical parameters into an easily expressible and understandable format (single score) by selecting and weighting the water quality parameters and applying an aggregation function (Gao et al., 2020; Fang et al., 2020; Zotou et al., 2020; Ponsadailakshmi et al., 2018; Abtahi et al., 2015). WQI has been widely used to assess groundwater suitability for drinking purposes (Heiβ et al., 2020; Udeshani et al., 2020; Varol 2020; Khangembam and Kshetrimayum, 2019; Kawo and Karuppannan, 2018; Wu et al., 2017). It is a very effective method to present water quality data in a simple way to the public as well as policymakers and competent authorities (Keesari et al., 2016)

Jordan is an arid country, that is ranked as the second water-poor country, worldwide. Moreover, about 40% of its water resources are shared by the neighbouring countries. Instability and conflicts in the region have pushed hundreds of thousands of immigrants to flee to the country, putting more burden over the limited water resources. Climatic change is not overriding Jordan; observed effects include decreased precipitation, temperature rise, shifting of the rainy season, and deteriorating water quality (Al-Qaisi, 2010). The overall objective of this study is to assess groundwater quality suitability for drinking purposes using a water quality index method in the area surrounding Al-Zaatari Camp, Jordan. The results of the present study may assist competent authorities by providing baseline information for sustainable management of groundwater in the area under consideration.

2. Study area

2.1 Location and climate

The study area is located within the Amman-Zarqa basin (AZB), east of Mafraq city (Figure 1). The AZB is a transboundary basin of which 3,739 km^2 are in Jordan and 310 km^2 in Syria. It is one of the most important groundwater basins in Jordan and represents a transitional area between the semi-arid highlands in the west to the arid desert in the east. The study area is characterized by arid to semi-arid climatic conditions with a mean annual precipitation in the range of 100 mm in the eastern part to about 300 mm in the south-west (Figure 2). The study area tends to exhibit short and intense rainfall during the rainy season (Al-Rawabdeh et al., 2021). The dominant land use/land cover in the study area (Figure 3) is a sparse vegetative cover, followed by irrigated agriculture, and rangeland (Jawarneh and Biradar, 2017).

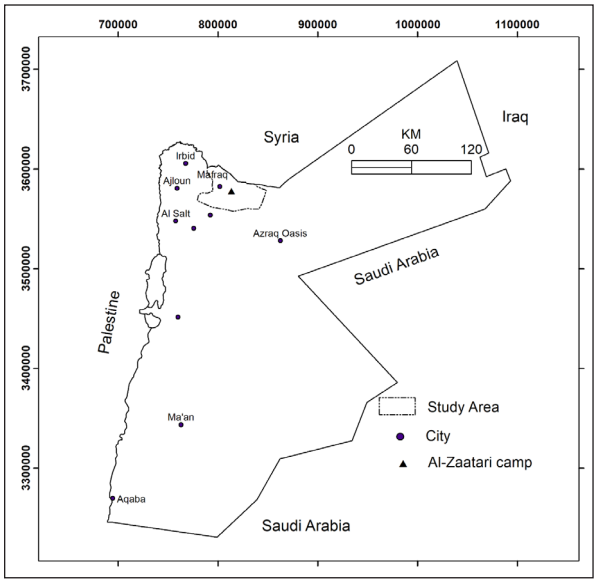

Figure 1. Location map of the study area.

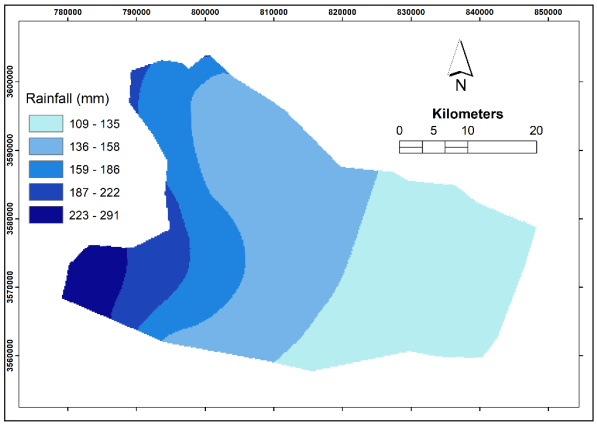

Figure 2. Rainfall map of the study area.

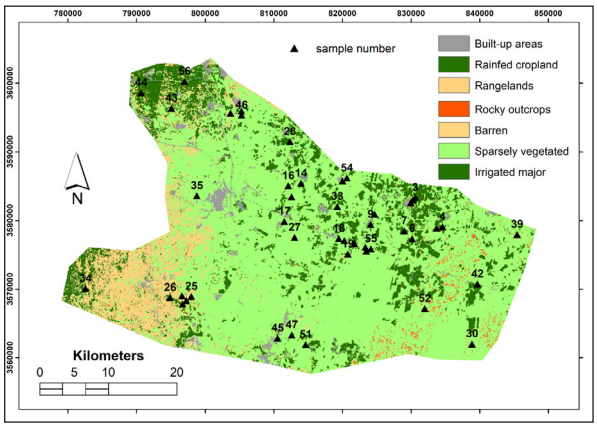

Figure 3. Land use-land cover of the study area with the sampled wells.

2.2 Geological and hydrogeological setting

From a hydrogeological point of view, three aquifer systems (Table 1 and Figure 4) are found in the study area: a composite system of the basalt and Amman Silicified Limestone /Wadi As Sir Limestone formation (B2/A7), the Umm Rijam/Wadi Shallala aquifer (B4/B5), and the Lower Ajlun aquifer which consists of Hummar (A4) and Na'ur

(A1/2) Formations (Al-Zyoud et al. 2015; Al-Rawabdeh et al. 2013). The basalt and the Amman-Wadi As Sir aquifers are hydraulically interconnected and form the main aquifers in the study area. In the eastern parts of the study area, a succession of six lava flows lies unconformably on the sedimentary rocks of the Late Cretaceous Balqa and Ajlun Groups (Bender, 1968). The transmissivity of this system ranges between 2.2 X 10-^{5} and 7x 10^{-3} m^{2} s^{-1} with an average of 3.2x10^{-4} m^{2} s^{-1}. The water is transferred laterally or vertically from the basalt aquifer into the Amman-Wadi As Sir aquifer (Obeidat and Alwaneh, 2019).

Based on pumping tests, the uppermost basaltic aquifer, which is formed by highly vesicular lava flows has transmissivity values in the range from 5.0×10^{-5} to 5.4×10^{-1} m2·s^{-1}, and the average is about 8×10^{-2} m^{2} s^{-1}, corresponding to a mean hydraulic conductivity of 2.3×10^{-4} m·s−1. The transmissivity of the limestone aquifer (B2/A7) varies between 5.4×10^{-5} and 2.5×10^{-2} m^{2} s^{-1}, with an average close to 5×10^{-3} m^{2} s^{-1}, corresponding to a mean hydraulic conductivity of 8.1×10^{-5} m^{2} s−1 (Al Mahamid, 2005). The Jordan Ministry of Water and Irrigation indicated that the water table of Amman/Wadi Sir aquifer is depleting at a rate of 0.67 to 2 m/yr. On the other hand, the mean annual recharge to the basin is 80 MCM/yr (Al Kuisi et al., 2009; Ta'any et al., 2009).

The Wadi Shallala Formation (B5) of early Middle-early Late Eocene age consists of chalk, chalky limestone and marl with chert intercalations, while the Umm Rijam Chert Limestone Formation (B4) of Paleocene age consists of alternations of limestone, chalk, and chert. The Muwaqqar Chalk Marl

Formation (B3, aquiclude/aquitard) of Maastrichtian age separates the upper aquifer system (B5/B4) from the middle aquifer system (B2/A7). It consists of bituminous marl and marly limestone.

The aquifer (B4) is highly fractured and characterized by cavernous and karstic features. The B5/B4 aquifer has a hydraulic conductivity in the range of 10^{-4} and 10^{-6} m/s with an average 5×10^{-5} m/s (Margane et al., 1999). The aquifers of Lower Ajloun group are composed of limestone, dolomitic limestone, and marl. Naur formation (A1/A2), mainly of marls, limestone and marly limestone, whereas the Hummer (A4) formation consists of hard dense limestone and dolomitic limestone (Awawdeh et al., 2020).

Table 1. Geological and hydrogeological classification of the rock units in the study area

Age	Group	Formation name	Symbol	Lithology	Thickness (m)	Aquifer potentiality
Paleocene	Belqa	Umm Rijam Chert Limestone	B4	Chert and limestone	30-50	Good
Maastrichtian		Muwaqqar Chalk Marl	B3	Chalk, marly chalk, marl	>300	Poor
Campanian		Amman Silicified Limestone	B2	Chert, limestone, with phosphate	30-120	Excellent
Santonian		Wadi Umm Ghudran	B1	Chalk, marl, marly limestone	0-75	Poor
Turonian	Ajloun	Wadi As Sir Limestone	A7	Limestone, dolomite, chert	65-300	Excellent
Turonian		Shueib	A5/6	Limestone, marly limestone	70	Fair-good
Cenomanian		Hummar	A4	Dolomite, dolomitic limestone	60-120	Fair-good
Cenomanian		Fuheis	A3	Marl and marly limestone	80-120	Poor
Cenomanian		Naur	A1/2	Limestone, dolomitic limestone, marly limestone	250-350	Good

2.3 Al-Zaatari Camp for Syrian Refugees

There are five Syrian Refugees camps in Jordan, which were built following the influx of about 1.4 million Syrians, fleeing the war erupted in 2011. Among the 5 refugees camps, only 3 camps are official: Al-Zaatari, Mrajeeb-Al Fhood, and Azraq. Al-Zaatari camp, established in 2012 is the world largest refugees camp in Jordan (Al-Harahsheh et al., 2015). The camp hosts 78,558 Syrian refugees, 20% of the population are under four years, and 40% are females (UNHCR, 2020). The camp close to Jordan's northern border with Syria is located about 10 km east of Mafraq city (Figure 1). Currently, three groundwater wells exist inside the camp which provides about 3000 m^{3} a day. In terms of the sources of drinking water, 51% of the households are using trucked water stored in private tanks, 26.7% of households are using purchased bottled water, and 22. 3% are using water from the communal tank (UNICEF, 2017). A wastewater treatment plant with a capacity of 3600 m^{3} was established to treat wastewater.

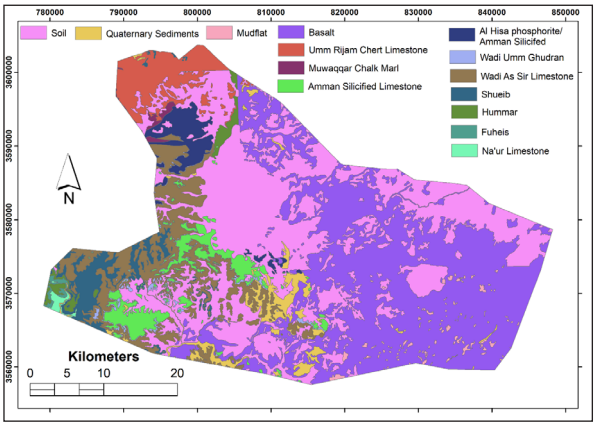

Figure 4. Geological map of the study area.

3. Material and Methods

3.1 Analytical procedure

A total of 450 samples representing 56 groundwater wells were used in this study. These included 26 samples collected by the authors in January 2019, and the rest were retrieved from the open files of the Water Authority of Jordan (Figure 3). It is assumed that after/during the rainy season, pollutants may have been subjected to downward leaching, and thus contaminating the underlying aquifers The samples were collected from the upper aquifer systems and involved 26 wells from the basalt aquifer, and 30 wells from the B2/A7 aquifer. The hydrochemical parameters used in this study represent average values.

The collected samples were field filtered through 0.45 µm Millipore filters into HDPE sample bottles with appropriate storage and preservation methods (refrigeration, freezing, acidification, the addition of chloroform). The methods described by APHA (1998) were followed during fieldwork and laboratory chemical analyses. Electrical conductivity (EC), temperature and pH were measured in situ using portable meters. Before sample collection from the wells, intensive purging was performed, to ensure representativeness and reproducibility of the groundwater sample. Chemical analyses were carried out at the laboratories of Jordan University of Science and Technology and Yarmouk University. Calcium (Ca^{+2}), magnesium (Mg^{+2}), sodium (Na^{+}), potassium (K^{+}), chloride (Cl^{-}), and sulfate (SO_4^{-2}) concentrations were determined by Ion Chromatography (Dionex ICS-1600). Bicarbonate (HCO_3^{-}) and nitrate (NO_3^{-}) were determined by titration method and spectrophotometry, respectively. Total Hardness (TH) was calculated using calcium and magnesium concentrations (Todd, 1980). All samples were analyzed in triplicate with analytical uncertainty of less than 4%. To check the correctness of the analysis, the cations–anions balance was used, where it was within ±5%, which guarantees the reliability of the chemical analysis.

3.2 K-means cluster analysis

K-means analysis is a tool designed to assign cases to a fixed number of groups (clusters) whose characteristics are not yet known but are based on a set of specified variables (Hartigan, 1975). It is useful for the classification of a large number of cases. The computer software IBM SPSS Statistics version 21 was used to carry out the cluster analysis.

3.3 Water quality index calculation

The determination of the WQI includes four major steps (Ismail et al., 2020; Njuguna et al., 2020):

1. Measurement of the selected water quality parameters.
2. Transformation of the measurement of the water quality parameters into a dimensionless number (quality rating).
3. Assignment of weight to each water quality parameter based on its degree of importance for drinking water (Table 2).
4. Aggregation of the quality rating to obtain the final WQI using a suitable aggregation function.
5. The weight was assigned to each parameter according to Adimalla and Qian (2019), Ismail et al. (2020), and Nagaraju et al. (2016).

Quality rating (Qi) was calculated according to the following equation:

$$Qi = 100 * Ci/S \quad \text{..... (1)}$$

whereCi is the measured parameter concentration and S is the WHO (2011) guidelines (Table3).

The final WQI was calculated using the following equation:

$$\text{WQI} = \sum_{i=1}^{n} RWi * Qi \quad \text{..... (2)}$$

Where Wi is the relative weight of the parameter, which was calculated as follows:

$$RWi = AWi / \sum_{i=1}^{n} AWi \quad \text{..... (3)}$$

Where RWi is the relative weight and AWi is the assigned weight.

Groundwater quality in the study area was classified into different groups based on the WQI. The obtained WQI values were categorized into the following categories (Ismail et al., 2020):

- Excellent: <50
- Good: 50-100
- Poor: 100-200
- Very poor: 200-300
- Unsuitable: >300

Table 2. Weights and the relative weight assigned to the hydrochemical parameters in the study area (Ismail et al., 2020).

Parameter	Assigned weight (AWi)	Relative weight (RWi)
TDS	5	0.15
Cl	5	0.15
SO_4	5	0.15
NO_3	5	0.15
Na	4	0.13
Ca	3	0.09
Mg	3	0.09
K	3	0.09
Sum of weights	33	1

4. Results and Discussion

4.1 Major ion chemistry and hydrochemical facies

The descriptive statistics of the hydrochemical parameters are presented in Table 3. The pH value is in the range of 6.68-8.19 with an average of 7.73, indicating that the groundwater is generally neutral. The EC is in the range of 390-2580 µS/cm with an average of 1002 µ/cm (Figure 5a). TDS is in the range of 223-1372 mg/L with an average of 583 mg/L. Based on Davis and Dewiest (1966) classification, about 96.6% of the samples are classified as freshwater. Except for three samples, the TDS content of all samples is below the maximum permissible limit of the drinking water quality guidelines of WHO (2011). The TH as $CaCO_3$ is in the range of 79-607 with an average of 254 mg/L. Based on Sawyer and McCarty (1967) classification, about 32.6% of the samples are classified as moderately hard, 33.7% hard, and 33.7 % very hard water. Three samples have TH above the maximum permissible limit of WHO (2011) drinking water quality guidelines of 500 mg/L.

Table 3. Descriptive statistics of the hydrochemical parameters.

Parameter	Min	Max	Mean	Std. Dev.	Coefficient of variation (C_V, %)	WHO (2011)
Ca (mg/L)	13	150	48	27.2	56.2	75
Mg (mg/L)	8	78	33	16.3	49.5	100
Na (mg/L)	39	288	98	36.1	36.7	200
K	2	14	6	2.6	46.6	10
HCO_3 (mg/L)	19	327	135	63.9	47.4	--
SO_4 (mg/L)	24	405	84	52.5	62.7	250
NO_3 (mg/L)	1	101	17	14.6	85.2	50
Cl (mg/L)	38	651	193	122.8	63.6	250
T (°C)	22	43	31	4.0	12.9	--
pH	7	8	8	0.3	3.9	6.5-8.5
EC (µS/cm)	386	2580	1002	399.2	39.8	--
TH (mg/L)	79	607	254	126.8	50.0	--
TDS (mg/L)	223	1372	583	218.7	37.5	1000
CAI	-0.97	0.93	0.02	--	--	--
WQI	18.5	155.5	50.6	25.1	49.6	--

The Ca and Mg concentrations are in the range of 14-150 mg/L, and 8-78 mg/L, with an average of 48 mg/L, and 33 mg/L, respectively (Figure 5b). All samples have Ca and Mg concentrations which are below the permissible limit of 200 and 100 mg/L, respectively. The main sources of Mg in groundwater include weathering of Mg-containing rocks, and contamination by domestic, animal, and industrial waste (Selvam et al., 2016). Na and K concentrations are in the range of 39-288 mg/L, and 2-14 mg/L, with an average of 98 mg/L, and 6 mg/L, respectively. Only one sample has Na concentration higher than the permissible limit of drinking water quality of 200 mg/L, and all samples have K concentration which is within the permissible limit of WHO (2011) drinking water quality guidelines. The main sources of Na in groundwater include weathering of rock-forming minerals such as Na-plagiocalse, and halite, in addition to contamination by human and animal waste (Selvam et al., 2016). HCO_3 and SO_4 concentrations are in the range of 19-327 mg/L, and 24-405 mg/L, with an average of 135 mg/L and 84 mg/L, respectively. All samples have HCO_3 and SO_4 concentrations which are within the maximum permissible limit of 600 mg/L.Cl and NO_3 concentrations are in the range of 38-651 mg/L, and 1-101 mg/L, with an average of 193 mg/L and 17 mg/L, respectively (Figure 5c & d). Only one sample (sample 24) has Cl concentration above the maximum permissible limit of WHO (2011) drinking water quality guidelines of 600 mg/L.This sample is located in the southwest part of the study area and has a nitrate concentration much higher than the natural background concentration of 5-10 mg/L (Panno et al., 2006), and more than the maximum permissible limit of drinking water quality set by the WHO (2011). Nitrate is the most common human-induced pollutant into groundwater (Babiker et al., 2006). The association of high concentrations of both chloride and nitrate indicates that the source of these ions is anthropogenic, and most likely domestic wastewater. About 28% of the samples have nitrate concentrations above the natural background concentration of 20 mg/L.Three samples have nitrate concentration above the maximum permissible concentration of drinking water quality set by the WHO (2011). According to Nagaraju et al. (2016), the concentration of a chemical component with a single source should have a low coefficient of variation (<10%). Among the major ions, NO_3 has the highest coefficient of variation reaching 85%, followed by Cl (64%), and SO_4 (63%). This may indicate a multi-source of these components, hydrochemical, and mixing processes affecting the spatial distribution of the hydrochemical parameters.

The major ions of the groundwater in the study area showed the following order:

Na>Mg>Ca>K, and Cl>HCO_3>SO_4>NO_3. Groundwater chemistry may reflect the influence of hydrochemical processes occurring in the subsurface (Gaikwad et al., 2020; Jain et al., 2018). The geochemical data of the main cations and anions were plotted using Piper diagram (Piper, 1944), where it revealed two water types (Figure 6): 1) mixed Ca-Mg-Cl type (suggesting interplay of complex geochemical processes in the aquifer), and 2) Na-Cl water type. Seven samples fall in the Ca-Mg-SO_4 field, and only one sample falls in the Ca-Mg-HCO_3 field. The majority of the samples falls in the Na-dominant zone, and no dominant zone in the cations facies. This may reflect the effect of the aquifer mineral make up (basalt), and hydrochemical processes, particularly base ion exchange process where Ca and Mg are sequestered onto the aquifer material and Na is released into the water. Additionally, the majority of samples falls in the Cl-dominant zone, and no dominant zone in the anions facies. The samples fall in both zones 1 and 2 of the diamond plot, revealing that the samples are divided into two main groups: alkaline earth exceeding alkalis, and alkalis exceeding earth alkaline.

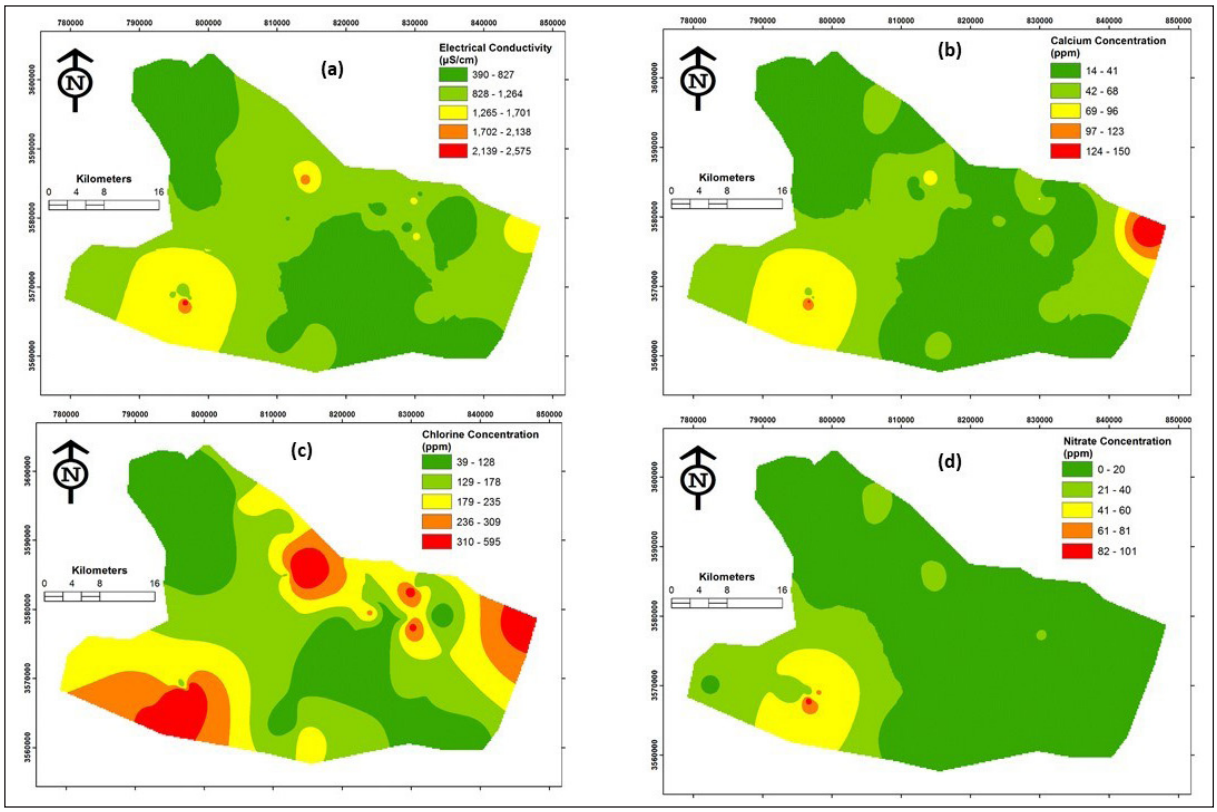

Figure 5. Spatial distribution of (a) EC, Ca (b), Cl (c), and NO_3 (d).

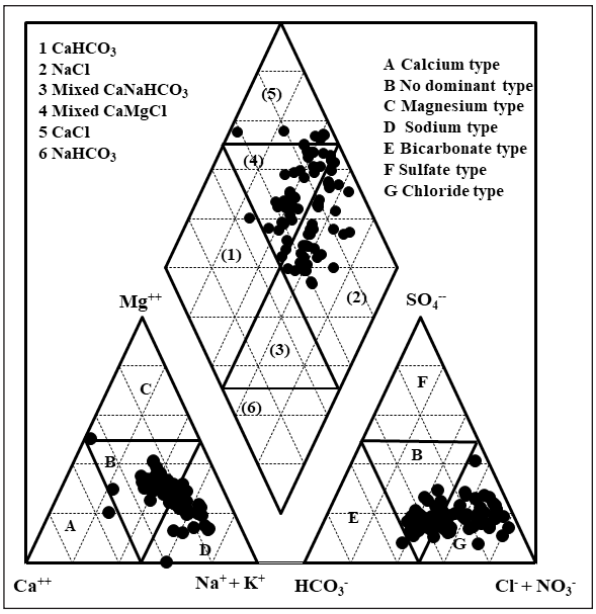

Figure 6. Piper diagram of the groundwater samples.

Gibbs diagram is a useful tool that can be used to investigate the effects of geochemical processes on groundwater chemistry. Evaporation, rock, and precipitation were the main factors identified by Gibbs (1970) that control or modify groundwater chemistry. The groundwater data in the study area was plotted using Gibbs diagram and presented in Figure 7, which revealed that rock weathering is the main process affecting groundwater in the study area. Groundwater-aquifer interaction has significantly impacted the groundwater chemistry. Ion exchange is another geochemical process that controls groundwater chemistry. Ion exchange and adsorption play an important role in regulating solute transport in the soil and aquifers (Appelo and Postma, 2005).

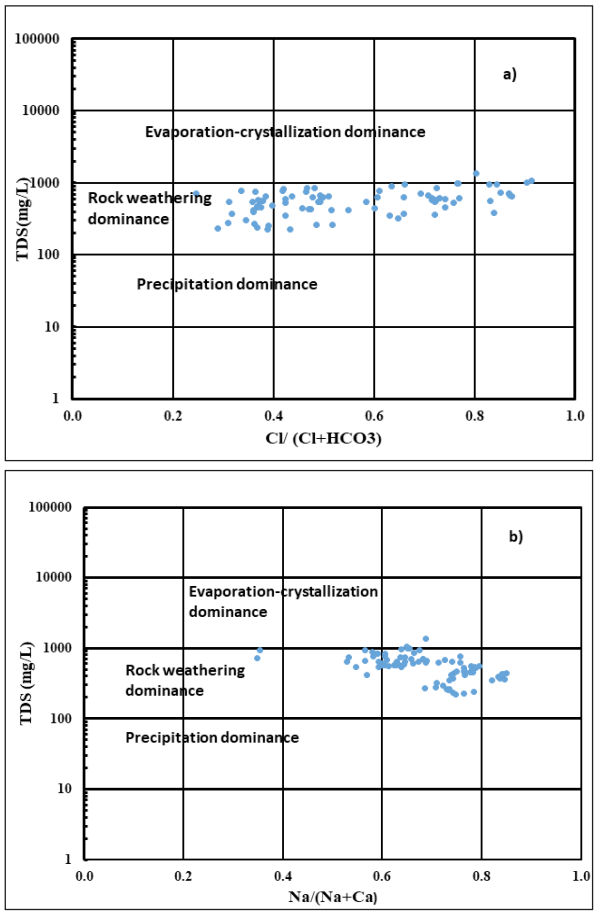

Figure 7. Gibbs diagram of the groundwater samples using anion vs. TDS (a), and cation vs. TDS (b).

Schoeller index (chloro-alkaline indices, CAI) have been used to get insights about ion-exchange reactions between groundwater and the hosting aquifer material, as well as information about freshening or salinizing processes of the groundwater (e.g. Tiwari et al., 2019; Abu-alnaeem et al., 2018; Stuyfzand, 2008). The CAI can be determined using the following equation (Schoeller, 1965):

$$CAI = (Cl - (Na + K))/Cl \quad \text{.....(4)}$$

where concentration is in meq/l

The CAI values could be negative or positive depending on whether the exchange of Na and K is from the water with Mg and Ca in rock/soil or vice versa (Tiwari et al., 2019). There are two types of ion exchange processes (Ayadi et al., 2018): the first one is known as reverse ion exchange process, where Na and K are sequestered onto the aquifer material, and Ca and Mg are released into the water. The CAI values in this case are positive, and there is a hardening of water (Zaidi et al., 2015). The second type of ion exchange processes is known as the base ion exchange process, where Ca and Mg are sequestered onto the aquifer material and Na and K are released into the water. The CAI values in this case are negative, and there is softening of water (Argamasilla et al., 2017). The CAI values of the groundwater in the study area ranged between -0.97 and 0.67 with an average of 0.01, and most of the samples cluster between -0.5 and 0.5(Figure 8), indicating that low level of the ion exchange process. Meanwhile, about 62% of the wells have positive CAI values, indicating hardening of the groundwater; about 38% have negative CAI values, indicting softening of the groundwater.

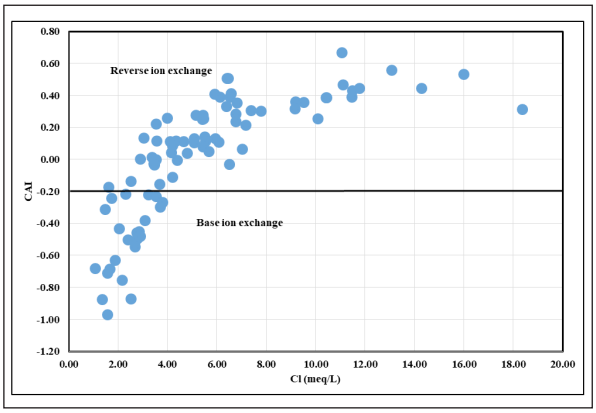

Figure 8. Chloride concentration vs. chloro-alkaline index (CAI).

Generally, areas with low salinity (means negative CAI values), signifying that the groundwater of these areas is undergoing freshening processes. Besides, the aquifer material released sodium into the groundwater and fixed calcium. About 67% of the samples collected from the B2/A7 has positive CAI values, and about 54% of the samples have negative CAI values, signifying to aquifer lithology effect on the groundwater chemistry.

The bivariate statistics of the physiochemical parameters of the groundwater are presented in Table (4). The terms, "strong" "moderate" and "weak" were used to describe the correlation coefficient values (r), and they refer to a range of >0.75, 0.5-0.7, and 0.3-0.5, respectively (Wang et al., 2007). EC is strongly correlated with Ca, Mg, Na, SO_4 and Cl, indicating that dissolution of these ions are the main source of the groundwater salinity. A moderate correlation exists between EC and NO_3, indicating that the more salinization of groundwater, the more accumulation of NO_3 in the groundwater. The Ca is strongly correlated with each of Mg and Cl, and moderately correlated with Na, NO_3 and SO_4. The Mg is strongly correlated with Cl, and moderately correlated with Na and SO_4. Na is strongly correlated with Cl and SO_4, and moderately correlated with NO_3. SO_4 is strongly correlated with Cl, and moderately correlated with NO_3. The weak correlation between HCO_3 and other hydrochemical parameters can be attributed to the sources of alkalinity, which includes dissolution of atmospheric and soil CO_2 (Moquet et al., 2011).

4.2 Cluster analysis and the WQI

The results of the k-means cluster analysis revealed two clusters with distinct ionic concentrations (Table 5). Cluster 1 includes 14% of the samples (7 samples: samples 1, 14, 24, 25, 37, 38, 39), whereas cluster 2 includes 86% of the samples (43 samples). Both clusters are of Ca-Mg-Cl water type (Figure 9). This water type can be related to the fourth group of Rimawi and Udluft (1985), which corresponds to freshwater mixed with saline water or freshwater which has passed through evaporates. The two clusters plotted in the no dominant zone in the cation facies (no one cation-anion pair exceeds 50%). On the other hand, the two clusters fell in the Cl-dominant zone in the anion facies. Based on the TDS, the two clusters can be classified as freshwater. However, cluster 1 has TDS content more than double than that of cluster 2. Additionally, cluster 1 has nitrate concentration much higher than the natural background concentration of 5-10 mg/L. The sources of nitrate in the study area include domestic wastewater and agricultural fertilizers.

Groundwater quality and its suitability for drinking were assessed using WQI. Eight hydrochemical parameters (TDS, Ca, Mg, Na, K, Cl, SO_4, NO_3) were taken into account for WQI calculation and considering the WHO (2011) guidelines for drinking water quality. The weights were assigned to calculate the WQI values for each hydrochemical parameter, depending on their prominence on water quality. TDS, Cl, SO4, and NO3 were assigned a weight of 5; Na was assigned a weight of 4, and K, Mg, and Ca were assigned a weight of 3. The relative weight of each parameter (Table 2) was calculated according to Eq. (3).

Table 4. Bivariate statistics of hydrochemical parameters.

Parameter	Ca	Mg	Na	K	HCO_3	SO_4	NO_3	Cl	EC	pH	TH	TDS
Ca	1	0.77	0.58	0.16	0.34	0.57	0.60	0.76	0.85	-0.73	0.94	0.90
Mg	0.77	1	0.53	0.43	0.09	0.50	0.38	0.80	0.85	-0.57	0.94	0.84
Na	0.58	0.53	1	0.36	-0.11	0.87	0.60	0.84	0.85	-0.28	0.59	0.78
K	0.16	0.43	0.36	1	-0.41	0.27	-0.05	0.50	0.42	-0.12	0.31	0.34
HCO_3	0.34	0.09	-0.11	-0.41	1	-0.13	0.18	-0.21	0.05	-0.12	0.22	0.29
SO_4	0.57	0.50	0.87	0.27	-0.13	1	0.67	0.78	0.78	-0.31	0.58	0.69
NO_3	0.60	0.38	0.60	-0.05	0.18	0.67	1	0.54	0.62	-0.23	0.52	0.62
Cl	0.76	0.80	0.84	0.50	-0.21	0.78	0.54	1	0.95	-0.60	0.83	0.86
EC	0.85	0.85	0.85	0.42	0.05	0.78	0.62	0.95	1	-0.59	0.90	0.95
pH	-0.73	-0.57	-0.28	-0.12	-0.12	-0.31	-0.23	-0.61	-0.59	1	-0.68	-0.61
TH	0.94	0.94	0.59	0.31	0.22	0.58	0.52	0.83	0.90	-0.68	1	0.92
TDS	0.90	0.84	0.78	0.34	0.29	0.69	0.62	.86	0.95	-0.61	0.92	1

Table 5. Final cluster Centers.

Parameter	Cluster no.		WHO (2011)
	1	2	
Ca (mg/L)	103.20	39.18	75
Mg (mg/L)	57.95	27.26	100
Na (mg/L)	164.74	89.08	200
K (mg/L)	6.31	5.43	10
HCO_3 (mg/L)	122.67	106.33	--
SO_4 (mg/L)	184.23	75.32	250
NO_3 (mg/L)	36.87	14.29	50
Cl (mg/L)	455.93	167.23	250
pH	6.77	7.33	6.5-8.5
EC (S/cm)	1829.1	861.8	--
TH (mg/L)	495.6	209.7	--
TDS (mg/L)	981.3	484.4	1000

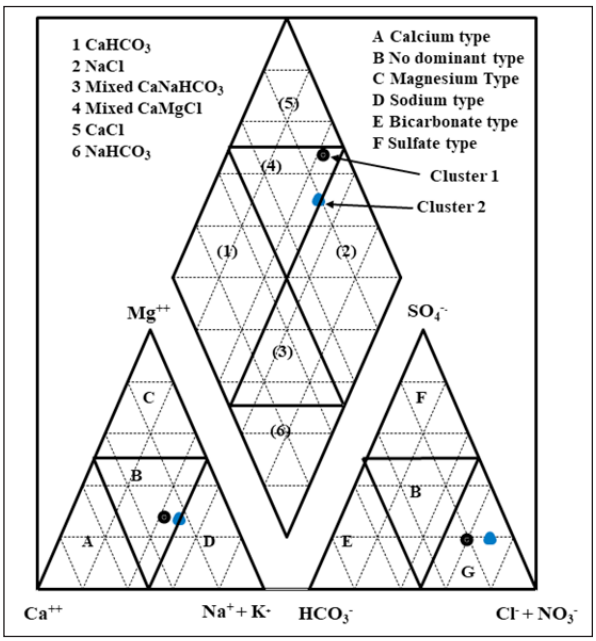

Figure 9. Piper diagram of the two clusters of the groundwater samples.

The WQI was computed following Eqs. (1) and (2). The results of WQI calculations indicated that it was in the range of 18.5 to 155.5 with an average of 50.6. Based on WQI values, the samples were categorized into three groups (Figure 10):

- Excellent: this groups comprised 26 samples, which forms about 46% of the sampled wells.
- Good: this group comprised 28 sampled wells, which forms 50% of the sampled wells.
- Poor: this group comprised only two wells, which forms 4% of the sampled wells.

The high values of WQI observed in two locations may be due to high concentrations of TDS, Cl, Ca, Na, SO_4 and NO_3. It is worth mentioning that cluster 1 members belong to the WQI classes good and poor, whereas cluster 2 involved both the WQI classes good and excellent

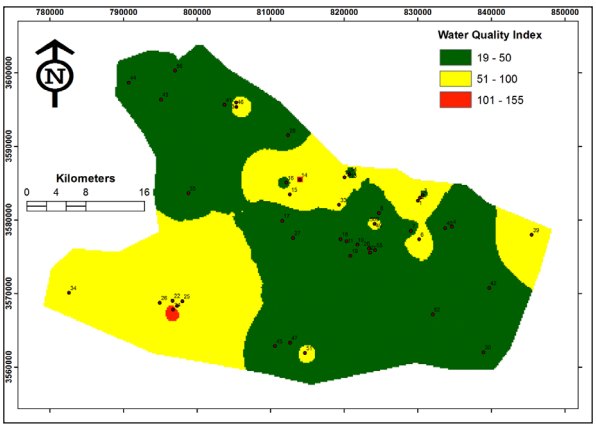

Figure 10. Spatial distribution of WQI of the groundwater samples. samples.

5. Conclusions

In arid areas, identifying the hydrogeochemical evolution of groundwater is essential for effective water resource management. So, the results of this study may form a baseline study for researches as well as relevant authorities responsible for groundwater management. Two hydrochemical facies were identified: mixed Ca-Mg-

Cl type, and Na-Cl, reflecting an interplay of complex geochemical processes in the aquifer. Gibbs diagram and CAI values revealed that the main geochemical processes influencing groundwater chemistry are rock weathering and ion exchange processes. Anthropogenic impacts on the water quality were limited. Based on WQI calculations, 96% of the sampled wells (54 wells) is of good-excellent water quality, authenticating the suitability for drinking.

References

Abanyie, S.K., Sunkari, E.D., Apea, O.B., Abagale, S., Korboe, H.M. (2020). Assessment of the quality of water resources in the Upper East Region, Ghana: a review. Sustainable Water Resources Management 6 (52) (2020). DOI:10.1007/s40899-020-00409-4.

Abbasnia, A., Yousefi, N., Mahvi, A.H., Nabizadeh, R., Radfard, M., Yousefi, M., Alimohammadi, M. (2019). Evaluation of groundwater quality using water quality index and its suitability for assessing water for drinking and irrigation purposes: case study of Sistan and Baluchistan province (Iran). Human and Ecological Risk Assessment: An Internal Journal 25(4): 988-1005.

Abed, A.M. (2000). Geology of Jordan. Jordanian Geologists Association, Amman.

Abtahi, M., Golchinpour, N., Yaghmaeian, K., Rafiee, M., Jahangiri-rad, M., Keyani, A., Saeedi, R. (2015). A modified drinking water quality index (DWQI) for assessing drinking source water quality in rural communities of Khuzestan Province, Iran.Ecological Indicators 53: 283-291.

Abu-alnaeem, M. F., Yusoff, I., Ng, T. F., Alias, Y., Raksmey, M.(2018). Assessment of groundwater salinity and quality in Gaza coastal aquifer, Gaza Strip, Palestine: An integrated statistical, geostatistical and hydrogeochemical approaches study. Science of the Total Environment 615: 972-989.

Adimalla, N., and Qian, H. (2019). Groundwater quality evaluation using water quality index (WQI) for drinking purposes and human health risk (HHR) assessment in an agricultural region of Nanganur, south India. Ecotoxicology and Environmental Safety 176: 153-161.

Aghazadeh, N., Chitsazan, M., Golestan, Y. (2017). Hydrochemistry and quality assessment of groundwater in the Ardabil area. Iran. Applied Water Science 7: 3599-3616.

Ahmed, A., Shabana, A.R., Saleh, A. (2019). Using hydrochemical and isotopic data to determine sources of recharge and groundwater evolution in arid region from Eastern Desert, Egypt. Journal of African Earth Sciences 151: 36-46.

Al-Harahsheh, S. Al-Adamat, R., Abdullah, S. (2015). The Impact of Za'atari Refugee Camp on the Water Quality in Amman-Zarqa Basin. Journal of Environmental Protection 6: 16-24.

Al Kuisi, M., Al-Qinna, M., Margane, A., Aljazzar, T. (2009). Spatial assessment of salinity and nitrate pollution in Amman Zarqa Basin: a case study. Environmental Earth Sciences 59 (1): 117-129. DOI: 10.1007/s12665-009-0010-z.

Al Mahamid, J. (2005). Intergration of water resources of the upper vaquifer in Amman-Zarqa basin based on mathematical modeling and GIS, Jordan. Freiberg Online Geology 12: 1- 223.

Al-Qaisi, B.M. (2010). Climate change effects on water resources in Amman Zarqa Basin, Jordan. Water Authority of Jordan, Ministry of Water and Irrigation, Jordan. Individual Project Report-Climate Change-Mitigation and Adaptation, 39p.

Al-Rawabdeh, A., Hazaymeh, K., Nusiar, S., Shdaifat, R., Al Hseinat, M. (2021). A GIS-EIP model for a mechanic industrial zone site selection in Al-Mafraq City, Jordan. Jordan Journal of Earth and Environmental Sciences 12 (1): 72-80.

Al-Rawabdeh, A.M., Al-Ansari, N.A., Al-Taani, A.A., Knutsson, S. (2013). A GIS-Based Drastic Model for Assessing Aquifer Vulnerability in Amman-Zerqa Groundwater Basin, Jordan. Engineering 5: 490-504.

Al-Zyoud, S., Ruehaak, W., Forootan, E., Sass, I. (2015). Over Exploitation of Groundwater in the Centre of Amman Zarqa Basin-Jordan: Evaluation of Well Data and GRACE Satellite Observations. Resources 4: 819-830.

Andrade, E.M., Palacio, H.A.Q., Souza, I.H., Leao, R.A.O., Guerreiro, M.J. (2008). Land use effects in groundwater composition of an alluvial aquifer (Trussu River, Brazil) by multivariate techniques. Environmental Research 106: 170-177

APHA. (1998). Standard Methods for the Examination of Water and Wastewater, 20th. edn.

American Water Works Association, Water Environment Federation: Washington.

Appelo, C.A.J., and Postma, D. (2005). Geochemistry, Groundwater and Pollution, second edn.

CRC Press - Taylor & Francis Group, Boca Raton, Fl, USA.

Argamasilla, M., Barbera, J.A., Andreo, B. (2017). Factors controlling groundwater salinization and hydrogeochemical processes in coastal aquifers from southern Spain. Science of the Total Environment 580: 50-68.

Awawdeh, M., Al-Kharbsheh, N., Obeidat, M., Awawdeh, M. (2020). Groundwater vulnerability assessment using modified SINTACS model in WadiShueib, Jordan. Annals of GIS. DOI: 10.1080/19475683.2020.1773535.

Ayadi, Y., Mokadem, N., Besser, H., Khelifi, F., Harabi, S., Hamad, A., Boyce, A., Laouar, R., Hamed, Y. (2018). Hydrochemistry and stable isotopes (δ18O and δ2H) tools applied to the study of karst aquifers in southern mediterranean basin(Teboursouk area, NW Tunisia). Journal of African Earth Sciences 137: 208-217.

Babiker, I.S., Mohamed, M.A.A., Terao, H., Kato, K., Ohta, K. (2004). Assessment of groundwater contamination by nitrate leaching from intensive vegetable cultivation using geographical information system. Environmental International 29 (8): 1009-1017.

Bender, F. (1968). Géologie von Jordanian, BeitraegeZurRegionalenGéologie, Region. Geol. d. Erde 7. GebruederBrontrager, Berlin.

Bodrud-Doza, Md., Towfiqul Islam, A.R.M., Ahmed F., Das, S., Saha, N., Safiur Rahman. (2016).

Characterization of groundwater quality using water evaluation indices, multivariate statistics and geostatistics in central Bangladesh. Water Science 30: 19-40.

Davis, S.N., and DeWiest, J.M. (1966). Hydrogeology: New York, John Wiley and Sons, 463 pp.

Fang, Y., Zheng, T., Zheng, X., Peng, H., Xin, J., Zhang, B. (2020). Assessment of the hydrodynamics role for groundwater quality using an integration of GIS, water quality index and multivariate statistical techniques. Journal of Environmental Management 273: 111185. DOI: org/10.1016/j.jenvman.2020.111185.

Gaikwad, S.K., Kadam, A. K., .Ramgir, R. R., Kashikarc, A. S, Wagh, V. M , Kandekar, A. M.,

Gaikwad, S. P., Madale, R. B, Pawar, N. J., Kamble, K. D. (2020). Assessment of the groundwater geochemistry from a part of west coast of India using statistical methods and water quality index. HydroResearch 3: 48-60.

Gao, Y., Q., H., Ren, W., Wang, H., Liu F., Yang, F. (2020). Hydrogeochemical characterization and quality assessment of

groundwater based on integrated-weight water quality index in a concentrated urban area. Journal of Cleaner Production, 260: 121006. DOI: org/10.1016/j.jclepro.2020.121006.

Gibbs, R.J. (1970). Mechanisms controlling world water chemistry. Science 170: 1088-1090.

Gibrilla, A., Fianko, J.R., Ganyaglo, S., Adomako, D., Anornu, G., Zakaria, N. (2020). Nitrate contamination and source apportionment in surface and groundwater in Ghana using dual isotopes (15N and 18O-NO3) and a Bayesian isotope mixing model. Journal of Contaminant Hydrology 233: 103658. DOI: org/10.1016/j.jconhyd.2020.103658.

Gopinath, S., Srinivasamoorthy, K., Saravanan, K., Prakash, R. (2019). Tracing groundwater salinization using geochemical and isotopic signature in Southeastern coastal Tamilnadu, India. Chemosphere 236: 124305. DOI: org/10.1016/j.chemosphere 2019.07.036.

Han, D., Post, V.E.A., Song, X. (2015). Groundwater salinization processes and reversibility of seawater intrusion in coastal carbonate aquifers. Journal of Hydrology 531: 1067-1080.

Hartigan, J.A. (1975). Clustering algorithms. John Wiley & Sons, New York, 349p.

Hegeu, H., Kshtrimayum, K.S. (2019). Hydrochemical characterization of groundwater in geomorphic units using graphical and multivariate statistical methods in the Dimapur valley, Northeast India. Groundwater for Sustainable Development 8: 484-500.

Heiβ, L., Bouchaou, L., Tadoumant, S., Reichert, B. (2020). Index-based groundwater vulnerability and water quality assessment in the arid region of Tata city (Morocco). Groundwater for Sustainable Development, 10: 100344. DOI:org/10.1016/j.gsd.2020.100344.

Hem, J.D. (1985). Study and Interpretation of the Chemical Characteristics of Natural Water (Vol. 2254). Department of the Interior, US Geological Survey.

Ismail, A., Hassan, G., Sarhan, A-H.(2020). Hydrochemistry of shallow groundwater and its assessment for drinking and irrigation purposes in Tarmiah district, Baghdad governorate, Iraq. Groundwater for Sustainable Development, 10: 100300. DOI: org/10.1016/j.gsd.2019.100300.

Jain, C.K., Sharma, S.K., Singh, S. (2018). Physico-chemical characteristics and hydrogeological mechanisms in groundwater with special reference to arsenic contamination in Barpeta District, Assam (India). Environmental Monitoring and Assessment, 190 (7): 417. DOI: org/10.1007/s10661-018-6781-5.

Jawarneh, R. and Biradar, C. (2017). Decadal National Land Cover Database for Jordan at 30 M Resolution. Arabian Journal of Geosciences 10 (22): 483. DOI:10.1007/s12517-017-3266- 8.

Kawo, N.S., and Karuppannan, S. (2018). Groundwater quality assessment using water quality index and GIS technique in Modjo River Basin, central Ethiopia. Journal of African Earth Sciences 147: 300-311.

Keesari, T., Sinha, U.K., Deodhar, A., Krishna, S.H., Ansari, A., Mohokar, H., Dash, A. (2016).

High fluoride in groundwater of an industrialized area of Eastern India (Odisha): inferences from geochemical and isotopic investigation. Environmental Earth Sciences 75 (14): 1-17.

Khangembam, S., and Kshetrimayum, K.S. (2019). Evaluation of hydrogeochemical controlling factors and water quality index of water resources of the Barak valley of Assam, Northeast India. Groundwater for Sustainable Development 8:541-553.

Kumar, M., Ramanathan, A.L., Rao, M.S., Kumar, B. (2006). Identification and evaluation of hydrogeochemical processes in the groundwater environment of Delhi, India. Environmental Geology 50: 1025-1039.

Lermi, A., and Ertan, G. (2019). Hydrochemical and isotopic studies to understand quality problems in groundwater of the Niğde Province, Central Turkey. Environmental Earth Sciences 78 (12): 365. DOI: org/10.1007/s12665-019-8365-2.

Li, P., Wu, J., Qian, H., Zhang, Y., Yang, N., Jing, L., Yu, P. (2016). Hydrogeochemical characterization of groundwater in and around a wastewater irrigated Forest in the southeastern edge of the Tengger Desert, northwest China. Exposure and Health 8 (3): 331-348.

Liu, F, Wang, S, Wang, L., Shi, L., Song, X., Yeh T-C.J. (2019). Coupling hydrochemistry and stable isotopes to identify the major factors affecting groundwater geochemical evolution in the Heilongdong Spring Basin, North China. Journal of geochemical Exploration 205: 106352.DOI: 10.1016/j. gexplo.2019.106352.

Machiwal, D., Islam, A., Kamble, T. (2019). Trends and probabilistic stability index for evaluating groundwater quality: the case of quaternary alluvial and quartzite aquifer system of India. Journal of Environmental Management 237: 457-475.

Margane, A., Hobler, M., Subah, A. (1999). Mapping of groundwater vulnerability and hazards to groundwater in the Irbidb area, N Jordan. Zeitschrift fur Angewandte Geologie 45(4): 175-187.

Moquet, J-S., Crave, A., Viers, J, Seyler, P., Armijos, E., Bourrel, L., Chavarri, E., Lagane, C., Laraque, A., Casimiro, W.S.L., Pombosa, R., Noriega, L., Vera, A., Guyot, J-L. (2011).

Chemical weathering and atmospheric/soil CO2 uptake in the Andeanand Foreland Amazon basins. Chemical Geology 287 (1-2): 1-26.

Nagaraju, A., Thejaswi, A., Sun, L. (2016). Statistical analysis of high fluoride groundwater hydrochemistry in southern India: quality assessment and implications for source of fluoride. Environmental Engineering Science 33: 1-7.

Njuguna, S.M., Onyango, J.A., Githaiga, K.B., Gituru, R.W., Yan, X. (2020). Application of multivariate statistical analysis and water quality index in health risk assessment by domestic use of river water. Case study ofTana River in Kenya. Process Safety and Environmental Protection 133: 149-158.

Obeidat, A., and Alawneh, M. (2019). Hydrochemistry and groundwater quality assessment in Mafraq Province, Jordan. Open Access Library Journal 6: e5365.

Obeidat, M.M., Awawdeh, M., Abu Al-Rub, F. (2013). Multivariate statistical analysis and environmental isotopes of Amman/Wadi Sir (B2/A7) groundwater, Yarmouk River Basin, Jordan Hydrological Process 27: 2449-2461.

Obeidat, M., M. Awawdeh, F. Abu Al-Rub, and A. Al-Ajlouni. (2012). "An Innovative Nitrate Pollution Index and Multivariate Statistical Investigations of Groundwater Quality of Umm Rijam Aquifer (B4), Yarmouk River Basin, Jordan." In Water Quality Monitoring and Assessment, edited by K. Voudouris and D. Voutsa. INTECH Open Access Publisher, Rijeka, Croatia. ISBN 978-953-51-0486-5.

Panno, S., Kelly, W., Martinsek, A., Hackley, K.C. (2006). Estimating background and threshold nitrate concentrations using probability graphs. Ground Water 44: 697-709

Piper, A.M. (1944) A Graphic Procedure in the Geochemical Interpretation of Water-Analyses. Eos, Transactions American Geophysical Union 25: 914-928.

Ponsadailakshmi, S., Sankari, S.G., Prasanna, S.M., Madhurambal, G. (2018). Evaluation of water quality suitability for drinking using drinking water quality index in Nagapattinam district, Tamil Nadu in Southern India. Groundwater for Sustainable Development, 6: 43-49.

Qin, R., Wu, Y., Xu, Z., Xie, D., Zhang, C. (2013). Assessing the

impact of natural and anthropogenic activities on groundwater quality in coastal alluvial aquifers of the lower Liaohe River Plain, NE China. Applied Geochemistry 31: 142-158.

Rashid, A., Khattakm S.A., Ali, L., Zaib, M., Jehan, S., Ayub, M., Ullah, S. (2019). Geochemical profile and source identification of surface and groundwater pollution of District Chitral, Northern Pakistan. Microchemical Journal 145: 1058-1065.

Rimawi, O. and Udluft. P. (1985). Natural water groups and their origin of the shallow aquifers complex in Azraq depression, Jordan. Geologisches Jahrbuch C38: 17-38.

Sawyer, C.N. and McCarty, P.L. (1967). Chemistry and sanitary engineers. New York, McGraw-Hill, 2nd ed., 518 pp.

Schoeller, H. (1965). Qualitative evaluation of groundwater resources. In methods and Techniques of Groundwater Investigations and development UNESCO: 54-83.

Selvam, S., Venkatramanan, S., Chung, S.Y., Singaraja, C. (2016). Identification of groundwater contamination sources in Dindugal district of Tamil Nadu, India using GIS and multivariate statistical analyses. Arabian Journal of Geosciences 9: 407. DOI: org/10.1007/s12517-016-2417-7.

Stuyfzand, P.J. (2008). Base exchange indices as indicators of salinization or freshening of (coastal) aquifers. 20th Salt Water Intrusion Meeting, Naples, Florida, USA.

Ta'any, R.A., Tahboub, A.B., Saffarini G. (2009). Geostatistical analysis of spatiotemporal variability of groundwater level fluctuations in Amman-Zarqa basin, Jordan: a case study. Environmental Geology 57: 525-535.

Tiwari, A.K., Pisciotta, A., De Maaio, M. (2019). Evaluation of groundwater salinization and pollution level on Favignana Island, Italy. Environmental Pollution 249: 969-981.

Todd, D.K. (1980). Groundwater Hydrology, Second Edition, Wiley, New York, 522 pp.

Udeshani W.A.C., Dissanayake, H.M.K.P., Gunatilake, S.K., Chandrajith, R. (2020). Assessment of groundwater quality using water quality index (WQI): A case study of a hard rock terrain in Sri Lanka. Groundwater for Sustainable Development, 11: 1004421. DOI: org/10.1016/j.gsd.2020.100421.

UNHCR FACTSHEET. 2020. Jordan-Zaatari Refugee Camp. https://reporting.unhcr.org/sites/default/files/UNHCR%20Jordan%20Zaatari%20Refugee%20Camp%20Fact%20Sheet%20-%20August%202020.pdf.

UNICEF. (2017). Wash infrastructure and services assessment in Zaatari Camp-assessment report.https://reliefweb.int/report/jordan/jordan-wash-infrastructure-services-assessment-zaatari-camp-assessment-report-march.

Varol, M. (2020). Use of water quality index and multivariate statistical methods for the evaluation of water quality of a stream affected by multiple stressors: A case study. Environmental Pollution 266: 115417. DOI: org/10.1016/j.envpol.2020.115417.

Wakida, F.T., and Lerner, D.N. (2005). Non-Agricultural Sources of Groundwater Nitrate: A Review and Case Study. Water Research 39 (1): 3-16.

Wang Q., Dong, S., Wang, H., Yang, J., Huang, H., Dong, X., Yu, B. (2020). Hydrogeochemical processes and groundwater quality assessment for different aquifers in the Caojiatan coal mine of Ordos Basin, northwestern China. Environmental Earth Sciences 79: 199. DOI: org/10.1007/s12665-020-08942-3.

Wang, S.W., Liu, C.W., Jang, C.S. (2007). Factors responsible for high arsenic concentrations in two groundwater catchments in Taiwan. Applied Geochemistry 22: 460-476.

WHO. (2011). Guidelines for Drinking-Water Quality, vol. 216. World Health Organization, pp. 303–304.

Wu, Z., Zhang, D., Cal, Y., Wang, X., Zhang, L., Chen, Y. (2017). Water quality assessment based on the water quality index method in Lake Poyang: the largest freshwater lake in China. Scientific Reports 7: 17999. DOI: 10.1038/s41598-017-18285-y.

Wu, J., Zhou, H., He, S., Zhang, Y. (2019). Comprehensive understanding of groundwater quality for domestic and agricultural purposes in terms of health risks in a coal mine area of the Ordos basin, north of the Chinese Loess Plateau. Environmental Earth Sciences 78(15): 446. DOI: org/10.1007/s1266 5-019-8471-1.

Zaidi, F. K., Nazzal, Y., Jafri, M. K., Naeem, M., Ahmed, I. (2015). Reverse ion exchange as a major process controlling the groundwater chemistry in an arid environment: a case study from northwestern Saudi Arabia. Environmental Monitoring and Assessment, 187: 607. DOI: 10.1007/s10661-015-4828-4.

Zango, M.S., Sunkari, E.D., Abu, M., Lermi, A. (2019). Hydrogeochemical controls and human health risk assessment of groundwater fluoride and boron in the semi-arid North East region of Ghana. Journal of Geochemical Exploration 207: 106363. DOI: org/10.1016/j.gexplo.2019.106363.

Zhang, H., Yang, R., Wang, Y., Ye, R. (2019). The evaluation and prediction of agriculture-related nitrate contamination in groundwater in Chengdu Plain, southwestern China. Hydrogeology Journal 27(2): 785-799.

Zotou, I., Tsihrintzis, V.A., Gikas, G.D. (2020). Water quality evaluation of a lacustrine water body in the Mediterranean based on different water quality index (WQI) methodologies. Journal of Environmental Science and Health Part A 55: 537-548.

JJEES

JJEES (2021) 12 (3): 198-205
ISSN 1995-6681

Jordan Journal of Earth and Environmental Sciences

Effect of Broken Tile Waste on Strength Parameter of Dune Sand

Mohammad Khabiri* and Bahareh Ebrahimialavijeh

Faculty of Civil Engineering, Yazd University, Yazd, Iran.

Received 26 August 2020, Accepted 16 December 2020

Abstract

Nowadays, the limitation of borrow resources with suitable soil in the roadbed, especially in sandy soil areas, has caused the existing soils to be improved by engineering methods. Since the focus in the central regions of Iran is on the tile industry, and a large part of the soil in the region is sand, so broken tile waste (BTW) is recommended to stabilize the pavement subgrades. Because sand and broken tile wastes have not enough adhesion, so a small amount of cement has been used to create the adhesion. In the present study, two Particle size of tile wastes at10%, 20% and 30% by soil dry weight and cement at 2.5%, 5% and 7.5% by soil dry weights have been used. Unconfined compressive strength, California Bearing Ratio (CBR) and durability tests were performed for created mixtures. Results showed that increase in cement content has led in increase the durability, CBR and compressive strength, but in CBR test, increasing the BTW content up to 20% caused increasing the CBR and above this has a reverse effect. The CBR was increased from 19% to maximum 83% and 89% for fine-grained and coarse-grained BTW, respectively. The maximum unconfined compressive strength was 3.7MPa and 3.2MPa for coarse and fine-grained BTW, respectively. Durability test also showed that increasing the BTW (both coarse and fine-grained)content up to 20% is optimal.

Keywords: Dune sand, stabilization, Tile Waste, CBR test, Compressive test, freeze-thaw cycle

1. Introduction

Usually, quicksand is not ideal for bearing the pavement loading alone at the site of road and railway building. Mechanical properties of sand soils are affected by soil structure, density, grain distribution, shape and mineralogy, soil interlocking degree, particles adhesion and shape. Non-sticky fine-grained soils such as quick (dune) sand, are not applicable unlimitedly and without additional adhesives in the flexible pavement of subgrade.

Compressive strength and operation against wet environmental conditions and freezing of dune sand soils are among the most important issues in the geotechnics and pavement engineering. Another environmental problem is the production of broken tile waste (BTW), which in Iran the production of this waste reaches at least 4000 tons. It can save a lot and benefit the ecosystem if it can be used optimally. In other countries with a ceramic tile industry, the development of such waste materials is also high. By replacing these wastes, the amount of cement usage for stabilizing this type of soil is reduced. Therefore, in the present study by replacing particles with coarser dimensions and adding adhesion materials, the strength of sand subgrades can be reinforced. This means that both improvement methods including modification grading and adhesion can be used simultaneously.

One of the methods for improvement and modification of subgrade soil is using the stabilizing methods. Various materials such as lime, cement and some polymeric materials have been used by several researchers for soil stabilization (Dutta, 2008; Tang et al., 2007; Rezaeimalek et al., 2017; Mousavi and Karamvand, 2017; Al-Tabbal and Al-Zboon, 2019, Liu et al., 2019; Saride et al., 2013; Consoli et al., 2010). Using cement in soils has increased strength parameters of soil and also has increased the soil fragility (Jamshidi et al., 2018). Using waste materials in development projects has led to a reduction in costs and also helped the environment. The waste materials include recycled asphalt and waste construction materials (Khabiri, (2010)). Using recycled asphalt in the soil has led to increase in bearing capacity and strength soil and has made the soil suitable for use in base or subbase layer (Hasan et al., 2018; Mousa et al., 2017; Alhaji and Alhassan, 2018; Cabalar et al., 2016a and Cabalar et al., 2016b). James and Pandian (2014) investigated the effect of broken ceramic on the compressive strength of clay soil stabilized with cement. Their results showed that increasing the broken ceramic percentage will increase the compressive strength of clay stabilized with cement. Application of BTW in loose black clay has improved strength parameters of the soil for use in subgrade construction (Raghudeep et al., 2015; Al-slaty, 2018). Same results were obtained for expansive soil (Rani et al., 2014; Sumayya et al., 2016; Kumar et al., 2015; Sabat, 2012). Ameta et al. (2013) investigated the application of waste tile in the dune soil. The results of direct cutting and CBR test indicate the improvement in the strength parameters of dune soil by adding broken tile. Cabalar et al. (2017) studied the use of construction and demolition materials with clay and natural aggregate utilization for road pavement subgrade. They found that the use of construction and demolition materials could be mixed with clay at specific contents for road pavement subgrade in order to reduce the environmental and economic problems across the world.

* Corresponding author e-mail: mkhabiri@yazd.ac.ir

Cabalar et al. (2016 b) found that the addition of construction and demolition materials to the clay reduced the optimum moisture content and increased the unconfined compressive strength. Also, the swelling percentage of the clay was found to decrease with an increase in the amount of waste material.

Therefore, given the necessity of using these soil improvement methods in the sand subgrades and also the emphasis on the use of tile wastes, more detailed studies are needed to be done in this field. This study aims to investigate the effect of the addition of tile wastes in different sizes, fine and coarse-grained, with different cement ratio, also investigates the effect of research variables on the stabilized sand subgrade by using pavement subgrade-related standard tests including soil capacity bearing ratio (CBR), durability and unlimited compressive strength. Also, the effect of freezing in the Freeze-thaw cycle has been investigated. The elasticity module obtained from different soil cases in numerical analysis software was used and the amount of deformation of modified subgrade soil and rutting life were calculated separately. The innovation of the present study is the simultaneous investigation the effect of two sand subgrade modification methods on the performance, and also the effect of use of BTW on the sand subgrade soil modification which has not been addressed in the previous studies.

2. Materials and methods

2.1 Sample Preparation

The soil used in this analysis is sandy soil from the Ardakan-Yazd plain (Figure 1), which is located at a latitude of 29°36 to 33°22 in the north and a longitude of 52°48 in the east and 56°36 in the north. This type of soil can be found in wide areas of middle-east and other countries with the climate of desert regions. The specifications of this soil have been defined based on the ASTM standard and are provided in Table 1.

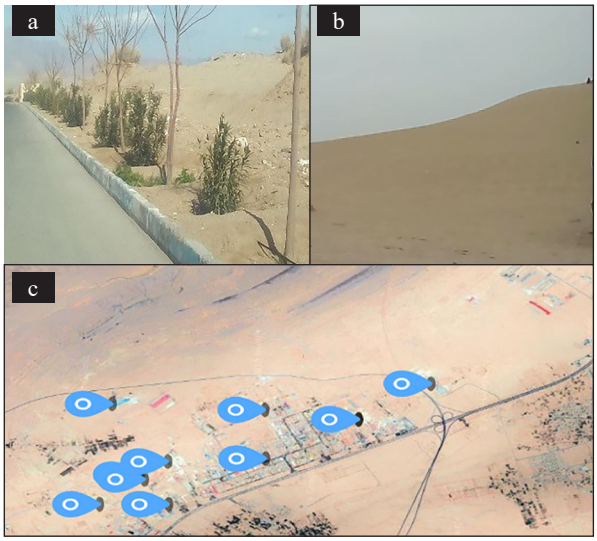

Figure 1. (a). Position of the path along the dune sands. (b). The volume of dune sand hills. (c). Location of tile factories located in the studied area.

Figure 2 shows the grading of this soil, which based on this grading and the specifications of Table 1 as well as based on the ASTM: D421, D422 standard, the naming of this soil will be SP. Thermal conductivity of these type of soils in terms of (w/mºk) is 0.795.

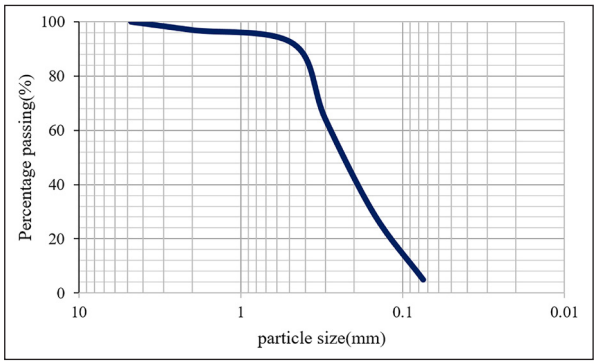

Figure 2. Particle size distributions for sand.

Based on the studies of Golami et al (2015), the findings of the XRF test of the chemical sand compounds used in the geographical area of the present research are beyond the range of the change in Table 2.

Table 1. Specifications of dune sand soil sample of Ardakan-Yazd plain area.

Specifications	Standard No	Unit	Content
Liquid limit	ASTM: D 4318-00	%	4
Plastic Limit	ASTM: D 4318-00	%	-
Moisture content	ASTM:D2216-98	%	3
Optimum moisture content	ASTM:D698-00	%	8
Maximum dry density	ASTM:D698-00	gr/cm3	1.75
Specific gravity	ASTM:D4546-08	-	2.64

Table 2. Specifications of dune sand materials of the studied area, XRF test results, chemical compounds decomposition.

Detected element	Quantity (%)
SiO2	48
Al2O3	8.3
MgO	4.5
P2O3	14
TiO2	8
MnO	0.1
CaO	22.5
Na2O	0.8
K2O	19
Others	8.5

The cement used in the present study is manufactured from a cement type 2 plant with the commercial name “Tejarat Mehriz” which has the characteristics so that it can be used in general civil engineering projects and its specifications are provided in Table 3.

Table 3. Physical and chemical specifications of cement used in the present study.

Chemical Properties of Cement		Abbreviation	Amount(Percent)
Silicon oxide		SiO2	20
Aluminium oxide		Al2O3	6
iron oxide		Fe2O3	6
Magnesium oxide		Mg O	5
Sulfur trioxide		SO3	3
Weight loss due to blush		-	3
Remaining insoluble		-	0.75
Three calcium aluminates		C3A	8
Physical properties of cement		Amount	
The specific surface area of 1 square centimeter per gram		2800	
Extension of the autoclave test (percent)		0.8	
Setting time of ordinary Portland cement	Basic (min)	45	
	Final(hours)	6	
Compressive (MPa)	3days	10	
	7days	17.5	
	28days	31.5	
Heat hydration calories per gram		70	

Broken tile waste (BTW) was supplied from tile plants in the studied area with the commercial name "Meybod Tile Factory," which at first had sizes 20cm×20cm and 30cm×60cm, and part of the tile was broken or split into two parts and was broken manually with the compaction hammer in the laboratory. Figure 3 provides a sample of these broken, fine-grained and coarse-grained tiles along with other materials used in this analysis.

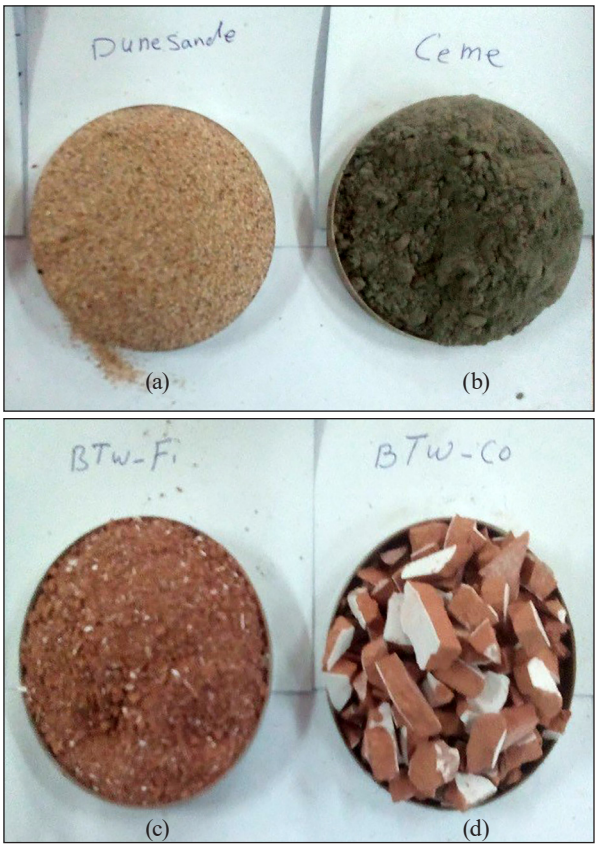

Figure 3. Consumable materials in the present study (a) dune sand, (b) cement type 2, (c) fine-grained BTW, (d) coarse-grained BTW.

Based on the findings of Tavakolia et al. (2013) and the grading of these two forms of broken tiles, the chemical components are differentiated by Figure 4 and Figure 5. The fine-grained and coarse-grained separation screening was 0.425 mm and the maximum size of the broken tile waste was 10 mm. Some of the specifications for these broken tile waste are given in Tables 4-5.

Table 4. Specifications of chemical compounds decompositions of tile.

Detected element	Quantity (%)
SiO2	69
Al2O3	18.5
MgO	0.72
P2O3	0.03
TiO2	0.73
SO3	0.06
MnO	0.08
CaO	1.5
Na2O	2.01
K2O	1.63
Fe2O3	4.81
LOI	0.5

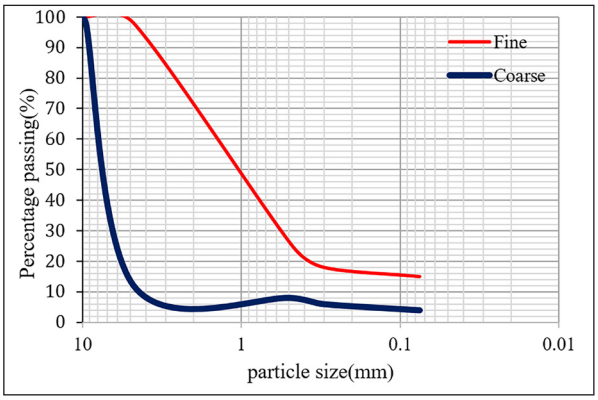

Figure 4. The particle size distribution of broken waste material (coarse-grained and fine-grained).

Table 5. Physical specifications of fine- and coarse-grained waste broken tiles.

Properties	Standard. No	Dimension of broken tile waste	
		Coarse-grained	Fine grained
Absorption of water	ASTM: C642-06	5	7
Particle Shape	IS- 2386-63	cubical angular-shaped	unpredictable
Bulky density	ASTM: C29-03	(gr/cm3) 2.33	(gr/cm3) 2.35
Coefficient of thermal conductivity	ASTM: C177-04	(w/mºk) 1.04	

3. Sample preparation and testing methods

Based on the previous researches include (Shooshpasha and Shirvani, 2015) and (Rudramurthy et al., 2019), the cement content for sand soils is in the range of 2.5% to 9% by soil dry weight. The maximum content of granular and solid wastes for addition to soils is about 15% (Prasanna, 2019). In the initial review of this study and before the main study it was found that the extreme use of broken tile waste has led to non-uniformity of the mixture and even has led to lack of adhesion which is in accordance with results of researches (Fauzi et al., 2016). In this study, the cement content was of 2.5%, 5% and 7.5% and BTW content was 10%, 20% and 30% by soil dry weight. Durability tests were also done for Freeze-thaw cycle. Since the road construction operation is done in a short time, the curing time was selected as 3 days. During the curing time, the samples were kept in a plastic bag to prevent moisture change. Based on the ASTM: C-109-07 standard, test specimens were made for durability and compressive strength tests and also these tests were done based on the ASTM: C-666-03 standard. For mixing the specimens, first, the sand was mixed with BTWand then the cement was added to the mixture and in less than 15min, it was entered in the standard mold and was compacted with a small hammer.

For determining the bearing capacity of modified sand subgrade soil a CBR test was done based on the ASTM: D1883-99 standard. For moisture used in the mixture, constant moisture (i.e.optimum moisture content) plus the percentage of water absorbed by the BTW and half of cement weight were added to the mixture.

4. Results and discussion

4.1. Compaction test

In this experimental study, the compaction test was performed for 6 different mixtures. The results of the present study can be applicable for compressive in the site. At Inroads pavement, operational standards defined minimum compaction of 95%, where of course is based on the road type and the amount of traffic (Kim and Kim, 2007). Figure 5 indicates the highest dry density difference at 5 percent of the cement material for both the fine-grained and the coarse-grained. According to this figure 5, it has been shown that the optimum moisture content and the maximum dry density of the soil has increased by addition to the untreated soil. It was found that the more the BTW became finer, the required moisture increased an also the maximum dry density is increased too. Increasing the coarse-grained BTW content in the soil reduced the optimum moisture and maximum dry density. In coarse-grained BTW, the glazed surface inhibits water absorption, which decreases the optimal soil moisture content. Also, the large grain size of the tiles and their lower density compared to sand particles, as well as the non-cohesive, will reduce the maximum dry density of the stabilized soil. Results of Taha et al. (2002) showed that increasing the recycled materials has a direct effect on the increasing the optimum moisture (Taha et al., 2002), when the particles are coarse, the water absorption of the ceramic particles is also higher than that of the sand particles, so they need more water per unit volume. Variations of maximum dry density of modified sandy soil is due to variation of BTW percentage and also due to the adhesion between sand soil particles.

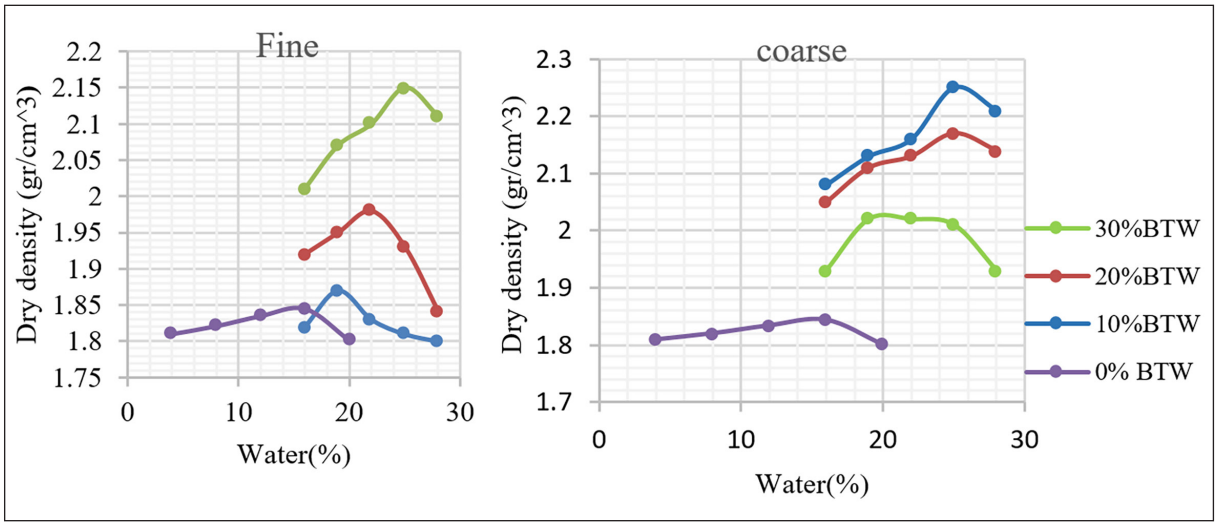

Figure 5. Variations of maximum dry density and optimum moisture in different percentages of BTW and cement (5%).

4.2. California Bearing Ratio test of sand

In the design of pavements, based on international standards, it is important to research the CBR of the subgrade to be specified (Patel et al., 2019) and hence the CBR variations with different content fine- and coarse-grained BTW and different content of cement have been studied and the results are shown in Figure 6. According to Figure 6, the addition of cement and BTW to the soil has increased the bearing capacity. Increasing the content of cement increases the bearing capacity and increasing the BTW content up to 20% increases the bearing capacity and then a decrease in bearing capacity is observed, which is quite evident in the figure. The test results show that the coarse-grained BTW has a higher bearing capacity. Therefore, the highest bearing capacity is obtained in soil that stabilized with 7.5% cement and 20% BTW, which was 89% for coarse-grained BTW and 83% fine-grained BTW. The bearing capacity of untreated soil is equal to 19%, so the carrying capacity with these stabilizers has increased more than 4 times.

4.3. Durability and compressive strength of stabilized soil

One topic which happened in subgrades is the possibility of freeze-thaw cycle occurrence. In the present study, the strength reduction in 3, 6 and 12 repeats of freeze-thaw cycles at moderate cement content and optimum content of BTW (20%) was investigated. These tests were performed for 5cm cubic specimens. The results showed that 3 and 6 cycles have not significant effect on stabilized sand soil and the reduction is about 3%, but in 12 repeats of freeze-thaw cycle, the reduction in strength reaches to 18%. These results are shown in Table 6. The coding of the samples in Table 6 is BXYC or BXYF. "X" represents the content of cement (%), "Y" the content of BTW (%), "F" means fine-grained BTW and "C" means coarse-grained BTW. The results of previous studies (Simonsen and Isacsson, 2001; Zhou et al., 2018; Xu et al., 2019) also showed that the number of cycles has a significant effect on the reduction of stabilized sand soil.

Table 6. Compressive strength variations of cubic specimen at different freeze-thaw cycle.

Sample Code	Compressive strength (Pa)		
	3 cycles	6cycles	12 cycles
B2025F	8	7	6
B2050F	17	16	13
B2075F	28	26	22
B2025C	11	10	9
B2050C	23	22	18
B2075C	36	34	32

It can be seen that the effect of freeze-thaw cycle for sand soil with coarse-grained BTW is less than fine-grained BTW. The reason may be due to the high thermal capacity of tile, which the finer it is, the heat transfer increases as a result of the increase in the specific surface and the internal thermal variations are also increased. For this purpose, it is recommended that in the regions with cold weather and the long period of frost the coarse-grained BTW be used for stabilized sand soils.

Figure 7 shows the compressive strength of soil stabilized with different content of cement and BTW. According to Figure 7, the addition of cement and BTW, both have increased the compressive strength of sand soil. Increasing the cement content has increased the compressive strength of the soil. Increasing the fine-grained BTW increased the compressive strength, but increasing the coarse-grained BTW by up to 20% increased the compressive strength, and no significant effect was observed. Increasing the dimensions of the BTW has also increased the compressive strength. Therefore, the highest compressive strength was observed in the soil stabilized with 7.5% cement and 20% coarse-grained BTW, which is 3.7 MPa.

These results are in good agreement with results of Hossain et al. (2019) which concluded that excessive additives do not have a significant effect on increased strength.

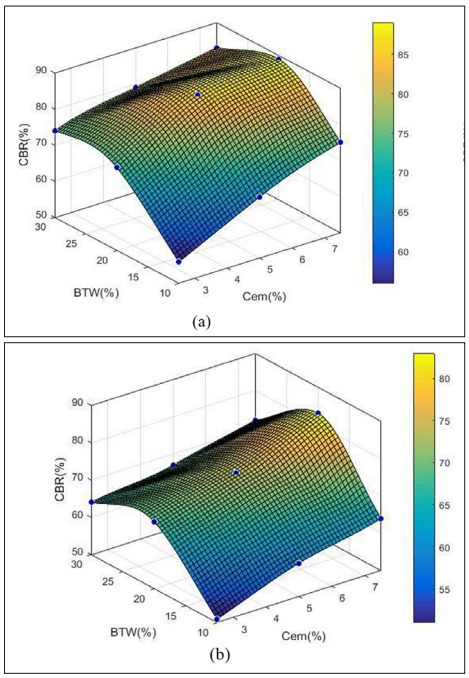

Figure 6. 3D plot of BTW-cement percentage variations in CBR (a) coarse-grained BTW and (b) fine-grained BTW.

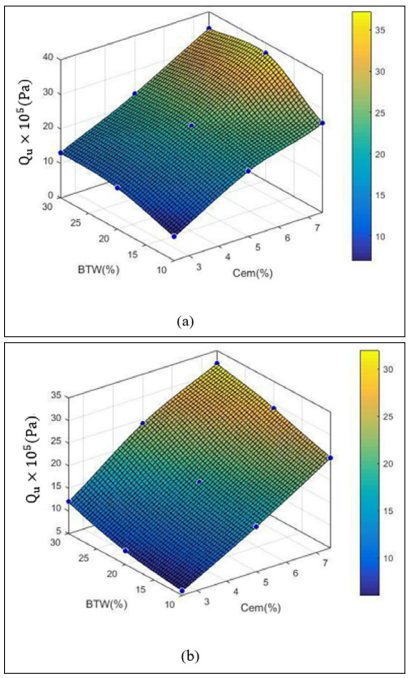

Figure 7. Compressive strength variations at different content of BTW-cement after 3-days curing. (a) coarse-grained BTW and (b) fine-grained BTW.

4.4. SEM image of samples

The SEM image of soil stabilization is shown in Figure 8, in which the distribution of the particles was uniform. Figure 8 indicates that the addition of cement to the sand-BTW mixture created adhesion between the particles. Increasing the adhesion of the particle increases the compressive strength and the bearing capacity.

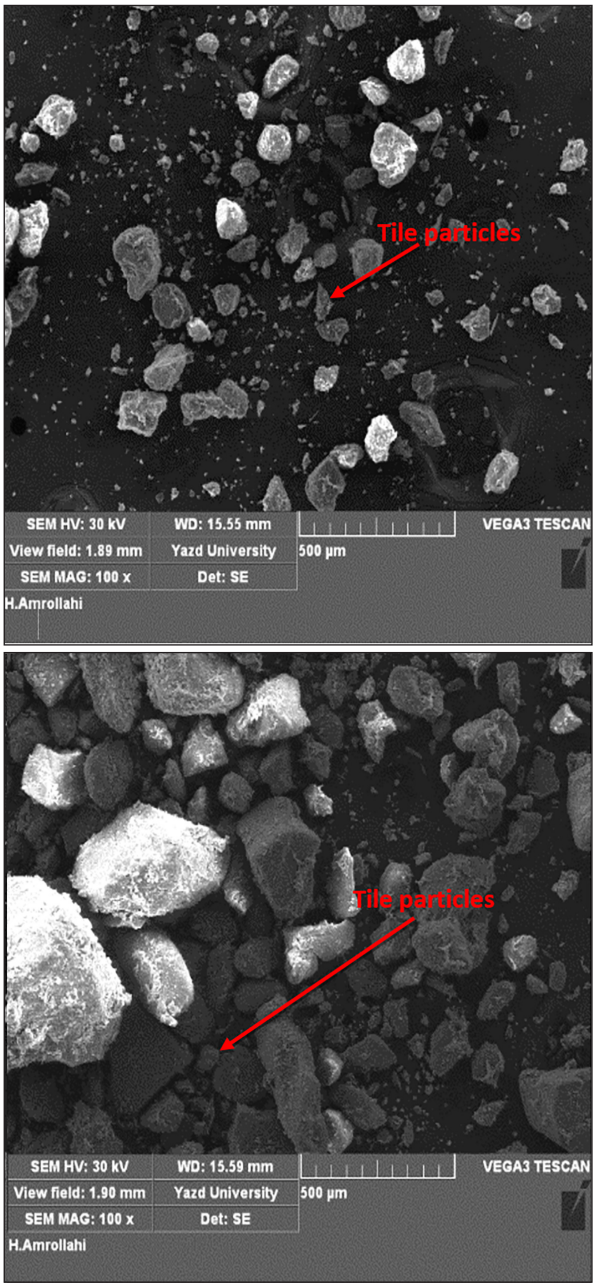

Figure 8. Grading plot of BTW and dune sand grains, (the right) coarse-grained and (the left) fine-grained.

5. Conclusions

Behavior of durability and strength of dune sand of subgrades having cement and BTW was studied in this study. 18 mixtures of this sand soil with different ratio of additives were made and tested. A series of load tests were conducted on the improved pavement test sections with cement and BTW reinforcement and the following conclusions can be drawn:

Results obtained from compaction test for different mixtures of cement, sand and BTW, shows that by adding coarse-grained BTW up to 20%, more optimum moisture than fine-grained, but the more moisture in-field compaction, the easier it will be to operate.

In regions with high freezing conditions, use of coarse-grained BTW is more proper than fine-grained BTW for providing enough strength of frozen subgrade. Besides, by considering the cost of breaking the tiles to smaller dimensions, use of coarser-grained BTW is more economical.

In sand soils by an extensive increase in BTW, and because the volume of adhesive materials around the BTW particles is reduced then the divided stress on the adhesive cement and mortar increased and the fracture possibility increased too and as a result, the resistance against loading decreased.

Adding BTW to the soil increases the bearing capacity of the sand. Also, increasing the dimensions of BTW will increase the bearing capacity. For fine-grained and coarse-grained tiles, the bearing capacity has increased from 19 to a maximum of 83% and 89%, respectively (for 7.5% cement and 20% BTW).

Addition of BTW has increased soil compressive strength. Increasing the amount of BTW and increasing its dimensions has increased the compressive strength and improved the durability against freeze–thaw cycle. The highest strength of soil stabilized was observed in 7.5% cement for20% coarse-grained BTW or 30% fine-grained BTW. This value is 3.7MPa and 3.2MPa for coarse and fine-grained BTW, respectively.

Finally, using BTW in both type of fine- and coarse-grained according to reinforcing sand subgrade and environmental issues, the proper amount of these materials and the ratio of cement can be different based on the type and chemical compounds mixture of tile. In line with these researches, the real conditions of such sand subgrades can be investigated in full scale, and in addition, ceramic waste, which is another form of tile, can be used in future studies.

References

Alhaji, M. M. and Alhassan, M. (2018). Free Swelling and Modulus of Elasticity of Compacted Black Cotton Soil Treated with Reclaimed Asphalt Pavement. The Egyptian International Journal of Engineering Sciences and Technology 25: 60-67.

Al-Slaty, M.F. (2018). Index properties of alkali-activated cement mortar affected by the addition of phosphatic clay. Jordan Journal of Earth and Environmental Sciences 9(1): 63 - 66.

Al-Tabbal, J. and Al-Zboon, K. (2019). The potential of the application of olive cake and stone cutting waste for soil amendment. Jordan Journal of Earth and Environmental Sciences 10 (1): 28-34.

Ameta, N. K., Wayal, A. S., Hiranandani, P. (2013). Stabilization of dune sand with ceramic tile waste as admixture. American journal of Engineering Research 2(09): 133-139.

ASTM: D-2216. (1998). Standard Test Method for Laboratory Determination of Water (Moisture) Content of Soil and Rock by Mass.

ASTM: D-1883. (1999). Standard Test Method for CBR (California Bearing Ratio) of Laboratory-Compacted Soils.

ASTM: D-4318. (2000). Standard Test Methods for Liquid Limit, Plastic Limit, and Plasticity Index of Soils.

ASTM: D-698. (2000).Standard Test Methods for Laboratory Compaction Characteristics of Soil Using Standard Effort (12,400 ft-lbf/ft3 (600 kN-m/m3)).

ASTM: C-29. (2003).Standard Method of Test for Bulk Density ("Unit Weight") and Voids in Aggregate.

ASTM: C-666. (2003). Standard Test Method for Resistance of Concrete to Rapid Freezing and Thawing.

ASTM: C-177. (2004). Standard Test Method for Steady-State Heat Flux Measurements and Thermal Transmission Properties by Means of the Guarded-Hot-Plate Apparatus.

ASTM: C-642. (2006). Standard Test Method for Density, Absorption, and Voids in Hardened Concrete.

ASTM: C-109. (2007). Standard Test Method for Compressive Strength of Hydraulic Cement Mortars (Using2-in. or [50-mm] Cube Specimens).

ASTM: D-4546. (2008). Standard Test Methods for One-Dimensional Swell or Collapse of Cohesive Soils.

Cabalar, A. F., Abdulnafaa, M. D., Karabash, Z. (2016a). Influences of various construction and demolition materials on the behavior of a clay. Environmental Earth Sciences 75 (841). Doi: 10.1007/s12665-016-5631-4.

Cabalar, A. F., Hassan, D. I., Abdulnafaa, M. D. (2016b). Use of waste ceramic tiles for road pavement subgrade. Road Materials and Pavement Design 18 (4): 882-896.

Cabalar, A. F., Zardikawi, O. A. A., Abdulnafaa, M. D. (2017). Utilisation of construction and demolition materials with clay for road pavement subgrade. Road Materials and Pavement Design 20 (3): 702-714.

Consoli, N. C., Bassani, M. A. A., Festugato, L. (2010). Effect of fiber-reinforcement on the strength of cemented soils. Geotextiles and Geomembranes 28(4): 344-351.

Dutta, RK. (2008). Effect of cement on the engineering properties of sand: A comparative study. Road Materials and Pavement Design 9(2): 323-332.

Fauzi, A., Djauhari, Z., Fauzi, U. J. (2016). Soil engineering properties improvement by utilization of cut waste plastic and crushed waste glass as additive. International Journal of Engineering and Technology 8(1): 15-18. doi.org/10.7763/IJET.2016.V6.851.

Golami, H. Ahmadi, J, Nazari Samani, A.A. (2015). Study of sedimentological characterizes and chemical index of alteration in Aeolian sediments Enverimontal Erosion esaerch 19(3): 15-27.

Hasan, M. M., Islam, M. R., Tarefder, R. A. (2018). Characterization of subgrade soil mixed with recycled asphalt pavement. Journal of Traffic and Transportation Engineering 5(3): 207-214.

Hossain, M. A., Afride, M. R., Nayem, N. H. (2019). Improvement of Strength and Consolidation Properties of Clayey Soil Using Ceramic Dust. American Journal of Civil Engineering 7(2): 41-46.

IS-2386. (1963). Indian Standard, Methods of Test for Aggregates for Concrete. Part I (Particle Size and Shape).

James, J. I. J. O. and Pandian, P. (2014). A study on the early UCC strength of stabilized soil admixed with industrial waste materials. International Journal of Earth Sciences 7(3): 1055-1063.

Jamshidi, C., R., Fatahi, B., Ghorbani, A., Alamoti, M. N. (2018). Evaluation of strength properties of cement stabilized sand mixed with EPS beads and fly ash. Geomechanics and Engineering 14(6): 533-544.

Kim, D. Kim, J.R. (2007). Resilient behavior of compacted subgrade soils under the repeated triaxial test,Construction and Building Materials 21(7): 1470-1479.

Khabiri, M. M. (2010). The effect of stabilized subbase containing waste construction materials on reduction of pavement rutting depth. Electronic Journal of Geotechnical Engineering 15: 1211-1219.

Kumar, A., Gupta, S. S., Chauhan, R. S. (2015). A review of the techniques of strength improvement of expansive soils by waste ceramic dust material. Discovery 40 (185): 344-348.

Liu, Y., Wang, Q., Liu, S., ShangGuan, Y., Fu, H., Ma, B., Chen, H., &Yuan, X. (2019). Experimental investigation of the geotechnical properties and microstructure of lime-stabilized saline soils under freeze-thaw cycling. Cold Regions Science and Technology 161: 32-42.

Mousa, E., Azam, A., El-Shabrawy, M., El-Badawy, S. M. (2017). Laboratory characterization of reclaimed asphalt pavement for road construction in Egypt. Canadian Journal of Civil Engineering 44(6): 417-425.

Mousavi, S. E. and Karamvand, A. (2017). Assessment of strength development in stabilized soil with CBR PLUS and silica sand. Journal of Traffic and Transportation Engineering 4(4): 412-421.

Patel, D., Kumar, R., Chauhan, K., Patel, S. (2019). Effects of Stabilization on Engineering Characteristics of Fly Ash as Pavement Subbase Material. Geotechnics for Transportation Infrastructure (pp. 127-137). Springer, Singapore.

Prasanna S. (2019) Utilization of Waste Plastic Shreds for Stabilization of Soil. In: Sundaram R., Shahu J., Havanagi V. (Eds), Geotechnics for Transportation Infrastructure. Lecture Notes in Civil Engineering 29. Springer, Singapore. DOI: 10.1007/978-981-13-6713-7_49.

Raghudeep, V., Lakshmayya, M. T. S., Prasad, K. S. B. (2015). Improvement in CBR value of black cotton soil by stabilizing it with vitrified polish waste. International Journal of Innovative Research in Science, Engineering and Technology 4(8): 6894-6902.

Rani, T. G., Shivanarayana, C., Prasad, D. S. V., Raju, G. V. R. (2014). Strength behaviour of expansive soil treated with tile waste. International Journal of Engineering Research and Development 10(12): 52-57.

Rezaeimalek, S., Nasouri, A., Huang, J., Bin-Shafique, S., Gilazghi, S. T. (2017). Comparison of short-term and long-term performances for polymer-stabilized sand and clay. Journal of traffic and transportation engineering 4(2): 145-155.

Rudramurthy G., Ramasamy P., Rajendran A. (2019) Stabilization of Clayey Soil Using Lime and Prosopis Fibers. In: Kallel A. et al. (eds) Recent Advances in Geo-Environmental Engineering, Geomechanics and Geotechnics, and Geohazards. CAJG 2018. Advances in Science, Technology & Innovation (IEREK Interdisciplinary Series for Sustainable Development). Springer, Cham. DOI: 10.1007/978-3-030-01665-4_60.

Sabat, A. K. (2012). Stabilization of expansive soil using waste ceramic dust. Electronic Journal of Geotechnical Engineering 17 (Bund. Z).

Saride, S., Puppala, A. J., Chikyala, S. R. (2013). Swell-shrink and strength behaviors of lime and cement stabilized expansive organic clays. Applied Clay Science 85: 39-45.

Shooshpasha, I., and Shirvani, R. A. (2015). Effect of cement stabilization on geotechnical properties of sandy soils. Geomechanics and Engineering 8(1): 17-31.

Simonsen, E. and Isacsson, U. (2001). Soil behavior during freezing and thawing using variable and constant confining pressure triaxial tests. Canadian Geotechnical Journal 38(4): 863-875.

Sumayya, K. P., Rafeequedheen, M., Sameer, V. T., Firoz, Khais, P. T., Jithin, K. (2016).

Stabilization of expansive soil treated with tile waste. International Journal of Civil Engineering 3(22): 67-75.

Taha, R., Al-Harthy, A., Al-Shamsi, K., Al-Zubeidi, M. (2002). Cement stabilization of reclaimed asphalt pavement aggregate for road bases and subbases. Journal of materials in civil engineering 14(3): 239-245.

Tang, C., Shi, B., Gao, W., Chen, F., Cai, Y. (2007). Strength and mechanical behavior of short polypropylene fiber reinforced and cement stabilized clayey soil. Geotextiles and Geomembranes 25(3): 194-202.

Tavakolia, D. Heidari, A., Karimian, M. (2013). Properties Of Concretes Produced With Waste Ceramic Tile Aggregate. Asian Journal of Civil Engineering (BHRC) 14(3): 369-382.

Zhou, Z., Ma, W., Zhang, S., Mu, Y., Li, G. (2018). Effect of freeze-thaw cycles in mechanical behaviors of frozen loess. Cold Regions Science and Technology 146: 9-18.

Xu, X., Li, Q., Lai, Y., Pang, W., Zhang, R. (2019). Effect of moisture content on mechanical and damage behavior of frozen loess under triaxial condition along with different confining pressures. Cold Regions Science and Technology 157: 110-118.

JJEES

Jordan Journal of Earth and Environmental Sciences

JJEES (2021) 12 (3): 206-213
ISSN 1995-6681

Assessment of the physicochemical and microbiological water quality of Al-Zahrani River Basin, Lebanon

Nada Nehme[1], Chaden Moussa Haydar[1], Zaynab Al-Jarf[1], Fatima Abou Abbass[1], Najah Moussa[2], Genane Youness[2], Khaled Tarawneh[*3]

1Faculty of Agricultural Engineering and Veterinary Medicine, Lebanese University, Dekwaneh, Libanon.
2Cnam-ISSAE Department of Statistics, Libanon
*3*Civil Engineering Department, Faculty of Engineering, Amman Arab University, Jordan.*

Received 23 September 2020; Accepted 28 December 2020

Abstract

Lebanon is a mountainous country with an area of 10452 km^2, and it is characterized by a Mediterranean climate having a variable rainfall rate from which a significant amount is manifested as snow. The dense population of Lebanese is located in the coastal zone creating a strong anthropic pressure on the water resources. The civil war (1975-1990) and the post-war period (1990-2000) have led to a shortage in Lebanese watersheds data due to discontinuation of regular measurements.

This study aims at investigating the hydrological response of the Al-Zahrani River Basin by tackling various physicochemical and microbiological parameters that are related to human activities' influence on the water quality in six selection sites. The water tested physiochemical parameters of the basic temperature (T), the potential of hydrogen (pH), electrical conductivity (EC) and total dissolved solids (TDS), the anions (NO_3^-, SO_4^{2-} and PO_4^{3-}), the cations (Na^+, K^+, Ca^{2+}, and Mg^{2+}), and the heavy metals (Cd, Cr, Fe, Cu and Zn). The microbial parameters are Salmonella, Escherichia coli, Total Coliforms, Clostridium perfringens and Staphylococcus aureus. Furthermore, the most polluted site was assessed through conduction of principal component analysis (PCA) statistics.

Microbiological pollution was found at a high level in all sites with a total absence of heavy metals contamination. High nitrate levels were observable in two sites (WadiAkhdar 2 and Zahrani), in addition to a high potassium rate in NabehKfarwah. The PCA assessment highlighted the Zahrani site as the most polluted. The main pollution causes are correlated with wastewater discharges and industrial activities.

Keywords: Watershed, heavy metals, water quality, pollution, PCA, Mediterranean Region.

1. Introduction

The demand for water which is the key element for the survival of human beings is rising gradually. On one hand, the population growth with their associated modern way of living favors a high water consumption rate. On the other hand, scarcity in the water volume is the case due to the arising pollution problems with its adverse effects on natural water resources (Shaban, 2010).

In Lebanon, rivers, natural springs and groundwater continue to be negatively affected by sewage, various household and industrial wastes which are haphazardly discharged without any regulation or control from establishments. All water resources are susceptible to bacteriological contamination in agricultural areas (Naameh, 1995). Moreover, runoff and infiltration of residues from fertilizers and pesticides additionally contribute to their environmental degradation.

Rivers in Lebanese are affected by several sources of pollution resulting in the depopulation of numerous ones. This issue has had negative repercussions on the ecology of these causing many of them to lose their capacity for flow regulation (Comair, 2010) and CAL (1971).

The absence of land management has led to an increase in the erosion rate and a substantial decrease in the regulation of watercourses. This is because sustainable human activities are crucial to the ecological balance of watersheds (DGAC, 1999).

Lebanon has always stood out for having available water resources per capita (1350 m^3/capita/ year) than neighboring countries. This is mainly attributed to its topography which favors a moderately high precipitation rate as rain and snow (Shaban, et al., 2004). More than 2000 karstic sources were discovered at the country (MOEW, 2010). The majority are used as a supply of drinking water and for irrigation purposes in the mountainous regions. The sources are known to have similar characteristics as reduced latency, a cloudy water outlet, and maximum floods around the period of March-May (Hakim, 1986). Among these sources which feed Ibrahim River are Afka Spring (1113 km altitude) has the highest flow rate (2.8 l/s), followed by the Roueiss Spring (1800 m altitude) with a flow rate of 1.7 l/s (Hakim, 1986).

The groundwater in Lebanon is studied to a much lower extent than the surface water. The main source of formation and recharge (i.e. feeds water resources by about 60%). The

* Corresponding author e-mail: khtarawneh62@yahoo.com

source rock massifs of Lebanon consist of limestone which is characterized by fractures and karstification allowing the absorption and infiltration of water from precipitation (Nehme et. al, 2020). The water infiltrates the limestone layers and collide with impermeable rock layers of marl, clay and basalt (Ayoub et al., 2000).

In the coastal region of Lebanon, there are 19 main watersheds, 35 intermediate and 40 minor secondary watersheds (Shaban and Darwish, 2010). The interior region of Lebanon has three major watersheds including Litani River that emerges from Bekaa Plain and outlets in the sea. In other words, it can be described as an interior coastal watershed, where water is captured. Two of these basins contain important rivers which divert water outside the Lebanese territory forming trans-boundary water resources. Within the interior region, it was detected four other trans-boundary watersheds which are commonly shared with Syria and one restricted hydrographic basin in the region of Yammounah (CNRS, 2005).

It can be considered that there are three large rivers shared between Lebanon and the neighboring regions. One exists in the north and constitutes the border with Syria forming the El-Kabir River. Another one originates from the plain of Bekaa and called Orontes River (named domestically as Al-Assi River) and runs in the northern direction towards Syria. The third one referred to as Hassbani-Wazzani that shared with Palestine at the South forming a major tributary of Jordan River.

The areas of the watersheds excluding the Litani River, the Orontes River and the Hassbani-Wazzani River are relatively small. According to the MEDRUSH model, they can be described as small hydrographic basins or sub-watersheds compared to the nested Ladders. This suggests that the entire Lebanese coastal zone constitutes an ordinary watershed that spans several valleys due to the steep slope and the relatively short distance between the thresholds and the outlets (Shaban and Darwish, 2010). This hypothesis is not only limited to Lebanese territory but also extends northward to Syria and to Palestine in the south, which means that the entire area including the regional watershed that supplies water to the Mediterranean.

The surface runoff of the Al-Zahrani River is almost west of the sea. Therefore, the Al-Zahrani River has been described as a coastal watershed since it first entered the sea. According to Shaban (2003), watersheds in Lebanon have been divided into three main types. These are: major, intermediate and minor watersheds. Large watersheds are those linked to rivers with permanent water flows. Al-Zahrani River watershed is considered an important watershed. The main objectives of this study are to present a general overview of the Al-Zahrani River: its route, the limits of its watershed and land use. The present study investigates the sources of contamination of the river with its watershed using statistical methods.

2. Materials and methods

2.1. Study area

In this study, the Al-Zahrani River basin, including major and minor watersheds, which has its source at Nabeh Al-Tasseh Spring between Jarjouh and Al-Lowaizeh (governorate of Al-Nabateyyeh) at 695m a.s.l. The peripheral zones of Jarjouh, Arabsalim, KafarRumman, Habbush, HouminFawqa, Azza, Deir Al-Zahrani, Kfarwah, and Al-Hajjeh end in the Mediterranean on the coast of Al-Zahrani. Al-Zahrani River has an average annual discharge of about 202 Mm^3/year (Litani River Authority, 2012), where it collects water in a catchment area of approximately 140 km^2 (Shaban et al., 2009). The length of the river is approximately 25 km. The region of our study is located in south Lebanon and extends from the source "Nabeh El-Tasseh Spring" to the region "Al-Zahrani" (Figure 1).

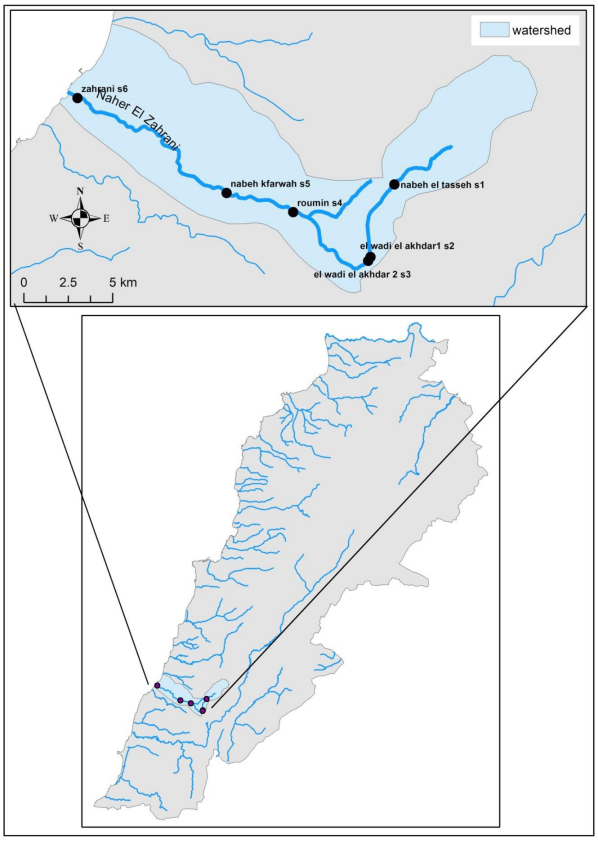

Figure 1. The study area of Al-Zahrani River Basin.

According to the physical and hydrological characteristics, two main parameters are used to characterize the Al-Zahrani watershed:

1. Dimensional parameters: which are expressed through the identification of the Al-Zahrani watershed. The dominant form has L shape. The area extends more than 140 km^2 with an altitude of the threshold or upstream more than 700 m.
2. Hydrological parameters: This includes the length of the primary stream around 25 km, and the number of outing games in the sea is 1 game with an average volume of discharged water around 202 Mm^3/year.

The sites that have been selected in this study are Nabeh El-Tasseh Spring, Wadi Al-Akhdar 1, Wadi Al-Akhdar 2, "Roumin, and NabehKfarwah. Water samples were collected from six selected sites at the outlet of the Zahrani coast. These sites represent typical source points for investigating pollution since they are situated at different geographic localities (Table 1).

Table 1. Coordinates of the sampling sites of the study area and the types of activities.

Sites	Coordinates			Types of economic activities
	Latitude	Longitude	Altitude (m)	
Nabeh El- Tasseh (S1)	33°27′08.3" N	35°31′56.9" E	690	Agriculture, irrigation and tourist area.
Wadi Al-Akhdarl (S2)	33°24′54.7" N	35°31′07.8" E	447	Agriculture and tourist area.
Wadi Al-Akhdar 2 (S3)	33°24′47.5" N	35°31′03.0" E	471	Agriculture and tourist area.
Roumin (S4)	33°26′14.2" N	35°28′17.1" E	435	Agriculture, irrigation and urban zone.
NabehKfarwah (S5)	33°26′46.9" N	35°25′50.9" E	405	Agriculture, irrigation and tourist zone.
Zahrani (S6)	33°29′35.5" N	35°20′21.1" E	12	Urban and industrial zone and outlet.

It is worth mentioning that the study area includes vegetation cover, arable lands and urban areas. The sites are considered as forest areas which are surrounded by vast agricultural areas. Contrarily, the final Zahrani site (S6) which is a coastal one is located in an urban area.

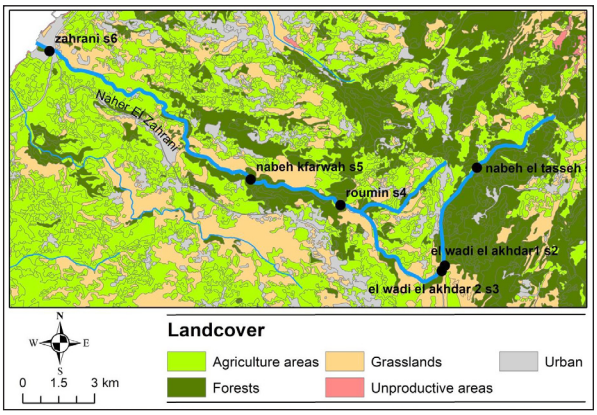

Figure 2. Land cover/ use map of Al-Zahrani River and its surrounding.

2.2. Sampling and treatment methods of water

Water samples were collected from various locations in the river basin of the mentioned sites.To assess adequately the pollution factor from each site 2000 ml were collected. Furthermore, each sample was replicated twice from each site. To conserve water samples polyethylene bottles were used. The method of sampling and collection followed the Standards Methods by WHO and Lebanese standard for drinking water (2016).

The physiochemical parameters of the water were analyzed to quantify its quality. The pH and EC of water samples were determined using a pH /ECmeter (HANNA, number type 8417 serial number 1143732). The concentration of heavy metals was determined using Atomic Absorption using the Atomic Absorption Spectrophotometric method (Spectrophotometer (RAYLEICH – MFX-210) with an air/ acetylene flame and background correction and a deuterium lamp to remove solid impurities before testing (AOAC 974.27). Ammonia, sulfate, nitrate and phosphate were determined using Spectrophotometer Jenway (Type 6300 serial number 6734. Several microbiological estimations have been conducted in this study such as total colony counts, total coliforms group, Escherichia Coli, Salmonella, Staphylococcus aureus and Clostridium Perfringens.

2.3. Statistical analysis

The Spearman correlation examines whether there is a relationship between the rank of observations for two characters X and Y, which makes it feasible to detect the existence of monotonic relationships as increasing or decreasing, and whatever their precise form if linear, exponential or power. This coefficient is appropriate when one or both variables are skewed or ordinal1 and is robust when extreme values exist.

Data analysis by principal component analysis (PCA) is performed by SPAD software. PCA is a technique for reducing the dimensionality of numerical datasets that increase interpretability and at the same time minimize information loss. It creates new uncorrelated variables that successively maximize the variances and exploratory tools for data analysis. PCA allows the reduction in the number of variables, and detection the type of structure in the relationships between variables, which amounts to ordering the variables. In this study, two potentials of this statistical tool were applied. Finally, the unsupervised learning k-means clustering was used to classify the sites.

4. Results and discussion

4.1. Physical and chemical assessment

The results obtained revealed that the temperature, pH, EC and TDS in the water samples of the underground tanks conform with the permissible limits of WHO (Table 2). The nitrate concentrations were significantly high in both sites of Wadi El Akhdar 2 and Al-Zahrani concerning the other ones. The sulfate concentrations ranged between 3 and 35 mg/L with the highest concentration detected at Al-Zahrani (42.75 mg/L). All the sites have sulfate concentrations below the maximum acceptable WHO threshold (250mg/L) indicated the absence of any sort of contamination from this parameter. The same applies to calcium and magnesium cations (Table 2). The average concentration of sodium at Nabeh El Tasseh, Kfarwah, Roumin and Zahrani surpassed the acceptable WHO standard (>150 mg/L), whereas the potassium level of Kfarwah exceeded the maximal allowable limit by 1mg/L (Table 2).

Table 2. Physical and chemical parameters of water samples.

Element	Average	Standard WHO	Situation
pH	7.59	(6.5-8.5)	Basic media:Wadi al akhdar 1&2, Zahrani
EC (µs/cm)	220	1500	Acceptable
TDS (ppm)	229	<1000	Acceptable
Nitrate (mg/L)	0.193	0.2	Only Al-Zahrani not accepted:0.67 mg/L
Sulphate (mg/L)	13.8	50	No contamination
Calcium (mg/L)	54.8	250	No contamination
Magnesium (mg/L)	18.52	50	No contamination
Sodium (mg/L)	168	150	Nabeh El Tasseh : 170 Nabehkfarwah: 160 Roumin : 190; Zahrani: 192 mg/L
Potassium (mg/L)	2	12	Roumin : 13mg/L

4.2. Microbial Assessment

The results of this study revealed a high level of microbial contamination in most of the investigated sites. Thus, Salmonella and staphylococcus aureus were highly detectable in all sites with figures significantly above the WHO threshold limits (Table 3) (Figures 3 and 4). Moreover, Nabeh El Tasseh Spring, Roumin and Zahrani zones recorded exceedingly high levels of total coliforms (>10000) (Table 3) (Figure 5). Total coliforms do not usually cause a disease, but their presence indicates contamination of the water by other more harmful bacterial microorganisms (Subin, 2013). No contamination from E.Coliand Clostridium perfringens was detected in any site.

Table 3. Microbial quality of water samples.

Sites	Coliforms totaux	EC	Salmonella	Staphylococcus aureus	Clostridium perfringens
Nabeh El Tasseh Spring	>10000	0	2000	20000	0
El Wadi Al Akhdar 1	1200	0	2200	2400	0
El Wadi Al Akhdar 2	1000	0	300	200	0
Kfarwah	1000	0	10	100	0
Roumin	>10000	0	4300	4200	0
Zahrani	>10000	0	>10000	20000	0

This study highlight on the danger of using this microbial polluted water for drinking purposes due to the associated negative impacts on human health and the environment regarding the norms of WHO.

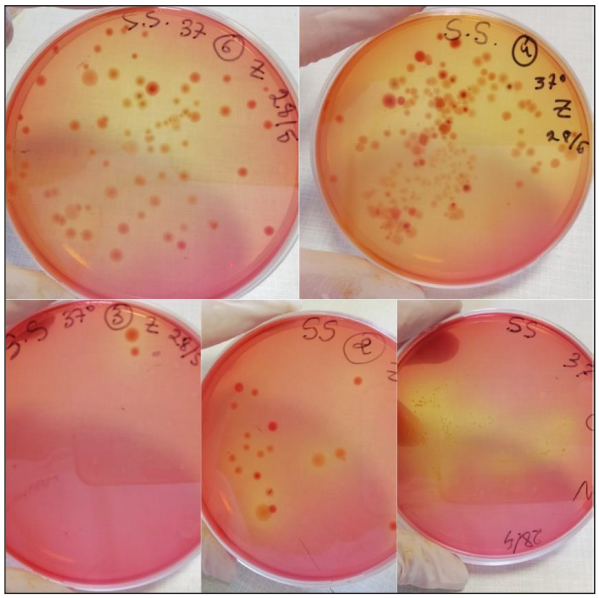

Figure 3. Photomicrograph showing Salmonella in the culture medium.

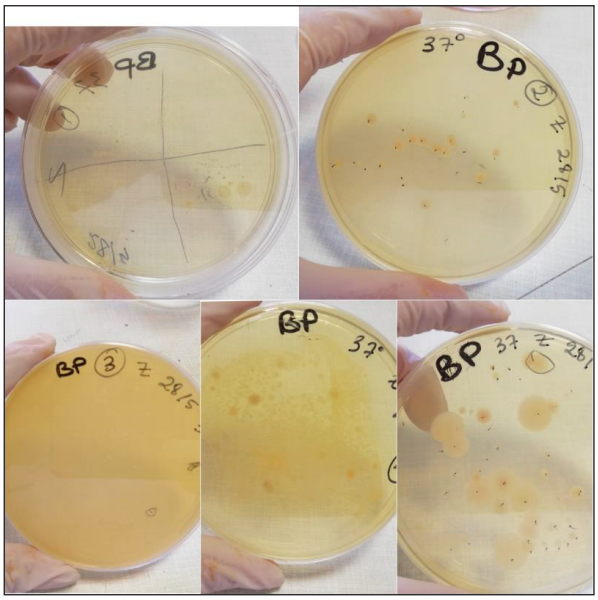

Figure 4. Photomicrograph showing Staphylococcus aureus in the culture medium.

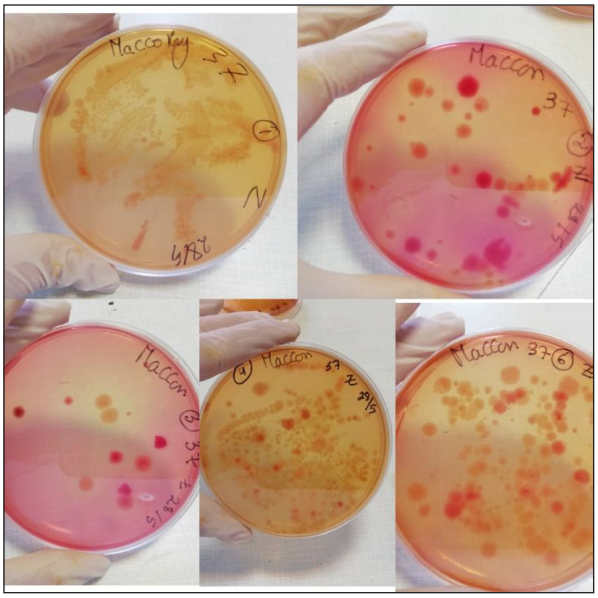

Figure 5. Photomicrograph showing total Coliforms in the culture medium.

4.3. Correlation analysis of water quality parameters

Water quality parameters were evaluated using the Spearman Correlation (Table 4). Total coliforms and Staphylococcus aureus are directly correlated with the conductivity of water and the total dissolved matter. Thus, as the concentration of dissolved solids increases, the conductivity factor mounts parallel causing an increase in the Total coliforms and Staphylococcus aureus counts. Salmonella is highly susceptible to pH mode. As the pH becomes more basic, the presence of Salmonella elevates.

Table 4. Correlation between bacteria and physicochemical parameters

	pH	EC	TDS	Nitrate	Sulfate	Ca	Mg	Na	K
ColiformesTotaux	Weak	Very strong	Very strong	Very strong	Average	Strong	Average	Strong	Average
Salmonella	strong	No Relation	No Relation	Very strong	Average	Strong	Very strong	Strong	Average
Staphylococcus aureus	Weak	Strong	Strong	Very strong	Average	Strong	Average	Strong	Weak

- Very Strong correlation: r>0.8
- Strong correlation : 0.5<r<0.8
- Average correlation : 0.2<r<0.5
- Weak correlation: 0<r<0.2

Excess of the magnesium is not harmful for kidneys, but a prolonged overdose can have a laxative and hypertensive effect (Rylander, 2014). However, an increase in magnesium concentration results in another increase of Salmonella in the water

4.4. Analysis of the Main Components

The principal component analysis is a statistical procedure that allows summarizing the information content in large data tables through a smaller set of "summary indices" that can be more easily visualized and analyzed (Mahapatra, et. al, 2012). The analysis considered on three bacteria as illustrative variables. The eigenvalue corresponds to the inertia intercepted by the factorial axis, obtained by the diagonalization of the inertia matrix, from which we choose the largest eigenvalues λi, which helps to determine the numbers of factorial axes for establishing a reduced dimension subspace. The choice of axes carrying the maximum inertia is equivalent to the construction of new variables that are associated with the axes of maximum variance. The principal axes of inertia are called the direction axes; the eigenvectors of the matrix of variances-covariance's normalized to 1. The number of axes is decided based on the Scree Plot, the Kaiser criterion, the modified Kaiser criterion and the Anderson criterion.

4.4.1. Scree plot

A scree plot is a graph that displays the proportion of variance explained and the number of principal components found. Choosing the number of principal components by eyeballing the scree plot and identifying a point at which the proportion of variance explained by each subsequent principal component drops off (Figure 6).

HISTOGRAMME DES 6 PREMIERES VALEURS PROPRES

NUMERO	VALEUR PROPRE	POURCENTAGE	POURCENTAGE CUMULE	
1	6.3508	70.56	70.56	**********
2	1.6947	18.83	89.39	**********
3	0.7511	8.35	97.74	**********
4	0.1727	1.92	99.66	***
5	0.0308	0.34	100.00	*
6	0.0000	0.00	100.00	*

Figure 6. The graph of scree plot.

It can be noticed from the scree plot in Figure 6 that the point at which the proportion of variance explained by each subsequent principal component drops off from the second principal component.

4.4.2. Kaiser's criterion

The number of axes was taken according to Kaiser's criterion modified by Sapota and Karlin. In this case, the main components were retained corresponding to the eigenvalues λ such as: $\lambda > 1 + 2\sqrt{((p-1)/(n-1))}$, where p=9 the number of active variables, and n = 6 the number of individuals. According to the Figure 6 the value of λ1 = 6.3508 and λ2 = 1.6947, therefore it is used 2 axes to collect and classify most of the datasets that are explained at 89.39% of the revealed results.

4.4.3.Variables Coordinates and Correlation Circle

The correlation circle shows an effect on the first axis since the first main component is negatively correlated with all the variables that give information to this axis (Table 5). The second component is positively correlated with pH, EC, Mg, TDS and Nitrate, and negatively with K, Na, Ca, and Sulfate.

It can be noticed on the graph of the illustrative and active variables that the bacteria Salmonella and Staphylococcus Aureus influence negatively on axis 1, so there is a correlation with these bacteria with TDS, Nitrate, Ca, Mg and sulfate. The total coliform bacteria negatively influences on axis 2, and this evidences a correlation with Na (Figure 7).

Table 5. The variables coordinate on the axes.

Elements	Axe 1	Axe 2
PH	-0.13	0.53
EC	-0.38	0.18
TDS	-0.39	0.09
Concentration of Nitrate	-0.39	0.13
Concentration of Sulfate	-0.37	- 0.08
Concentration of Ca	-0.38	- 0.19
Concentration of Mg	-0.39	0.12
Concentration of Na	-0.31	- 0.46
Concentration of K	-0.05	- 0.63

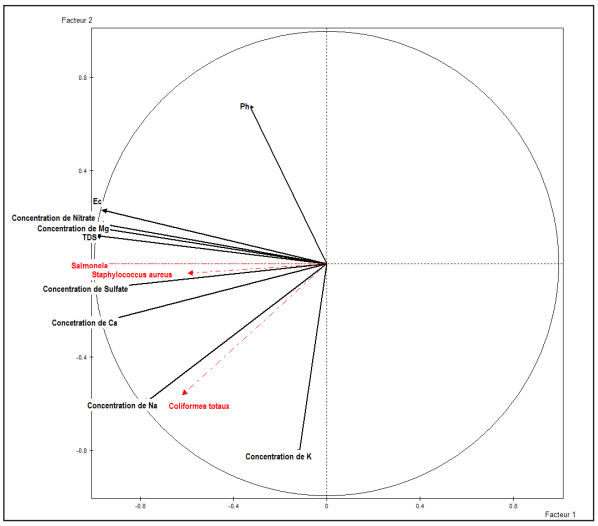

Figure 7. Correlation circle of elements.

4.4.4. Individuals Coordinate

The individuals who positively influence on axis 1 areNabehKfarwahSpring with a contribution of 6.69, Wadi Akhdar1 with a contribution of 7.46, Wadi AKhdar2 with a contribution of 5.12, while Roumin has the smallest contribution on axis 1 with 1.19. The individuals who negatively influenced on axis 1: Al-Zahrani with a large contribution of 74.86 and Roumin with a contribution of 1.19 (Figure 8).

On axis 2 theWadiAlkhdar 1, wadiAlKhdar 2 and Al-Zahrani influence positively on axis 2 with contributions from 21.79, 11.01 and 6.2, respectively, while Roumin, Nabeh el Tasseh Spring and NabehKfarwah Spring influenced negatively on axis 2 with the contributions of 56.16, 3.73 and 1.10, respectively.

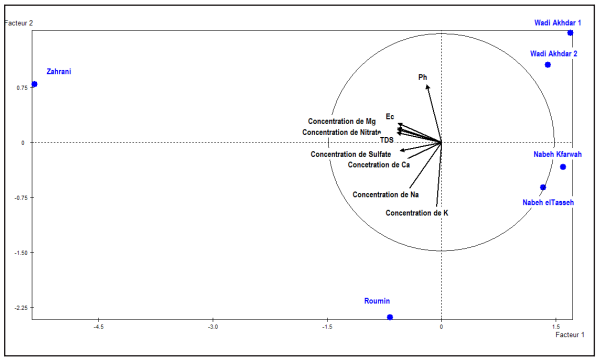

Figure 8. Graph showing the sites along with the correlation circle.

4.4.5. Clustering of sites

K-means clustering was used to classify the sites into clusters. It is the process of partitioning the entire data set into disjoint groups or clusters that are based on the pattern in the datasets, so the specific clustering criteria are optimized. It can be noticed that the sites can be classified into three clusters (Figure 9).

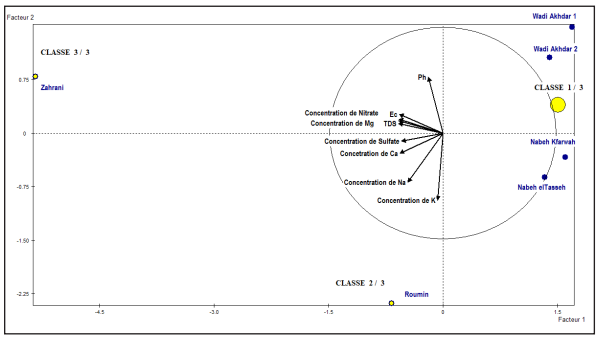

Figure 9. Classification of the sites in three clusters.

The elements which affected the clustering of the sites are: EC, TDS, Nitrate and Magnesium, the concentration of these elements in the clusters are all within WHO standards, but according to the correlation table, EC, TDS, Nitrate and Magnesium have a strong correlation with Total Coliform Bacteria, Salmonella and Staphylococcus aureu. It can be noticed Staphylococcus aureu that has a medium correlation with Mg. It can be concluded that all the sites are contaminated by three types of bacteria and that the Al-Zahrani Site is the most contaminated one since it represents the highest average for the four elements. The second cluster contains Roumin site, it is the only site that has a high

concentration of Potassium. The least affected cluster is the one having sites WadiAkhdar 2, NabehKfarwahSpring, NabehElTassehSpring, WadiAkhdar 1, since it has lower averages.

5. Conclusions and recommendations

Generally, the discharge of Al-Zahrani River is decreasing over the last few decades. This may compose an external element affecting the water balance of Al-Zahrani River and its basin. This element is believed to be the limited human impact of water consumption, as mentioned earlier in connection with the large number of villages that benefit from drinking water drawn from the source of Nabeh Al-TassehSpring by large-scale water supply network and because of unlicensed wells in the river basin.

The coastal river in Lebanon appears to be a very important element that could be useful in various active sectors of the population's life, from domestic uses to agriculture and industrial. Emphasis should be paid to the common surface and groundwater resources and their hydrological characterization in this area. The Zahrani River Basin is a typical example showing the absence of integrated studies and management approaches and lack of comprehensive datasets. This study helps to provide some of the comprehensive information necessary for the management of the Al-Zahrani River and its watershed and to highlight the hydrological and flow characteristics of the river. The results of this study are essential for the continuation of the future proposed works on the Al-Zahrani River basin. These include water strategies and policies, notably in the view of dams for the construction, and the supply canals and the abstraction of groundwater.

In this study, six sites were studied along the Al-Zahrani River. It is based on the evaluation of the physico-chemical parameters of water (T, pH, EC and TDS), anions of NO_3^-, SO_4^{2-} and PO_4^{3-}, cations of Na^+, K^+, Ca^{2+}, Mg^{2+} and metals of Cd, Cr, Fe, Cu and Zn, in addition to the evaluation of the levels of bacteria as Salmonella, Escherichia coli, Total coliforms, Clostridium perfringens and Staphylococcus aureus.

It obvious that the sites are not contaminated with Mg, Ca and PO_4^{-3}, since their concentrations are generally lower than the standards set for the WHO, while they are contaminated by Nitrate, Sulfate, Potassium, Sodium and bacteria since their concentrations are higher than the standards in certain sites. This pollution is linked to the use of fertilizers in agriculture on one hand, and a mixture with sewage on the other hand. Thus, the quality of the water is deterioratedat these sites. However, the values of heavy metals in the water were not detected. The microbiological analysis indicated that all sites are contaminated by total coliforms that have a very high contamination, which exceeds the limit acceptable by WHO. The contamination with Salmonella and Staphylococcus aureus are high, which indicates that all the sites are discharges of wastewater and agricultural waste.Onthe other hand all the sites are not contaminated by Escherichia Coli and Clostridium perfringens. The results of the physico-chemical parameters for the values of TDS, EC and pH for all sites are acceptable. The PCA of the statistical analysis showed that the Zahrani site is the most polluted.

Finally, legislation must be made to control and protect the Lebanese watersheds against pollution including water strategies, construction of wastewater treatment unit and adopting efficient irrigation approached in the agricultural areas.

References

Ayoub, G., Gannam, G., Khoury, R, Acra, A., Hamdar, B. (2000). The submarine springs in Cheka, Lebanon.

CAL, (1971). Atlas Climatique du Liban, Tome 1. Service Météorologique, Ministère des Travaux publics et Transports, Beirut, Lebanon.

Chaugan, k., Maheshwari, k., Bajpai, K., Vivek, A. (2017). Isolation and preliminary characterization of a bacteriocin-producer Bacillus strain inhibiting Methicillin resistant Staphylococcus aureus. Acta Biologica Hungarica 68(2): 208-219.

Comair, F. (2010). Water Resources in Lebanon, Documentation provided by Dr Comair, DG of Water and Electrical Resources, MOEW to ECODIT.

DGAC. (1999). Direction Générale de l"Aviation Civile, rapport annuel, Beyrouth, Liban, 32p. Etudes Géopolitiques publiées par l"Observatoired"études géopolitiques, Thème sur la Géopolitique de l"eau pour la revue.

Hakim, B. (1986). Recherches hydrologiques et hydrochimiques sur quelques karsts méditerranéens au Liban, en Syrie et au Maroc. Publications de l"Université Libanaise.

Libnor (Lebanese Standard Institution), (2016). No 464, ICS 43.060.20.

Litani River Authority, (2012). Unpublished report.

Mahapatra, S., Sahu, M., Patel, R., Panda, N. (2012). Prediction of water quality using principal component analysis, water Qual Expo Health 4: 93-104.

MOEW. (2010). Ministry of Environment. Climate change: Technical annex to Lebanon's First National Communication. Assessment of Lebanon's vulnerability to climate change. Final Report. UNDP; GEF.

National Council for Scientific Research (CNRS), (2005).

Naameh, M. (1995). "Water problems of Lebanon." National Congress on Water Strategic Studies Center. Beirut (in Arabic), 67p.

Norm of World Health Organization (WHO). 2006.

Nehme, N., Haydar, C M., Dib, A., Ajouz, N., Tarawneh, K. (2020). Quality Assessment of Groundwater in the Lower Litani Basin (LLRB), Lebanon. Geosciences Research 5(1): 1-14.

Rylander, R. (2014). Magnesium in drinking water - a case for prevention- Journal of Water and Health 12(1): 34-40.

Shaban, A. (2003). "Studying the hydrogeology of occidental Lebanon: utilization of remote sensing." Ph.D. dissertation. Bourdeaux 1 University. 202p.

Shaban, A., Bou K., Khawlie, M., Froidefond, J., Girard, M. (2004). Caractérisation des facteurs morphométriques des réseaux hydrographiques correspondant aux capacités d"infiltrations des roches au Liban occidental. Zeitschrift fur Geimorphologie 48(1): 79-94.

Shaban, A., Robinson, C., El-Baz, F. (2009). Using MODIS Images and TRMM Data to Correlate Rainfall Peaks and Water Discharges from the Lebanese Coastal Rivers. Journal of Water Resource and Protection 4: 227-236.

Shaban, A. (2010). Unpublished report report about geology and hydrology of Litani/Lebanon.

Shaban, A. and Darwich A. (2010). Mapping watershed for Sustainable Management in Lebanon. The Lebanese National Council for scientific Research (CNRS), Final Report.

Subin, H. (2013). An Assessment on the Impact of Waste Discharge on Water Quality of Priyar River Lets in Certain Selected Sites in the Northern Part of Ernakulum District in Kerala, India. International Research Journal of Environnemental Sciences 2: 8: 76-84.

JJEES

Jordan Journal of Earth and Environmental Sciences

JJEES (2021) 12 (3): 214-229
ISSN 1995-6681

Technological and provenance aspects of Umayyad and Ayyubid-Mamluk pottery from Umm as-Surab, north-eastern Jordan: A multi-method approach.

Khaled Al-Bashaireh*[1], Maen Omoush[1], Mahmoud Al-Kofahi[2], Pierre-Marie Blanc[3], Piero Gilento[4]

[1]*Department of Archaeology, Faculty of Archaeology and Anthropology, Yarmouk University, Jordan.*
[2]*Physics Department, College of Arts and Sciences, Baker University, USA.*
[3]*Archéologie du Proche-Orient hellénistique et romain (APOHR), Centre National de la Recherche Scientifique (CNRS), University Paris 1 Panthéon-Sorbonne, UMR7041, France.*
[4]*Archéologie du Proche-Orient hellénistique et romain (APOHR), University Paris 1 Panthéon-Sorbonne, UMR7041, France.*

Received 19 August 2020; Accepted 28 December 2020

Abstract

This research deals with an archaeometric study of the pottery of the Umayyad (661-750AD) and Ayyubid-Mamluk (1171-1250AD, 1250-1517 AD) periods excavated from the Umm as-Surab archaeological site (north-eastern Jordan), using a multi-analytical approach, consisting of thin-section petrography, X-ray powder diffractometry, X-ray fluorescence spectrometry and thermal gravimetry. The data collected on ceramic fabric, raw materials, and chemical and mineralogical compositions were used to shed light on the provenance of the potsherds and reconstruct various aspects of their production technology, such as production recipes (base clay versus tempers), firing temperature and atmosphere. Chemical data were statistically treated using a multivariate method. The cluster analysis was performed using the software package of SPSS version 25 and the squared Euclidean distance in the Ward's method. The results indicate that the samples were locally produced using the available raw materials: few samples have different recipes that might indicate a different source for them. The production technology was well controlled, using ferruginous calcareous and non-calcareous clays mixed with quartz and limestone, among others, non-plastic inclusions and fired at temperatures between 750 and 950°C.

Keywords: Islamic pottery, Umm as-Suarb (Umm el-Surab), Jordan, production technology, provenance, high-temperature mineral phase.

1. Introduction

The potsherds, referable to the Umayyad (661-750AD) and Ayyubid-Mamluk (1171-1250AD; 1250–1517 AD) periods, were unearthed from the upper layers of 2018 excavations in sector 2 of area A; located between the topographic units TU24 and TU29, at Umm as-Surab (or Umm el-Surab, north-eastern Jordan) (Figures 1-2). The joint archaeological excavation, carried out by Yarmouk University (Jordan) and the University of Paris 1-Panthéon Sorbonne, and the CNRS - the French Center for the Scientific Research, (France), aimed to: i) deeply understand the history of this part of the site which has witnessed continuous occupational phases from the Roman till the Medieval (Ayyubid- Mamluk) Islamic periods; and ii) compare the occupational phases of the growth and distribution of occupations of the whole site, and more generally to reflect on the settlement the dynamics of the entire region, i.e. the Jordanian Ḥawrān. The excavations highlighted the occupation phase of the Ayyubid-Mamluk periods, which is still little known and studied in other nearby sites, such as Umm el-Jimal (Osinga, 2017). The archaeometric study of some representative Umayyad and Ayyubid-Mamluk pottery samples from Umm as-Surab aims to better understand their production technology, in terms of selection and provenance of raw materials, production recipes and firing technology (atmosphere and temperature) during the Umayyad, Ayyubid and Mamluk periods. The technological features will be compared to those of Tal al-Husn (Otoom, 2019), Dohaleh (Al-Tawalbeh, 1996), Hayyan al-Mushrif (Al-Bataineh, 2003), and Al-Bediah (Al-Bataineh, 2005) to reveal the similarities (or differences) of the potters' technologies and define possible skill connections and exchanges during the same periods.

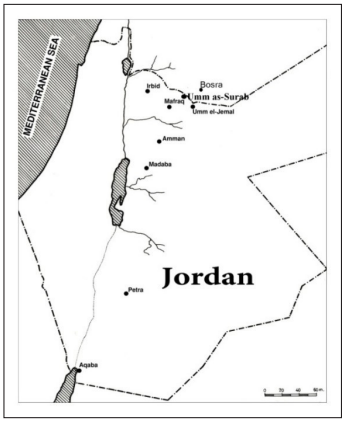

Figure 1. Geographical location map of the archaeological site of Umm as-Surab.

* Corresponding author e-mail: khaledsm@email.arizona.edu

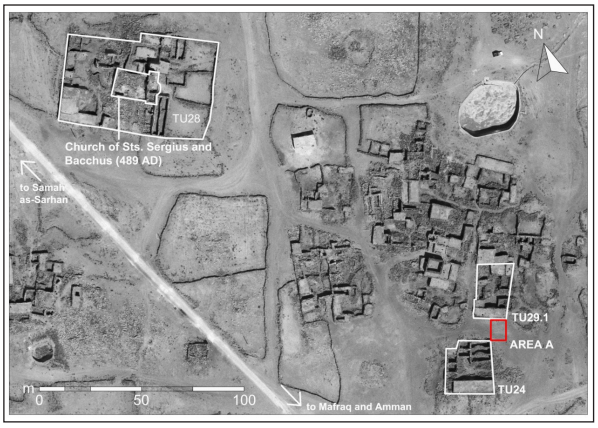

Figure 2. Aerial image showing the location of the excavated area A (red rectangle) between TU24 and TU29. (Image by Piero Gilento elaborated on an aerial image of the Spanish Archaeological Mission in Jordan, courtesy of Antonio Almagro, CSIC-Spain).

2. Umm as-Surab Archaeological Site

Umm as-Surab (MEGA Jordan n. 2806) is located in north-eastern Jordan, close to the border with Syria, and within the basaltic plateau of Harrat Ash Shaam that covers the north-eastern Jordan. It is about 13 km north-west of the city of Mafraq and about 12 km north of Umm el-Jimal, the most important archaeological site in Mafraq governorate (Figure 1).

Umm as-Surab stemmed its importance from its location close to Bosra (south-eastern Syria) and on a directory of the "Via Traiana Nova" from Bosra to Gerasa (Anastasio et al., 2016). Basalt is the main, and almost the only, building stone used in the construction of its buildings that have been dated by architectural, archaeometric and typological studies, at least to the Roman, Byzantine and Islamic periods (Parenti, 2012). However, various Nabataean and Greek inscriptions were identified and cataloged at the beginning of the 20th c. AD by the Princeton Archaeological Expedition to Syria (Butler, 1909). Lithics and inscriptions found in the surrounding areas, especially in the wadis (ephemeral river beds), showed that the area was inhabited during the Iron Age (King, 1989). Houses and churches at the site indicate that it reached its peak during the Byzantine Period (4-7th c. AD) and the rehabilitation of the church of Sts. Sergius and Bacchus into a mosque indicates its occupation during the Muslim times (King, 1983a; Gilento, 2014).

This church represents the most important and preserved structure at the site. It is an apsed church with three naves and slightly south-east oriented (Figure 2), and dated to AD 489, based on a dedicatory inscription inscribed on the lintel of the main entrance, currently not in situ (Butler, 1909).

Various archaeological researches were conducted at the site during the 1930s (Bartoccini, 1941), 1960s (Mittmann,1966), 1980s (King, 1983b), in 2002 (Bucarelli, 2007), and during the period between 2008 and 2012 (Parenti and Gilento, 2010; 2012). More recently, new projects have started in 2017 (the Jordan Hawrān Archaeological Survey), and in 2018 the joint project between Yarmouk University, Paris1-Panthéon Sorbonne and the CNRS.

3. Materials and methods

A set of 28 potsherds were selected from the pottery collection excavated from area A: the Umayyad potsherds are 6 (namely SRB19, SRB22, SRB23, SRB27, SRB32, SRB33), while the rest of the potsherds are Ayyubid-Mamluk (Figure 3).

Figure 3. Photographs of the Umm as-Surab (Jordan) studied potsherds.

Most of the Umayyad potsherds are made by wheel and have bodies with light colors of buff, pink, grey and white, which resemble the characters of the Umayyad pottery (Sauer, 1982; Merkel, 2019; Bes et al., 2020). The Ayyubid-Mamluk pottery potsherds are coil and wheel-shaped and decorated. The Hand Made Painted Potteries (HMPP) are largely dominant comprising jars, juglets and pitchers (with one handle). They are decorated in black, brown or dark red lines and geometric motives by the freestyle or freehand brushwork. The HMPP which originated as early as the late 11th century AD became most popular from the 12th c. AD to the 15th century AD and widely distributed throughout Jordan archaeological sites and other regions in the Levant (Peterson, 2018; Barfod et al., 2019; Walker, 2012). The main geometric decorations of the potsherds include spirals, either round, square or triangular lines (see samples SRB6, SRB7, SRB9, SRB10, SRB11, SRB12, and SRB14), parallel and vertical lines (SRB6, SRB9, and SRB15), triangles (SRB7,

SRB8, SRB11, and SRB12) and tilted squares (SRB9 and SRB15).

Because most of the pottery findings are fragments, having variable sizes, the selection strategy aimed at choosing the most suitable potsherds of identifiable form which would represent the Umayyad and Ayyubid-Mamluk pottery recorded in the excavated area (Table 1). The samples were classified into Umayyad and Ayyubid-Mamluk groups according to their stratigraphic layers which display phases related to the Islamic settlement in the excavated area. The selection was based also on their decoration, color, size, etc. Although many of the unearthed potsherds could not be attributed to a specific vessel form; some of them represent jars, bowls, and small juglets (Figures 3-4). The selected potsherds are mainly rims (9 potsherds), bodies (4 potsherds), bases (6 potsherds), nicks (4 potsherds), and handles (5 potsherds) (Table 1). The description of the samples is given in Table 1.

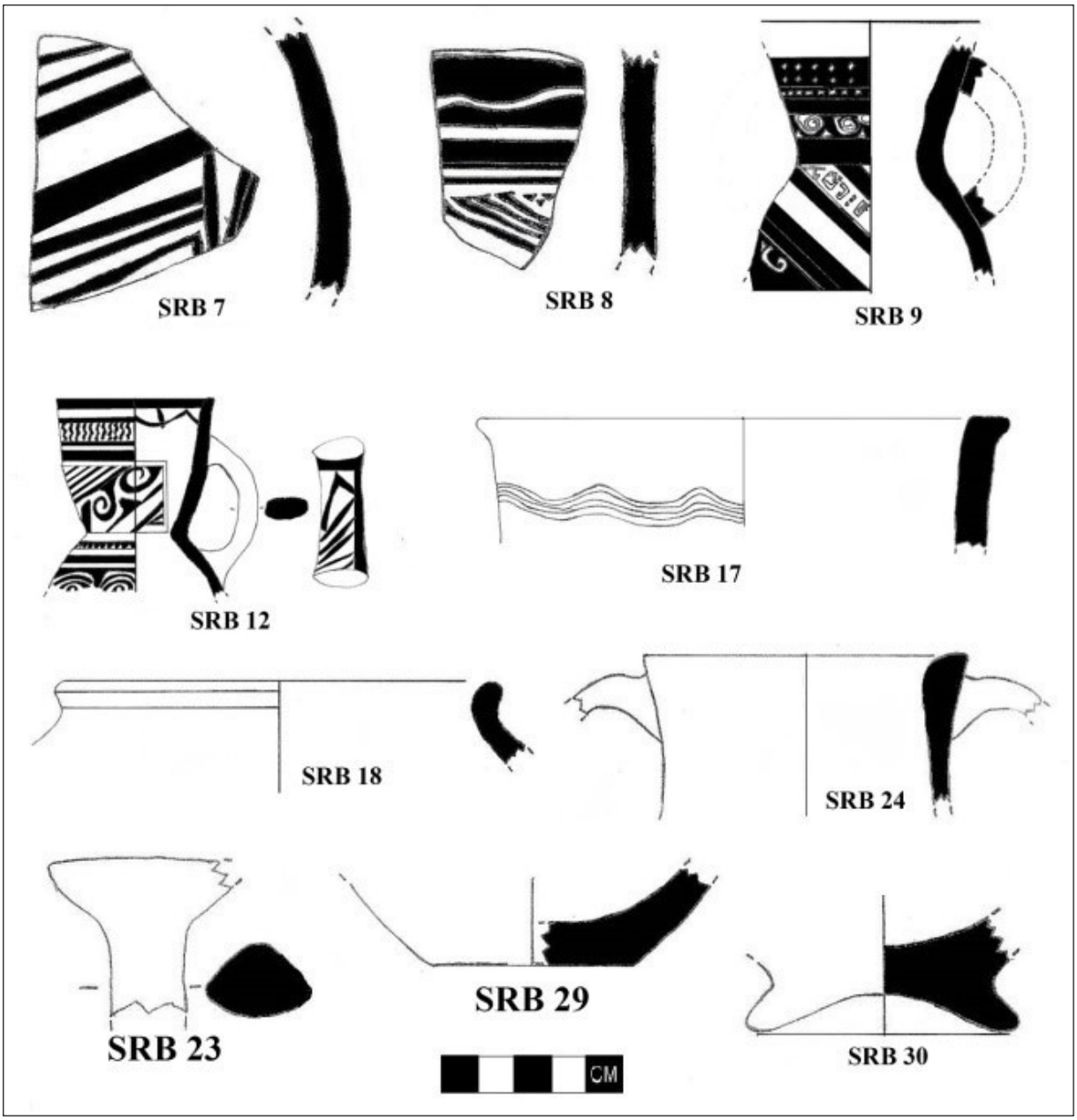

Figure 4. Decorative motives of selected potsherds from Umm as-Surab, Jordan.

All the potsherds were analyzed according to a multi-analytical approach. They were firstly brushed and washed to reduce possible contamination from the archaeological soil. A small part of each sample was used for thin section preparation and the rest was ground in an agate mortar for the mineralogical, thermal and chemical analyses by X-ray powder diffraction (XRPD), thermal gravimetry (TGA) and energy dispersive X-ray fluorescence (EDXRF).

Thin sections were prepared according to the standard procedure discussed by Camuti and McGuire (1999) and examined using a Leitz 7062 model polarizing microscope at the laboratories of the Faculty of Archeology and Anthropology at Yarmouk University. XRD patterns were obtained by the analysis of powders from whole samples using a Rigaku X-ray diffractometer with an Ultima IV (185mm) Goniometer under the following conditions:

scanning 2θ: 5–60°, Max Power 1.8KW, Cu Ka radiation (1.5418 Å), 40 kV and 40 mA energy. Thermal gravimetric analyses (TGA) were performed by Netzsch TG 209F1 Iris instrument supported by the Netzsch Proteus software. Samples were heated from 20 to 900 °C under a nitrogen atmosphere at a heat rate of 3 °C/min. The relative mass loss of the samples was recorded. The XRPD and TG analyses were carried out at the Pharmaceutical Research Center at the Jordan University of Science and Technology.

XRF analyses were carried out under vacuum using the Rigaku NEX CG spectrometer at the Physics Department, Baker University, Kansas, USA. Five grams of each sample in powder form were used to prepare 30 mm pressed pellets using a 25-ton hydraulic press (samples 9 and 18 could not produce the needed 5 grams). The spectrometer uses advanced Cartesian geometry EDXRF for rapid qualitative and quantitative elemental analysis of major and minor atomic elements. It has a simplified user interface and uses a novel software called "EZ Analysis" developed by Rigaku which reduces the need for standards and use the Fundamental Parameter Method (FPt) for the analysis of XRF spectra. This method is based on two calibrations: the MCA energy calibration, and the intensity's library calibration. In the MCA calibration, a standard containing known concentrations of Sn, Cu, and SiO2 is used to identify the relationship between the energy of the characteristic peaks and the corresponding channel numbers in the spectrum. In the intensity's library calibration, 99.99% pure standards of Cu, Sn, and SiO2, were used to identify the relationship between peak profiles (count numbers) and the corresponding concentrations of the elements based on a sensitivity library measurement intensity. The RIGAKU NEX-CG spectrometer used in the analysis uses a RIGAKU's Patented ULTRA CARRY filter method that brings the limits of detection of most metals down to 20ppb (0.02ppm) and better. The results reported are as determined by the software of the system. X-rays from the primary source in NEX CG are used to bombard four targets made of Al, Cu, Mo, and RX9 (an alloy of several metals) to allow optimal irradiation for all elements in the samples. However, because of the spectrometer limitations, sodium and the lighter elements were not measured. The spectrometer uses a 3D geometry to detect the characteristic x-rays for the elements in the sample.

4. Results and discussion

A general description of the samples is presented in Table 1. The texture varies from fine silt to very coarse sand, while the voids are rare to common and vary in size from <1 to about 3mm. The thickness of the samples varies from about 0.5cm to about 2.5cm. Five samples (SRB8, SRB17, SRB22, SRB29, SRB31) show a sandwich-like structure (Nodari et al., 2004) with a black or grey core bracketed by creamy to brown-reddish outermost portions of the body. This known feature most probably indicates firing at low heating rates in a kiln of partial opening and in a reducing atmosphere at the initial stage and oxidizing one at the end (Gosselain, 1992; Nodari et al., 2004; Maritan et al., 2006; Daszkiewicz and Maritan, 2017; De Bonis et al., 2017). However, the same result can be obtained by firing the potsherds in an oxidizing atmosphere with high amounts of organic materials (Rye, 1981; Maritan et al., 2006; Bong et al., 2008).

4.1 Petrography

A summary of the petrographic description of the samples is illustrated in Figure 5 and presented in Table 1. The petrographic examination showed similar types of inclusions, mainly consisting of quartz grains (Figure 5) and fragments of micritic limestone (Figures 5C, E, F), with some grog (Figures 5E, F) and basalt grains (Figure 5D) of sub-angular to angular boundaries, forming a well-sorted grain size distribution. The coarse grains of quartz are sub-angular to angular indicating deliberate addition after their crushing, while the rounded fine quartz grains indicate their natural presence in the clay used in manufacturing the potsherds. The wavy extinction, exhibited by quartz grains, resulted from production processes of firing or/and crushing. The reddish color of some samples resulted from hematite detected by XRD analysis, indicates firing under an oxidizing atmosphere (Rice, 1983). The elongated vesicles (channels and planar voids), partially filled with secondary calcite (Figure 5H), mainly represent secondary fissures, cavities or voids left after the burning out of organic materials like straws (Figures 5E, F). At higher magnification on the microscope, foraminifera (Figure 5 I) was noticed in several samples and a crystal of Gehlenite (Figure 5J) was noticed in sample 30, indicating a high firing temperature, see below.

Based on the amounts of quartz inclusions, the samples could be classified in four main groups: Group 1- with low quartz (5-15%) (samples SRB14, SRB23, SRB28, SRB29, SRB32); Group 2- with moderate quartz (16-30%) (samples: SRB6, SRB7, SRB8, SRB12, SRB15, SRB16, SRB24, SRB25, SRB30); Group 3- with rich quartz (31-40%) (samples: SRB9, SRB10, SRB11, SRB13, SRB17, SRB19, SRB20, SRB21, SRB26, SRB27, SRB31); Group 4- with very rich quartz (>40%) (samples: SRB18, SRB22, SRB33), (Figure 5, see table 1 for details).

According to the grain-size of the quartz inclusions, two different fabrics can be distinguished: fine-medium (Figure 5A) and fine-coarse fabrics (Figure 5B). Samples SRB7, SRB9, SRB18, SRB19, SRB24, SRB25, SRB26 and SRB30 have fine-medium fabric while the rest of the samples have fine-coarse fabric (Figure 5, see Table 1for more details). The fine-medium fabric has optically active and homogeneous groundmasses of brown to dark brown color in plane polarized Light (PPL) and light brown to dark brown in Crossed Polarized Light (XPL). The samples of the fine-coarse fabric have different percentages of the non-plastic inclusions, and in PPL their groundmass color varies from brown and dark brown to very dark brown, while in XPL it varies from light brown and brown to yellowish and reddish brown.

These results show that most of the Umayyad potsherds (4 of 6) were made of rich (SRB19, 27) to very rich (SRB 22, 33) quartz inclusions, and all of them (except SRB19) have fine-coarse fabrics. On the contrary, the Ayyubid-Mamluk samples have fine-coarse and medium-coarse fabrics and their quartz contents range between low to very rich.

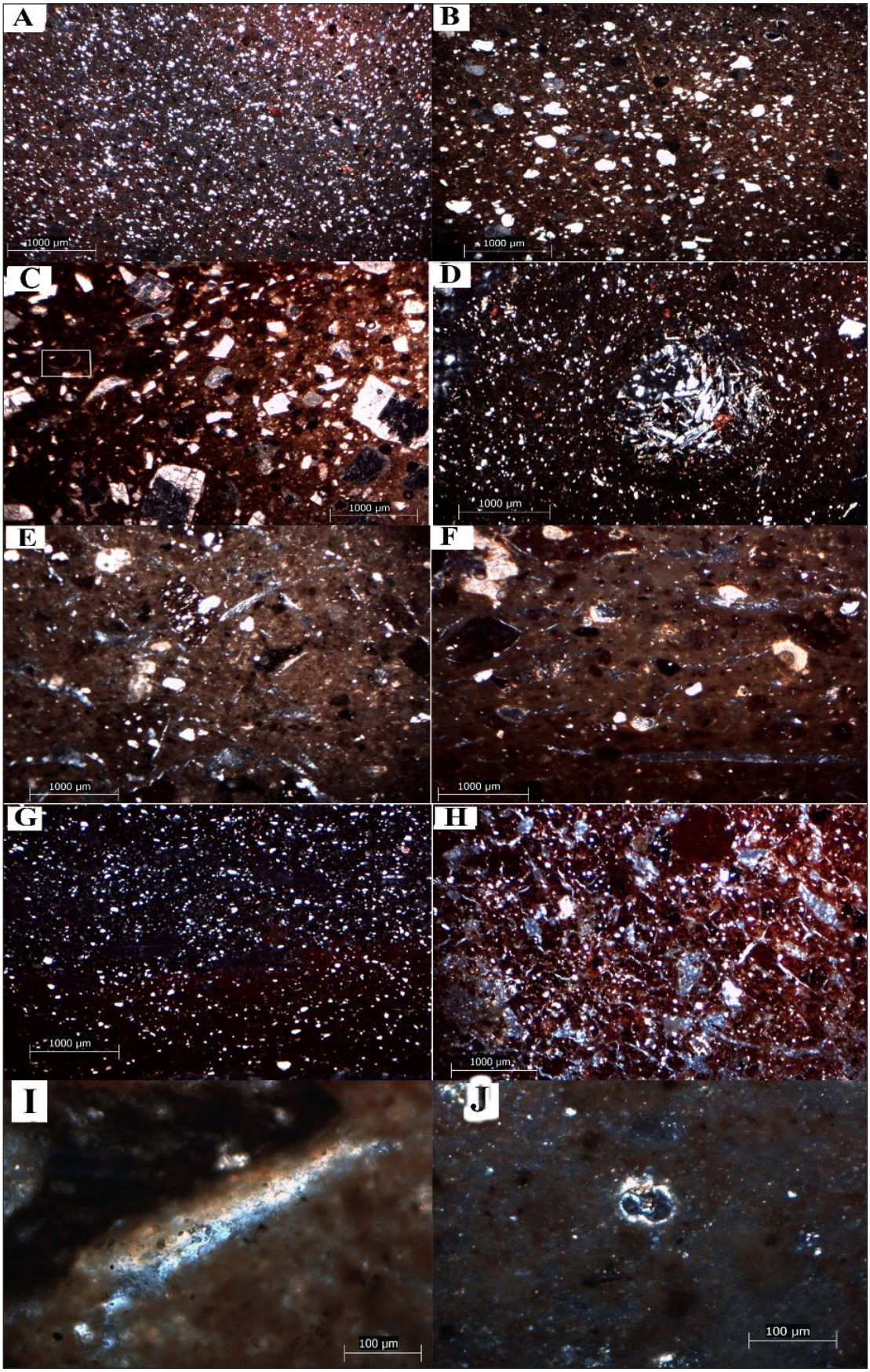

Figure 5. Photomicrographs showing different petro-fabric of the studied pottery sherds under cross-polarised light (XPL). A. Very rich in quartz (Group 4) and fine-medium fabric (SRB 18). B. Moderate in quartz (Group 2) and fine-coarse fabric (SRB 16). C. Scarce in quartz (Group 1), very coarse abundant limestone-tempered and bivalve-bearing (SRB 29). D. Rich in quartz (Group 3) and very coarse basalt-tempered (SRB 17). E. Moderate in quartz (Group 2) and grog-tempered (SRB 30). F. Scarce in quartz (Group 1) and longitudinal voids remnants of burnt straws (SRB 28). G. Very rich in quartz (Group 4) and grey core ware (SRB 22). H. Rich in quartz (Group 3) and abundant voids (SRB 9). I. Gehlenite in sample 30, and J. foraminifera in sample 32.

Table 1. Brief macroscopic and, petrographic description, parallels,firing temperature, and XRD results of the studied potsherds (Qz=quartz, G=Gehlenite, F= Feldspar, C= Calcite, H=Hematite, D= Diopside, Mj= major, Mn= minor, Tr= trace, Ab= absent, Qz. G. S.=Quartz grain size, very high > 40%, high (30-40%), moderate (15-30%), low (5-15%), scarce (3-5%), rare < 3%, very fine < 63µ, fine 63µ-0.5mm, medium 0.5-1mm, coarse 1-2mm, verycoarse > 2mm).

Sample No, Context, Period	Pottery type/shape,color, (parallels).	Minerals by XRD			Firing T.	Inclusions (abundance %)	Grain Size/shape	Notes
		Mj	Mn	Tr/ Ab				
SRB6 SRB.341.14 Ayyubid-Mamluk	Rim/body, small jar. Ware: 7.5YR (7/3) pink. Decoration 5YR(3/2) dark reddish brown.(Avissar and Stern, 2005: 114, fig. 47; Gabrieli et al., 2014: 200, fig.5, b,c,d; Barfod et al., 2019: 150, fig. 11. 5:J16-Tc-67-18).	Qz, G	F, C, H, illite	D	900- 950	Quartz (20), Gr 2, Grog (5)	Fine-coarse/ Sub rounded-Sub angular	Fine-coarse fabric, few micritic limestone granules, calcite fills boundaries of some fissures, iron oxide staining. Dark brown PPL and brown color XPL.
SRB7 SRB.320.5 Ayyubid-Mamluk	Body, jar. Ware: YR(5/3) reddish-brown. Decoration: 7.5YR(3/1) very reddish-grey. (Avissar and Stern, 2005: 114, fig. 47, Lichtenberger and Raja, 2016: 67, fig. 3).	Qz, F, C	G, H	D, Illite	800-850	Quartz (16), Gr 2 Grog (4)	Fine-medium/ Sub rounded-Sub granular Fine/ Sub rounded	Fine-medium fabric, few micritic limestone granules, calcite fills boundaries of some fissures, iron oxide staining. Very dark brown PPL and dark brown-brown XPL.
SRB8 SRB.320.13 Ayyubid-Mamluk	Rim/body, jar. Ware: 2.5YR (6/6) light red. Core: 7.5YR (5/3) brown. Decoration: 7.5YR (2.5/1) black.(Avissar and Stern, 2005: 114, fig. 47, Lichtenberger and Raja, 2016: 67, fig. 3).	Qz,	F, C, G, H	D, illite	800-850	Quartz (25), Gr 2 Micritic limestone (5), basalt (2)	Fine/Sub rounded-rounded/ Subangular Very coarse/ Sub rounded-rounded	Fine-coarse fabric, secondary calcite fills boundaries of some fissures, very coarse basalt grains, iron oxide staining. Dark brown PPL and reddish-brown XPL.
SRB9 SRB.340.9 Ayyubid-Mamluk	Neck/handle/Body, Jar or Juglet. Ware: 5YR (5/4) reddish brown. Decoration: 5YR(3/1) very gray. (LaGro, 2002: 92, fig. 3.50, Avissar and Stern, 2005: 114, fig. 47).	Qz, F	C, H	G, Illite	800-850	Quartz (32), Gr 3 Grog (3), basalt (1)	Fine/ Sub rounded-Sub angular Medium/Sub rounded	Fine-medium fabric, unimodal grain size, voids and residues of abundant organic matter of longitudinal shape (straw), iron oxide staining. Very dark brown PPL and reddish-brown XPL.
SRB10 SRB.326.20 Ayyubid-Mamluk	Body/ jar Ware 7.5YR(5/1) gray. Decoration: 2.5YR(3/1) very reddish gray.(Gabrieli et al., 2014: 200, fig.5.b, c,d, Lichtenberger and Raja, 2016:83, table 8.b).	Qz, F, C	G, H	D, illite	800-850	Quartz (30), Gr 2 Micritic limestone (20), Grog (5), Basalt (1)	Fine/Sub rounded-rounded Medium–very coarse/ Sub rounded Coarse/ Sub rounded Fine, surrounded	Fine- coarse fabric, bimodal grain size, few grog, secondary calcite fills boundaries of cracks and fissures, residues of organic matter of longitudinal shape, iron oxide staining. Dark brown-black PPL and dark brown XPL.
SRB11 SRB.376.11 Ayyubid-Mamluk	Rim/body, small jar. Ware: 10YR (7/6) yellow. Decoration: 2.5YR(4/3) reddish brown.(Avissar and Stern, 2005: 114, fig. 47, Gabrieli et al., 2014: 200, fig.5.b, c,d, Lichtenberger and Raja, 2016: 83, table 8.b; Peterson, 2017: 69, fig.4: J13-D-g-2).	Qz,	C, F, H	G, Illite	800-850	Quartz (30), Gr 2 Micritic limestone (10), Grog (5), Basalt (1)	Fine-coarse/ Sub rounded-Sub angular Fine-very coarse/ Sub rounded, Fine-coarse/ subrounded Fine, rounded	Fine-coarse fabric, bimodal grain size, fractured quartz, secondary calcite fills boundaries of some fissures and residues of organic matter of longitudinal shape(straw), iron oxide staining, some argillaceous granules. Dark brown PPL and brown XPL.
SRB12 SRB.310.2 Ayyubid-Mamluk	Neck/body, small jar. Ware: 7.5YR (7/4) pink. Decoration: 10YR(3/1) very dark grey. (LaGro, 2002: 71, fig. 3.6, Avissar and Stern, 2005: 114, fig. 47).	Qz, G, C, F	H	D, illite	850-900	Quartz (25), Gr 2 Micritic limestone (5)	Fine-coarse/ Sub rounded-Sub angular Medium/ subrounded	Fine-coarse fabric, bimodal grain size, fractured quartz, secondary calcite fills boundaries of some fissures and residues of organic matter of longitudinal shape (straw), iron oxide staining, some argillaceous granules. Brown PPL and light brown–brown XPL.
SRB13 SRB.340.4 Ayyubid-Mamluk	Body, jar. Ware: 5YR (6/6) reddish yellow. Decoration: 5YR (4/2) dark reddish gray. (Barfod et al., 2019: 149, fig. 10, 4:J16-Td-13-15).	Qz, F	G, C, H	D, Illite	800-850	Quartz (30), Gr 2 Micriticlimestone(15) Grog (5), Basalt (1)	Fine/Rounded-Sub angular Fine-coarse/ Sub rounded Coarse/sub rounded-subangular Fine, sub-rounded	Fine- coarse fabric, bimodal grain size, secondary calcite fills boundaries of some fissures, iron oxide staining, residues of organic matter of longitudinal shape (straw). Dark brown PPL and brown XPL.

Continue Table 1

Sample No, Context, Period	Pottery type/shape,color, (parallels).	Minerals by XRD			Firing T.	Inclusions (abundance %)	Grain Size/shape	Notes
		Mj	Mn	Tr/ Ab				
SRB14 SRB.320.17 Ayyubid-Mamluk	Body, jar. Ware: 10YR (7/3) pale brown. Decoration: 5YR(2.5/6) dark reddish brown.(Avissar and Stern, 2005: 114, fig. 47 Gabrieli et al., 2014: 208, fig. 9a,b; Barfod et al., 2019: 148: fig. 8, J16-Tc-53-2).	Qz, C, G, F	H	D, illite	900-950	Quartz (12), Gr 1 Micritic limestone(13), Grog (10)	Fine-coarse/ Sub rounded-Subangular medium-coarse/ Sub rounded coarse/sub-rounded	Fine-coarse fabric, bimodal grain size, secondary calcite fills boundaries of fissures, iron oxide staining. Brown PPL and light brown XPL.
SRB15 SRB.340.3 Ayyubid-Mamluk	Neck/body, jar. Ware: 7.5 YR (6/6) reddish-yellow. Decoration: 5YR(2.5/1) black. (Avissar and Stern, 2005: 89, fig. 38).	Qz, C	G, F, H	D, Illite	800-850	Quartz (20), Gr 2 Micriticlimestone(15) Grog (5), basalt (1)	Fine/ Rounded- Subangular Fine-coarse/rounded Fine /rounded	Fine-coarse fabric, bimodal grain size, few basalt, grog and argillaceous granules, secondary calcite fills boundaries of some fissures and residues of organic matter of longitudinal shape, iron oxide staining. Dark brown PPL and light brown-brown XPL.
SRB16 SRB.327.18 Ayyubid-Mamluk	Rim/body, jar. Ware: 7.5YR (7/6) reddish yellow. (McPhillips and Walmsley, 2007: 152, fig. 13:1).	Qz, G	F, C, H	D, Illite	850-900	Quartz (20), Gr 2 Micritic limestone (15) Grog (10)	Fine-coarse/ Sub rounded-Subangular Coarse/ Subangular- Sub rounded Fine/rounded	Fine-coarse fabric, bimodal grain size, wavy extinction and fractured quartz, secondary calcite fills boundaries of some fissures, iron oxide staining. Light brown- yellowish-brown PPL and brown XPL.
SRB17 SRB.341.19 Ayyubid-Mamluk	Rim/neck/body, crater (basin). Ware: 2.5YR (6/6) light red. Core: 10YR (5/1) gray.(McPhillips and Walmsley, 2007: 154, fig. 14:3).	Qz	F, H, C	G, Illite	<800	Quartz (40), Gr 3 Basalt (10)	Fine/ Sub rounded-Subangular Very coarse/ Subangular-angular	Fine-coarse fabric, bimodal grain size, wavy extinction and fractured quartz, secondary calcite fills boundaries of some fissures, argillaceous grains, iron oxide staining. Brown PPL and dark brown XPL.
SRB18 SRB.301.6 Ayyubid-Mamluk	Rim/neck/body, jar. Ware: 2.5YR (5/6) red.	Qz,	F, C, H	G, illite	800-850	Quartz (50), Gr 4 Basalt (1)	Fine-coarse/ Sub rounded-Granual Fine rounded	Fine-medium fabric, unimodal grain size, wavy extinction and fractured quartz, secondary calcite fills boundaries of some fissures and residues of organic matter of longitudinal shape (straw), iron oxide staining, two clays brown and grey. Dark brown PPL and brown-reddish brown XPL.
SRB19 SRB.376.4 Umayyad	Rim/neck, bowl. Ware: 5YR (5/4) reddish brown. (McNicoll et al., 1982: 168, plate 144.5, Sauer and Herr, 2012: 518. Fig.4:4:13).	Qz	C, F, H	G, illite	800-850	Quartz(40), Gr 3 Micriticlimestone(5) Grog (5), basalt (1)	Fine/ Sub rounded-rounded Fine/ sub rounded Fine/ subrounded	Fine–medium fabric, fine grog and basalt, unimodal grain size, voids and residues of organic matter of longitudinal shape, iron oxide staining. Brown-orange brown PPL and light brown-brown XPL.
SRB20 SRB.368.1 Ayyubid-Mamluk	Rim/body, jar. Ware 7.5YR(7/8) reddish yellow. (Sauer, 1982. 334: fig.7).	Qz, F	G, C,	H, D, Illite	800-850	Quartz (30), Gr 2 Micriticlimestone(8) Grog (2)	Fine-coarse/ Sub rounded-Subangular Sub rounded Medium/subrounded	Fine-coarse fabric, fractured quartz, bimodal grain size, few fine grog, bad mixing, iron oxide staining, secondary calcite fills boundaries of some fissures. Dark brown-grey PPL and greyish brown XPL.

Continue Table 1

Sample No, Context, Period	Pottery type/shape,color, (parallels).	Minerals by XRD			Firing T.	Inclusions (abundance %)	Grain Size/shape	Notes
		Mj	Mn	Tr/ Ab				
SRB21 SRB.317.6 Ayyubid-Mamluk	Rim/body, jar. Ware: 5YR (7/4) pink. (McPhillips and Walmsley, 2007: 154, fig. 15:3).	Qz	F, C, G,	H, D, illite	800-850	Quartz (40%) Gr 3	Fine-coarse/ Sub rounded-sub angular	Fine-coarse fabric, bimodal grain size, fractured quartz, few fine grog, secondary calcite fills boundaries of some fissures and residues of organic matter of longitudinal shape (straw), iron oxide staining. Dark brown PPL and brown XPL.
SRB22 SRB.374.10 Umayyad	Loop handle, jar . Ware: 10YR (5/8) red. Core: 2.5Y (4/1) dark gray.	Qz	C, F, H	G, Illite	<800	Quartz (40-50%) Gr 4 Grog (1), basalt (1)	Fine-coarse/ Sub rounded-Sub angular Fine sub-rounded	Fine-coarse fabric, bimodal grain size, fractured quartz, few fine grog and basalt, secondary calcite fills boundaries of fissures and residues of organic matter of longitudinal shape (straw), iron oxide staining. Two parts, lower: dark reddish-brown and upper: greyish brown PPL; and lower: reddish-brown – dark red; and upper dark grey XPL.
SRB23 SRB.376.23 Umayyad	Loop handle, jar. Ware 2.5YR (5/6) red. Outside: YR(4/3) reddish brown. (Almagro et al., 2000: 449, fig.15: 5).	C	Qz,	F, H, G, illite	<800	Quartz (10), Gr 1 Limestone (40)	Fine/ rounded Very coarse/angular Sub angular- angular	Fine-very coarse fabric, bimodal grain size, fractured quartz, secondary calcite fills boundaries of fissures and residues of organic matter of longitudinal shape (straw), iron oxide staining. Light brown- light Orange-brown PPL and brown – light brown XPL.
SRB24 SRB.320.15 Ayyubid-Mamluk	Rim/handle/Body, jar. Ware: 7.5YR (6/3) light brown. (McPhillips and Walmsley, 2007: 151, fig. 11:3).	Qz, G, F, C	H, Illite	D	900-950	Quartz (25), Gr 2 Basalt (1)	Fine/ Sub rounded Fine-rounded	Fine-medium fabric, fractured quartz, few plagioclase grains, abundant fissures and cracks, iron oxide staining. Dark brown PPL and brown XPL.
SRB25 SRB.314.9 Ayyubid-Mamluk	Handle, jar. Ware: 2.5YR (6/6) dark yellow. (Barfod et al., 2019: 151, fig. 14 a-b, 7: J16-Uc-1-13).	Qz, G, C, F	H, Illite	D	900-950	Quartz (20), Gr 2 Micritic limestone (5)	Fine-medium/ Sub rounded-rounded Fine-medium/ Sub rounded	Fine-medium fabric, unimodal grain size, few basalt and grog grains, secondary calcite fills boundaries of voids and residues of organic matter of longitudinal shape (straws), iron oxide staining. Orange-brown PPL and light brown-light reddish-brown XPL.
SRB26 SRB.341.2 Ayyubid-Mamluk	Handle, jar. Ware: 2.5YR (6/8) light red. (McPhillips and Walmsley, 2007: 154, fig. 14:2).	Qz	C	F, H,G, illite	<800	Quartz (40), Gr 3 Micritic limestone (5), grog (1)	Fine-medium/ Sub rounded Fine-medium/ Sub rounded	Fine-medium fabric, bimodal grain size, wavy extinction and highly fractured quartz, secondary calcite fills boundaries of voids. Dark brown-reddish brown PPL and brown XPL.
SRB27 SRB.372.10 Umayyad	Handle/rim, cooking pot. Ware: 2.5YR (4/1) dark gray. (Almagro et al., 2000: 449, fig.15:1).	Qz		C, F, H, G, Illite	<800	Quartz (40), Gr 3 Micritic limestone (5), grog (1)	Fine-coarse/ Sub rounded-Sub angular Medium–coarse/Sub rounded	Fine-coarse fabric, bimodal grain size, wavy extinction and highly fractured quartz, fine-grained basalt, iron oxide staining. Very dark brown-grey PPL and dark grey- black XPL.

Continue Table 1

Sample No, Context, Period	Pottery type/shape,color, (parallels).	Minerals by XRD			Firing T.	Inclusions (abundance %)	Grain Size/shape	Notes
		Mj	Mn	Tr/ Ab				
SRB28 SRB.340.17 Ayyubid-Mamluk	Base/ body, plate. Ware: 10YR(7/4) very pale brown. Decoration 7.5YR (4/2) brown.(Peterson, 2018: 143, fig.5).	G, Qz, C, F	H, illite	D	900-950	Quartz (15), Gr 1 Micritic limestone (12) Grog (15), Basalt (1)	Fine/ Sub rounded-Subangular Fine-coarse/ Sub rounded Fine-very coarse/ Sub rounded Fine, Sub-rounded	Fine-coarse fabric, bimodal grain size, secondary calcite fills boundaries of cracks, voids, and residues of organic matter of longitudinal shape (straws), iron oxide staining. Dark brown PPL and light brown - dark brown XPL.
SRB29 SRB.340.2 Ayyubid-Mamluk	Base/body, bowl. Ware: 7.5YR (7/4) pink Core: 2.5YR (4/1) dark gray.	C	Qz,	F, H, G, illite	<800	Quartz (10), Gr 1 Primary calcite (35), Basalt (1)	Fine-coarse/ Sub rounded Medium – very coarse/ Sub angular- angular. Fine, sub-angular	Fine-very coarse fabric, bimodal grain size, few plagioclase, bivalve fossils, secondary calcite fills boundaries of void, iron oxide staining. Very dark brown-black PPL and brown- dark brown XPL.
SRB30 SRB.341.17 Ayyubid-Mamluk	Base/body, plate. Ware: 5YR (7/4) pink.	Qz, G, C, F	H, Illite	D	900-950	Quartz (18), Gr 2 Micritic limestone (5) Grog (7)	Fine –frequently medium/ Sub rounded-rounded Fine- frequently medium/ Sub rounded-Sub angular Medium/ Sub angular-angular	Fine-medium fabric, bimodal grain size, secondary calcite fills boundaries of cracks and fissures, residues of organic matter of longitudinal shape, (the presence of two types of clay indicates bad type), iron oxide staining. Light brown- yellowish-brown PPL and light brown - brown XPL.
SRB31 SRB.320.9 Ayyubid-Mamluk	Base, bowl. Ware: 2.5YR (6/6) light red. Core: 2.5YR (4/1) dark gray. (Bagatti, 1947: figs 53: 5,10. Tel abu-Gourdan; Franken and Kalsbeek, 1975: 166-167, figs. 50, 51).	Qz, C, G	F, H	D, illite	850-900	Quartz (25), Gr 2 Micritic limestone (5), basalt (1)	Fine-coarse/ Sub rounded-sub angular Fine- very coarse/ Sub rounded –rounded. Fine, rounded	Fine-coarse fabric, bimodal grains size, fractured quartz, few plagioclase and basalt grains, few grog, secondary calcite fills boundaries of cracks and fissures, residues of organic matter of longitudinal shape, iron oxide staining. Dark brown PPL and dark reddish-brown XPL.
SRB32 SRB.340.3 Umayyad	Base/body, bowl. Ware: 5YR (5/4) reddish brown. Decoration: 10YR (4/2) light red	Qz, G, C, F	H, Illite	D	900-950	Quartz (7), Gr 1 Micritic limestone (16) Grog (1)	Fine-medium/Sub rounded-Subangular Fine- coarse /Subangular-Sub rounded	Fine-coarse fabric, bimodal grain size, fractured quartz, secondary calcite fills boundaries of cracks, few grog, voids and residues of organic matter of longitudinal shape, iron oxide staining. Brown – yellowish-brown PPL and light brown- dark brown XPL.
SRB33 SRB.374.1 Umayyad	Base/body, plate. Ware: 2.5YR (4/2) light red	Qz	F, C	H, G, illite	<800	Quartz (50), Gr 4 Micritic limestone (2)	Fine- coarse/ Sub rounded-Subangular	Fine-coarse fabric, bimodal grain size, wavy extinction and highly fractured quartz, fine-grained basalt, iron oxide staining. Dark brown PPL and dark reddish brown XPL.

4.2 Chemical analysis

The XRF results are presented in Table 2. The potsherds are distinguished by very high variability in the concentration of silica, ranging between 21% (sample SRB29) and 70.5% (sample SRB27), and that of calcium oxide, which is quite low (1.76-4.49%) in few potsherds, and higher in others ranging between 7.3% (sample SBR19) and 64% (sample SBR29). The disparity of the calcium oxide contents is displayed in the ternary system of Figure 6 where the values are mainly scattered toward the quartz–Calcite border line within the silica - diopside – gehlenite, and silica (quartz) - gehlenite - anorthite areas, except two samples SRB23 and SRB29, indicating the use of mostly calcareous raw materials in the manufacture of the samples.

The results show that the Umayyad potters mainly used low calcium and high silica raw materials in the production of most of their potsherds (four out of six); while to the contrary, Ayyubid-Mamluk potters used high calcium raw materials in the production of most of their potsherds. These results agree with the function of the studied samples and their decorations. Calcium-rich materials increase the workability of the object and produce better quality for bright surface and modifications (Noll 1991; Emami et al., 2008).

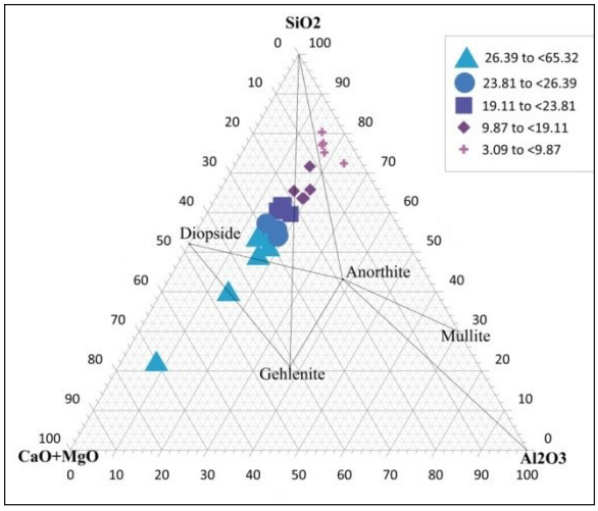

Figure 6. CaO+MgO-SiO_2-Al_2O_3 ternary diagram showing the distribution of the studied samples within sub-triangles(the values in the index are of the CaO concentrations).

Table 3. Chemical analysis (in %) of major and minor elements determined by XRF, LOI stands for loss of ignition).

	SiO_2	CaO	Fe_2O_3	MgO	Al_2O_3	K_2O	P_2O_5	TiO_2	MnO	Cr_2O_3	Co_2O_3	V_2O_5	NiO	ZnO	LOI 1050 (550)°C
SRB6	48.7	23.8	5.6	2.0	15.0	2.5	0.49	1.02	0.09	0.03	0.02	0.02	0.01	0.01	4.51(1.20)
SRB 7	56.1	13.2	5.6	2.2	16.7	3.6	0.87	1.04	0.07	0.03	0.02	0.03	0.01	0.01	2.10(0.50)
SRB8	55.4	12.3	8.2	3.2	13.7	3.1	0.75	1.37	0.16	0.03	0.03	0.03	0.01	0.02	5.36(1.10)
SRB10	53.6	16.6	7.9	3.2	13.1	2.5	0.65	1.27	0.19	0.03	0.03	0.03	0.01	0.01	4.65(3.80)
SRB11	52.3	17.7	7.5	3.5	12.9	3.2	0.55	1.16	0.16	0.02	0.03	0.02	0.01	0.01	7.39(3.30)
SRB12	49.4	22.1	5.9	1.7	15.5	3.2	0.44	1.00	0.07	0.02	0.02	0.02	0.01	0.01	5.60(1.10)
SRB13	53.0	15.9	8.2	3.2	13.5	2.8	0.79	1.36	0.20	0.03	0.03	0.03	0.01	0.01	4.49(1.10)
SRB 14	43.8	28.8	5.9	1.6	14.6	2.7	0.43	0.95	0.10	0.02	0.02	0.01	0.01	0.01	10.84(6.80)
SRB 15	52.5	18.5	7.2	2.8	13.3	2.7	0.79	1.25	0.13	0.03	0.03	0.03	0.01	0.02	5.87(3.10)
SRB 16	53.8	18.5	4.4	1.3	16.6	2.4	0.69	1.16	0.04	0.02	0.01	0.02	0.01	0.01	5.21(3.40)
SRB 17	57.6	1.76	13.3	1.3	18.8	2.9	0.67	2.67	0.21	0.03	0.04	0.06	0.01	0.02	3.4(2.85)
SRB 19	60.2	7.3	9.4	2.6	13.9	3.0	0.55	2.07	0.18	0.03	0.03	0.04	0.01	0.02	6.06(2.60)
SRB20	60.8	12.2	3.3	1.3	18.1	1.9	0.41	1.44	0.03	0.02	0.01	0.03	0.00	0.01	4.34(2.00)
SRB21	57.7	14.1	4.5	1.4	17.5	2.1	0.54	1.24	0.06	0.03	0.02	0.03	0.01	0.01	4.72(1.40)
SRB22	66.1	3.47	8.0	2.0	14.2	2.7	0.74	1.71	0.19	0.03	0.03	0.04	0.01	0.02	3.96(1.20)
SRB23	35.8	39.4	6.5	1.0	12.9	2.5	0.23	0.97	0.08	0.03	0.02	0.02	0.01	0.02	25.62(3.10)
SRB24	47.9	25.0	6.6	3.5	12.4	2.1	0.46	1.01	0.13	0.02	0.03	0.02	0.01	0.01	5.22(3.50)
SRB25	47.4	22.5	6.3	1.5	16.2	3.6	0.51	0.97	0.08	0.02	0.03	0.02	0.01	0.01	6.47(4.40)
SRB26	68.0	4.59	4.4	1.5	16.3	2.6	0.39	1.52	0.06	0.03	0.02	0.02	0.01	0.01	2.36(1.60)
SRB27	70.5	3.86	4.6	1.5	15.1	2.1	0.29	1.46	0.07	0.03	0.02	0.03	0.01	0.01	1.89(0.90)
SRB28	45.9	25.7	5.9	1.8	15.7	1.9	1.11	0.97	0.07	0.03	0.02	0.02	0.01	0.02	6.38(2.00)
SRB29	21.0	64.0	2.7	1.3	7.06	2.5	0.24	0.41	0.04	0.01	0.01	0.01	0.01	0.01	36.12(1.90)
SRB30	48.2	24.2	5.7	2.2	14.7	2.7	0.35	1.02	0.06	0.02	0.02	0.02	0.01	0.01	6.22(2.90)
SRB31	49.1	21.5	7.1	2.9	12.2	3.9	0.51	1.15	0.16	0.02	0.02	0.03	0.01	0.01	9.87(9.60)
SRB32	48.2	22.6	6.2	2.2	16.5	2.0	0.60	0.94	0.09	0.02	0.02	0.02	0.01	0.01	4.83(2.60)
SRB33	69.5	2.66	9.3	1.4	12.9	1.1	0.29	1.99	0.25	0.04	0.04	0.04	0.01	0.01	0.70(0.61)

Al_2O_3 concentrations that range between 12.2% (sample SRB 31) and 18.8% (sample SRB 17); (sample 29 is an exception (7.06%); most probably reflect the samples' content of clays and feldspar, which was detected by XRD analysis. Fe_2O_3 concentrations vary from 2.74% (sample SRB 29) to 13.3% (sample SRB 17); the high values most probably reflect the presence of iron content in the form of hematite (detected in XRD analysis) in the tempers or clays derived from the volcanic rock minerals spread in the Umm as-Surab area. The pyroxene and other volcanic rock minerals and dolomite present in the clays or tempers are possible reasons for the concentration of MgO, that ranges between 0.961% (sample SRB 23) and 3.51% (sample SRB 11). K_2O concentrations are in a moderate range between 1.12% (sample SRB 33) and 3.84% (sample SRB 31), the higher concentrations might be related to a high content of K-feldspar and clay minerals (Iordanidis et al., 2009; İssi et al., 2011). These alkalis may act as fluxes during firing, promoting sintering and vitrification. Other oxides concentrations could be seen in Table 2.

It could be inferred that potters were conscious of producing potsherds that will not withstand high temperatures. The potsherds are low refractory since all the sums of the concentrations of K_2O, Fe_2O_3, CaO, MgO and TiO_2 oxides in all the samples are more than 9% (Ravisankar et al., 2014).

The first group of the multivariate analysis shown in (Figure 7) and characterized by CaO ≥ 21.1% and SiO2 ≤ 49.4% contents, consists of 11 potsherds; while the second group consists of 15 potsherds characterized by CaO ≤ 18.5% and SiO2 ≥ 52.3% contents. The results show that all the 4 plates and 6 jars (in addition to 1 bowl) are included in the first group, while 11 jars (in addition to 2 bowls, 1 pot, 1 crater) are included in the second group. The Umayyad plate and one of the two jars belong to the first group, while the two Umayyad bowls, the pot and the second jar belong to the second group. The Ayyubid-Mamluk jars are included in both groups; the three plates and one bowl belong to the 1st group, while the crater belongs to the 2nd group.

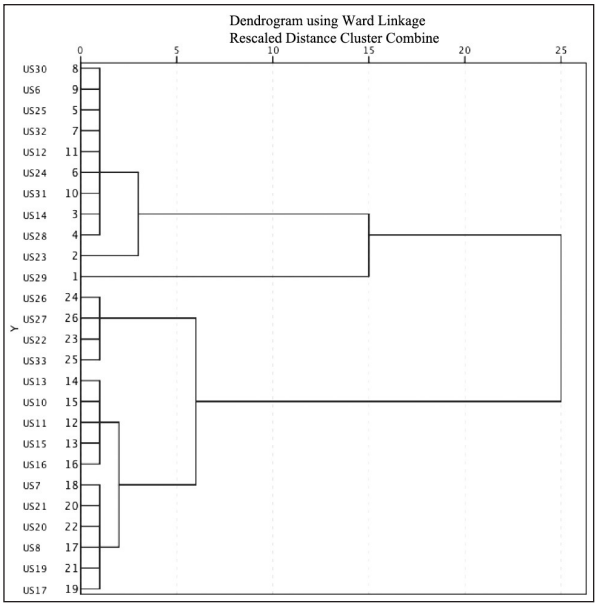

Figure 7. Pottery sample dendrogram based on Ward's method and squared Euclideandistance(The cluster analysis was performed using the software package of SPSS version 25 and the squared Euclidean distance in the Ward's method).

4.3 XRD results

The results of the XRD analysis generally agree with the petrographic and chemical analyses. The main mineral phases recurring in most of the samples are calcite, quartz, gehlenite, feldspar, diopside and hematite (Figure 8). The iron mineral of hematite found in most of the samples indicate an oxidizing firing atmosphere of the samples (Van der Weerd et al., 2004).

Quartz diffraction peaks are intense in all the samples, except in samples SRB23 and SRB29 in which they are moderate (Figure 8: SRB23). The diffraction peaks of gehlenite, calcite and feldspar are more variable; and therefore, more useful in the classification of the samples into four groups (A-D) as shown in Figure 8.

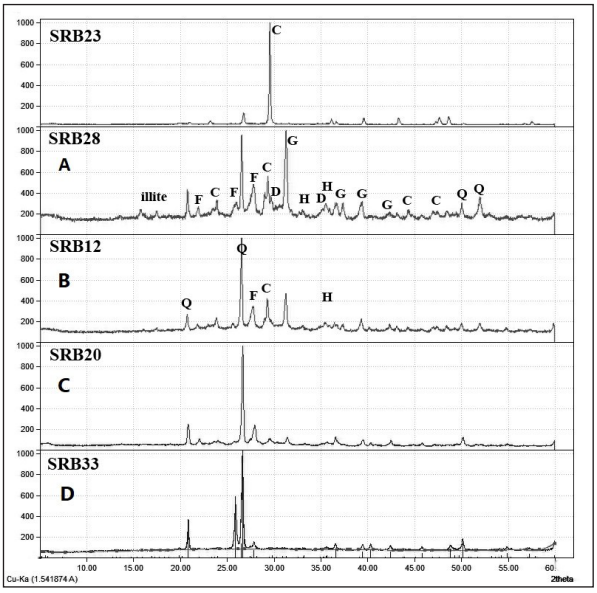

Figure 8. XRD patterns of pottery samples from Umm as-Surab, Jordan showing the samples' difference in their content of minerals. (Q= quartz, F= feldspar, C= calcite, G= gehlenite, H= Hematite, D = diopside).

Gehlenite ($Ca_2Al_2SiO_7$) is a sorosilicate mineral of the melilite family and forms in pottery during the firing process at temperatures in the range of 800-950°C from the reaction between silica and alumina, and the lime of carbonate phases (Maggetti, 1982; Noll, 1991; Duminuco et al., 1998; Cultrone et al., 2001). The pyroxene mineral diopside ($CaMgSi_2O_6$) starts to form at a temperature around 900°C (Maritan et al., 2006; Grammatikakis et al., 2019). Therefore, in group A, the high amount of gehlenite and low amount of diopside (see Figure 8: SRB28) indicate that samples (SRB6, SRB14, SRB24, SRB25, SRB28, SRB30, SRB32) were fired at temperatures around the upper limit of the above-mentioned temperature range (900-950°C). The XRD results are supported by the microscopic examination that observed at high magnification a gehlenite crystal at the carbonate-silicate interface in sample 30 (Figure 5I). The medium amount of gehlenite and absence of diopside in the samples of group B (SRB12, SRB16, SRB31) (Figure 8: SRB12) indicates a firing temperature between 850 and 900°C. The low-intensity peaks of gehlenite in the samples of group C (SRB7, SRB8, SRB9, SRB10, SRB11, SRB13, SRB15, SRB18, SRB19, SRB20, SRB21) (Figure 8: SRB20) indicates a firing temperature between 800 and 850°C, while the very low-intensity peaks (or absence) of gehlenite in the samples of group D (SRB17, SRB22, SRB23, SRB26,

SRB27, SRB29, SRB33) (Figure 8, SRB33) indicates a firing temperature around or below 800°C. It is worth noting that the intensity of Gehlenite peaks and the concentration of CaO have a positive relationship (Table 2), indicating more free CaO at a higher temperature to react with silica and alumina.

The calcite peaks indicate an incomplete decomposition, which starts at around 650°C and ends at around 900-1100°C, depending on the calcite grain size and the kiln's heating rate (Trindade et al., 2009). Therefore, the calcareous clay, limestone coarse inclusions and/or rapid heating might be the probable reasons for the $CaCO_3$ presence in several samples although fired at temperatures up to 950°C. The two samples (SRB23 and SRB29) of group D (Figure 8: SRB23) have very high-intensity peaks of calcite, because of their content of high calcareous (marl) clay and very coarse limestone inclusions.

The XRD results show that 5 of the 6 Umayyad potsherds (SRB19, SRB22, SRB23, SRB27, SRB33) belong to the D-group, i.e. were fired at temperatures below 800°C, while the sixth sample SRB32 (A-group), was fired at a temperature between 900-950°C. The function of these samples does not imply the resistance to thermal shocks. However, the cooking pot SRB27 has very low CaO content and high amount of inclusions which increase its thermal shock properties (Papachristodoulou et al., 2006; Hein et al., 2008). The potter was probably aware of the larger thickness of SRB32 than the other Umayyad potsherds, therefore he added lower amount of inclusions and fired it at a higher temperature.

The results show that the Ayyubid-Mamluk potsherds were fired at higher temperatures than those of the Umayyad ones. The Ayyubid-Mamluk handmade painted jars, except samples (SRB 6, 14) fired at 900-950°C, were fired at 800-900°C, while the unpainted jars (SRB 16, 24, 25) were fired at 850-950°C. It is most probable that Ayyubid-Mamluk raised the firing temperature to these values to reduce the jars' porosity and permeability. The two Ayyubid-Mamluk plates were fired at 900-950°C, while the Umayyad plate was fired below 800°C. On the contrary, the two Umayyad bowls were fired at higher (or similar) temperatures (800-950°C) than the three Ayyubid-Mamluk ones (<800-900°C).

4.4 Thermogravimetric (TG) analysis

The thermogravimetric (TG) curves show to some extent similar patterns of weight loss during the gradual increase of the firing temperature of the potsherds from room temperature to 900°C. All the samples showed different percentages of gradual weight losses when heated (Figure 9), but the weight losses were significant within the temperature ranges between (0-200 °C and 600-850 °C), and for few samples between (400-550°C). Characteristic patterns are shown in Figure (9B-C).

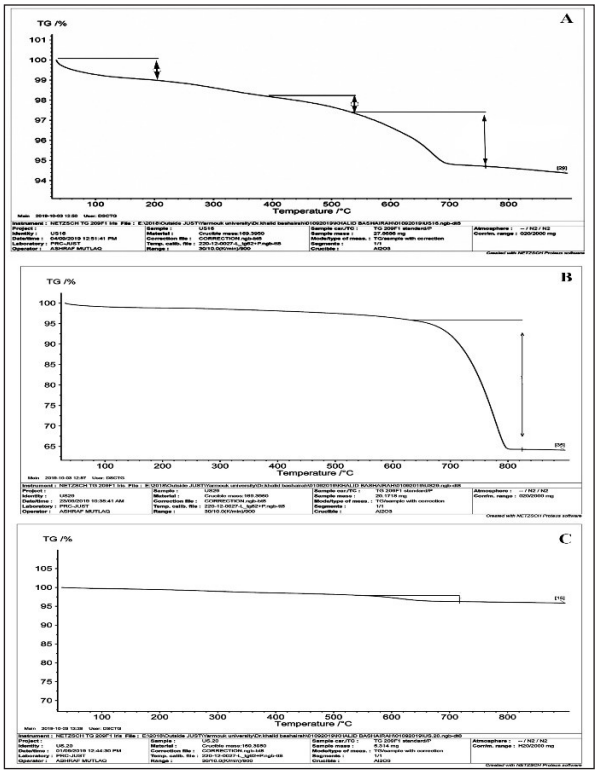

Figure 9. Themogravimetric diagrams of Umm as-Surab potsherds. The common pattern of most samples (A), characteristic patterns of samples SRB23, SRB29, SRB32 (B), and SRB20, SRB26 (C).

In general, the gradual weight losses could be attributed to the evaporation of water molecules also adsorbed at the mineral surface, at the low-temperature range (between 0 and 100 °C), the dehydration of adsorbed water in smectite-like minerals (120-200°C), the decomposition of organic material between 400 and 600°C, and the dehydroxilation of clay minerals between 550 and 950°C (wide range depending on the type of phyllosilicate), the decomposition of calcite between 650 and 850°C (Moropoulou et al., 1995; Drebushchak et al., 2005). All the above samples from both groups show the decomposition of calcite evidenced by the mass loss at temperatures between 650-900°C indicating a firing temperature below 850-950°C. Furthermore, the TG analyses do not show the clear decomposition of clay materials between 550-650°C indicating firing the potsherds at temperatures above 650°C (Findik et al., 2014). The TGA results agree with the chemical and XRD mineralogical analyses where the samples of low CaO concentration (or calcite content) show less weight loss than the samples of higher CaO concentration (or calcite content), when heated at temperatures between 600-900°C.

5. Raw materials and their source

It is possible to shed light on the sources of the raw materials used in the production of the potsherds by correlating the mineralogical composition and fossils found in the limestone and other added inclusions to the possible raw materials deposited in the surroundings of the archaeological site. The recipe of pottery production comprises the clay and non-plastic inclusions of sub-angular to angular quartz and sub-rounded to angular limestone. They also contain crushed ceramic (grog) in different amounts. However, the most noticeable inclusions are the fine rounded basalt grains present in several samples, large angular basalt grains in several ones, and fossil traces in others (Figure 5). These petrographic components are consistent with the geology of the Umm as-Surab area, which is covered by Harrat Ash-Sham basalt rocks and soils and has outcrops of alluvium and wadi sediments (Figure 8) including clays, Pleistocene sediments, and Umm Rijam Chert Limestone (Garaibeh, 2003). Therefore, the presence of the fine basalt grains in the clay resulted from weathering and erosion of the basalt surrounding the site, while the larger angular crushed basalt grains were deliberately added to the clay paste. Similarly, crushed limestone grains were deliberately added. The fossiliferous Umm Rijam Chert Limestone comprising several kinds of fossils and outcropping about 8 km from Umm as-Surab are the probable source of the limestone and fossil inclusions noticed in the samples. The geological map of the region (Figure 8) shows possible clay and sand quarries within the Pleistocene alluvium and wadi sediments distributed in the region, since few of them are close to Umm as-Surab. All of this data suggests a local origin of the potsherds since they are formed of local raw material available in the region.

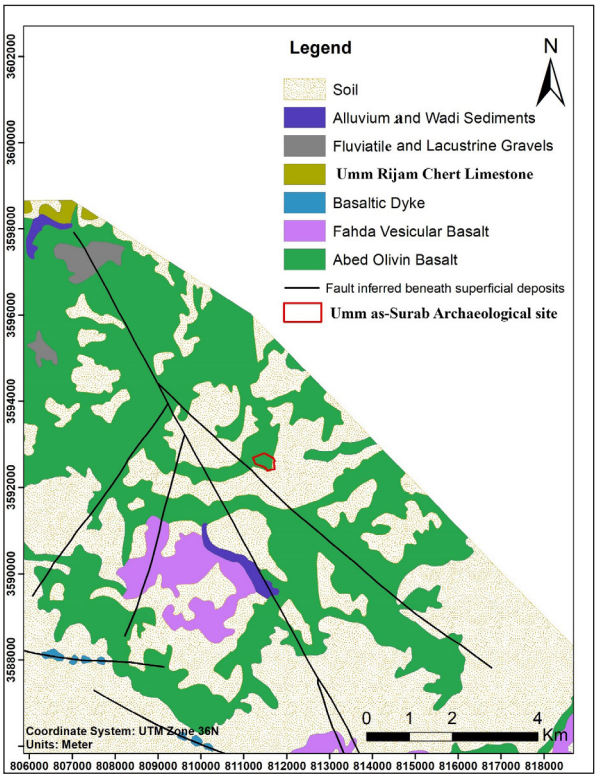

Figure 8. Figure 8. The geological map of Umm as-Surab area showing the probable sources of the raw materials.

6. Conclusions

The application of multidisciplinary analyses to study the pot samples, collected at Umm as-Surab archaeological site, northeast Jordan, offered more data on the production technology of the Umayyad and Ayyubid-Mamluk pottery in the area. The results show disparities in the concentration of their mineralogical and chemical composition reflecting different production recipes of the samples. The results could be attributed to several reasons: probable use of different sources of raw materials, the use of clays of the moderate and high content of carbonates, the addition of different amounts of non-plastic inclusions, varying firing conditions, and/or the import of wares from nearby workshops.

The Umayyad tableware potsherds appeared to contain clays of low carbonates and high silica contents and were fired at temperatures below than 850°C to resist thermal shocks (Papachristodoulou et al., 2006; Hein et al., 2008), while several of the Mamluk-Ayyubid water jars that contain higher amounts of carbonates and moderate to high content of silica were fired at temperatures around 800-950°C to reduce their permeability and porosity. Cooking wares were also manufactured by the addition of higher amounts of inclusions to the clay paste, as in sample SBR 27 (Tite el., 2001). However, it is also possible to achieve these properties in the ceramic body by mixing two or more different clays instead of adding inclusions (Neff et al., 1988).

The results agree with other studies on Umayyad and Ayyubid-Mamluk pottery. Most recently, Otoom (2019) found that the Umayyad potsherds of her study were imported to Tell al-Husn from other neighboring workshops, probably from Gerash and were fired at temperatures between 800 and 900oC. The recipes used in the production of the Umm as-Surab potshers disagree with those of the Ayyubid-Mamluk potsherds from Dohaleh, Hayyan al-Mushrif and Al-Bediah archaeological sites, examined by Al-Tawalbeh (1996), Al-Batainah (2003) and Al-Bataineh (2005), respectively. At Umm as-Surab, the potsherds could be distinguished by the presence of non-plastic basalt grains and absence of dolomite; while, the potsherds of Dohaleh and Hayyan al-Mushrif could be distinguished by the presence of non-plastic dolomite grains and absence of basalt.

The results show technological differences in ceramic production between the Umayyad and Ayyubid-Mamluk periods, which could be reflected in their historical and social contexts. While the tradition of Umayyad ceramic production was concentrated in urban centres such as Bosra or Jerash, with a large commercial exchange network, the Ayyubid-Mamluk ceramic was, to the contrary, mainly produced by workshops on a local scale.

From a macroscopic point of view, the Umayyad pottery of Umm as-Surab shows similarities to the pottery findings at the urban site of Bosra, located only 12 km to the northeast of Umm as-Surab. Administratively, Umm as-Surab followed Bosra during the Byzantine period, and most likely it remained under Bosra's economical and social influence during the Islamic periods.

However, the most interesting data for the settlement history of this site come from the ceramic context of the Ayyubid-Mamluk period, confirming the data of the

settlement trends of other research projects, which concern the western part of Jordan, i.e. the area included between Irbid and the Yarmouk River (Walker, 2005; 2007). The data from ceramic studies of the eastern part of northern Jordan, on the contrary, have shown so far a paucity of information on the Middle-Islamic period, as the case of Umm al-Jimal (Osinga, 2017).

The Umm as-Surab research project, therefore, opens up a new moment of reflection on the dynamics of the population of the countryside in the Islamic Middle Ages. The ceramic analyses show that the production is mostly local but, in any case, with a good knowledge of production technologies. A comparison with ceramic assemblages from other sites in the region, such as those of Dohaleh, Hayyan al-Mushrif and Al-Bediah, confirms this hypothesis. Despite a rather local productive activity, the occupation of Umm as-Surab in the Ayyubid-Mamluk period demonstrates a historical context favourable to a revitalization of the countryside, supported by economic and social stability of the Mamluk sultanate which is reflected in an occupation program and exploitation of geological and agricultural resources at a larger scale.

Acknowledgement

The study was supported by a grant from the Deanship of Research and Graduate Studies at Yarmouk University. The authors would like to acknowledge the Department of Antiquities of Jordan for permission to study the samples and thank Dr. Lara Maritan for reading and commenting on the paper.

References

Almagro, A. Jiménez, P., Navarro, J. (2000). Excavation of Building F of the Umayyad Palace of Amman: Preliminary Report. ADAJ: 44, 433-457.

Al-Bataineh, M. (2005). AyyubidMamluk pottery excavated from Al-Bedia site, area “E” fifth season 2003. Master thesis, Yarmouk University.

Al-Bataineh, S. (2003). AyyubidMamluk pottery in Hayyan Al-Mushrif site: Analytical Study. Master thesis, Yarmouk University.

Al-Tawalbeh, D. (1996). Painted and glazed Ayyubid –Mamluk pottery from Dohaleh/north Jordan, 12th to 15th century A.D. Master thesis, Yarmouk University.

Anastasio, S., Gilento, P., Parenti, R. (2016). Ancient Buildings and Masonry Techniques in the Southern Hauran, Jordan. Journal of Eastern Mediterranean Archaeology and Heritage Studies 4(4): 299-320.

Avissar, M. and Stern, E. J. (2005). Pottery of the Crusader, Ayyubid, and Mamluk Periods in Israel (IAA Reports 26), 1-179, Jerusalem.

Bagatti, B. (1947). I monumenti di Emmaus el-Qubeibeh e deidintorni. Jerusalem.

Franken, H. J. and Kalsbeek, J. (1975). Potters of a Medieval Village in the Jordan Valley. North Holland Publishing Company, Amsterdam.

Barfod, G., Lichtenberger, A., Peterson, A., Raja, A., Ting, C. (2019). “Middle Islamic pottery from Jerash. New research on ceramic fabrics and the implications for production patterns of HMGP pottery in Northern Jordan”, ZeitschriftfürOrientarchäologie 12: 140-167.

Bartoccini, R. (1941). Un decennio di ricerche e di scaviitaliani in Transgiordania. Bollettino del RealeIstituto di archeologia e storiadell’arte 9: 1-10.

Bes, P., Brughmans, T., Lichtenberger, A., Raja, R., Romanowska, I. (2020). “Ceramics in Cities in Context: An Overview of Published Roman Imperial to Umayyad Pottery in the Southern Levant”, in: Lichtenberger, A. and Raja, R. (eds.), Hellenistic and Roman Gerasa: The Archaeology and History of a Decapolis City, Jerash Papers 5, Turnhout, pp. 55–118.

Bong, W. S., Matsumura, K., Nakai, I. (2008). Firing technologies and raw materials of typical early and Middle Bronze Age pottery from Kaman-Kalehöyük: a statistical and chemical analysis. Anatolian Archaeological Studies 17: 295-311.

Bucarelli, O. (2007). Umm es-Surab (Giordania). Indagini archeologiche topografiche nel settore ovest. Temporis Signa II: 309-331.

Butler, H.C. (1909). Ancient Architecture in Syria, Division II, Section A, Part 2, The Sourthern Hauran. Brill: Leiden.

Camuti, K. S. and McGuire, P. T. (1999). Preparation of polished thin sections from poorly consolidated regolith and sediment materials. Sedimentary Geology 128(1-2): 171-178.

Cultrone, G., Rodriguez-Navarro, C., Sebastian, E., Cazalla, O., De La Torre, M. J. (2001). Carbonate and silicate phase reactions during ceramic firing. European Journal of Mineralogy 13(3): 621-634.

Daszkiewicz, M. and Maritan, L. (2017). “Experimental Firing and Re-Firing”. In A. W. M. Hunt (eds.). The Oxford Handbook of Archaeological Ceramic Analysis, 487 – 508. Oxford University Press, Oxford.

De Bonis, A., Cultrone, G., Grifa, C., Langella, A., Leone, A. P., Mercurio, M., Morra, V. (2017). Different shades of red: The complexity of mineralogical and physico-chemical factors influencing the colour of ceramics. Ceramics International 43(11): 8065-8074.

Drebushchak, V. A., Mylnikova, L. N., Drebushchak, T. N., Boldyrev, V. V. (2005). The investigation of ancient pottery. Journal of Thermal Analysis and Calorimetry 82(3): 617-626.

Duminuco, P., Messiga, B., Riccardi, M. P. (1998). Firing process of natural clays. Some microtextures and related phase compositions. Thermochimica Acta 321(1-2): 185-190.

Emami, S. M. A., Volkmar, J., Trettin, R. (2008). Quantitative characterisation of damage mechanisms in ancient ceramics by quantitative X-ray powder diffraction, polarisation microscopy, confocal laser scanning microscopy and non-contact mode atomic force microscopy. Surface Engineering 24(2): 129-137.

Fındık, N. Ö., Akyol, A. A., Sarı, N. (2014). Archaeometric analyses of Hasankeyf unglazed ceramics. Mediterranean Archaeology and Archaeometry 14(1): 261-271.

Gabrieli, R. S., Ben-Shlomo, D., Walker, B. (2014). Production and Distribution of Geometrical-Painted (HMGP) and Plain Hand-Made Wares of the Mamluk Period: A Case Study from Northern Israel, Jerusalem and Tall Hisban. Journal of Islamic Archaeology 1(2): 193-229.

Garaibeh A. (2003). Geological Map of Umm el-Jimal. Geological Mapping Division, Natural Resource Authority: Amman.

Gilento, P. (2014). La Chiesa dei Santi Sergio e Bacco, Umm as-Surab (Giordania). Risultati storico-costruttivi dall’analisi archeologica degli elevati. Arqueología de la Arquitectura (11): 013. doi: http://dx.doi.org/10.3989/arq.arqt.2014.015.

Gosselain, O.P. (1992). Bonfire of the enquiries. Pottery firing temperatures in archaeology: What for?. Journal of

Archaeological science 19(3): 243-259.

Grammatikakis, I. E., Kyriakidis, E., Demadis, K. D., Cabeza Diaz, A., Leon-Reina, L. (2019). Mineralogical Characterization and Firing Temperature Delineation on Minoan Pottery, Focusing on the Application of Micro-Raman Spectroscopy. Heritage 2(3): 2652-2664.

Hein, A., Müller, N.S., Day, P.M., Kilikoglou, V. (2008). Thermal conductivity of archaeological ceramics: the effect of inclusions, porosity and firing temperature. Thermochimica Acta 480(1-2): 35-42.

Iordanidis, A., Garcia-Guinea, J., Karamitrou-Mentessidi, G. (2009). Analytical study of ancient pottery from the archaeological site of Aiani, northern Greece. Materials characterization 60(4): 292-302.

İssi, A., Kara, A., Alp, A. O. (2011). An investigation of Hellenistic period pottery production technology from Harabebezikan/Turkey. Ceramics International 37(7): 2575-2582.

King, G.D. (1983a). Two byzantine churchs in northern Jordan and their Re-use in the islamic period. Damaszener Mitteilungen 1: 111-136.

King, G.D. (1983b). Byzantine and Islamic sites in northern and eastern Jordan. In Proceedings of the Seminar for Arabian Studies, pp. 79-91. Seminar for Arabian Studies, Archaeopress, Oxford.

King G.D. 1989. Um el Surab. D. Homès-Fredericq/J. B. Hennessy (eds.), Archaeology of Jordan II, vol.1, Field Reports, Surveys and Sites (A–K). Akkadica Supplement 7, Leuven: Peeters, pp. 621–24.

LaGro, H. E. (2002). An Insight IntoAyyubid-Mamluk Pottery: Description and Analysis of a Corpus of Mediaeval Pottery from the Cane Sugar Production and Village Occupation at Tell Abu Sarbut in Jordan: Preceded by Pertinent Remarks on Contemporaneous Cane Sugar Production. Deetje publications.

Lichtenberger, A. and Raja, R. (2016). Ğeraš in the Middle Islamic Period: Connecting Texts and Archaeology through New Evidence from the Northwest Quarter. Zeitschrift des Deutschen Palästina-Vereins 63-81.

Maggetti, M. (1982). Phase analysis and its significance for technology and origin. In: Olin, J.S. and Franklin, A. D. (eds.), Archaeological ceramics, Smithsonian Institution Press: Boston, MA: 121-133.

Maritan, L., Nodari, L., Mazzoli, C., Milano, A., Russo, U. (2006). Influence of firing conditions on ceramic products: experimental study on clay rich in organic matter. Applied Clay Science 31(1-2): 1-15.

McNicoll, A., Smith, R. H., Hennessy, B. (1982). Pella in Jordan 1. Canberra: Australian National Gallery.

Mcphillips, S. and Walmsley, A. (2007). MamlukFahl during the Early Mamluk Period: Archaeological Perspectives. Mamluk Studies Review, MEDOC, University of Chicago, 9 (1): 119-156.

Merkel, S. (2019). "Ceramic petrography of locally produced Byzantine/Umayyad pottery from Jerash". In: Lichtenberger A. and Raja, R. (eds.), Byzantine and Umayyad Jerash Reconsidered: Transitions, Transformations, Continuities, Jerash Papers 4, Turnhout, 229-238.

Mittmann, S. (1966). The Roman Road from Gerasa to Adraa. ADAJ 11: 65-87.

Moropoulou, A., Bakolas, A., Bisbikou, K. (1995). Thermal analysis as a method of characterizing ancient ceramic technologies. Thermochimica acta, 269: 743-753.

Neff, H., Bishop, R.L., Sayre, E.V. (1988). A simulation approach to the problem of tempering in compositional studies of archaeological ceramics. Journal of Archaeological Science 15(2): 159-172.

Nodari, L., Maritan, L., Mazzoli, C., Russo, U. (2004). Sandwich structures in the Etruscan-Padan type pottery. Applied Clay Science 27(1-2): 119-128.

Noll, W. (1991). Alte Keramiken und ihrePigmente: Studienzu Material und Technologie, Stuttgart: Schweizerbart.

Osinga, E. (2017). The countryside in context: stratigraphic and ceramic analysis at Umm el-Jimal and environs in northeastern Jordan (1st to 20th century AD). PhD Dissertation, the University of Southampton, Southampton.

Otoom, R. (2019). The Umayyad pottery from Tal Al-Husn archaeological site, Aera A, season 2018: (descriptive and analytical study). Master thesis, Yarmouk University.

Papachristodoulou, C., Oikonomou, A., Ioannides, K., Gravani, K. (2006). A study of ancient pottery by means of X-ray fluorescence spectroscopy, multivariate statistics and mineralogical analysis. AnalyticaChimica Acta 573: 347-353.

Parenti, R. (2012). Building archaeology in Jordan: Preliminary report on the 2009-2011 surveys at Umm as-Surab. ADAJ 56: 187-195.

Parenti, R. and Gilento, P. (2010). Orient and Occident: continuity and evolution in construction know-how from the 4th to the 9th centuries. Archeologia dell'architettura (15): 181-196.

Parenti R. and Gilento P. (2012). Limes Arabicus and still-standing buildings.In. G. Vannini & M. Nucciotti (éd.), La Transgiordanianeisecoli XII-XIII e le 'frontiere' del Mediterraneomedievale (BAR S2386): 111-124.

Peterson, A. (2017). "Medieval pottery from Jerash: The Middle Islamic settlement". In: Lichtenberger, A. and Raja, R. (eds.), Gerasa/Jerash: From the Urban Periphery, Aarhus: 67-74.

Peterson, A. (2018). "Medieval Jerash: Investigating the pottery of a Middle Islamic hamlet in the Northwest Quarter". In: Raja, R. and Sindbæk, S. M. (eds.), Urban network evolutions: Towards a high-definition archaeology, Aarhus: 139-146.

Ravisankar R, Naseerutheen A, Annamalai GR, Chandrasekaran A, Rajalakshmi A, Kanagasabapathy KV, Prasad MV, Satpathy KK. (2014). The analytical investigations of ancient pottery from Kaveripakkam, Vellore dist, Tamilnadu by spectroscopic techniques. Spectrochim Acta A Molecular and Biomolecular Spectroscopy. 121: 457-63. doi: 10.1016/j.saa.2013.10.110. Epub 2013 Nov 8. PMID: 24287055.

Rice, P.M.(1983). Pottery Analysis: A Source book. University of Chicago Press, Chicago.

Rye, O. S. (1981). Pottery technology: principles and reconstruction 4. Washington, DC: Taraxacum.

Sauer, J. (1982). The Pottery of Jordan in the Early Islamic Period. SHAJ 1: 329-337.

Sauer, J. A. and Herr, L. G. (2012). Ceramic finds: typological and technological studies of the pottery remains from tell Hesban and vicinity. Andrews University Press.

Tite, M. S., Kilikoglou, V., Vekinis, G. (2001). Strength, toughness and thermal shock resistance of ancient ceramics, and their influence on technological choice. Archaeometry 43(3): 301-324.

Trindade, M. J., Dias, M. I., Coroado, J., Rocha, F. (2009). Mineralogical transformations of calcareous rich clays with firing: a comparative study between calcite and dolomite rich clays from Algarve, Portugal. Applied Clay Science 42(3-4): 345-355.

Van der Weerd, J., Smith, G. D., Firth, S., Clark, R. J. (2004). Identification of black pigments on prehistoric Southwest

American potsherds by infrared and Raman microscopy. Journal of Archaeological Science 31(10): 1429-1437.

Walker, B. (2005). The northern Jordan survey 2003 – Agriculture in Late Islamic Malka and Hubrasvillages: A Preliminary report on the first season. Bulletin of the American Schools of Oriental Research 339: 67-111.

Walker, B. (2007). The politics of land management in Medieval Islam: The village of Malka in northern Jordan. SHAJ 9: 253-261.

Walker, B. (2012). The Islamic Age. In Ceramic Finds: Typological and Technological Studies of the Pottery Remains from Tell Hesban and Vicinity. In: J. A. Sauer and L. G. Herr (eds), Hesban 11. Berrien Springs, MI: Andrews University Press, pp. 507–594.

JJEES

Jordan Journal of Earth and Environmental Sciences

JJEES (2021) 12 (3): 230-240
ISSN 1995-6681

Assessment of Water Resources Management in Azraq Basin, Jordan

Atef Al-Kharabsheh

Department of Water Resources and Environmental Management, Faculty of Agricultural Technology, Al-Balqa Applied University, Jordan

Received 6 September 2020; Accepted 4 January 2021

Abstract

Azraq basin is located in the northeastern part of Jordan with an area of 12710 km^2. The climate is classified as an arid to semi-arid zone with high evaporation rates and low rainfall amounts. This paper was conducted to interpret geological and hydrogeological data of aquifers to study the effects of overpumping on the hadrochemical characteristics of aquifers. Three aquifer systems are forming the basin; the upper one, which is composed of basalts and carbonates (B4) is the most important aquifer, due to its good water quality and low pumping costs. This aquifer is overpumped since the beginning of the eighties from AWSA governmental production wells and increasing the private agricultural activities. The calculated safe yield of the upper aquifer during the period 1967 to 2018 is about 23 MCM while the pumping may reach about 100 MCM including the private wells. This overpumping resulted in the dryness of Azraq Oasis, decreasing the water table by more than 17 meters and increasing the electrical conductivity to more than 7000 µS/cm in Azraq depression. According to the chemical analyses carried out in this study, there are three types of water: earth alkaline water with an increased portion of alkalis and with prevailing sulfate and chloride (mixed type), alkaline water with prevailing bicarbonate (mixed type) and alkaline water with prevailing sulfate and chloride (sodium chloride type). The mixed types of water assure that there is saltwater intrusion bodies began to occur as a result of the artesian pressure from the middle and lower aquifer systems. To solve the water problems associated with crises in Azraq basin, it is highly recommended to stop overpumping from the upper aquifer, decrease agricultural activities and apply artificial recharge projects of the upper aquifer system especially in the recharge areas in the northern and northwestern parts. This will increase recharge to the upper aquifer, since the natural recharge is less than 3 percent of the total precipitation over Azraq Basin, due to thunderstorm effects and clayey type of soil.

Keywords: water, Jordan, Azraq, aquifer, overpumping.

1. Introduction

Jordan falls within the arid to semi-arid climatic region. The climate is characterized by a long dry season extending from May to October and a rainy season, which starts mainly in late October to the middle of May. The peak precipitation occurs in the winter months of December, January, and February. Snowfall occurs occasionally a few times a year over the highlands of elevation above 800 m above sea level. The areal distribution of rainfall is mainly governed by the topographic features of the region. The highest rainfall is recorded in the northern and central highlands of Ajlun and Salt. The long-term average of these two stations is about 620 and 608 mm/year, respectively. Rainfall decreases significantly from west to east and from north to south (Al-Kharabsheh, 2020).

Azraq basin covers an area of about 12710 km^2, about 94 percent is located in Jordan, while the rest lies in Syria (5 percent) and Saudi Arabia (1 percent) (Figure 1). An important oasis is located at the central part of Azraq basin known as Azraq Oasis, which was recharged by large springs (Shishan and Drouz springs). The wetland supports rich and varied aquatic fauna and flora with freshwater habitats (Water Authority, 1989). The highest point is located at Jebel El-Arab area in Syria with an elevation of about 1576 m above the mean sea level (amsl), while the lowest is at the center of Azraq depression (Qa) with an elevation of about 500 m (amsl). The elevation increases to about 900 m in the southern part of the basin.

The average annual rainfall ranges from more than 325 mm in the north at Salkhad to 150 mm in the west at Muwaqqar and less than 50 mm in the south and east at El-Umary (Figure 2), with an average total of around 122 mm. As a desert area, the thunderstorm rainfall types are forming the major rainfall in Azraq Basin (Al-Kharabsheh et al., 1997).

The purpose of this paper is to determine the geological formation including stratigraphy and structure, interpret the hydrological data including meteorological data, rainfall and runoff, interpret the hydrogeological data including aquifer characteristics and dynamics and study the impacts of overpumping on the hydrochemical attributes of aquifers.

* Corresponding author e-mail: atefkh@bau.edu.jo

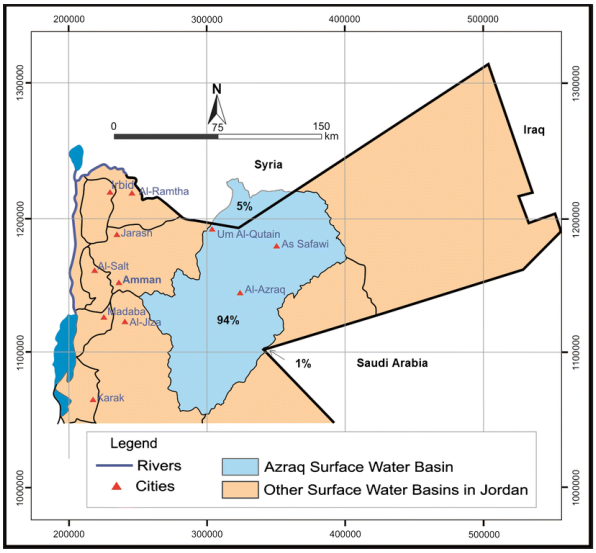

Figure 1. Location Map of Azraq Basin (Ayed, 1996).

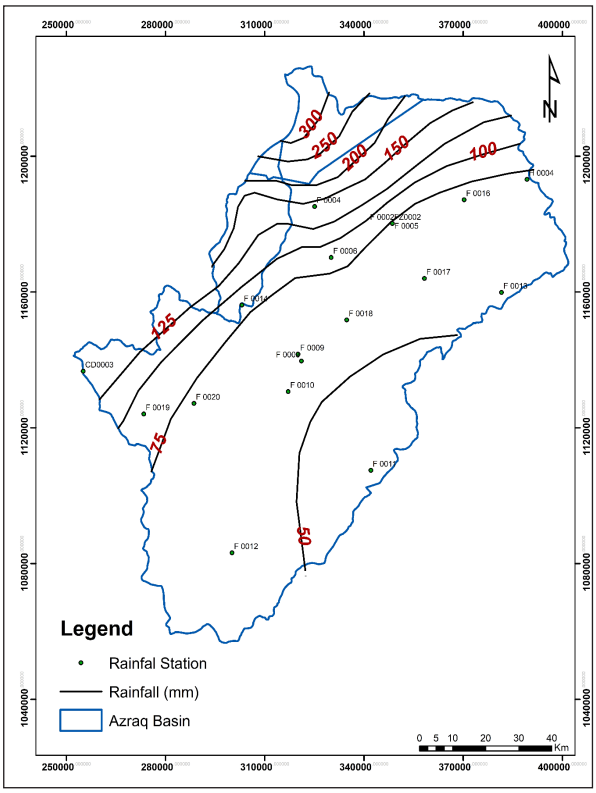

Figure 2. Isohythal Map of Azraq Basin during the Period 1967 to 2018 (WAJ Files Data).

2. Materials and Methods

The climatic parameters representing Azraq Basin were determined and evaluated to obtain the water budget. The long-term monthly and annual means of relative humidity, temperature, wind speed and direction and the class A pan evaporation in Azraq basin are going to be evaluated in this paper. Despite the prevailing thunderstorms, cyclonic rainfall may reach the area, particularly in December, January, February and March.

The methodology used in this study is collecting hydrological and hydrogeological data from different resources, conducting statistical analyses of hydrological data for the different periods, analyzing hydrological data including meteorological data, rainfall and runoff, calculating the runoff volumes affecting the recharge of groundwater, determining modified water budget of Azraq basin, studying the hydrogeological data affecting characteristics of different aquifers, making a relation between overpumping and groundwater salinity and determining methods to evaluate the hydrological characteristics affecting oasis discharge management with time.

3. Water Budget

All the wadis in the Azraq basin are ungauged and no flow measurements are available. The heavy thunderstorm rainfall causes high peak discharges and consequently causes severe inundation in parts of the drainage area. Many ungauged wadis drain into the Qa-Azraq area. Water from these wadis remains several months in Qa-Azraq area as puddles, before evaporating. Water flows to Qa-Azraq area where the good field is located (Al-Kharabsheh, 1991). The ground slopes range between 5-10 percent in the northern part, 3-5 percent in the other directions and exceed 15% in Jebel El-Arab area (Ayed, 1986).

Surface runoff measurements were achieved by using the United States Soil Conservation Service Method (Soil Conservation Service, 1969, 1972 and 1975)) as follows:

$$R = (P-0.2S)^2/(P+0.8S) \quad \text{..... (1)}$$

Where R is the accumulated depth of runoff, P is the accumulated depth of storm rainfall and S is the maximum retention of the soil related to an assigned Curve Number (CN) given to each type of soil. This relation is known as (United States Department of the Interior, 1960):

$$S = (1000/CN)-10 \quad \text{..... (2)}$$

Where R is the accumulated depth of runoff, P is the accumulated depth of storm rainfall and S is the maximum retention of the soil related to an assigned Curve Number (CN) given to each type of soil. This relation is known as (United States Department of the Interior, 1960):

Initial abstraction (Ia) can be calculated as Ia=0.2S.

Penman equation is used to calculate the potential evapotranspiration, which is shown below:

$$E = \Delta / (\Delta + \gamma)\, Rc(1 - r) - \Delta / (\Delta + \gamma)\, Rb + \gamma / (\Delta + \gamma)\, Ea \quad \text{.. (3)}$$

Where R is the accumulated depth of runoff, P is the accumulated depth of storm rainfall and S is the maximum retention of the soil related to an assigned Curve Number (CN) given to each type of soil. This relation is known as (United States Department of the Interior, 1960):

Initial abstraction (Ia) can be calculated as Ia=0.2S.

Penman equation is used to calculate the potential evapotranspiration, which is shown below:

$$I = P-E-R-I_a \quad \text{..... (4)}$$

Where I is the infiltration (mm), P is the precipitation, E is the actual evapotranspiration (mm), R is the runoff and Ia is the initial abstraction (mm). The evapotranspiration, runoff and initial abstraction are subtracted from the rainfall every year to calculate the water budget.

Fourteen rainfall stations are located in the basin of which, eleven stations are located in the Jordan side of the basin, and three stations are in Syria. Table 1 represents the rainfall stations, their locations, type of gauges, and their approximate record period. Table 2 shows annual statistical analyses of rainfall stations in the Azraq Basin. Table 3 summarizes the monthly and annual averages of the main rainfall stations in the study area. Generally, the heaviest rainfall occurs between December and March. The highest monthly rainfall values were recorded in Salkhad (Syria), and the minimum monthly values were measured in EI-Umary station, while Um El-Quttein rainfall station represents the average monthly values in the basin.

The direct runoff in Azraq Basin is estimated using SCS method. Table 4 shows elements of the water budget of the Azraq Basin. Volumes of rainfall, runoff, evaporation and infiltration range from 254, 0.5, 193 and 3.3 MCM, respectively during the dry seasons, to about 1736, 66, 433 and 72 MCM for the same respective components during the wet seasons. The average of the infiltration is about 32 MCM, while the recharge is about 23 MCM since about 8 MCM of the infiltrated water is lost by evapotranspiration into the atmosphere and 1 MCM is flowing into the adjacent areas.

According to Figure 3 and table 5, the Azraq basin is divided into 11 sub-catchments, the highest estimated natural recharge is occurring through Wadi Hassan, while the lowest is occurring in Wadi Jesha. The catchment subdivisions are accomplished according to many factors like geology, topography and drainage pattern.

Table 1. Rainfall Stations in Azraq Basin during the period 1967 to 2018 (WAJ Files Data).

Station Code No.	Name of Rainfall Station	Coordinates (Palestine Grid)		Altitude (m)	Type of station	Ann. Av. Rainfall in mm (1967-2018)
		East	North			
F 0001	UM E1-Quttein	303.5	192.5	986	Daily	140.7
F 0002	H 5 (Safawi)	348.5	180	715	Daily	66.5
F 0004	Deir E1-Kahf	325	185	1025	Daily	108.1
F 0006	E1 Aritain	330	170	800	Daily	91.7
F 0009	Azraq Evap. St.	320	141.5	533	Daily	59.5
F 0011	E1-Umary	342	107.3	525	Daily	48.9
F 0012	Qasr Tuba	300	83	750	Daily	55.9
F 0013	Wadi Salahib	381.5	159.7	700	Totalizator	64.5
F 0020	Qasr E1–Kharrana	288.5	127	650	Daily	73
CD 0003	E1–Muwaqqar	255	136.5	910	Daily	156.2
H 0004	Tullul E1-Ashqaf	389.2	193	900	Totalizator	67.9
S 0001*	Salkhad	311	210	1447	Daily	325.6
S 0002 *	Imtan	321	203	1260	Daily	247.5
S 0003 *	Khirbet Awwad	310	194	1065	Daily	198.7

* Stations located in Syria

Table 2. Long-term annual rainfall of Azraq Basin during the period 1967 to 2018 (WAJ Files Data).

Rainfall Station	Maximum Annual Rainfall (mm)	Minimum Annual Rainfall (mm)	Mean Annual Rainfall (mm)
Salkhad	533	163.0	325.6
Um EI-Quttein	277	59.4	140.7
Safawi (H5)	189	15.5	66.5
EI-Aritain	170	39.5	91.7
Azraq Evap. Station	149	9.8	59.5
Qasr EI-Kharrana	134	21.0	73
Qasr Touba	108	10.0	55.9
EI-Muwaqqar	323	68.5	156.2
EI-Umary	97	8.5	48.9
Tullul EI-Ashqaf	121	15.0	67.9
Wadi Salahib	110	21.5	64.5
Deir El-Kahf	168	36.1	108.1
Khirbet Awwad	368	76.1	198.7

Table 3. Long-term monthly and annual rainfall averages (mm) for rainfall stations of Azraq Basin during the period 1967 to 2018 (WAJ Files Data).

Rainfall Station	Months								Annual
	Oct.	Nov.	Dec.	Jan.	Feb.	Mar.	Apr.	May	Total
Um EI-Quttein	3.7	14.8	25.4	29.9	29.8	23.2	7.7	6.2	140.7
H5 (Safawi)	3.9	9.4	10.9	12.2	12.7	10.5	5.8	1.1	66.5
EI-Aritain	8.2	10.2	12.2	26.7	10.8	12.5	7.1	4	91.7
Azraq Evap. Station	4.2	6.7	10.4	10.4	9.8	11.8	4.3	1.9	59.5
EI-Umary	3.7	5.9	7.6	9.7	6.1	10.5	4.8	0.6	48.9
Qasr Touba	2.9	8.0	10.9	12.4	6.2	12.2	2.9	0.4	55.9
Wadi Salahib	4.2	9.9	9.8	11.2	11.9	11.2	5.8	0.5	64.5
Qas EI-Kharrana	3.7	9.7	14.8	16.8	8.2	16.9	2.3	0.6	73.0
EI-Muwaqqar	4.0	16.8	29.5	34.0	30.0	31.0	10.7	0.2	156.2
Tullul EI-Ashqaf	4.1	10.5	9.9	11.8	12.7	10.3	7.5	1.1	67.9
Salkhad	10.9	34.0	57.8	68.7	69.0	62.6	19.4	3.2	325.6
Imtan	7.3	21.8	43.5	65.2	45.8	42.5	16.2	5.2	247.5
Khirbet Awwad	5.7	17.8	33.0	52.0	43.0	28.5	17.4	1.3	198.7
Deir El-Kahf	3.4	10.4	19.9	28.9	25.4	12.6	4.9	2.6	108.1
Average	5.0	13.3	21.1	27.9	23	21.2	8.3	2.1	121.8

Table 4. Calculated Water Budget for Azraq Basin during the period 1967 to 2018 (WAJ Files Data).

Water Year	Rainfall (MCM)	Runoff (MCM)	Loss (MCM)			Infilt. (MCM)	Runoff Rate (%)	Infilt. Rate (%)	Loss Rate (%)		
			Ed	Ia	Total				Ed	Ia	Total
1967/1968	1119.8	5.7	251.8	857.5	1109.3	4.8	0.5	0.4	22.5	76.6	99.1
1968/1969	1273.5	48.8	560.5	618.6	1179.1	45.6	3.8	3.6	44.0	52.6	92.6
1969/1970	784.2	12.5	341.1	414.2	755.3	16.4	1.6	2.1	43.5	52.8	96.3
1970/1971	1471.8	69.3	646.3	703.3	1349.6	52.9	4.7	3.6	43.9	47.8	91.7
1971/1972	1657.4	13.2	307.8	1317.5	1625.3	18.9	0.8	1.1	18.6	79.5	98.1
1972/1973	730.8	21.0	204.2	483.2	687.4	22.4	2.9	3.1	27.9	66.1	94.0
1973/1974	2043.8	80.0	421.7	1452.5	1874.2	88.8	4.0	4.3	20.6	71.1	91.7
1974/1975	1244.3	13.3	211.9	964.7	1176.6	54.4	1.1	4.4	18.0	76.5	94.5
1975/1976	1240.5	21.6	354.7	841.0	1195.7	23.2	1.7	1.9	28.6	76.8	96.4
1976/1977	719.4	13.0	419.8	266.7	686.5	19.5	1.8	1.8	37	58.3	95.3
1977/1978	738.5	3.3	117.0	613.8	730.8	4.4	0.4	0.6	15.8	83.2	99.0
1978/1979	542.7	3.1	110.5	421.6	532.1	7.5	0.6	1.4	20.4	77.6	98.0
1979/1980	1736.2	65.8	433.4	1165.3	1598.7	71.7	3.8	4.1	25.0	67.1	92.1
1980/1981	1165.5	54.8	361.2	702.8	1064.0	46.7	4.7	4.0	31.0	60.3	91.3
1981/1982	1137.5	6.9	164.4	953.4	1117.8	12.8	0.6	1.1	14.5	83.8	98.3
1982/1983	995.2	53.1	322.2	549.0	871.2	70.9	5.3	7.1	32.4	55.2	87.6
1983/1984	610.1	15.5	332.7	240.9	573.6	21.0	2.5	3.4	54.6	39.5	94.1
1984/1985	1075.3	18.9	429.0	583.4	1012.4	44.0	1.8	4.1	39.9	54.2	94.1
1985/1986	1042.2	19.1	351.4	649.8	1001.2	21.9	1.8	2.1	33.7	62.4	96.1
1986/1987	1009.2	48.2	364.6	544.7	909.3	51.7	4.8	5.1	36.1	54.0	90.1
1987/1988	1629.4	17.5	438.7	1136.3	1575.0	36.9	1.1	2.3	26.9	69.7	96.6
1988/1989	1422.2	26.3	301.0	1054.6	1355.7	40.2	1.8	2.8	21.2	74.2	95.4
1989/1990	1182.0	10.8	227.3	928.7	1156.0	15.2	0.9	1.3	19.2	78.6	97.8
1990/1991	1238.0	47.2	309.8	822.3	1132.1	58.7	3.8	4.7	25.0	66.5	91.5
1991/1992	1074.0	38.9	312.9	670.4	983.3	51.8	3.6	4.8	29.0	62.5	91.0
1992/1993	795.7	22.1	406.5	349.4	755.9	17.7	2.8	2.2	15.2	43.9	95.0
1993/1994	866.8	2.2	31.9	827.4	859.3	5.3	0.3	0.6	3.7	95.4	99.1
1994/1995	1150.3	13.4	255.9	855.4	1111.3	25.6	1.2	2.2	22.2	74.4	96.6
1995/1996	610	5.2	354.4	238.0	592.4	12.4	0.85	2.03	58.1	39.0	97.1

Continue Table 4

Water Year	Rainfall (MCM)	Runoff (MCM)	Loss (MCM)			Infilt. (MCM)	Runoff Rate (%)	Infilt. Rate (%)	Loss Rate (%)		
			Ed	Ia	Total				Ed	Ia	Total
1995/1996	610	5.2	354.4	238.0	592.4	12.4	0.85	2.03	58.1	39.0	97.1
1996/1997	1037	18.7	352.0	642.5	994.5	23.9	1.80	2.30	33.9	62.0	95.9
1997/1998	1033	13.4	399.5	593.2	992.7	26.9	1.30	2.60	38.7	57.4	96.1
1998/1999	254	0.5	56.5	193.5	250.0	3.3	0.20	1.30	22.2	76.3	98.5
1999/2000	258	1.1	75.9	176.4	252.3	4.1	0.43	1.60	29.4	68.6	98.0
2000/2001	1011.1	18.3	340.2	632.1	972.3	20.5	1.8	2.0	33.6	62.5	96.2
2001/2002	1575.3	59.3	371.5	1079.1	1450.6	65.4	3.77	4.2	23.6	68.5	92.1
2002/2003	1175.0	44.3	288.3	787	1075.3	55.4	3.77	4.7	24.5	67.0	91.5
2003/2004	975.3	47.9	332.8	544.1	876.9	50.5	4.9	5.2	34.1	55.8	89.9
2004/2005	653.2	6.3	382.3	251.5	633.8	13.1	1.0	2	58.5	38.5	97.0
2005/2006	1034.5	37.8	298.4	647.2	945.6	51.1	3.7	4.9	28.8	62.6	91.4
2006/2007	912.3	5.7	338.1	561.7	899.8	6.8	0.6	0.7	37.1	61.6	98.6
2007/2008	1588.3	15.7	422.3	663.2	1085.5	35.1	1.0	2.2	26.6	41.7	96.8
2008/2009	289	2.1	91.3	190.4	281.7	5.2	0.7	1.8	31.6	65.9	97.5
2009/2010	1399.5	25.8	291.0	1043.8	1334.8	38.9	1.8	2.8	20.8	74.6	95.4
2010/2011	789.5	4.9	132.1	674.4	806.5	5.1	0.6	0.6	16.7	85.4	98.7
2011/2012	1088.5	5.5	240.3	838.1	1078.4	4.6	0.5	0.4	22.1	77.0	99.1
2012/2013	1248.3	48.1	552.5	603.9	1156.4	43.8	3.9	3.5	44.2	48.4	92.3
2013/2014	1501.5	71.3	652.8	722.9	1375.7	54.5	4.7	3.6	43.5	48.4	91.6
2014/2015	1644.9	12.8	301.5	1312.5	1614	18.1	0.8	1.1	18.3	79.8	98.1
2015/2016	1198.6	21.1	334.5	820.3	1154.8	22.7	1.8	1.9	27.9	68.4	96.3
2016/2017	995.2	55.3	320.7	558.7	879.4	60.5	5.6	6.1	32.2	56.1	88.4
2017/2018	1321.5	62.3	243.8	945	1188.8	70.4	4.7	5.3	18.4	71.5	90.0
Average	1084.1	26.4	316.9	700.2	1017.1	32.2	2.2	2.8	29.3	64.7	94.9

Total loss =(Evapotranspiration of the storm (Ed)+ Initial Abstraction (Ia)

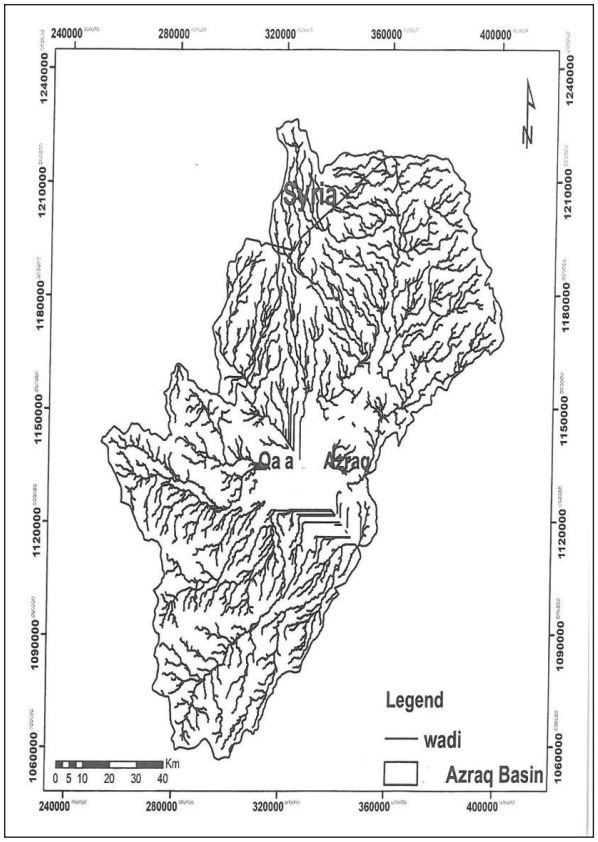

Figure 3. Azraq Subcatchment Areas.

Table 5. Estimated Recharge Quantities of Azraq Subcatchments (mm) during the Period 2000 to 2028 (Al Shamil Engineering Office, 2000).

Year	Wadi Butum	Wadi Ghadaf	Wadi Harth	Wadi Hassan	Wadi Jesha	Qa'a Khanna	Wadi Mudeisisat	Wadi Rajil	Wadi Rattam & Wadi Unqiya	Wadi Uweinid	Wadi Aseikhim
2000	0.92	0	0	0	0	0.6	0.95	0.5	0	0.27	0.00
2001	0.21	0	0	5.79	0	1.25	0.15	2.63	0	0	4.63
2002	7.6	0	4.15	6.81	0	2.34	9.53	3.28	0.74	4.51	5.45
2003	0.21	0	0	9.28	0	3.26	0.01	4.01	0	0.57	7.42
2004	7.14	0.44	3.74	8.81	0.18	4.48	15.02	6.77	0	0.04	7.05
2005	0.56	1.43	0	1.02	0	1.89	0.51	2.26	0	0	0.82
2006	0.49	0	0	4.74	0	2.63	0.65	2.53	0	0.92	3.79
2007	12.7	0.71	10.6	7.61	0.34	2.66	13.94	4.3	2.94	6.67	6.09
2008	1.9	4.21	0	4.08	2.48	1.29	0.89	1.59	1.18	4.63	3.26
2009	3.61	1.76	0	11.88	1.14	3.13	4.53	3.25	0.07	3.38	9.50
2010	2.55	0	0	13.95	0.09	2.62	2.96	3.5	0	0	11.16
2011	1.49	0	0	1.17	0	0.38	1.85	0.7	0	0	0.94
2012	6.34	0	2.12	12.52	0.14	2.02	11.25	4.07	0	0	10.02
2013	14.83	0.81	7.97	10.81	0	4.05	19.9	8.52	1.07	4.03	8.65
2014	0	0	0	1.28	0	0.61	0	0.96	0	0	1.02
2015	1.06	0	0	5.12	0	1.39	1.27	1.72	0	0	4.10
2016	0.06	0	0	14.59	0	4.36	0	6.56	0	0	11.67
2017	0.35	0	0	13.63	0	3	0.27	6.46	0	0.1	10.90
2018	4.47	1	1.8	10.96	0	4.03	5.58	5.7	0	1.35	8.77
2019	2.34	0	0	13.67	0	3.84	2.9	5.08	0.01	3.49	10.94
2020	0	0	0	17.52	0	2.61	0	6.21	0	0.02	14.02
2021	9.61	3.26	2.54	20.89	0.75	6.18	11.52	7.69	0.87	3.39	16.71
2022	2.34	0	0.03	1.69	0	0.54	3.02	0.47	0	0	1.35
2023	0.42	0.44	0	8.49	0	2.11	0.4	3.57	0	0.68	6.79
2024	9.44	3.91	1.59	11.08	2.37	2.89	8.01	7.85	0.12	2.23	8.86
2025	2.72	0	0	6.64	0	2.33	6.24	4.01	0	0.24	5.31
2026	0.26	0	0.72	3.54	0	2.31	0.42	3.02	0	0	2.83
2027	2.7	0.39	0	5.45	4.14	0.66	8.5	1.53	0	0	4.36
2028	0.42	0	0	3.42	0	0.92	0	0.53	0	0	2.74

4. Aquifer Characteristics of Azraq Basin

There are three aquifer systems in the Azraq basin namely: the upper, middle and lower aquifer systems.

The upper aquifer system consists of alluvial deposits (Quaternary), Basalts Miocene-Quaternary), Wadi Shallala (Eocene) and Umm Rijam Chert Limestone (Paleocene) formations. The basalt aquifer is connected with layers of clay, which may give rise to perched groundwater bodies. A gradual thinning of the basalt from east to west and a sharp increase in the hydraulic gradient of the system (Al-Momani, 1991). The transmissivity of the basalt ranges from 3.1x10-3 to 0.76 m2/s (Humphreys, 1982). Wadi Shallala Formation is composed of marl clayey materials. It acts as an aquitard to the groundwater between the Basalt and Rijam aquifers at the northern part of the basin. The Rijam aquifer is considered as a good aquifer and composed of white-coloured chalky limestone and brown chert, underlain by the green marls, and contains occasional gypsum (Al-Kharabsheh, 1995).

The middle aquifer system is composed of Amman Silicified Limestone Formation (Campanian), Wadi Umm Ghudran Formation (Santonian) and Wadi As Sir Limestone Formation (Turonian). This aquifer outcrops at the west and southwest of the basin and underlie most of the area (Ayed, 1996). The Amman Silicified Limestone Formation is composed of chert and limestone. Depth to the aquifer water ranges between 420 and 590 m. The hydraulic conductivity ranges between $3.06x10^{-6}$ and $4.73x10^{-3}$ m/s with an average value of $7.16x10^{-4}$ m/s (Water Authority, 1989).

The lower aquifer system is separated from the middle one by low permeability marls and marly limestone. This aquifer system consists of poorly consolidated multicolored sandstones of the Early Cretaceous age intercalated with thin beds of shales and clays (Lloyd, 1992).

5. Groundwater Recharge and Movement

Groundwater movement depends on the hydraulic conductivity and hydraulic gradient. Groundwater elevations are highest in the northeast of the basin, decreasing from 564 to about 500 m.a.s.l towards Azraq depression. Groundwater flow in the outcropping (B4) Formation is from west and northeast towards Qa-Azraq. The average transmissivity of the upper aquifer system is 11000 m^2/d.

The aquifers are hydraulically interconnected, due to major faults. Groundwater is flowing in different flow

directions: water of the upper aquifer system flows from the north at Jebel El-Arab area toward the Qa-Azraq in the south, the water of the middle aquifer system flows from the west and the southwest (Zerqa and Mujib basins) and from the east (Hammad Basin) to reach the Azraq depression, the water of the lower aquifer system flows from east to west to discharge in its lowest point at the Dead Sea Basin (Figure 4). The groundwater flow pattern of the upper aquifer system shows that groundwater flow direction is in the direction Azraq depression (Figure 5), while in the middle aquifer system it flows in the northeastern direction of the depression (Figure 6). Areas of Outcropping Aquifers in Azraq Basin are presented in Figure (7).

The water budget approach was applied to estimate the recharge to the groundwater. The water budget equation is used to perform the water balance on daily basis for each storm event during the period under investigation. The rainfall is the only measured parameter; therefore, daily runoff and initial abstraction were calculated using the SCS-Curve Number method for each storm during a specific year. The potential evapotranspiration was computed by Penman's Equation. Then, the water budget was solved for all storms the occurred during the period of water years (1967/1968-1999/2000). The water budget of the Azraq basin shows that the average yearly infiltration is 32 MCM (Table 4). About 1 MCM flows through the Sirhan structure to adjacent areas and about 8 MCM of the infiltrated water is lost by evapotranspiration. This shows that net recharge to the upper aquifer system is about 23 MCM annually.

6. Results and Conclusions

There were two groups of springs forming the Azraq Oasis in the central part of the Azraq basin near the good field area. The first group, Drouz consists of the Aura and Mustadhema springs; the second group, Shishan includes the Souda and Qaisiyeh springs. They were recharged from the same resource of the upper aquifer system (Jebel El Arab). These two groups of springs run dry, due to the overpumping from the good field area upstream of the springs (Table 6).

Azraq basin suffers environmental problems including loss of biodiversity, drought and pollution, due to human and agricultural activities.

Table 6. Withdrawal from the Upper Aquifer System Compared to the Natural Discharge from Azraq Springs (WAJ Files Data).

Year	Withdrawal from Upper Aquifer System (MCM)	Discharge from Springs (MCM)
1981	1.5	10.49
1982	11	8.35
1983	13.81	6.60
1984	16.36	6.04
1985	19.14	5.27
1986	18.22	3.57
1987	22	4.11
1988	31.64	2.15
1989	28.92	1.96
1990	34.9	0

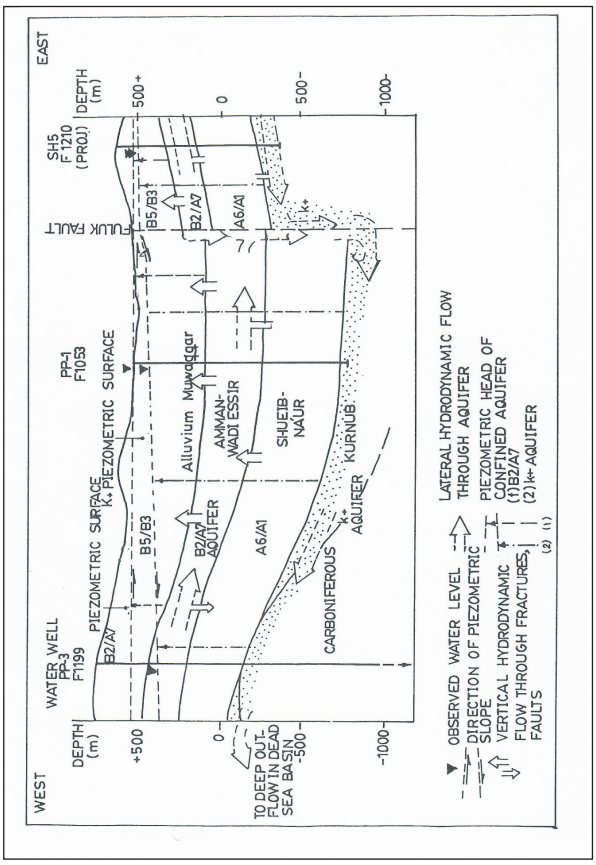

Figure 4. Hydrodynamic Characteristics of Groundwater Flow in Azraq Basin (Salameh and Udluft, 1985).

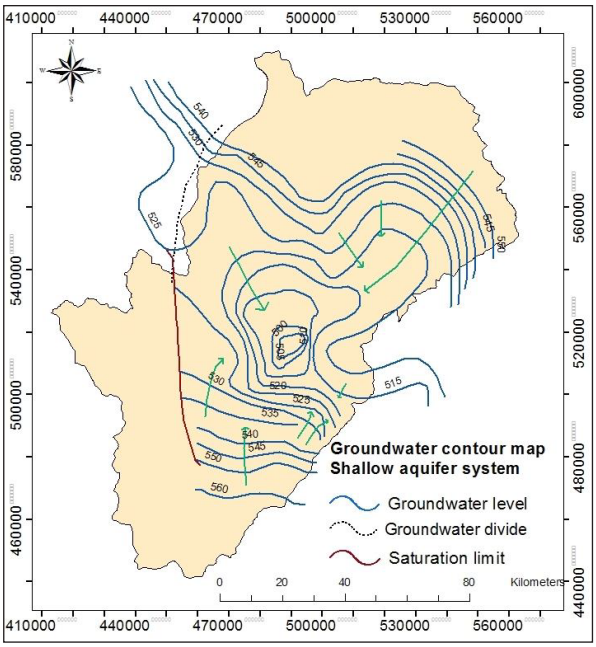

Figure 5. Groundwater flow pattern of the Upper Aquifer System (Hobler et al., 2001).

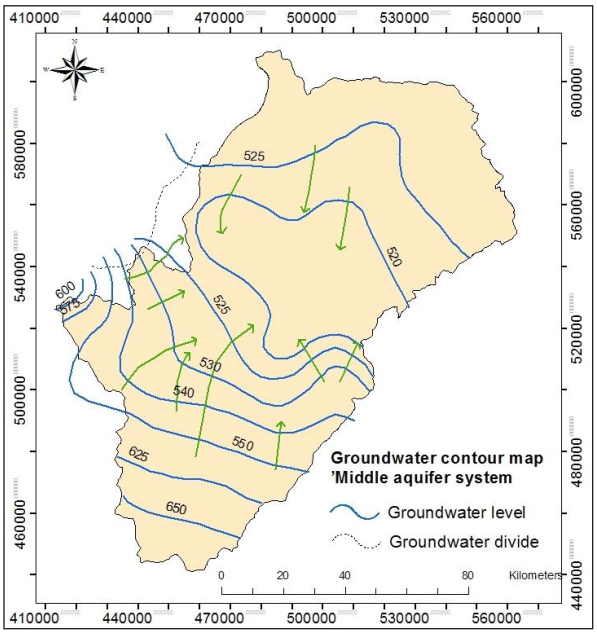

Figure 6. Groundwater flow pattern of the Middle Aquifer System (Hobler et al., 2001)

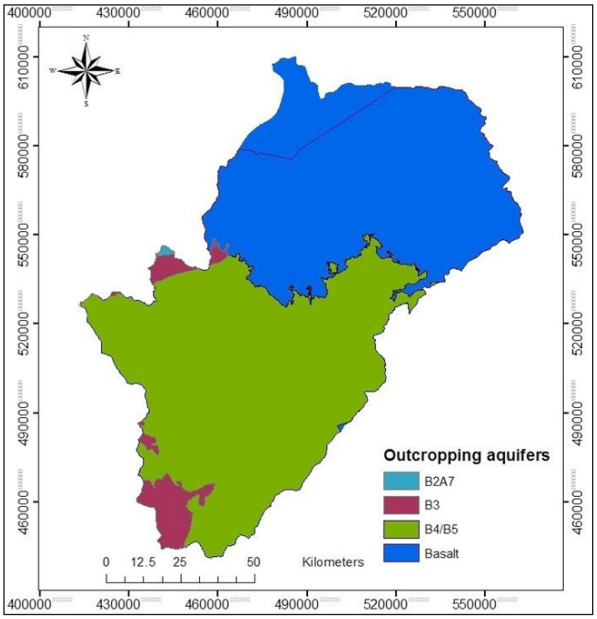

Figure 7. Areas of Outcropping Aquifers in Azraq Basin (Alkhatib, 2017).

The severe pumping is alarming environmental disaster. The groundwater overpumping has also caused environmental, social and economic negative impacts (WAJ Files Data).

Due to the overpumping from the basin for agricultural activities, water tables are dropped significantly at a rate of 80-90 cm/y. Consequently, there is severe ecosystem deterioration. People are losing most of their products and large cropping areas being irreversibly damaged due to lack of water, salinity and soil quality deterioration (Al Wreikat and Al-Kharabsheh, 2020).

Well F 1014 is an example of a declining water table by -0.8/y m at Ain El-Beida. This well penetrates the basalt and the underlying B4 aquifers (Figure 8). The expected saturated thickness of this well is expected to decrease more than 90 percent if the recent pumping continues.

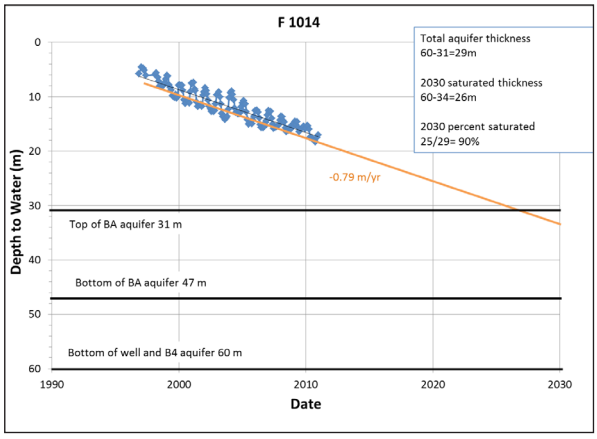

Figure 8. Actual and Estimated Groundwater level Fluctuations at Ain El-Baida Well (F 1014).

Based on the water table fluctuation measurements at the well F 1022, the current trend is -1 m/y. The saturated thickness of B4/B5 aquifer is forecast to decline to 53 percent by the year 2030 (Figure 9).

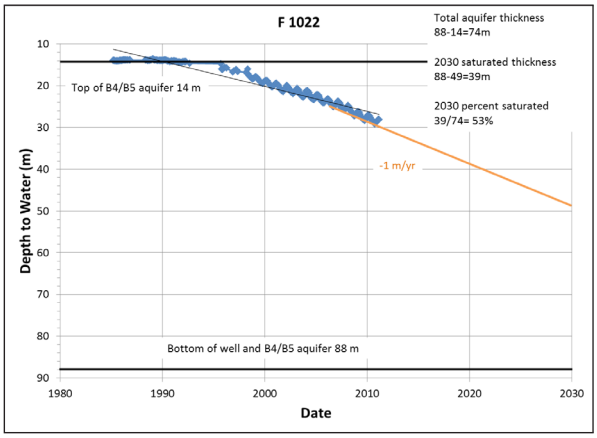

Figure 9. Actual and Estimated Groundwater level Fluctuations at Azraq Oasis Well (F 1022).

Well F 1043 is located in the Azraq oasis area, near several wells with high abstraction rates. The current trend is -0.42 m/y, which is less than the long-term trend of the linear fit to all data. The combined saturated thickness of the Basalt and B4 aquifers is forecast to decline to 85 percent at this location in the year 2030 (Figure 10).

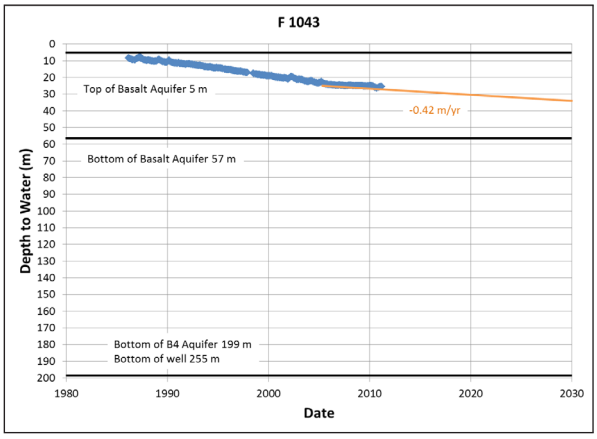

Figure 10. Actual and Estimated Groundwater level Fluctuations at Azraq Oasis Well (F 1043).

Water quality and amount have suffered to incredible significance in Azraq basin over the most recent four decades. The allocated water per capita is expected to decrease from 120 m^3 recently to 91 m^3 by the year 2025, which is far below the international standard (1000 m^3). Water deficiency is a huge challenge affecting the future of different activities in the country, especially after the refugee crises.

The investigations of groundwater of Azraq basin, which is one of the amongst the most vital basins in Jordan. The groundwater withdrawal from Azraq basin reached about 50 MCM/year is utilized to supply Amman, Zarqa and Jordan-northern governorates with a new water supply and about 50 MCM/year from the private agricultural wells. Azraq Oasis is the core of the basin where a large number of transitory flying birds reset in consistently amid their trip from Siberia to Africa. Lack of water affects the hydrochemical and biological system in the basin, due to overpumping from the upper aquifer system. The water level dropped significantly and indications of salinization and exhaustion occurred. The serious drawdown in the Azraq well field caused saltwater intrusion in the central part of the basin (Qa-Azraq). The salinization in the upper aquifer (basalt/B5/B4) likely resulted from the switch of Sabkha water to the AWSA well field and the artesian pressure from the saline middle and lower aquifers, due to the serious drop of the water table of the upper aquifer.

The huge increase in electrical conductivity is occurring at the Azraq depression, due to the saltwater intrusions. The electrical conductivity values increased to about 7000 µS/cm but they could decrease to about 4500 µS/cm in the year 2030 if the pumping from the upper aquifer system decreases to the safe yield average (Figures 11-12). Continuous dropping in the water table also could be stopped by decreasing pumping to a safe yield average (Figure 13).

According to piper plot classification, 1944 for about 33 water samples during the year 2018 (Figure 14), the groundwater of the upper aquifer system shows three types of water according to the major cations (sodium, potassium, magnesium and calcium) and anions (bicarbonate, sulphate, chloride and nitrate) (Figure 15) as follows:

1. Earth alkaline water with an increased portion of alkalis and with prevailing sulfate and chloride (mixed type).
2. Alkaline water with prevailing bicarbonate (mixed type).
3. Alkaline water with prevailing sulfate and chloride (sodium chloride type).

It can be seen clearly that the aquifers are composed of a group of different rock formation, which affects the chemical constituents of the groundwater. The analyses also show a formation of saltwater bodies at the central part of the depression.

Matrics of linear correlation for the combination of parameters of chemical constitutes are shown in table (7). It can be seen a positive relationship affecting the increase of different cations and anions in groundwater.

Groundwater artificial recharge involves collecting surface water in ponds, sand dams, recharge releases, underground dams, recharge wells, drilled wells or other facilities where water infiltrates into the permeable soil to recharge the upper aquifer system, which is composed of fractured carbonates and basalts (Gale, 2005). Trenches and shafts can be used in the unsaturated zone, or water can be directly injected into aquifers through recharge wells. Applying artificial recharge techniques will help in the followings:

1. Increase the safe yield of the basin aquifers
2. Decrease the effects of thunderstorm rainfalls on the basin recharge
3. Decrease the effects of thunderstorm rainfalls on the soil erosion
4. Improve the groundwater quality
5. Alleviate the formation of saltwater intrusions in the upper aquifer system
6. Improve the natural discharge of Azraq springs
7. Increase the tourist activities in the basin
8. Increase the activities of the immigration birds in the eastern deserts
9. Avoid the increasing salinity of the soils as a result of agricultural activities
10. Develop new agricultural activities in the basin.
11. Combat desertification of the ecosystem

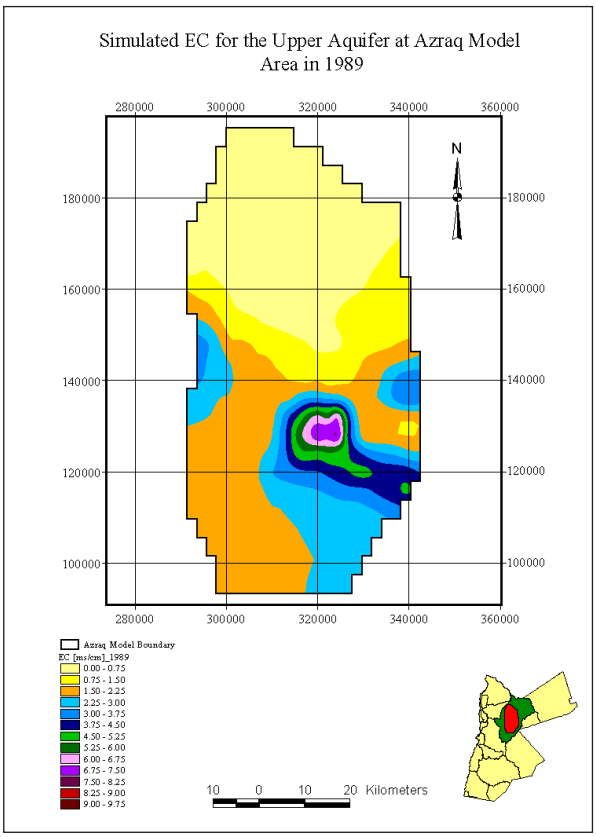

Figure 11. Simulated Groundwater Salinity of the Upper Aquifer System in Azraq Basin in the Year 1989 (WAJ Files Data).

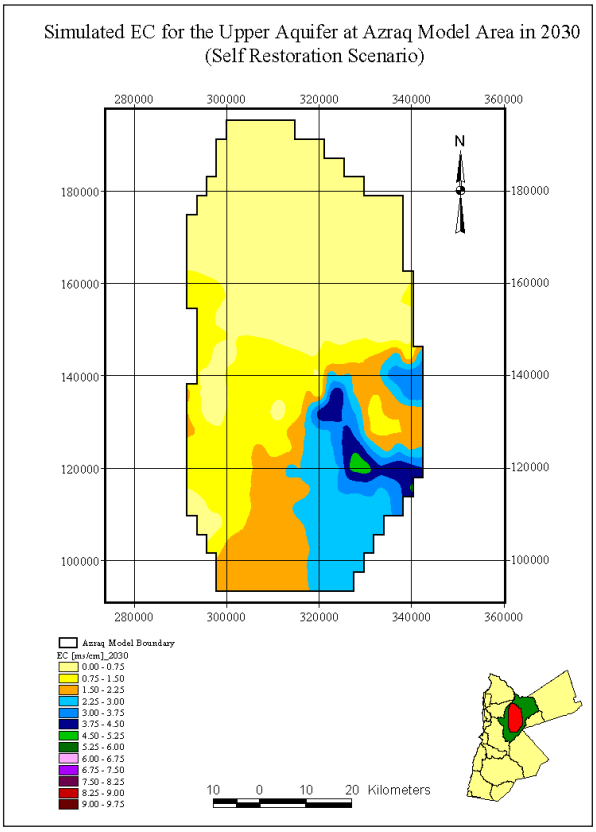

Figure 12. Simulated Groundwater Salinity of the Upper Aquifer System in Azraq Basin in the Year 2030 using Self Restoration Scenario (WAJ Files Data).

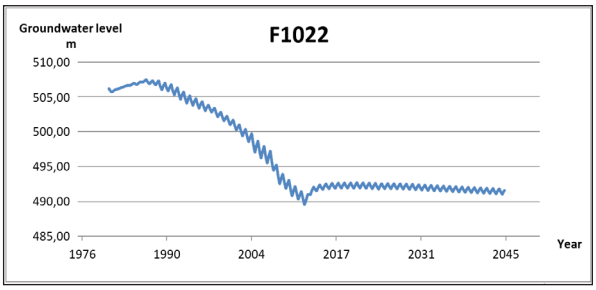

Figure 13. Simultaion of Groundwater Levels under Safe Yield Conditions in the Well F1022 during the Period 1976-2045 (Alkhatib, 2017).

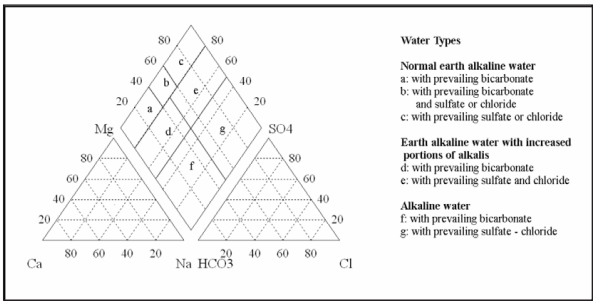

Figure 14. Trilinear Classification of Water Types according to Chemical Constituents (Piper, 1944).

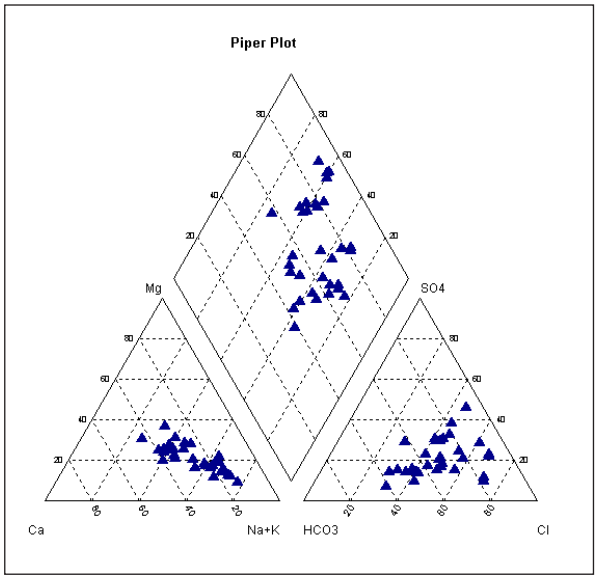

Figure 15. Trilinear presentation of groundwater in the Upper Aquifer System of Azraq Basin.

Table 7. Matrix of Linear Correlation Coefficient of the Chemical Analyses in Azraq Basin (mg/L).

	pH	Na	Mg	Ca	Cl	K	SO4
pH	1	-0.47	-0.565	-0.638	-0.488	-0.407	-0.541
Na		1	0.874	0.89	0.953	0.85	0.867
Mg			1	0.954	0.942	0.724	0.903
Ca				1	0.917	0.731	0.93
Cl					1	0.751	0.825
K						1	0.828
SO4							1

References

Alkhatib, J. (2017). An Integrated Approach of Analyzing Management Solutions for Water Crisis in Azraq Basin, Jordan, Ph. D Thesis, Georg-August University, Germany.

Al-Kharabsheh, A. (2020). Challenges of Sustainable Water Management in Jordan. Jordan Journal of Earth and Environmental Sciences 11 (1): 38-48.

Al-Kharabsheh, A. (1991). Hydrogeological and Hydrochemical Study of the Upper Aquifer System in Azraq Basin. M.Sc. Thesis, Yarmouk University, Jordan.

Al-Kharabsheh, A. (1995). Possibilities of Artificial Groundwater Recharge in the Azraq basin: Potential Surface Water Utilization of Five Representative Catchment Areas (Jordan). Journal of Hydrogeologie und Umwelt 10, 205 pp.

Al-Kharabsheh, A. Al-Weshah, R., Shatanawi, M. (1997). Artificial Groundwater Recharge in the Azraq Basin (Jordan). Dirasat 24(3): 357-370.

Al-Momani, M. (1991). Relationship between AWSA Well Field and Northeast Desert Groundwater (Upper aquifer) and Sources of Salinity in Deep B2/A7 Aquifer, Azraq basin. Unpubl. Report, Water Authority, Jordan.

Al Shamil Engineering Office. (2000). Vulnerability of the Azraq Groundwater System to Climate Change, Amman, Jordan.

Al Wreikat, M. and Al-Kharabsheh, A. (2020). Impact of over pumping on groundwater resources sustainability at Amman Zarqa basin, Jordan: a case study of arid areas affected by Syrian refugees crisis. Environmental Earth Sciences (2020) 79:19 https://doi.org/10.1007/s12665-019-8768-0.

Ayed, A. (1986). Surface Water Resources in Azraq Basin. Unpubl. Report, Water Authority, Amman, Jordan.

Gale, L. (2005). Strategies for Managed Aquifer Recharge (MAR) in semi-arid areas, UNESCO's International Hydrological Programme (IHP).

Hobler, M., Margane, A., Almomani, M., Subah, A. (2001). Groundwater resources of northern Jordan Volume-4 contribution to the hydrogeology of Northern Jordan. BGR-WAJ technical cooperation project.

Humphreys, H. (1982). Azraq Well Field Evaluation (Hydrochemistry & Monitoring), Water Authority 37 pp.

Lloyd, J. W. (1992). Deep Aquifers and the Impact of their Exploitation, Jordan's Water Resources and their Future Potential. Symposium 27th and 28th October 1991 Organized by Friedrich Ebert Stiftung, Higher Council for Science and Technology, Water Research and Study Center: 49-67.

Piper, A.M. (1944). A graphical interpretation of water analysis, Transactions of the American Geophysical Union 25: 914 -928.

Salameh, E. and Udluft, P. (1985). The Hydrodynamic pattern of the central part of Jordan. Geoloisches Jahresbuch 38 (C): 39-53.

Soil Conservation Service (1969). Computer Program for Project Formulation, Technical Release. 20, U.S. Department of Agri¬culture, Washington D., USA.

Soil Conservation Service (1972). National Engineering Hand¬book. Section 4, Hydrology, U.S. Department of Agriculture, Wa¬shington, D.C., USA.

Soil Conservation Service (1975). Urban Hydrology of Small Watersheds, Technical Release No.55, Engineering Division, U.S. Department Agriculture, Washington, D.C., USA.

Ayed, R. (1996). Hydrological and Hydrogeological Study of the Azraq Basin, Jordan, Ph. D. thesis, Baghdad University, Iraq.

United States Department of the Interior, (1960). Design of Small Dams, United States Government Printing Office, 1st edition, 611 p, Washington, USA.

WAJ Files Data, Water Authority of Jordan (Rainfall, Evaporation and Wells Data), Amman, Jordan.

Water Authority (1989). North Jordan Water Resources Project. Investigation Project Staff. Unpubl. Report, Water Authority, Jordan.

JJEES

JJEES (2021) 12 (3): 241-253
ISSN 1995-6681

Jordan Journal of Earth and Environmental Sciences

Impacts of Brick Kilns on Environment around Kiln areas of Bangladesh

MK Saha[1], SJ Ahmed[2], AH Sheikh[3], MG Mostafa[1*]

[1]Institute of Environmental Science, University of Rajshahi, Rajshahi 6205, Bangladesh
[2]Department of Physics, Dhaka University of Engineering and Technology (DUET), Gazipur, Bangladesh
[3]Department of Geography and Environmental Studies, University of Rajshahi, Rajshahi 6205, Bangladesh

Received 11 November 2020; Accepted 21 January 2021

Abstract

The study aimed to assess the impacts of the brick kiln on the environment around the kiln areas. The study conducted a survey based on a structured questionnaire and sampling at selected 12 brick kiln clusters in Rajshahi and Gazipur Districts of Bangladesh. The sampling analysis results were compared with the national and international standard limits. The survey results illustrated that about 69% of respondents thought that the brick kilns were the vital source of air pollution in the areas. The study revealed that the criteria air pollutants (CO, SO_2, NO_x, PM 2.5, PM 10, SPM) except CO exceeded the National Ambient Air Quality Standard (NAAQS) limits. The higher level of lead (Pb) and chromium (Cr) in the fly ash samples might have influenced the heavy metals pollution in the farm soil and surface water. About 100% of surface water samples exceeded the permissible standard limit for Pb. The noise level was found higher than the acceptable level (75 dB) of the Department of Environment, Bangladesh (DoE, BD) standard. Thus, the study observed that the brick kilns cause a threat to the environment and human health in the study areas.

Keywords: Brick kiln, environment, impact, pollution, toxic, Bangladesh.

1. Introduction

The industries discharged or emitted several toxic elements including, salinity, organic load (chemical oxygen demand, biological oxygen demand), inorganic matter, dissolved, suspended solids, heavy metals, and other salt residues to the environment caused severe environmental pollution (Manjushree et al., 2013). Industrial wastewater contains heavy metals that degraded the aquatic ecosystem, as well as aquatic life. Surface water in Bangladesh has been contaminated with heavy metals, causing a significant health hazard for humans (Helal et al., 2011). The brick kilns are blamed for adding environmental pollution in different parts of Asia including, Bangladesh, India, and Sri Lanka. The number of brick kilns in Bangladesh is likely to exceed 10,000 (BUET, 2007). The annual rate of demand for the bricks is rapidly increasing every year for profligate industrialization. Industrialization in Bangladesh is growing without any proper planning and management. The brick-making sector is the largest buyers of coal as brick burning is an energy-intensive process (around 24 million tons/year) in Bangladesh. It is also the source of the largest air pollutants (World Bank, 2011). The brick kiln emissions the trends in air quality over the past decade stated that seasonal variations in both the PM 2.5 and PM 10 concentrations occurred and exceeded the national standards during the dry season while they were below the standards during the rainy season (Islam and Afrin, 2015). The hazardous elements are presently brought forward from the brick kilns every year. The elements mixed up with air, soil, and water resulting in changes of physical, chemical, and biological properties, and it causes environmental pollution. Most of the brick kilns have not well designed with enough ventilation facilities that resulted in incompetent fuel-air mixing and incomplete combustion of fuel (Maithel et al., 2012). It produces blackish smoke containing harmful gases and short-lived climate pollutants (SLCPs) such as black carbon. The emission of CO_2 and SLCPs from the traditional brick kilns impact on the meteorological conditions of South Asia (CCAC, 2014). It also contributes to regional and global warming (Skinder et al., 2014). Brick kilns smoke and haze engulfed is a regular phenomenon in South Asia. Islam (2002) stated that half a dozen brick-manufacturing factories spewing out brown smoky haze at Gaffargaon Upazilla of Mymensingh district in Bangladesh. Another study reported that the brick kilns smoke and haze are engulfed every morning and evening in the Panchkhal Valley of Kavrepalanchowk district in Nepal (Bam, 2018). Brick manufacturing in Bangladesh and among the top three sectors, along with vehicle exhaust and suspended road dust, contributing to the air pollution and health problems in Dhaka. A research report illustrated that a total of released gases and particulate matters from the brick kilns in the Dhaka region of Bangladesh were estimated to be 15,500 tons of SO_2, 302,000 tons of CO, 23,300 tons of PM 2.5, 6,000 tons of BC, and 1.8 million tons of CO_2 emissions. It produced severe air pollution in the region (Guttikunda et al., 2013). The brick kilns have both long-term and short-term impacts in the agricultural sector including, vegetation hampers, loss of crop yield, plant fruits fall, etc. It also impacted ozone depletion, global warming, photochemical smog's, land fertility decreases, etc. (Pokhrel

* Corresponding author e-mail: mgmostafa@ru.ac.bd

and Lee, 2011). Moreover, the brick kilns are considered to be vital for environmental contamination of surrounding areas. Dey and Dey (2015) analyzed the various physicochemical properties of like WT, pH, EC, Transparency, TA, DO, FCO_2, nitrate, and phosphate to study the impact of brick industries of Cachar district, Assam on the aquatic bodies by using Standard Methods. They found that the water temperature (WT) in the aquatic system near the brick kilns increased due to the emissions of heat from the kilns, which slightly raise the water temperature in nearby aquatic systems. Morley (2012) reported that each kiln burned an average of 350 tons of woods per year, and the number of kilns is increasing every year resulted in devastating effects on the forests. A survey conducted on the brick kiln areas and stated that inhabitant near the kilns is more likely to suffer from health hazards caused by pollution of kilns, comparing those who are not living in the areas of the brick kilns (Joshi and Dudani, 2008). The brick-making sector in Bangladesh relies on the manual labor of millions of workers. Ghoshal (2008) conducted a study in Tripura of Indian that illustrated the working and living conditions of the brick kiln workers were not satisfactory. The Government of Bangladesh amended the Brick Kiln Control Act (2001) that prohibits the setup of the brick kilns within a three-kilometer radius of human inhabitation as well as an orchard. However, with the lack of administrative manpower and infrastructure facilities, the act remains a useless one, as the kilns are even operating less than one kilometer of a densely colonized area (DoE, 2013). The adverse effects on the physical and chemical properties of the ambient air, surface water, farm soil, sound quality, crop production, and human communities affected by the brick kilns emissions are now a matter of great concern. The study aimed to assess the impacts of brick kilns on the environment around the kiln areas of Bangladesh.

2. Materials and Methods

The study consisted of two parts, i.e., one was a questionnaire survey, and another was laboratory experiments through sample collection and analyses. The study selected twelve (12) brick kiln clusters in Rajshahi and Gazipur Districts. Rajshahi is a district in the north-western part of Bangladesh. It is lying between 24°22′26″ in north longitude and 88°36′4″ in east latitude. The climate of Rajshahi is generally marked with monsoons, high temperature, considerable humidity, and moderate rainfall. The hot season commences early in March and continues till the middle of July. The maximum mean temperature observed is about 32 to 36 °C (90 to 97°F) during April, May, June, and July. The minimum temperature recorded in January is about 7 to 16°C (45 to 61°F). The highest rainfall is observed during the months of monsoon. The average height of the Rajshahi district from the mean sea level is 18 meters. The average annual rainfall in the district is about 1,448 mm (BBS, 2013a). Another sampling location, Gazipur is a district in the central part of Bangladesh. It is lying between 24°54′5″ in north longitude and 90°24′45″ in east latitude. Gazipur has a tropical climate. The summers are much rainier than the winters in Gazipur. The average minimum and maximum temperature in Gazipur are 12.7°C and 36.0°C, respectively. The average height of the Gazipur from the mean sea level is 34 meters. The average annual rainfall is 2376 mm (BBS, 2013b).

A structured questionnaire comprised of simple and direct questions was developed by the research team using focus group discussion (FGD). Finally, it was pre-tested by the opinions of the experts and respondents. The questionnaire survey was conducted to understand public awareness of different environmental and social issues due to the brick kiln emissions. The questionnaire survey was conducted through personal interviews of the respondents of the study areas. A total of seven hundred (700) respondents took part in the survey. There were five types of samples, i.e., ambient air, farm soil, fly ash, surface water, and noise sample collected, and some instant data were recorded from different sampling locations in the study area. A total of 72 representative samples were collected during the pre-production, production, and post-production seasons over two years. The ambient air and noise were recorded only in the production season. A high volume air sampler was used (Gray Wolf Sensing, Ireland, and Casella CEL, UK) to assess the air quality around the brick kiln area. The air quality parameters, namely CO, SO_2, NO_x, PM 2.5, PM 10, SPM, O_2, CO_2, AT, RH, H_2S, C_8H_6, C_6H_6, TVOC, respectively were recorded during the ambient air sampling. The farm soil samples were collected at the depth of 0-15 cm for laboratory analysis. The fly ash samples were collected from different types of crop and tree leaves at different sampling locations. The selection of the surface water body for the collection of water samples was based on nearness to brick kiln areas as the study comprised determination of contamination in water. Several physicochemical parameters, including temperature, pH, EC, DO, TDS, TSS, BOD_5, COD, NH_3, TC, FC, salinity, turbidity, heavy metals, and anions were considered for analysis of the farm soil, fly ash and water. A precision noise level meter (Lutron, SL-410, Taiwan) was used to detect the noise intensity of different sources. The samples were analyzed using different conventional and standard scientific methods. The results were then analyzed using various computer soft wares like MS Office, Arc GIS, Adobe Photoshop, etc., after QA/QC of the data and the analysis techniques and results obtained. The analysis data were compared with national and international standards.

2.1. Assessment of Pollution Load Index and Risk Index

The study was conducted to achieve the pollution load index and risk index of heavy metals in the farm soil using the method Hakanson, 1980. The computing equation for contamination factor (C^i_f) and the degree of contamination (C_d) are as follows:

$$C_f^i = \frac{c_i}{c_n^i} \quad \text{..... (1)}$$

$$C_d = \sum_{i=1}^{n} C^i_f \quad \text{..... (2)}$$

Where C^i is the measured concentration of the heavy metals in farm soil.

2.1.1. Pollution Load Index (PLI)

The extents of pollution by the heavy metals were assessed by employing the method based on the pollution load index (PLI) developed by Tomlinson et al. (1980) and the expression is shown below:

$$PLI = (C_{f1} \times C_{f2} \times C_{f3} \times \dots\dots\dots \times C_{fn})^{1/n} \quad \text{..... (3)}$$

Where n is the number of metals (n = 5 in this study) and C_f is the contamination factor.

2.1.2. Risk Index

The potential ecological risk factor (E^i_r) of a single element and the potential ecological risk index (RI) of multi-element can be computed by the following equations:

$$E^i_r = T^i_r \times C^i_f \quad \text{..... (4)}$$

$$RI = \sum_{i=1}^{n} E^i_r \quad \text{..... (5)}$$

Where,$C^i_f$is the contamination factor for the element of "i"; T^i_r is the toxic-response factor for the given element of "i", which accounts for the toxic requirement and sensitivity requirement.

3. Results and Discussion

The study determined the impacts of the brick kiln emissions around the kiln areas. The results obtained from the field survey and sampling analyses of different types of samples are incorporated in this study. The results are interpreted and discussed in the following sections.

3.1. Survey Responses

During the study, several respondents have given their opinions regarding the brick kiln impacts on environmental degradation, crop yield, soil and land condition, deforestation, occupational situation, etc. The responses to the survey questionnaire are discussed below.

3.1.1. Environmental Degradation

The respondents in the study area were assumed to face several environmental degradation issues surrounding the brick kiln areas. The study considered several assessment parameters to measure their extent of vulnerability (Table 1). The peoples' perception regarding various environmental degradation illustrated that about 69 and 68% of highly vulnerable to air pollution and hamper natural environment, respectively, due to brick kilns (Table 1). However, about 64% of the population did not make any comments on noise pollution due to brick kilns. The results indicated that most of the people thought that the brick kilns were high to medium level of vulnerable to different environmental degradation parameters. The vulnerability assessment results indicated that the selected parameters have significant influences on the environment in the brick kiln areas. Guttikunda and Khaliquzzaman (2014) reported that the brick kilns in agricultural lands, low quality wooden fuel in the brick kiln, improperly fixed chimneys, and the violation of laws to conserve the environment is leading this sector into a major cause of environmental pollution. Moreover, the study observed that there was almost no monitoring and controlling of the brick kiln operation process due to the lack of administrative and logistical supports towards improving environmental sustainability.

Table 1. Survey responses to vulnerability level on environmental degradation.

Assessment parameters	Assessment on vulnerability level			No comments (%)
	High (%)	Medium (%)	Low (%)	
Hamper the natural environment	67.86	17.14	9.28	5.72
Air pollution	69.28	19.29	5.00	6.43
Water pollution	27.86	25.00	12.86	34.28
Soil pollution	35.71	22.86	20.00	21.43
Noise pollution	9.29	16.43	10.00	64.28
Raising ambient temperature	46.43	24.99	17.86	10.72
Affected biodiversity	32.15	28.57	3.57	35.71
Overall assessment	44.23	22.04	11.23	25.51

3.1.2. Socio-Environmental Issues

There are some socio-environmental issues raised in the brick kiln areas. These issues were loss of crop production, land and soil degradation, solid waste generation, disrupted transportation system, deforestation, hampers labor rights, complexity in a social relationship, etc. The field survey responses to socio-environmental issues relevant to the brick kilns are summarized in Table 2. The survey result revealed that the farmers near the brick kilns got less food production due to brick kiln emissions. All types of agricultural plants near the kiln areas were in an exhausted condition. The temperature rise and emission gases from brick kilns have caused severe impacts on the fruit plants in Rajshahi areas. The diseases include mango splatter and damage in mango stalk, growth affected in jackfruits, root damage in banana, spotted leaves and production loss in litchi, sacking the vegetation, and finally expire in date palms and immaturity and spotted surface in green coconut. It also observed that the mango production near the brick kilns was hampered due to the increase in ambient temperature. The study results showed that about 65% of brick kilns were situated in agricultural land. The farm soil is used as a vital raw material for brick production, and about 95% of the brick-making soils were collected from the topsoil of the agricultural lands, so every year, the agricultural lands lose fertility. Besides, agricultural lands also lose by installing new brick kilns. Nusrat and Mahadev (1991) investigated the loss of soil fertility due to brick making soil in Mysore in India. The study also observed that the brick kiln created about 50 and 55% of unwanted wetland and waterlogging conditions in the study areas, respectively (Table 2). Mazumdar et al. (2018) reported that water logging is a serious problem around the brick kiln areas. The survey results showed that the brick kiln produced different types of solid waste, such as broken parts of bricks, coal, and wood, etc. The coal ash and wooden trash also the source of solid waste in the brick kilns. Moreover, over burnt and broken bricks also produced a substantial amount of waste. This excess amount of wastes gets dispersed to neighboring areas by blowing wind or by human activities. A study conducted by Das (2015) on

brick kilns and stated that the several negative impacts of brick kiln identified, solid waste generation is one of them at Khejuri blocks, Medinipur, West Bengal in India.

The study apparent that essential brick burning fuel used as forest wood, and about 40% used fuel as wood in the study areas. The brick kiln has a high impact on the deforestation process. The consumption of biomass fuels is generally considered to be neutral to emissions of carbonaceous greenhouse gases, which means the CO_2 emitted during the brick burning process. Morley (2012) reported that each brick kiln burned 350 tons of woods a year in Bangladesh, so more kilns mean having a devastating effect on the forests. The other parameters, such as disrupted transportation system, visibility reduction, Complexity in a social relationship, etc. have impacts on socio-environmental deprivation. Das (2015) conducted research on land degradation by brick kin setup stated that different types of socio-economic and environmental problems raised due to brick kiln at Khejuri blocks, PurbaMedinipur, West Bengal in India. Therefore, the brick kiln act as a genuine agent of land and soil degradation, deforestation, etc. and as well as environmental degradation.

Table 2. Field responses to socio-environmental issues.

Socio-environmental issue	Effect	Percentage (%) of loss
Loss of crop production	Crop disease	25% crops
	Low production	15% crops
Land and soil degradation	Agricultural land loss	65% brick kiln situated in ag. land
	Removal of topsoil	95% collected soil from ag. land
	Formation wet land	50% brick kiln areas
Threat for irrigation and water management	Water logging condition	55% brick kiln areas
	Damage command area	15% brick kiln areas
Solid waste generation	Affected areas	35% surrounding areas
Disrupted transportation system	Town road	15% damage
	Village road	35% damage
Degraded river condition	River grabbing	15% sampling locations
	River pollution	10% sampling locations
Deforestation	Brick kiln setup	30% brick kiln areas
	Fuel wood	40% used fuel
Visibility reduction	Smog formation	40% brick kiln areas
Hamper labors right	Physically damaged	35% labors injured
	Poor accommodation	Almost 100% kiln areas
	Child labor	15% labor were child
Complexity in social relationship	Conflict between kiln owner and community people	Almost 100% kiln areas

3.2 Ambient Air Pollution

The brick kiln in Bangladesh is highly energy-intensive and carbon-emitting. It includes land clearing for sand and clay, combustion of fuel for burning, uses of diesel engines on-site, and finally, transportation of the end product that's led to cause air pollution. The study results of ambient air quality showed that most of the parameters exceeded the permissible standard limit. The biomass fuels like firewood, coal and diesel were responsible for emitting particulates and toxic gasses such as SO_2, NO_x, and CO_2 in the kiln areas. The ash and sulfur-containing coals together with rubber tires are using as initial firing material for manufacturing brick has to lead to increasing enormous emissions. The heavy metal contaminations occurred in the atmosphere, aquatic bodies, and soil surface due to fossil fuels. The criteria air pollutants (CO, SO_2, NO_x, PM 2.5, PM 10, SPM) except CO exceeded the National Ambient Air Quality Standard (NAAQS) limits. Most of the parameters exceeded the NAAQS standards at all sampling locations. The particulate matter concentration in ambient air was found highest among all types of ambient air quality parameters. The concentrations of PM 2.5 and 10, and SPM were ranged from 57 to 2573, 287 to 3875, and 519 to 1950 $\mu g/m^3$, respectively (Table 3).

Guttikunda (2009) stated that brick kilns emitted PM 2.5, which considered being harmful to humans because it can travel deeper into the respiratory system and cause premature mortality and respiratory ailments. The concentration of criteria air pollutants was found higher in the Gazipur region than the Rajshahi due to the higher number of brick kilns per cluster in the areas (Figure 1). Some vital parameters of air quality monitoring, including O_2, ambient temperature (AT), relative humidity (RH), and C_6H_6 violated the permissible standard limit, which influenced the entire condition of ambient air quality. The study found that CO_2 present in the ambient air was within the limit (OSHA, 2010), but, the increase in CO_2 concentrations is known to cause smaller stomatal apertures in the plant. Hence the decrease in the leaf conductance for water vapor (Morison and Gifford, 1987). The study showed that the ambient temperature was found to be higher around the kiln areas due to kiln heat emitted during the brick production season. But the average temperature of Bangladesh ranges from 7.2 to 12.8°C during winter and 23.9 to 31.1°C during summer (Shahid, 2010).

The ambient temperature and relative humidity during the peak brick production season (January-February) were found to be higher than the areas about one Km away from a kiln indicating the kiln emitted heat has a significant influence on the environment. The gaseous pollutants, CO, H_2S, C_8H_6, and TVOC were found very low at all locations indicating not be harmful to the environment (Table 3). However, the inappropriate process of the kiln may increase emissions. Higher emissions are also expected during the stabilization period after startup in the new season. Cui et al. (2015) reported that air pollutants deposited on the ground and seeped into the soil affected the soil pH and lead to permanent degradation. Several plants are sensitive to air pollutants, as they can damage their leaves, impair plant, growth, and limit primary productivity (Ulrich, 1984). A study conducted the effects of ambient air pollutants including, NO_x, SO_2, and particulate matters on some crops grown in the urban and industrial areas of Haridwar city (Chauhan and Joshi, 2010). It observed that the gaseous (SO_2 and NO_x) and particulate pollutants have detrimental effects on the crops through changes in morphological characteristics, photosynthetic pigments, and yield of crops.

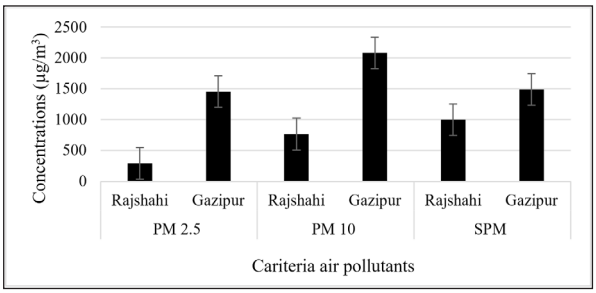

Figure 1. Biyearly concentrations of particulate criteria air pollutants during the brick production season (January-April) in 2016-2017.

Table 3. Statistical analysis of ambient air quality parameters and comparison with the standard limits.

Parameters	Study area	No. of Samples	Minimum	Maximum	Mean ± SD	No. of Sample exceed/below	Permissible standard
NO_x (ppm)	Rajshahi	16	0.008	0.222	0.075 ± 0.049	>07	0.053 ppm (AA, NAAQS, 2005)
	Gazipur	08	0.167	0.972	0.489 ± 0.327	>08	
SO_2 (ppm)	Rajshahi	16	0.039	0.423	0.148 ± 0.104	>16	0.03 ppm (AA, NAAQS, 2005)
	Gazipur	08	0.078	0.612	0.253 ± 0.181	>08	
CO (ppm)	Rajshahi	16	0.91	3.10	1.855 ± 0.626	Within the limit	35 ppm (AA, NAAQS, 2005)
	Gazipur	08	0.41	2.80	2.006 ± 0.860	Within the limit	
PM 2.5 (µg/m³)	Rajshahi	16	57	821	289.18 ± 249.07	>16	50 µg/m³ (AA, NAAQS, 2005)
	Gazipur	08	725	2573	1454.25 ± 697.75	>08	
PM 10 (µg/m³)	Rajshahi	16	287	1523	766.69 ± 315.59	>16	15 µg/m³ (AA, NAAQS, 2005)
	Gazipur	08	1134	3875	2083.25 ± 991.43	>08	
SPM (µg/m³)	Rajshahi	16	519	1653	998.69 ± 319.72	>16	140 µg/m³ (AA, NAAQS, 2005)
	Gazipur	08	1052	1950	1491 ± 408.61	>08	
O_2 (%)	Rajshahi	16	17.3	20.1	18.63 ± 0.80	16<	20.95% (IAC)
	Gazipur	08	17.7	18.5	17.85 ± 0.54	08<	
CO_2 (ppm)	Rajshahi	16	428	582	504.56 ± 38.70	Within the limit	5000 ppm (OSHA)
	Gazipur	08	415	814	651.37 ± 130.65	Within the limit	
AT (°C)	Rajshahi	16	29.80	35.00	32.54 ± 1.66	>16	25 °C (IAC)
	Gazipur	08	35.40	39.10	37.69 ± 1.29	>08	
RH (%)	Rajshahi	16	68.3	76.5	72.66 ± 2.87	>16	40-50% (IAC)
	Gazipur	08	65.0	73.5	68.85 ± 3.10	>08	
H_2S (ppm)	Rajshahi	16	0.014734	0.125239	0.059 ± 0.033	Within the limit	15 ppm (WSH Act, 2006)
	Gazipur	08	0.014734	0.176808	0.073 ± 0.054	Within the limit	
C_8H_6 (ppm)	Rajshahi	16	0.043	0.145	0.083 ± 0.031	Within the limit	50 ppm (WSH Act, 2006)
	Gazipur	08	0.0529	0.0835	0.069 ± 0.011	Within the limit	
C_6H_6 (ppm)	Rajshahi	16	0.0324	0.139	0.082 ± 0.031	>16	0.001608 ppm (AA, NAAQS, 2009)
	Gazipur	08	0.063	0.096	0.078 ± 0.010	>08	
TVOC (ppm)	Rajshahi	16	0.092	0.285	0.159 ± 0.063	-	Not set
	Gazipur	08	0.114	0.172	0.143 ± 0.020	-	

The enormity of air pollution has always been a matter of concern due to the rapid development of brick kiln over a long period. However, the pollutants including NO_x, SO_2, CO, O_2, C_6H_6, PM 2.5, PM 10, and SPM were detected at a higher level, violating the standard in ambient air in the brick kiln has deteriorated the air quality at an alarming rate.

3.3. Farm Soil Pollution

The soil is a natural resource made of mineral and organic constituents. Farm soil degradation is one of the most serious problems in the world. Three-quarters of the world soil degradation occurs in tropical areas, and about 7% of the total land area (13,391 km²) of Bangladesh is experiencing

land degradation but, the soil degradation has not been considered due to brick production so far (Eswaran, 1999). The pH and organic matter in the farm soil samples were found to be very low. So the nutrient elements and soil biota of the topsoil are destroyed through brick burning. Khan et al. (2007) found that the brick burning process decreased the average pH values of soils with the depth function. It has greatly influenced the concentrations of greenhouse gases in the atmosphere. Thus, it is essential to investigate the contribution of soil to the release and fixation of greenhouse gases (IUSS, 2002). The brick kilns emitted heat seriously degraded the farm soil quality. A report showed that the brick burning emitted heat reduces the surrounding soil moisture (Mazumdar et al., 2018). The nutrients of the farm soil, which are generally found in the top layer were affected and destroyed through heat emission. The results showed that most of the organic matter content in the production season was lower compared to other seasons. The lower values of organic matter (OM) and organic carbon in the soil are responsible for the lower cation exchange capacity, holding capacity, soil erosion, and reduces microbial activity (Van Loon and Duffy, 2007). The farm soil parameters, such as pH, organic matter, soil texture were found to be critical conditions. Most of the farm soil samples found more than 50% of sand particles in the production seasons (Table 4). There are no available standards of the above parameters, and therefore some published reports' observations were cited here to evaluate the soil status. A report showed that the soil texture might be affected by wind erosion that produced dust around the brick kiln (Abuduwaili and Mu, 2002). Under changing environmental conditions, the soil particles, i.e., sand, silt, and clay bound heavy metals like Pb, Cr, As, etc. may exhibit extreme toxicity even at low levels under certain conditions (Peerzada, 2004).

Table 4. Statistical analysis of farm soil parameters comparison with the standards.

Parameters	Study area	No. of Samples	Minimum	Maximum	Mean ± SD	Sample exceed / below (No.)	Reference of permissible standard
pH	Rajshahi	48	6.18	8.29	7.67 ± 0.46	>12/<1	6.5 - 8.0 Tisdale et al. (1999)
	Gazipur	24	6.60	8.48	7.44 ± 0.50	>4	
OM (%)	Rajshahi	48	0.58	3.21	1.51 ± 0.49	<20	> 1.38 % Neupane and Bishat (2015)
	Gazipur	24	0.34	1.47	0.93 ± 0.32	<22	
Soil texture	Rajshahi	48	Sample content > 50 % of sand particles		56.29%	>34	Hannan (1995)
	Gazipur	24			64.97%	>18	
Pb (ppm)	Rajshahi	48	9.53	31.27	16.66 ± 5.81	On limit	300.00 ppm (DEP, 2003)
	Gazipur	24	6.54	23.86	11.53 ± 5.09	On limit	
Cr (ppm)	Rajshahi	48	9.50	52.77	26.77 ± 12.22	>02	50.00 ppm (DEP, 2003)
	Gazipur	24	16.54	70.13	37.61 ± 13.94	>04	
Cd (ppm)	Rajshahi	48	0.42	1.95	0.97 ± 0.32	On limit	3.00 ppm (DEP, 2003)
	Gazipur	24	0.91	1.85	1.19 ± 0.24	On limit	
As (ppm)	Rajshahi	48	2.90	6.80	5.01 ± 0.91	On limit	20.00 ppm (DEP, 2003)
	Gazipur	24	1.10	3.40	2.02 ± 0.53	On limit	
Fe (ppm)	Rajshahi	48	1.12	3.03	2.02 ± 0.47	<48	20000 – 550000 ppm Bodek et al. (1988)
	Gazipur	24	1.59	2.81	2.16 ± 0.34	<24	
Zn (ppm)	Rajshahi	48	12.68	79.34	41.23 ± 18.21	>45	16.00 ppm Crommentuijn et al. (1997)
	Gazipur	24	11.24	78.51	40.58 ± 20.41	>20	

The brick kilns are one of the principal causes of topsoil degradation and environmental pollution. They degraded large areas of land every year, especially in Bangladesh. The brick-making soils collected from a depth of about 1 to 2 m of agricultural land. The land areas extended over about 5000 ha during the year 1998-99 in different pockets of brickfields (Rahman and Khan, 2001). The heavy metals, like Pb, Cd, and As were found to be very low at all of the farm soils indicated not harmful to the agricultural work (Table 4). The Cr, Fe, and Zn ion violated the permissible standard limits of soil samples among the heavy metals. The concentration of heavy metals, including Cr, Fe, and Zn ion varied from 9.50 to 70.13, 1.12 to 3.03, and 11.24 to 79.34 ppm in the study area, respectively (Table 4). The higher concentration of the toxic metal ions in the soils with the acidic pH affected the plants. Kudesia (1990) stated that brick kiln used low-quality coal seems to have high Cr concentration may also be the cause of plant growth reduction, soil fertility loss, and also, some hazardous diseases of the human being. The concentration of heavy metals at different locations varies might be attributed to the direction and velocity of wind, age of the topsoil, deposition of heavy metals, etc. The study observed that most of the heavy metal concentration in the farm soils of the Gazipur region is higher than the Rajshahi region (Figure 2). The results indicated that the maximum concentration of metal ions found in Gazipur may be due to the higher number of kilns per cluster in Gazipur districts compared to Rajshahi. Budhwar et al. (2006) studied the effect of brick kiln emitted heavy metals on the soil and plants around the brick kiln chimneys. The results showed that only Cr exceeded the permissible standard limit of some soil samples. Heavy metals like Pb, Cr are reported to have contaminated and reduced the soil quality and damaged the plant life (Maya et al., 2015). High concentrations of the toxic components in the soils with an acidic pH affected the plant community and posed a threat to human health, who consumed the contaminated crops (Ochieng et al., 2010).

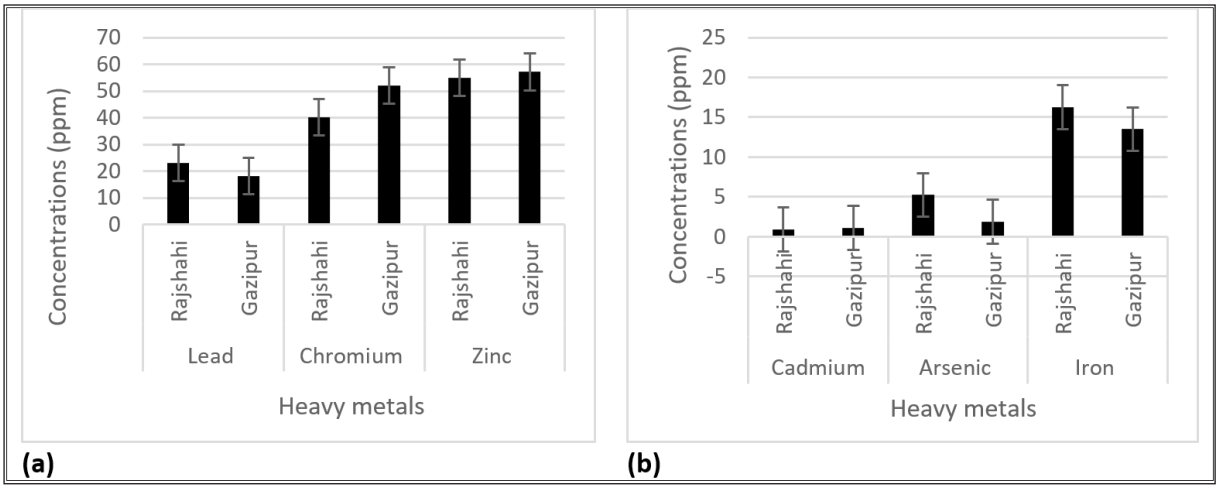

Figure 2. Biyearly concentrations of heavy metals in farm soil samples during the production season (January-April) in 2016-2017.

The study results showed that the values of contamination factor (C^i_f) and ecological risk factor (E^i_r) in the selected farm soil of Rajshahi and Gazipur districts existed in the order of Cd > As > Cr >Pb> Zn and Cd > As >Pb> Cr > Zn, respectively (Table 5). The study results showed that pollution load index and risk index values were found lower than 1 and 150, respectively, at all sampling locations indicating low risk and pollution from heavy metals in the areas (Table 5). A study conducted on the impacts of industrial effluents on the soil in BSCIC of Rajshahi revealed that the heavy metals contamination in the industrial areas showed a lower pollution load index and low-risk index. The observation supports the present finding (Hossain, 2018). However, the continuation of brick kilns operation in the areas would become threatened for soil fertility in the future.

The fly ash is a byproduct of a brick kiln disposed of in the form of ash slurry into the surrounding land, waterbody, vegetation, etc. Heavy metal contamination in the environment is a global problem that is a growing threat to human beings. The study conducted to estimate the content of heavy metal in the fly ash produced from the brick kiln. There is no standard permissible limit available for heavy metals in the fly ash. It contains an appreciable amount of Pb, Cr, and Cd (USEPA, 2003). The study observed that firewood, coal, and petroleum were used as fuel for brick burning, which produced fly ash enriched with heavy metals including Pb and Cr in the production seasons at the kiln areas. Al-Hiyaly et al. (1988) reported that the fly ash produced from coal burning, which added a higher concentration of Pb into the environment. The lead (Pb) and chromium (Cr) concentrations were found very high in the fly ash samples at different locations might have influenced the heavy metals pollutions in the soil and water (Table 6).

The study findings supported the report of Verma et al. (2017), which showed a higher concentration of heavy metals in the production season compared to other seasons. The heavy metals concentration of collected fly ash samples in the areas followed in the order: production season> post-production season > pre-production season (not shown in Table). The study results revealed that the fly ash produced from the combustion process of brick kilns is one of the sources of heavy metal pollution. The fly ash and surface run-off contaminated water from the kilns areas indisputably declines the soil fertility and crop production in the surrounding agricultural lands. The presence of heavy metals in the fly ash is a matter of concern. Moreover, the disposal of such huge amounts of fly ash degraded the entire environment.

Table 5. Biyearly of contamination factors (C^i_f), pollution load index (PLI), potential ecological risk factors (E^i_r) and risk index (RI) of heavy metals in farm soil samples during September 2015 - August 2017.

Study area	Contamination factors (C^i_f)					Pollution load index (*PLI*)	Potential ecological risk factors (E^i_r)					Risk index (*RI*)
	Pb	Cr	Cd	As	Zn		Pb	Cr	Cd	As	Zn	
Rajshahi	0.239	0.297	0.976	0.334	0.235	0.303	1.189	0.594	29.253	3.341	0.235	34.616
Gazipur	0.167	0.417	1.189	0.135	0.232	0.291	1.081	0.668	31.24	2.728	0.234	35.943

Table 6. Biyearly descriptive statistics ofheavy metal concentration in fly ash samples from September 2015 - August 2017.

Heavy metals	Study area	Minimum	Maximum	Mean ± SD
Lead (Pb)	Rajshahi	1.9862	26.2878	9.59 ± 7.96
	Gazipur	3.0458	24.8154	11.01 ± 7.83
Chromium (Cr)	Rajshahi	0.8517	18.2155	9.26 ± 5.90
	Gazipur	3.2065	19.2111	12.35 ± 5.70
Cadmium (Cd)	Rajshahi	0.0098	0.0934	0.032 ± 0.019
	Gazipur	0.0063	0.0643	0.026 ± 0.014
Arsenic (As)	Rajshahi	0.0001	0.0074	0.003 ± 0.002
	Gazipur	0.0005	0.0096	0.003 ± 0.002
Iron (Fe)	Rajshahi	0.0048	0.0640	0.020 ± 0.012
	Gazipur	0.0094	0.0738	0.032 ± 0.022
Zinc (Zn)	Rajshahi	0.0023	0.0917	0.041 ± 0.022
	Gazipur	0.0026	0.1124	0.040 ± 0.029

3.4 Surface Water Pollution

The surface water reflects its ecological potential and sustenance quality by its biological, chemical, and physical characteristics. The study analyzed the concentration of different parameters in aquatic bodies near the brick kilns. The DO concentration in most of the surface water samples was found lower, and the lowest concentration of DO was 1.0 mg/l found in the Gazipur area (not shown in Table). The study observed that the DO values of most of the surface water samples were found lower compared to the standard limit in both the study areas indicating surface water was not suitable for aquatic life. Cox (2003) reported that aquatic animals are forced to alter their breathing patterns or lower their level of activities in a reduced DO level in a water body. The study also revealed that very few numbers of samples exceeded the permissible standards limit in Gazipur, and the water was more turbid in affected water bodies. The biyearly mean value of turbidity in the collected surface water samples was 24.24 and 33.89 NTU in Rajshahi and Gazipur, respectively (Table 7). The turbidity variation in the surface water at different locations might be due to the pollution loads in the water. Mazumdar et al. (2018) reported that the high turbidity might be responsible for the high level of water temperature in the water bodies near brick kiln because the suspended particles absorb the heat from the sunlight making the water warm. The biyearly mean value of color in the collected surface water samples was 42.29 and 63.75 pt-co in Rajshahi and Gazipur, respectively (Table 7). The higher color concentration of water might be due to the presence of oxygen demanding wastes, dissolved solids, and particulate materials in the surface water. During brick production, huge amounts of particulates, including fly ashes and suspended particles, and finally, it fell into the surface water bodies. The study observed that the degree of color in the surface water increased every year and the rate of increasing the trend indicating declined the surface water quality. Saha et al. (2020a; 2020b) reported that oxygen depletion occurs by the pollutants affecting the taste, odors, and colors in surface water and also affects aquatic life.

Table 7. Statistical analysis s of physicochemical parameters of surface water and comparison with the standard limits.

Parameters	Study area	No. of Samples	Minimum	Maximum	Mean ± SD	Violation of No. of Samples	Permissible standard
pH	Rajshahi	48	5.15	7.64	6.72 ± 0.54	<5	6 – 9 (DoE, 2003)
	Gazipur	24	6.09	7.65	6.72 ± 0.44	0	
DO (mg/l)	Rajshahi	48	2.5	6.2	4.19 ± 0.92	<27	4.5 – 8.0 mg/l (DoE, 2003)
	Gazipur	24	1.0	4.9	2.70 ± 1.16	<23	
Turbidity (NTU)	Rajshahi	48	9	41.4	24.24 ± 8.83	0	1 - 50 NTU (USGS, 2006)
	Gazipur	24	11.0	55.1	33.89 ± 12.41	>3	
Color (pt – co)	Rajshahi	48	7	88	42.29 ± 22.29	>44	15 pt – co (WHO, 2003)
	Gazipur	24	32	97	63.75 ± 18.92	>24	
(mg/l)	Rajshahi	48	5.9	65.3	26.20 ± 18.73	>39	10 mg/l (DoE, 2003)
	Gazipur	24	7.0	68.4	30.71 ± 23.11	>21	
(mg/l)	Rajshahi	48	2.7	24.1	8.28 ± 5.17	16	10 mg/l (ECR, 1997)
	Gazipur	24	2.6	13.0	6.83 ± 3.28	>4	
F^- (mg/l)	Rajshahi	48	0.14	2.15	0.79 ± 0.57	>3	2 mg/l (ECR, 1997)
	Gazipur	24	0.23	1.89	0.89 ± 0.60	0	
Pb (ppm)	Rajshahi	48	0.1239	4.9528	2.32 ± 1.23	>48	0.10 ppm (DoE, 2003)
	Gazipur	24	0.7234	4.8152	2.09 ± 1.27	>24	
Cr (ppm)	Rajshahi	48	0.0015	3.9338	1.44 ± 1.18	>32	0.50 ppm (DoE, 2003)
	Gazipur	24	0.0294	3.1217	1.40 ± 1.20	>17	
Cd (ppm)	Rajshahi	48	0.009	0.018	0.040 ± 0.020	>8	0.05 ppm (DoE, 2003)
	Gazipur	24	0.095	0.0048	0.040 ± 0.026	>6	
Fe (ppm)	Rajshahi	48	0.154	0.512	0.316 ± 0.080	0	2.00 ppm (DoE, 2003)
	Gazipur	24	1.850	3.012	2.36 ± 0.354	>21	
FC (CFU/100 ml)	Rajshahi	48	26	95	48.06 ± 16.79	>48	0 CFU/100 ml (WHO, 2003)
	Gazipur	24	21	54	33.16 ± 8.51	>24	
TC (CFU/100 ml)	Rajshahi	48	<100	>200	>150	>48	0 CFU/100 ml (WHO, 2003)
	Gazipur	24	<100	>200	>150	>24	

Among the anionic parameters of the surface water, (NO_3^-), nitrite (NO_2^-), and fluoride (F^-) ions exceeded the standard limits. The (NO_3^-) and, nitrite (NO_2^-) ion concentrations in surface water exceeded the permissible limit at both the study areas indicating significantly harmful to humans, flora, and fauna (Table 7). Kacaroglu and Gunay (1997) reported that the presence of nitrate concentration was higher than 5 mg/l reflecting unsanitary conditions. So it may be called, due to combustion residue of the brick kiln and its blown fly ash and removal of the topsoil layer from the agricultural land, ultimately the eroded soil goes to the nearby aquatic system through catchment channels.

The concentrations of anions, including nitrate, nitrite, and fluoride ions were varied from 5.9 to 68.4, 2.7 to 24.1, and 0.14 to 2.15 mg/l, respectively (Table 7). Vandeviver et al. (1998) reported that the higher concentration of nitrite was highly toxic to humans, flora, and fauna. The result showed that a high concentration of anionic parameters might be due to the higher input load of pollutants like coal burned fly ash and different organic and inorganic pollutant in the aquatic bodies. The study observed that except for nitrite concentration, the other anions in surface water were found higher in the concentration level in the Gazipur region than the Rajshahi region due to the lower number of kilns per cluster (Figure 3). The results indicated that the maximum value of nitrite ions was found to be at Horian in Rajshahi. It may be due to the decomposed bagasse and sludge of Rajshahi sugar mills, Horian, which is very near to the sampling site. The Pb, Cr, and Fe concentrations in most of the surface water samples exceeded the permissible standard. The results illustrated that the heavy metals, including Pb, Cr, Cd, and Fe were in the range from 0.1239 to 4.9528, 0.0015 to 3.9338, 0.009 to 0.095, and 0.154 to 3.012 ppm, respectively (Table 7). Järup (2003) reported that the symptoms of acute lead poisoning are headache, irritability, abdominal pain, and various symptoms related to the nervous system. The concentrations of heavy metals in surface water at different locations were varied might be due to the fallout of pollutants in the aquatic bodies. Other studies reported that the presence of heavy metals in excessive amounts in soil, water, and air leads to several health problems including neurotoxicity, kidney toxicity, sterility, anemia, etc. (Islam and Mostafa, 2020). Al-Hiyaly et al. (1988) stated that fly ash was a vital source of ambient air pollution during the production period. It produced due to coal burning, which added a higher concentration of heavy metals like Pb into the environment. The study observed that the concentration of heavy metals like Pb, Cr, and Fe was found higher in the Gazipur region than the Rajshahi region, Fe concentration, in particular (Figure 4a).

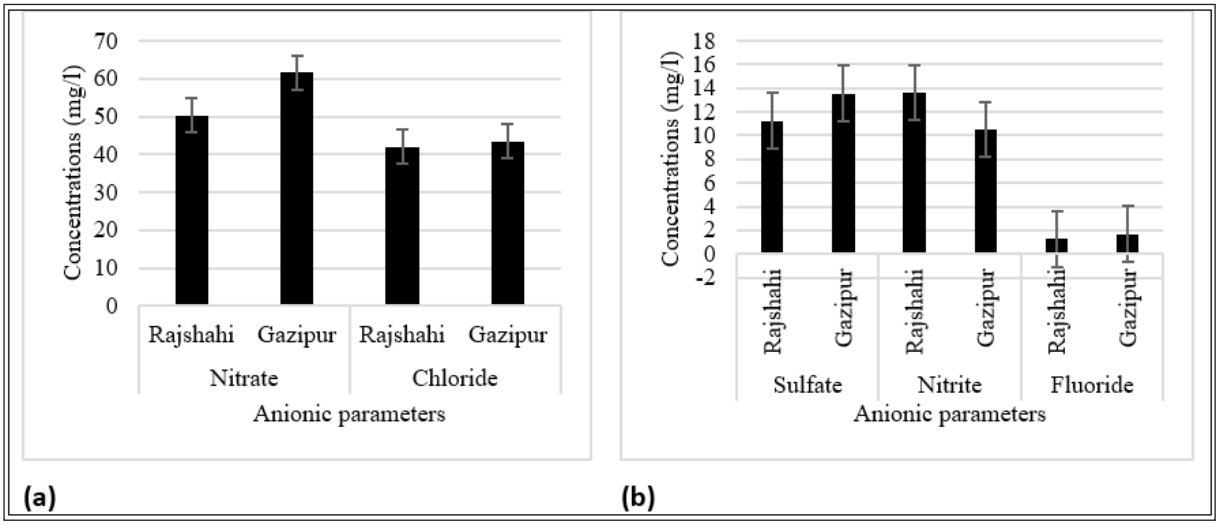

Figure 3. Biyearly concentrations of anionic parameters in surface water samples during the production season (January-April) in 2016-2017.

The results indicated that the higher numbers of brick kilns per cluster in the Gazipur than the Rajshahi areas emitted large amounts of fly ashes and other particles that might increase the heavy metals concentration of the surface water samples. The results showed that the maximum concentration of Fe found at all locations in Gazipur may be due to the presence of many wrought re-rolling mills in Gazipur districts. However, the concentration of heavy metals like Cd, As, and Zn was found lower in surface water of the Gazipur region than the Rajshahi region as the soils of the area contained these metals comparatively higher (Figure 4b). The concentrations of these heavy metals were found higher than usual concentration indicated the surface water contaminated with heavy metals. The study observed that both anions and cations were found higher concentrations in the brick production season (not shown in Table).

The other indicators of surface water, such as TC and FC values exceeded the permissible standard at all sampling locations. The TC and FC concentrations in all surface water samples exceeded the WHO's standard (0 CFU/100 ml) that may harm aquatic life and human health (Table 7). Lango et al. (2012) reported that an increased amount of bacterial population in aquatic ecosystems affected public health.

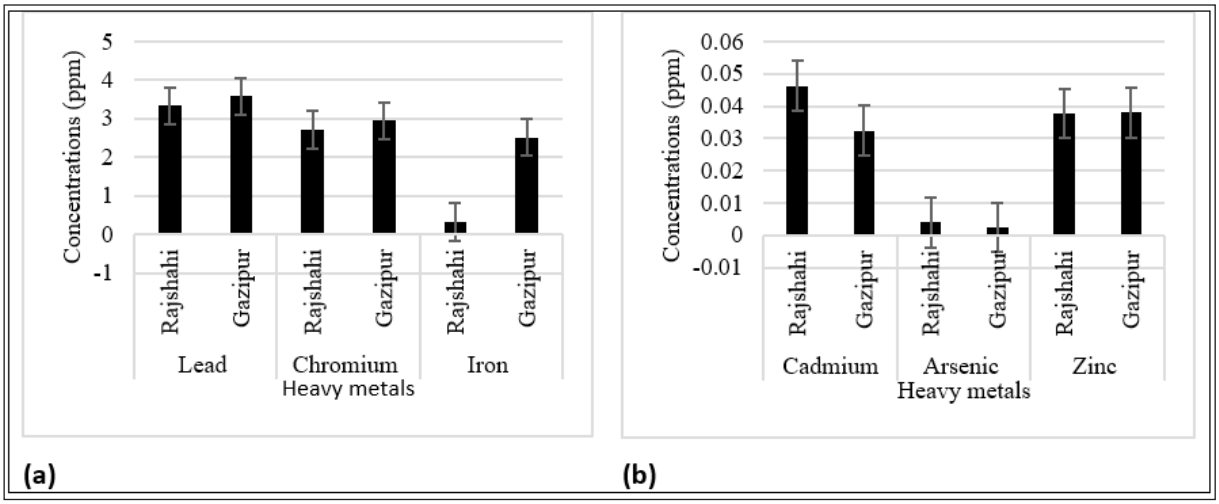

Figure 4. Biyearly concentrations of heavy metals in surface water samples during the production season (January-April) in 2016-2017.

The results indicated that the anions and cations were increased during the brick production season. It is impossible to control the dissolution of undesirable constituents in the waters once they enter into the ground (Mostafa et al., 2017; Sastri, 1994). These heavy metals in the surface water may be susceptible to severe health problems. Finally, these toxic metal ions and organometallic compounds are consumed by humans through water and foodstuffs.

3.5 Noise Pollution

The increased brick kiln activities use excessive machinery have led to several environmental problems in the study area. Jamatia et al. (2014) reported that the increase of brick kiln coupled with the haphazard manufactural set-up in a small area has resulted in a significant contribution to pollution load in the environment. A total of 24 sound sampling was done, and the noise levels were recorded during peak working hours (09:30 AM – 04:30 PM) at the kiln areas. The results showed that the average values of the noise levels were recorded to be 89.45 and 82.63 dB in Gazipur and Rajshahi, respectively (Table 8). The noise level of all the individual sources exceeded the permissible standard limit (75 dB) of noise in an industrial area (ECR, 1997). This noise level was alarming for kiln workers (Saha et al., 2019). High levels of occupational noise remain a problem in all regions of the world. NIOSH (1998) reported that 30 million and 4-5 million workers are exposed to hazardous noise in the USA and Germany, respectively. According to the World Health Organization (WHO), generally, 60 dB sounds can make deaf temporarily, and 100 dB sounds can cause complete deafness (WHO, 2002). However, the noise affects human beings physically and psychotically. The noise environment may cause hypertension, headache, sleeplessness, etc. The study observed that the machinery used in the brick kilns created a higher intensity of noise, and it has had harmful effects on human health and the environment. Eventually, the high levels of occupational noise are alarming for kiln workers.

Table 8. Average noiselevel during peak working hours.

Study Area	Sampling locations	No. of Samplings	Noise Level (dB)		
			Minimum	Maximum	Mean ± SD
Rajshahi	8	16	72.8	91.7	82.63 ± 6.51
Gazipur	4	8	80.4	94.8	89.45 ± 4.95

4. Conclusions

The survey results showed that about 69% of respondents blamed the brick kilns for the cause of air pollution in the areas. The survey study identified several impacts, including loss of crop production, river grabbing, deforestation, etc. The study revealed that the criteria air pollutants (CO, SO_2, NO_x, PM 2.5, PM 10, SPM) except CO exceeded the National Ambient Air Quality Standard (NAAQS) limits. The particulate matter concentration in ambient air was found the highest among all types of ambient air quality parameters. The particulate matters, including PM 2.5 and 10, and SPM were in the range from 57 to 2573, 287 to 3875, and 519 to 1950 μg/m^3, respectively. The brick kilns cluster emitted enormous amounts of gases in the surrounding areas would cause adverse effects on human health. The soil analysis results found that most of the farm soil samples contained more than 50% of sand particles during the production season. The pH and organic matter content in the collective farm soil samples were showed to be very low. The presence of a higher level of lead (Pb) and chromium (Cr) in the fly ash samples might have influenced the heavy metals pollution in the farm soil and surface water. About 100% of surface water samples exceeded the permissible standard limit for Pb. The fly ash and surface run-off contaminated water from the kilns areas indisputably declines the soil fertility and crop production in the surrounding agricultural lands. The study observed that the machinery used in the brick kilns created a higher intensity of noise that caused exceedances in the sound to the acceptable level in any industrial region (75 dB) of the DoE standard. Eventually, the high levels of occupational noise are alarming for kiln workers. Finally, it

may be concluded that the ambient air, farm soil, and surface water around the brick kiln areas were affected in the study areas, and the contamination process will continue in the future until any remedial measures have been introduced.

Acknowledgements

The authors would like to thank the Ministry of Science and Technology, Government of the People's Republic of Bangladesh for partial funding of this study.

References

Abuduwaili, J. and Mu, G.J. (2002). Analysis on the dust storms and their disasters in the lakebed regions of Ebinurlake, Xinjiang. Arid Land Geography 25: 149-154.

Al-Hiyaly, S.A., Mcneilly, T., Bradshaw, A.D. (1988). The effect of zinc concentration from electricity pylons-evolution in replicated situation. New Phytologist 110: 571–580. DOI: 10.1111/j.1469-8137.1988.tb00297.x.

Bam, B. (2018). Brick kilns smoke, haze engulfs human settlement. Face to Face, 5 June 2018.

BBS. (2013a). Districts statistics 2011 Rajshahi. Bangladesh Bureau of Statistics (BBS), Statistics and Informatics Division (SID), Ministry of Planning, Government of the People's Republic of Bangladesh.

BBS. (2013b). Districts statistics 2011 Gazipur. Bangladesh Bureau of Statistics (BBS), Statistics and Informatics Division (SID), Ministry of Planning, Government of the People's Republic of Bangladesh.

Brick Kiln Control Act (Amendment). (2001). Bangladesh Gazette (Act no.: 17, 11-04-2001), Ministry of Environment and Forest, Government of People's Republic of Bangladesh.

Bodek I., Lyman, W., Reehl, W.F., Roseblatt, D.H. (1988). Environmental organic chemistry. Pergamon Press, New York.

Budhwar, R., Bihari, V., Mathur, N., Srivastava, A., Kumar, S. (2006). DNA protein cross links as a biomarker of exposure to solar radiation: a preliminary study brick- kiln workers. Biomarkers 8(2): 162-166. DOI: 10.1080/1354750031000067495.

BUET (Bangladesh +University of Engineering and Technology) (2007). Small study on air quality of impacts of the North Dhaka brickfield cluster by modeling of emissions and suggestions for mitigation measures including financing models. Prepared by the Chemical Engineering Department.

CCAC. (2014). Time to Act: To Reduce Short-Lived Climate Pollutants. UNEP.

Chauhan, A., and Joshi, P.C. (2010). Effect of ambient air pollutants on wheat and mustard crops growing in the vicinity of urban and industrial areas. New York Science Journal 3(2): 52-60.

Chowdhury, M., Mostafa, M.G., Biswas, T.K., Saha, A.K. (2013). Treatment of leather industrial effluents by filtration and coagulation processes. Journal of Water Resource and Industry 3: 11- 22. DOI: 10.1016/j.wri.2013.05.002.

Cox, B.A. (2003). A review of currently available in-stream water-quality models and their applicability for simulating dissolved oxygen in low land. The Science of Total Environment 2003 Oct 1;314-316:335-77. DOI: 10.1016/s0048-9697(03)00063-9. PMID: 14499540.314-316.

Crommentuijn, T., Polder, M.D., Van de Plassche, E.J. (1997). Maximum Permissible Concentrations and Negligible Concentrations for Metals, Taking Background Concentrations into Account (RIVM Report 601501001), Bilthoven, Netherlands.

Cui, J., Zhou, J., Peng, Y. (2015). Effects of atmospheric deposition nitrogen flux and its composition on soil solution chemistry from red soil farmland, southeast China. Environmental Science Process and Impacts 17(12): 2082–2091.

Das, R. (2015). Land degradation in terms of environmental cost due to the emergence and development of brick kilns - A study on Khejuri CD blocks over coastal Medinipur in West Bengal. International Journal of Science and Research 4 (2): 1942-1951.

DEP (Department of Environmental Protection). (2003). Assessment levels for Soil, Sediment and Water, Contaminated Sites Management Series, Australia.

Dey, S., and Dey, M. (2015). Deterioration and degradation of aquatic systems due to brick kiln industries – A study in Cachar District, Assam. Current World Environment 10(2): 467- 472.

DoE (Department of Environment). (2003). A Compilation of Environmental Laws of Bangladesh. pp 212-214.

DoE (Department of Environment). (2013). Bangladesh Government-Memo no. 2565 DOE/Enforcement/37, DOE, GoB.

ECR (The Environment Conservation Rules). (1997). Department of Environment, Ministry of Environment and Forests, Government of Bangladesh, Bangladesh.

Eswaran, H. (1999). Recommendation in the proceedings of the 2nd international conference on land degradation. January 25-29, KhonKaen, Thailand. 9. Environment facing 21st Century, P.

Gain (eds) SEHD, Dhaka-1205, Bangladesh, p: 305.

Ghoshal, P.K. (2008). Prospects and Problems of Brick Industry. New Delhi: Mittal Publications.

Guttikunda, S. (2009). Impact Analysis of Brick Kilns on the Air Quality in Dhaka, Bangladesh. SIM-Air Organization. http://www.sim.org.

Guttikunda, S.K., and Khaliquzzaman, M. (2014). Health benefits of adapting cleaner brick manufacturing technologies in Dhaka, Bangladesh. Air Quality, Atmosphere and Health 7 (1):103–112.

Guttikunda, S.K., Begum, B.A., Wadud, Z. (2013). Particulate pollution from brick kiln clusters in the Greater Dhaka region, Bangladesh. Air Quality. Atmosphere and Health 6(2): 357-365.

Hakanson, L. (1980). An ecological risk index for aquatic pollution control: A sedimentological approach. Water Research 14(8): 975-1001.

Hannan, M.A. (1995). Structure and related physical properties of some soils of Bangladesh. Master thesis, University of Dhaka, Bangladesh.

Helal, U.S.M., Mostafa, M.G., Haque, A.B.M.H. (2011). Evaluation of groundwater quality and its suitability for drinking purpose in Rajshahi City, Bangladesh. Water Science and Technology. Water Supply 11(5): 545-559. DOI: 10.2166/ws.2011.079.

Hossain, M.M. (2018). Impact of industrial effluent on soil and water around BSCIC industrial zone in Rajshahi City. PhD Dissertation. University of Rajshahi, Bangladesh.

IAC (Ideal Atmospheric Condition). (1996). Natural Gas-Standard Reference Conditions. International Organization for Standardization, Geneva, Switzerland.

Islam, M.M., and Afrin, S. (2015). The Influence of Brick Kilns on Seasonal Variation of Particulate Matter Concentration in Dhaka City. 11th International Conference on Mechanical Engineering, ICME 2015, Dhaka, Bangladesh.

Islam, T. (2002). Smoke from Brick Kilns Damages Environment, Health. Inter Press Service, 24 November 2002. http://www.ipsnews.net/2002/11/bangladesh-smoke-from-brick-kilns-damages-environment-health.

Islam, M.R., and Mostafa, M.G. (2020). Characterization of textile dyeing effluent and its treatment using polyaluminium chloride. Applied Water Science (2020) 10:119. DOI: 10.1007/s13201-020-01204-4.

IUSS. (2002). Soil and the environment, IUSS Commission VIII. p. 66. World Congress of Soil Science. International Union of Soil Science 14-21 August, Thailand.

Jamatia, A., Chakrabarti, S., Chakraborty, S., Das, M.K. (2014). Assessment of Ambient Noise Quality in Jirania Brick Industries Cluster: a Case Study. International Journal of Engineering Research and Technology 3 (9):12-16.

Järup, L. (2003). Hazards of heavy metal contamination. British Medical Bulletin 68(1): 167–182.

Joshi, S.K., and Dudani, I. (2008). Environmental health effects of brick kilns in Katmandu valley. Katmandu University Medical Journal 6(1): 3-11.

Kacaroglu, F., and Gunay, G. (1997). Groundwater nitrate pollution in an alluvium aquifer, Eskisehir urban area and its vicinity. Environmental Geology Turkey 31: 178–184.

Khan, H.R., Rahman, K., Rouf, A.J.M., Sattar, G.S., Oki, Y., Adachi, T. (2007). Assessment of degradation of agricultural soils arising from brick burning in selected soil profiles. Journal of Environmental Science and Technology 4: 471-480.

Kudesia, V.P. (1990). Pollution, Pragoti Prakasani, India. P. 370.

Lango, F., Castañeda-Chávez, M., Zamora-Castro, J.E., Hernández-Zárate, G., Ramírez-Barragán, M.A., Solís-Morán, E. (2012). La acuariofilia de especiesornamentales marinas: unmercado de retos y oportunidades. Latin American Journal of Aquatic Research 40: 12-21.

Maithel, S., Uma, R., Bond, T., Baum, E., Thao, V.T.K. (2012). Brick kilns performance assessment, emissions measurements and roadmap for cleaner brick production in India. Study report prepared by Green Knowledge Solutions, New Delhi.

Maya, M., Musekiwa, C., Mthembi1, P. (2015). Remote sensing and geochemistry techniques for the assessment of coal mining pollution, Emalahleni (Witbank), Mpumalanga. South African Journal of Geomatics 4(2): 174–188.

Mazumdar, M., Goswami, H., Debnath, A. (2018). Brick Industry as a Source of Pollution-Its Causes and Impacts on Human Rights: A Case Study of Brick Kilns of Palasbari Revenue Circle. International Journal of Humanities and Social Science 6 (3): 220-240.

Morison, J.I.L., and Gifford, R.M. (1987). Plant growth and water use with limited water supply in high CO2 concentrations: I. leaf area, water use, and transpiration. Australian Journal of Plant Physiology 11:361-374.

Morley, T.W. (2012). Brick kilns Of Bangladesh. Sphericnews: journalism from around the world.

Mostafa, M.G., Helal U.S.M., Haque, A.B.M.H. (2017). Assessment of Hydro-geochemistry and Groundwater Quality of Rajshahi City in Bangladesh. Applied Water Science 7(8): 4663-4671. DOI:10.1007/s13201-017-0629-y.

NAAQS (National Ambient Air Quality Standards). (2005). Bangladesh Gazette (19th July 2005), Ministry of Environment and Forests, Government of People's Republic of Bangladesh. 7568-7569p.

NAAQS (National Ambient Air Quality Standards). (2009). Prevention and Control of Pollution Notification (18th November 2009), Central Pollution Control Board, India.

OSHA (Occupational Safety and Health Administration). (2010). Carbon Dioxide: Health Hazard Information Sheet. The FSIS Environmental Safety and Health Group (ESHG) ESHG-Health- 02.00. (https://www.osha.gov/dts/chemicalsampling/data/CH_225400.html).

Neupane, S., and Bishat, G. (2015). Impact of Brick Kilns' Emission on Soil Quality of Agriculture Fields in the Vicinity of Selected Bhaktapur Area of Nepal. Journal of Applied and Environmental Soil Science 2015. DOI: 10.1155/2015/409401.

NIOSH (National Institute for Occupational Safety and Health). (1998). Criteria for a recommended standard: occupational noise exposure. Revised criteria. Cincinnati, OH, USA. (http://www.cdc.gov/niosh/98-126.html).

Nusrat, A., and Mahadev, P.D. (1991). Environmental Impact of Brick Loam Quarrying on Agricultural Soil. The Indian Geographical Journal 6: 83-88.

Ochieng, G.M., Seanego, E.S., Nkwonta, O.I. (2010). Impacts of mining on water resources in South Africa: A review. Scientific Research and Essays 5(22): 3351–3357.

Peerzada, N., Morrow, M.L., Ryan, P. (2004). Distribution of heavy metals in rove harbors. Science of Total Environment 92: 1-12.

Pokhrel, R., and Lee, H. (2011). Stragety for the Air Quality Management for Brick Kiln Industries in Nepal. Society for Nepalese students in Korea. Retrieved from (http://sonsik.org.np/uploads/2_ pdf).

Rahman, M.K., and Khan, H.R. (2001). Impacts of brick kiln on topsoil degradation and environment pollution. Project report submitted to the Ministry of Science and Information and Communication Technology, Bangladesh Secretariat (Dhaka). 210.

Saha, M.K., Ahmed, S.J., Sheikh, A.H., Mostafa, M.G. (2019). Occupation Hazardous of Brick Kiln Worker at High Intensity Noisy Environment. Journal of Industrial Pollution Control 35(1): 2220-2223.

Saha, M.K., Ahmed, S.J., Sheikh, A.H., Mostafa, M.G. (2020a). Occupational and Environmental Health Hazards in Brick Kilns. Journal of Air Pollution and Health 5(2): 135-146.

Saha, M.K., Ahmed, S.J., Sheikh, A.H., NafizUl, A., Mostafa, M.G. (2020b). Impacts of Brick Kiln Emissions on Air Quality around Kiln Areas. International Journal of Natural and Human Sciences 1(1): 60–70.

Sastri, J.C.V. (1994). Groundwater chemical quality in river basins, hydrogeochemical modeling. Lecture notes-Refresher course, School of Earth Sciences, Bharathidasan University, Tiruchirappalli, Tamil Nadu, India.

Shahid, S. (2010). Recent trends in the climate of Bangladesh. Climate Research 42(3): 185-193.

Skinder, B.M., Pandit, A.K., Sheikh, A.Q., Ganai, B.A. (2014). Brick kilns: Cause of atmospheric pollution. Journal of Pollution Effects and Control 2(2): 1000112.

Tisdale, S.L., Nelson, W.L., Havlin, J.L., Beaton, J.D. (1999). An introduction to nutrient management soil fertility and fertilizers (eds). (3rd edt). The Prentice Hall, New Jersey. pp. 52-278.

Tomlinson, D.L., Wilson, J.G., Harris, C.R., Jeffney, D.W. (1980). Problems in the assessment of heavy metal levels in estuaries and the formation of pollution index. Helgolander Meeresunters 33: 566-572. DOI: 10.1007/BF02414780.

Ulrich, B. (1984). Effects of air pollution on forest ecosystems and waters—the principles demonstrated at a case study in Central Europe. Atmospheric Environment 18(3): 621-628.

USEPA (United States Environmental Protection Agency). (2003). Supplemental guidance for developing soil screening levels for superfund sites. U.S. Environmental protection agency, office of solid waste and emergency response, Washington, D.C.

USGS (United States Geographical Survey) (2006). Turbidity and Water, Standard for inland surface water, USGS. https://

www.usgs.gov.(special-topic/water-science- school / science/ turbidity-and-water?qt-science_center_objects=0#qt science).

Van Loon, G.W., and Duffy, S.J. (2007). Chemiaśrodowiskowa, Wyd. Naukowe PWN, Warszawa. pp. 23-27.

Vandeviver, P.C., Bianchi, R., Verstraete, W. (1998). Treatment and Reuse of Wastewater from the Textile Wet-Processing Industry: Review of Emerging Technologies. Journal of Chemical Technology and Biotechnology 72:289-302. DOI: 10.1002/(SICI)1097-4660(199808)72:4<289.

Verma C, Madan S., Hussain, A. (2017). Heavy metal contamination of groundwater due to fly ash disposal of coal-fired thermal power plant, Parichha, Jhansi, India. Cogent Engineering, 3: 1179243.

WHO (World Health Organization). (2002). World Health Report 2002 – reducing risks, promoting health life. Geneva.

WHO (World Health Organization). (2003). Guidelines for Drinking Water Quality. 3rd ed. Geneva. https: www.who.int/ water_sanitation_health / dwq/en/.

World Bank. (2011). Workshop on Public Policies to Mitigate Environmental Impact from Brick Production. Maxico. World Bank. Retrieved from: http://www.ine.gob.mx/decargas/ dgcenica/2012_ladrilleras_pon_s6_jli_eng.pdf.

WSH Act (Workplace Safety and Health). (2006). The Workplace Safety and Health Act (1st March, 2006), Republic of Singapore.

JJEES

JJEES (2021) 12 (3): 254-268
ISSN 1995-6681

Jordan Journal of Earth and Environmental Sciences

Water quality evaluation of Qunayya Spring- Jordan

Iyad Ahmed Abboud[1*] and Montaha Shawabkeh[2]

[1]Geology / Biology Department, Faculty of Science, Taibah University – Yanbu' Branch, Al-Madinah Al-Munawwarah, Saudi Arabia.
[2]Samra Station WWTP, Environmental Services, Jordan.

Received 30 April 2020, Accepted 9 March 2021

Abstract

Qunayya Spring, a catchment covers an area of about 111 km^2 with a total discharge of about 4.3 Million Cubic Meter (MCM)/year, where water flows from the Ajloun Group Formation located at the lower part of the Upper Cretaceous to the outlet of spring. Qunayya Spring is considered a major source of drinking water for many villages in the governorates of Zarqa and Mafraq, and a major source of irrigation for farms, nurseries, livestock, and poultry farms. Because of septic tanks in populated areas, and because of the use of chemical and natural fertilizers on farms, this led to pollution and deterioration of the quality of the Qunayya Springwater. Therefore, the physical, chemical and biological properties of the Qunayya Spring were studied to determine the water quality and assess its suitability for human and agricultural uses. The total number of samples collected from Qunayya Spring reached 84 samples distributed over 14 sites, with a total of 6 samples for each site over 9 months. The physical and chemical properties of 74 samples were evaluated to verify the hydrogeochemical processes and the background environment of ion concentration. In addition to 10 samples were taken for bacterial biological analysis of the cultivation faecal coliforms and total coliform bacteria. The biological consumed oxygen (BOD) and chemically (BOC) values were also calculated for all water samples. The hydrochemical of ionic relations show that the higher concentrations of Na^+ and Cl^-ions are due to ion exchange and evaporation processes. Anthropogenic sources are the other reason for increasing Mg^{2+}, Na^+, Cl^-, SO_4^{2-}, PO_4^{3-}, and NO_3^- ions. Besides, Piper's diagram shows an increased ratio of the normal earth alkaline with an increase in the content of bicarbonate and chlorine, or earth alkaline with an increase in bicarbonate. Thus, the groundwater quality is distinguished by Ca^{2+}> Mg^{2+}> Na^+> K^+: HCO_3^- + CO_3^{2-}> Cl^-> NO_3^-> SO_4^{2-}> PO_4^{3-}facies, while the predominate of hydrochemical types are Ca^{2+}–HCO_3^-, Ca^{2+}–Mg^{2+}–HCO_3^-, and Ca^{2+}–Mg^{2+}–Cl^-. Based on the concentrations of TDS and TH, the majority of groundwater samples are not suitable for drinking. According to EC versus SAR, the most dominant categories are C2-S1 and C3-S1, which have medium to high salinity hazards and low sodium hazards, and in a consideration of irrigation water, the quality is medium to low. The major ion concentrations are below the acceptable level for drinking water. Therefore, it is necessary to eradicate the high toxic salt concentration from the drainage system. Furthermore, the biological results showed that the water spring was highly polluted with total coliforms and faecal coliforms. Also, the spring water was shown to be free from biological contamination after treatment.

Keywords: Geochemical evolution, water quality, hydrochemical, Amman-Zarqa Basin, Qunayya, Jordan.

1. Introduction

Jordan is located within the arid to semi-arid climate zone, this plays a big role in decreasing the rainfall and thus recharge groundwater reservoirs with water, which makes daily groundwater withdrawals for daily uses more than feedback, and this, in turn, leads to total depletion for groundwater basins. This is one of the biggest environmental challenges facing the country. Besides, the water resources in Jordan flow around a constant volume annually, unlike the population, which increases continuously from year to year, due to natural increases, the high annual flow of immigrants from neighbouring countries, and the return of workers from abroad. This situation disturbs the balance of water between supply and demand (Abboud, 2018a). Whereas, in 2025, if the situation continues as such, it is expected that the Jordanian per capita share of water will decrease from 170 m^3/year to 91 m^3/year (Tabieh and Al-Horani, 2010). This will place Jordan among the countries that suffer from severe water shortages.

The water crisis in Jordan is represented in a scarcity of water resources and inefficient administration, the decline in quality because of agricultural development, groundwater pollution, and over pumping, which causes salination (Salameh, 1996; Abboud, 2018a; b).Also, there are many hydrogeochemical studies conducted on different areas of Jordan in an attempt to monitor the geological, hydrological, and hydrochemical conditions of the groundwater basins to identify the quality of water, the impact of pollution on it, and the level of the depletion (Al Kuisi et al., 2009; Abboud, 2014; Abboud, 2018a; b).

Water resources in Jordan were divided into surface and subsurface sources, as well as unconventional sources as treated wastewater (Abed, 1982; MWI, 2000). The developed available annual surface water quantity in Jordan is about 295 MCM in 2007 and is expected to reach 365 MCM in 2022 (UNESCO, 2012). Most of this water comes from Syria in the form of floods and surface flow (Abed, 1982; WAJ, 1995; 1996). Groundwater is considered the main water source in

* Corresponding author e-mail: iyad.abboud@yahoo.com

Jordan; there are 12 water basins, these water sources are renewable or nonrenewable. Some basins are classified as fossil aquifer, meaning that water is not renewed in them if it is extracted, such as the Al-Disi basin (Wardam, 2004). In 2000, more than 412 MCM renewable groundwater sources and 62 MCM non-renewable water resources were used in Jordan, although the total annual recharge for groundwater resources is about 275 MCM, which means that more than 199 MCM were over-pumped in 1997, and this quantity increases with time (Tabieh and Al-Horani, 2010). Treated wastewater is considered one of the most important non-conventional resources of water in Jordan. It is continuously increasing, and its treatment limits environmental pollution and provides water for use in agriculture (MWI, 2000).

Qunayya Spring water is a primary source of drinking water for ten villages in the governorates of Zarqa and Al-Mafraq, and also a main source of irrigation for many nearby farms, Mashtal, watering livestock, and poultry farms. Pollution water quality deterioration has been a noticeable problem at Qunayya Spring during the previous years since 2001 (CDM, 2002), resulting from septic tanks in the populated areas around it, and the use of chemical and natural fertilizers in the nearby farms. As a result, water pumping from the Qunayya Spring was stopped many times, since 2001 (MWI, 2004). The physical, chemical and biological features of Qunayya Spring were studied to define the water quality and compare it with the Jordanian and international standards, also evaluated the suitability for human and agricultural uses. Besides, the water pollution of Qunayya Spring and the leakage occurring in the spring channel were studied, with the quantity of discharge calculated to determine the water quality.

2. Study Area

2.1. Location and Physiography

The Qunayya Spring is located in the Amman-Zarqa Basin in northern Jordan, in Wadi Qunayya, northwest of Zarqa city with attitudes: 35°59`52.3”N and 32°12`53”E. The elevation of the Qunayya area is about 500 m above the mean sea level, as a trapezoidal shape, with a total catchment area of about 111 km^2 (Figures 1-2). The climate of the study area is of a Mediterranean type which is characterized by dry and hot summers, and mild wet winters with fluctuating rainfall during the years. The average annual rainfall is very low and ranges from 110 mm to 355 mm. While, the absolute monthly temperatures range from 2 °C in January to 45 °C in July (Elemat, 2012).

Physiographically, The morphology of the Amman-Zarqa Basin shows a gradual slope from east to west, where the elevation above the mean sea level varies, between 500 m in the east at Qunayya Spring 1000 m at the northwest part of the Qunayyaarea. The texture of the soil is mostly friable red soils in the west to clay, silty loam, and sandy soil in the east. The Amman-Zarqa Basin extends from the Ajloun mountains in the west to the Azraq Basin in the east and south, while to the north, the study area extends to the Yarmouk Basin (Figures 1-2). The catchment area is drained by many different wadis: Al-Dajanyeh, Um Rumana, Hammamt Al-Eleimat, Um Kharrouba, and Dahal. Irrigation in the study area has used both surface and subsurface water, giving rise to the recirculation of groundwater. Where the area of Qunayya Spring and other surrounding areas are used for agriculture, greenhouses, poultry farms, grazing lands, and olive farms.

Figure 1. Jordan map showing the 15surface water basins and Qunayya catchment areaas a study area (after MWI, 2010).

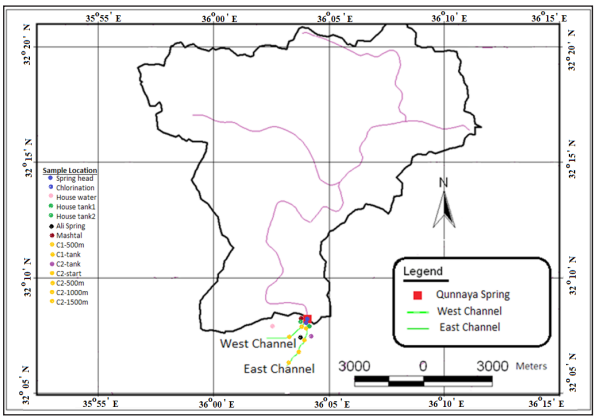

Figure 2. The catchment area of Qunayya Spring and locations of water samples.

2.2. Geological and Hydrogeological Setting

The geological setting of the study area shows that it from tectonism type causing the appearance of heights, cracks, and severe folds in the rock layers, especially from west to east (Brunke, 1997). Figure 3 shows the geological formations of the study area and the most important geological structures of the rock units spread in the study area. Most outcrops in the study area mostly trace the Triassic to Recent age through the dominance of the Cretaceous deposits. Upper Cretaceous was divided according to Quennel (1951) into the Ajloun and Belqa Groups, which consist of limestones, chert, phosphorite marl, and porcellainite (Abed et al., 2008). The rocks of the Lower Cretaceous Kurnub Group are distributed along the axis of the Suweileh structure and the Zarqa River Valley, while the northeastern part of the basin is largely covered by basalt flows (Figure 3).

Table 1 shows the geological and hydrogeological classification of the rock units in the Amman-Zarqa Basin based on Rimawi (1985) since the area of Qunayya Spring is considered a part of the Ajloun Group, which consists of five geological formations. Na'ur Formation (A1-2) consists oflimestone interbedded with thick sequences of marl and marly limestone witha thickness of about 130 m. This formation is considered as one of the oldest hydrogeological units in the Ajloun Groupat the Qunayya area, and this formation is considered a pooraquifer; Fuheis Formation (A3) consists ofsoft gray and green marl, marly limestone, and limestonewith a thickness of about 70 m. This formation forms an excellent and distinct aquifer in the study area. Al-Hummar Formation (A4) consists ofhard dense limestone and dolomitic limestonewith a thickness of about 50 m. This formation together with Na'ur Formation contributes to the discharge of the Qunayya Springwater. Shu'eib Formation (A5-6) consists ofgray limestone interbedded with marl and marly limestonewith a thickness of about 60 m and forms a fair to poor aquiclude. Wadi Sir Formation (A7)consists oflimestone, dolomitic limestone, dolomite, chert,and marl with a thickness of about 70 m andwas considered the main aquifers in the study area (Abed, 1982; Rimawi, 1985; Abed, 2000).The recent sediments in the Qunayya area, consist of silt, sands, and mud and their thickness ranges between 5 m to 15 m (Brunke, 1997).

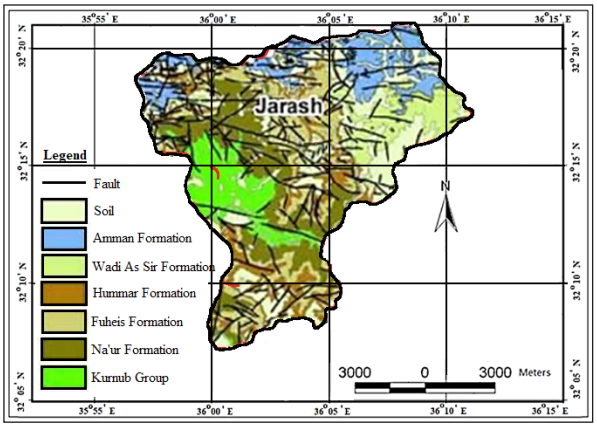

Figure 3. Geological and structural map of the study area (Catchment area of Qunayya Spring)

(Modified after the Natural Resources Authority (NRA), 2004 and Al Kuisi et al., 2014).

Table 1. Geological and hydrogeological classification of the rock units in Amman–Zarqa Basin (after Rimawi, 1985).

Epoch	Group	Formation	Symbol	Rock type	Thickness (m)	Aquifer potentiality
Tertiary	Balqa	Wadi fill		Soil, sand, gravel	10-40	Good
		Basalt	V	Basalt, clay	0-50	Good
Upper Cretaceous		Muwaqqar	B3	Chalk, marl, chalky limestone	60-70	Poor
		Amman	B2	chert, limestone with phosphate	80-120	Excellent
		Ghudran	B1	Chalk, marl, marly limestone	15-20	Poor
	Ajloun (Qunayya area)	Wadi Sir	A7	Limestone, dolomite, chert	90-110	Excellent
		Shu'eib	A5-6	Gray limestone interbedded with marl and marly limestone	75-100	Fair to poor
		Al-Hummar	A4	Hard dense limestone and dolomitic limestone	40-60	Good
		Fuheis	A3	Soft gray and green marl, marly limestone, and limestone	60-80	excellent
		Na'ur	A1-2	Limestone interbedded with a thick sequence of marl and marly limestone	150-220	Poor
Lower Cretaceous		Kurnub	K	Massive white and varicolored sandstone with layers of reddish silt and shale	300	Good

3. Methodology

3.1. Samples Collection

Eighty-four samples were collected from Qunayya Springwater, from more than 14 sites (Figure 2), with a total of 6 samples from each site, as listed in Table 3, for a period from December to August. Ten water samples placed in a suitable medium for biological bacterial analysis, for growing the Qunayya Spring is considered a major source of drinking water for many villages in the governorates of Zarqa and Mafraq, and a major source of irrigation for farms, nurseries, livestock, and poultry farms. Because of septic tanks in populated areas, and as a result of the use of chemical and natural fertilizers on farms, this led to pollution and deterioration of the quality of the Qunayya Spring water.

3.2. Chemical Analyses

The physical, chemical and biological properties of the Qunayya Spring were studied to determine the water quality and assess its suitability for human and agricultural uses. The total number of samples collected from Qunayya Spring reached 84 samples distributed over 14 sites, with a total of 6 samples for each site over 9 months. The physical and chemical properties of 74 samples were evaluated to verify the hydrogeochemical processes and the background environment of ion concentration. Forty-seven samples were taken for chemical analyses to determine the type and concentrations of the major ions using the standard methods book (APHA, 1998). Then, all samples were analyzed in the laboratories of Al al-Bayt University to determine the geochemical characteristics and groundwater quality of the Qunayya Springwater.

Hydrogen ion concentration (pH), specific electrical conductivity (EC), and temperature (T) were measured to all samples directly in the field, using pH and EC meters. Total dissolved solids (TDS) were measured in the field

and computed by multiplying the specific EC by a factor of 0.55 to 0.75, depending on the relative concentrations of ions. Carbonate (CO_3^{2-}) and bicarbonate (HCO_3^-) were estimated by titrating with HCl. The total hardness (TH) as $CaCO_3$ was calculated using Equation 1, while Ca^{2+} was analyzed by titration using standard EDTA. Magnesium (Mg^{2+}) was calculated from the TH and Ca^{2+}. Sodium (Na^+) and potassium (K^+) were measured by a flame photometer. Chloride (Cl^-) was estimated by standard $AgNO_3$ titration. Sulphate (SO_4^{2-}), nitrate (NO_3^-), and phosphorate (PO_4^{3-}) were analysed using a spectrophotometer. Finally, the error for the chemical analyses results was calculated with a percentage that doesn't exceed (5-10%) according to the Gibbs equation (Gibbs, 1972).

$$TH \text{ as } CaCO_3 = 2.5(Ca^{2+}) + 4.1(Mg^{2+}) \quad \text{.....(1)}$$

The percentage of sodium ($\%Na^+$) was measured related to the sodium hazard for judging the quality of water for irrigation, according to Equation 2, taking the ionic concentrations in milliequivalents per liter (meq/l).To determine the soil zone and quality, this is usually expressed in the process of ion exchange in the soil zone by using the concept of sodium adsorption ratio (SAR), as summarized in Equation 3, and the ion concentrations were taken in meq/l.

$$\%Na^+ = (Na^+ + K^+)*100/Ca^{2+} + Mg^{2+} + Na^+ + K^+ \quad \text{.....(2)}$$

$$SAR = Na^+/((Ca^{2+} + Mg^{2+})/2)^{0.5} \quad \text{.....(3)}$$

3.3. BOD and COD

The biological oxygen demand (BOD) and chemical oxygen demand (COD) were determined for all water samples. The value of BOD was defined by using an Oxytop device which was installed in a special container made for this purpose. After taking 432 ml of water sample in this container and putting two pills of NaOH in the plastic container, the device was put in a special incubator at 20˚C for 5 days with taking care to continuously stir the sample by using a magnetic stirrer. At the end of the period, the reading was taken directly from the device which represents the value of BOD (John and Holum, 1986; APHA, 1998). The value of COD was determined by titration after preparing the sample by adding 2.5 ml of water sample to 1.5 ml of potassium dichromate solution and 3.5 ml of sulfuric acid. Then put into a COD reactor for 2 hours at 150˚C. After cooling, 3 drops of ferrior detector were added. Then the titration was made by using ferror ammonium sulphate solution until a reddish-brown color appears. The COD value is calculated using Equation4 after John and Holum (1986) and APHA (1998).

Where:B: consumed volume of FAS solution at blank titration; S: The consumed volume of FAS solution at sample titration; M: The concentration of FAS.

3.4. Bacteriological Analyses

Ten samples were taken for bacterial biological analysis of the cultivation faecal coliforms and total coliform bacteria. Bacterial tests were performed in the form of two tests per sample to determine the type and number of bacterial colonies of total coliform and faecal coliform bacteria. The number of bacterial colonies was determined for the total coliform after filtering 100 ml of the spring water sample to be tested using sterilized filtration paper (0.45 µm) and a Partial Vacuum device. The filtration paper was then placed on a medium of Endo Broth in a Petri dish placed in an incubator at 35˚C for 22 hours. The bacterial colonies were counted in a colony-forming unit (CFU) for every 100 ml (CFU/100 ml). Each red or metal gold-colored colony was considered to be of the total coliform count (TCC). The number of bacterial colonies of the total of faecal coliform bacteria was defined after filtering the water sample and putting the filtration paper in a medium of multiple fermentation tube test for coliforms (MFC) Broth in a Petri dish previously placed in a water bath at 44.5˚C for 24 hours. Each blue-colored colony was considered to be a part of the faecal coliform group.

4. Results and Discussion

4.1. Discharge

The discharge quantity of the Qunayya Spring fluctuates according to the years and the amount of rainfall, so the maximum drainage of the Spring in recent years reached about 337.2 m^3/hr. The permanent discharge quantities vary between 237 m^3/hr to 268 m^3/hr, and the highest discharge level is 45-60 days after rainfall, with an annual of 2.95 Mm^3 in the period from 1960 to 2003. The discharge was calculated according to Equation 5 after Margane and Almomani (1995). The maximum discharge rate of Qunayya Spring water in the period from 1983 to 2004 was in April-1992 when it was 2142 m^3/hr. The minimum discharge was in November-2002 and it was 134.5 m^3/hr, while the maximum monthly rate of discharge was in the period between 1983-2004 in April, and it was 407.2 m^3/hr. The minimum monthly discharge rate for the same period was in September at about 251.7 m^3/hr (Table 2). The monthly rate of discharge for every 5 years was between (181.1 – 758.8) m^3/hr and the highest annual discharge was in 1991-1992 at about 8.47 MCM which equals 966.68 m^3/hr. The highest annual discharge rate for every 5 years ranged from 1.93 mm^3/year to 4.34 mm^3/year which equals (220.4 – 495.44) m^3/hr. The total discharge in the catchment area was about 4.3MCM/year (Table 2). Based on the available data at the Ministry of Water and Irrigation, it appears that water discharge peaks after 45-60 days of rainfall which is 288 ml/day, and that equals 32 MCM/year. The stored water is about 1.25 MCM/year since the unstored spring water into the spring is 4.5 MCM/year, this value equals the discharge at the catchment area which forms 14% of the total amount of rainfall (Brunke, 1997).

$$Q = A*V \quad \text{.....(5)}$$

Where: Q: Discharge rate; A: Surface area; V: Velocity of water (depends on distance and time).

Table 2. Monthly discharge of Qunayya Spring for the period (1983-2004) in (m^3/hr).

Year	OCT	NOV	DEC	JAN	FEB	MAR	APR	MAY	JUN	JUL	AUG	SEP	Average	MCM
1983/1984	360	591	434	484	-	418	265	380	435	285	250	-	390.2	3.42
1984/1985	266	317	328	266	300	558	386	310	298	282	271	245	318.9	2.79
1985/1986	240	231	258	293	308	248	212	358	240	236	270	223	259.8	2.28
1986/1987	213	292	279	328.5	309.3	432	213	225.8	171	272	200	217	262.72	2.30
1987/1988	208	235	246	302	431	334	416	276	389	454	237.8	253	315.2	2.76
Avr (83-88)	257.4	333.2	309	334.7	269.7	398	298.4	310	306.6	305.8	245.8	234.5	309.4	2.71
1988/1989	294	516	378	555	385	324	250	238	188	159	198	171	304.7	2.67
1989/1990	251	246	227	312	332	393	314	140	303	-	190	303	273.7	2.40
1990/1991	197	182	191	205	335	226	329	-	282	226	316	221	246.4	2.16
1991/1992	197	205.8	330	1288	605	-	2142	1468	923	1194	1314	-	966.7	8.47
1992/1993	891	801	857	1048	-	-	-	594	288	205	979	509	685.8	6.01
Avr (88-93)	366	390.2	396.6	681.6	414.3	239	758.8	610	396.8	446	599.4	301	495.4	4.34
1993/1994	-	-	-	-	473	-	-	-	-	339	-	330	380.7	3.33
1994/1995	298	309	-	264.5	-	-	-	415	-	-	285	-	314.3	2.75
1995/1996	287	376	322	362	239	341	-	288	323	281.3	227	347.6	308.5	2.70
1996/1997	240	302.2	-	-	-	268	288.2	-	278.1	-	210	219.4	258.0	2.26
1997/1998	224	244	279	230	274.3	361.8	-	282.8	195	272.4	237	255.8	259.7	2.27
Avr (93-98)	262.3	307.8	300.5	285.5	328.8	323.6	288.2	328.6	265.4	297.6	239.8	288.2	304.2	2.67
1998/1999	208.2	198.4	-	-	223.5	279	-	179.6	195.4	-	190.8	180.5	206.9	1.81
1999/2000	-	166.4	184.6	-	221	263.3	-	189.5	162.8	176.3	166.8	176.2	189.7	1.66
2000/2001	167.7	181.4	202.2	186.9	189.2	-	155.1	175.5	140.1	160.1	142.6	142.7	167.6	1.47
2001/2002	125.6	168	-	174.6	210.8	222.5	256.3	174.6	180	144.8	-	150.6	180.8	1.58
2002/2003	136.8	134.5	-	174.3	-	308.6	265.3	-	419.2	-	-	-	239.8	2.10
2003/2004	266.9	300.9	334.7	388.8	384.8	336.9	457.1	374.3	285.1	324.3	331.8	266.3	337.7	2.95
Avr (98-2004)	181.1	191.6	240.5	231.2	245.9	282.1	283.4	218.7	230.4	201.4	208	183.3	220.4	1.93
Avr (83-2004)	266.7	305.7	311.7	383.2	314.6	310.7	407.2	366.8	299.8	312.7	323.2	251.7	332.4	2.91

4.2. Field Measurements

The maximum, minimum, and average results of the field tests (pH, Electrical Conductivity (EC), Total Dissolved Solids (TDS), Total Hardness (TH), and Temperature (T)) are summarized in Table 3. The pH values of groundwater varied from 6.7 to 9.4 with an average of 7.8, indicating an alkaline condition of groundwater. This is caused by the inflow of carbonates in the groundwater aquifer due to the percolation of water through fractures, joints, permeability, and porosity of carbonate rocks (Hummar Formation-A4). The concentration of TDS, a measure of quality, values ranged from 300 to 788 mg/l with a mean of 383.4 mg/l in the spring water. There were no significant variations between TDS values in the house tank water or along the two channels and the spring water values. So, according to the TDS classification, all of the water samples of the groundwater belonged to the freshwater type (TDS<1,000 mg/l). The values of EC in the spring water varied between 728 and 749 µS/cm and in the house water varied between 700 and 789 µS/cm, which is directly linked to the concentrations of ions existing in the groundwater and its higher values that contribute to higher salinity. While the rest of the samples along the two channels varied between 446 and 848 µS/cm with an average of 738.4 µS/cm. Commonly, the slight variations in EC reflect a low variation in geochemical processes present in an area. The temperature of the spring water varied between 20 and 26˚C while in the water of the channel it varied between 20 and 27˚C. In general, the temperature of all the samples varied between 15.6 and 32.8˚C with an average of 25˚C, corresponding to the seasonal temperature variation.

Table 3. Physical properties results of Qunayya Springwater samples in the field.

Sample Location See Figure 2	pH			TDS (mg/l)			EC (µS/cm)			TH (mg/l)			Temperature (C°)			Coordinates		Elv. (m)
	min	max	mean	min	max	mean	min	max	mean	min	max	mean	min	max	mean	N	E	
Springhead	7.3	7.5	7.4	361	390	371.5	728	749	737.0	357	403	370	20.4	26.0	24.1	35° 59 52.3”	32° 13 53”	475
Chlorination	7.2	7.8	7.4	352	398	383.3	667	800	761.8	329	368	346	20.3	26.8	24.3	35° 59 51.9”	32° 13 53.2”	497
House water	7.1	7.4	7.2	349	420	386.3	700	802	762.7	301	342	325	23.4	27.9	25.9	35° 59 49.4”	32° 13 52.7”	477
House tank1	7.3	8.5	7.9	300	395	366.4	700	789	751.6	306	346	330	15.6	32.8	25.8	35° 59 44.7”	32° 13 20.3”	479
House tank2	7.5	8.7	8.2	369	391	379.5	739	768	754.2	298	340	317	24.2	31.7	28.9	35° 59 57.3”	32° 13 44.4”	475
Ali spring	6.7	7.6	7.3	349	470	431.8	667	943	834.6	254	276	265	19.3	24.5	21.5	35° 59 53.8”	32° 13 32.5	462
Mashtal	7.8	8.3	8.1	310	419	382	603	883	765.0	245	278	259	17.7	26.1	22.8	35° 59 29.3”	32° 13 23.5”	473
C1-500m	7.2	8.1	7.6	348	395	365.7	705	786	742.7	313	384	350	21.4	25.7	24.4	35° 59 53.4”	32° 13 49.6”	470
C1-tank	7.0	8.4	7.8	355	385	368.8	705	765	734.8	314	376	329	19.2	28.6	25.1	35° 59 53.4”	32° 13 49.6”	470
C2-tank	8.4	8.9	8.8	300	514	359.4	446	669	597.6	296	353	314	20.3	29.4	26.5	35° 59 25.7”	32° 13 23.1”	474
C2- start	7.2	8.1	7.5	352	588	463	470	835	703.2	336	391	351	22.2	26.6	24.9	35° 59 53.4”	32° 13 49.6”	467
C2-500m	7.7	8.5	7.9	355	401	370	712	800	738.5	322	379	344	18.7	26.5	24.1	35° 59 25.7”	32° 13 23.1”	446
C2-1000m	7.1	8.3	7.9	352	395	375	690	788	729.5	314	368	334	17.4	28.4	25.0	35° 59 53.9”	32° 13 29.9”	470
C2-1500m	7.9	8.9	8.5	331	419	365.1	662	848	724.5	299	359	325	20.0	31.0	26.7	35° 59 45.2”	32° 13 26.8”	450
Mean			7.8			383.4			738.4			326			25.0			

4.3. Water Chemistry

The total hardness (TH) is between 176 and 412 mg/l (Table 3). This is because of the alkaline earth metals (Calcium: $Ca^{2+}$and Magnesium: Mg^{2+}) of weak acidic anions (Bicarbonates: $HCO_3^-$and Carbonates: CO_3^{2-}) and the strong acidic anions (Chlorides: Cl^-, Sulfates: SO_4^{2-}, and Nitrates: NO_3^-). According to Sawyer and McCarty (1967) for TH classification, about 30% of the total groundwater samples from the study area were classified as hard water (150 – 300 mg/l) and the other water samples (70%) in the category of very hard (>300 mg/l; Table 4). The results of the chemical analysis of Qunayya Spring groundwater are presented in Table 5. The table shows the minimum, maximum, and mean values for the ions concentration of Na^+, K^+, Ca^{2+}, Mg^{2+}, Cl^-, HCO_3^-, SO_4^{2-}, NO_3^-, and PO_4^{3-}, and also shows a comparison between the results of water analysis of the two channels with the water from the Qunayya Springhead.

After analysing the water samples of the spring head, it appeared that there is a fair variation in the concentration of some ions, while others were more and some of them have a fixed rate. In the groundwater samples, the concentrations of Na^+, K^+, Ca^{2+}, and Mg^{2+}ions vary from 30.8 to 44.9, 4 to 6, 43 to 65.2, and 43.4 to 58.4 mg/l, respectively (Table 5). In general, the aquifer rocks of the study area are the main source of Na^+, K^+, Ca^{2+}, and Mg^{2+}ions in the groundwater, the differences in the concentrations of ions are probability to differences in their sources. The mean concentration of Ca^{2+} (53.1 mg/l) is mostly closer to the mean of Mg^{2+} (49.6 mg/l; Table 5), despite the Ca^{2+} generally exceeds the Mg^{2+}, depending on their relative abundance in rocks. This shows that the anthropogenic activities could be the source of increased concentration of Mg^{2+} than Ca^{2+} in normal conditions; thereby the Mg^{2+} shows the comparable concentration of the Ca^{2+} in the groundwater (Rao et al., 2012). The high concentration of Ca and Mg indicates that they are both derived from the same source, that is, from the dissolution of calcite and dolomite from the rocks of the B2/A7 Formation. Finally, the analysis of Ca^{2+} and Mg^{2+} didn't show any changes in their concentrations overall months of the year.

The mean concentration of Na^+ (37.15 mg/l) is much higher than that of K^+ (4.63 mg/l; Table 5). The high concentration of Na^+ among the other cation concentrations reflect a rock weathering process and/or dissolution of salts stocked in soil by the impact of evaporation (Stallard and Edmond, 1983) and also indicate higher solubility conduct (Rao et al., 2012), while the lower concentration of K^+ (less than 5 mg/l) is because of its compatibility at clay minerals (Hem, 1991). Mainly, the appearance of any anomalies in the concentration of K in the water is due to the addition of K in the groundwater coming from potassium fertilizers and clay minerals associated with the reservoir rocks. Also notice the decrease in the concentration of Na^+ in the summer months (32 mg/l) in comparison with the winter months (42 mg/l), while the K^+ didn't show any changes in the concentration (Table 5). As a result, the order of cationic abundances is, Ca^{2+}> Mg^{2+}> Na^+> K^+.

Given the anions, the concentrations mean of HCO_3^-, Cl^-, NO_3^-, SO_4^{2-}, and PO_4^{3-}ions distributed as thus 233.53, 73.61, 38.27, 25.13, and 0.662 mg/l, respectively (Table 5). So, carbonates (HCO_3^-) are the common ion in the groundwater. The concentration of HCO_3^-in groundwater is caused by the presence of CO_2 in the soil zone which is formed from the weathering of origin materials, or may also be coming from the dissolution of silicate minerals from country rocks (Rao, 2002). Therefore, the high concentration of bicarbonate in the water is attributed to the natural weathering processes of the basin rocks. As a result of the decay of organic matter and the root respiration process in the soil zone works to launch carbon dioxide, which reacts with water to produce HCO_3^-, which in turn converts to CO_3^{2-} as a result of rocks weathering through the infiltration of recharge water (Jacks, 1973; Berner and Berner, 1987). The excess content of carbonates indicates a strong weathering of rocks, which favors a vigorous mineral dissolution (Stumm and Morgan, 1996).

In general, chloride (Cl^-) is mainly derived from non-lithological sources (Hem, 1991), as well as nitrates-NO_3^- (Ritzi et al., 1993). Also, the possibility contributes to Cl^- in the groundwater maybe depends on the country rocks (shale) (Rao et al., 2012). Another source of Cl^- in the groundwater of the study area represented in the influences of irrigation practice, use of natural and chemical fertilizers, solid waste of the poultry farms and barns cattle and cows, waste of olive mills, and septic tanks. The solubility rate of Cl^- is also high (Rao et al., 2012) becomes the next dominant ion after HCO_3^- in the groundwater (Table 5). Therefore, the increase in chloride concentration is often attributed to excessive irrigation and overexploitation of groundwater aquifers in the study area. Excess concentration of NO_3^- more than 10 mg/l in the water reflects man-made pollution (Rao et al., 2012). However, under natural conditions the NO_3^- concentrations do not exceed 10 mg/l (Cushing et al., 1973). So, the concentration of NO_3^- in the study area varies from 10 to 72.8 mg/l with a mean of 38.27mg/l (Table 5). The high concentration of nitrates in the study area is attributed to the extensive agricultural activities and the intensive use of chemical fertilizers, also, to the use of treated wastewater effluents in irrigation of crops. Relatively, the higher concentration of SO_4^{2-} (mean 25.013 mg/l; Table 5) reflects the influence of the country rocks (Rao et al., 2012), and it may also be related to some agricultural activities (ammonium sulfate fertilizer) widely spread in the study area. The order of abundance is HCO_3^-> Cl^-> NO_3^-> SO_4^{2-} > PO_4^{3-}.Generally, the concentration of dissolved ions in groundwater controlled by; lithology, soil type and texture, velocity and proportion of groundwater flow, type of aquifer, nature of geochemical reactions, solubility ratio of salts, and human activities (Hem, 1970; 1991; Karanth, 1991; 1997; Ritzi et al., 1993; Bhatt and Saklani, 1996; Stumm and Morgan, 1996; Eraifej and Abu-Jabber, 1999; Rao, 2002; Al Kuisi et al., 2009; 2014; 2015; Pazand et al., 2012; Rao et al., 2012; Abboud, 2014; 2018a; 2018b).

Table 4. Distribution of groundwater samples based on the classification of TH (after Todd and Mays, 2005).

Classification of TH (mg/l)	Sample numbers	Percentage of samples	Water type
<75	-	-	Soft
75–150	-	-	Moderately hard
150–300	1, 6–9, 11, 12, and 14	44.44	Hard
>300	2–5, 10, 13, and 15–18	55.56	Very hard

Table 5. Chemical analysis results of Qunayya Springwater samples during 6 months.

Sample	Na^{2+}			K^{+}			Ca^{2+}			Mg^{2+}			Cl^{-}			HCO_3^{-}			SO_4^{2-}			NO_3^{-}			PO_4^{3-}		
	min	max	mean	min	max	mean	min	max	mean	min	max	mean	min	max	mean	min	max	mean	min	max	mean	min	max	mean	min	max	mean
Springhead	30.8	44.8	37.1	4	5	4.7	59.1	65.2	57.6	50.8	58.4	55.0	67.4	77.4	71.6	235	257	244	23.5	26.3	24.6	35.7	66.7	47.4	0	2.8	0.90
Chlorination	30.8	44.8	37.1	4	5	4.6	48.0	60.1	54.5	48.5	53.0	51.0	76.0	82.5	78.7	205	257	237	22.7	28.2	24.9	35.0	66.7	46.9	0	0.1	0.06
House water	30.8	44.9	37.1	4	5	4.7	44.0	53.0	49.8	46.3	51.0	48.8	77.2	79.4	77.9	195	251	226	19.5	25.8	23.7	10.0	15.4	12.8	0	0.1	0.05
House tank1	30.8	44.8	37.1	4	5	4.6	45.1	55.1	50.7	47.0	50.6	49.5	77.7	83.5	80.5	191	251	222	21.4	30.2	25.6	10.0	14.5	12.5	0	0.1	0.02
House tank2	30.8	42.2	36.9	4	6	4.9	43.0	53.0	49.6	46.3	50.5	47.6	72.8	80.4	77.8	191	251	224	19.3	34.3	25.5	12.4	30.0	16.1	0	0.3	0.08
C1-500 m	30.8	44.8	37.0	4	5	4.5	53.0	62.0	55.4	43.9	55.7	51.4	66.3	76.5	70.9	234	257	242	12.1	36.6	24.4	35.1	66.7	47.2	0	2.5	0.86
C1-tank	30.8	44.9	37.5	4	5	4.5	49.0	60.0	54.8	46.6	54.9	46.7	67.4	82.5	72.9	232	255	240	22.9	42.7	29.6	31.2	65.7	45.0	.1	2.6	0.91
C2-tank	30.8	44.8	37.1	4	6	5.0	47.0	57.9	50.7	43.4	50.7	45.4	65.7	80.2	71.6	220	256	237	23.3	30.6	25.7	37.5	68.7	48.3	0	2.5	0.85
C2-start	30.8	44.8	37.6	4	5	4.5	52.0	64.0	56.3	50.0	56.1	51.1	65.5	76.8	70.6	220	256	238	22.1	28.7	24.8	37.8	70.5	49.4	0	3.0	1.05
C2-500 m	30.8	44.8	37.1	4	5	4.5	50.5	64.1	54.1	47.5	53.2	50.8	66.2	74.1	70.3	208	256	235	21.1	29.5	24.5	37.2	72.8	49.9	0	3.5	1.16
C2-1000 m	30.8	44.8	37.2	4	6	4.8	49.0	61.0	52.7	46.5	52.3	49.2	66.8	73.5	70.3	208	256	234	21.1	26.5	24.0	31.5	65.1	45.7	0	3.0	1.06
C2-1500 m	30.8	44.8	37.0	3	5	4.3	46.0	58.0	50.7	44.7	51.9	48.1	66.4	73.7	70.2	195	256	227	21.3	31.5	24.3	12.9	66.7	38.0	0	2.8	0.95
Mean			37.15			4.63			53.1			49.6			73.6			234			25.1			38.3			0.66

4.4. Water Type

The distributions of the dissolved ions in Qunayya Springwater and modifications in water character using Piper's trilinear diagram (Piper, 1944) were shown in Figure 4 to determine the type of water and its potability over six months and to determine the geochemical processes. Waters in the study area are characterized by the dominance of carbonates, chloride, calcium, magnesium, sodium, and sulfate.The percentages of Ca^{2+} (28.2–38.1%), Mg^{2+} (44.3–52.5%), $Na^{+} + K^{+}$ (17.2–29.4%), $HCO_3^{-} + CO_3^{2-}$ (50.7–62.5%), Cl^{-} (29.8–40.2%), and SO_4^{2-} (4.8–11.4%) are calculated for all groundwater samples they are plotted in the Piper's diagram (Table 6; Figure 4). One hundred percent of the groundwater sampling points are fall in zone 5. This indicates that alkaline earth and weak acids are occupied over the alkalies and strong acids. So, the groundwater quality is characterized by carbonate hardness exceeds 50%. Based on dominant cations and anions in the Qunayya Springwater, one water type was found for the water samples that analysed: Ca^{2+}–HCO_3^{-}, Ca^{2+}–Mg^{2+}–HCO_3^{-}, and Ca^{2+}–Mg^{2+}–Cl^{-}. The first two characters are to connect with the mineral processes (limestone–dolomite weathering, dissolution, and precipitation) and to the aquifer recharge. While the third characteristic is related to groundwater pollution, as it is associated with ion exchange processes, rock weathering, and halite solution. Consequently, depending on the results of Piper's diagram, the geochemical classification of groundwater indicates that the origin of salts and other dissolved solids in the groundwater came of during infil tration of recharge water which loaded of the influences of anthropogenic sources.

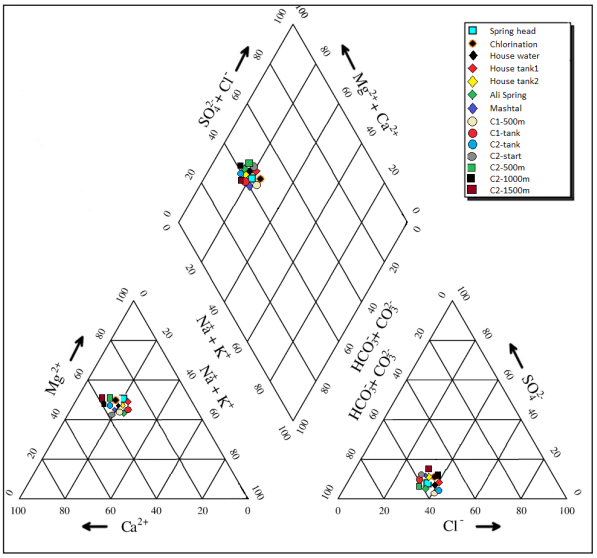

Figure 4. Piper's trilinear diagram of water chemistry in the study area (after Piper, 1944).

Table 6. Particulars of various parameters after Piper's diagram.

Particulars	Minimum	Maximum	Mean
Ca^{2+} (%)	28.2	38.1	34.2
Mg^{2+} (%)	44.3	52.5	49.4
$Na^{+} + K^{+}$ (%)	17.2	29.4	25.1
$HCO_3^{-} + CO_3^{2-}$ (%)	50.7	62.5	58.1
Cl^{-} (%)	29.8	40.2	36.6
SO_4^{2-} (%)	4.8	11.4	8.2

4.5. Water Quality

Water types depend on several factors to become suitable for several purposes: drinking, agriculture, and industrial purposes. These factors are codified into minimal standards required for the use of water. So the Jordanian standards (JS) (1997), World Health Organization (WHO) (1998, 2004, 2011), and the Environmental Protection Agency (EPA) have issued to set physical, chemical, and biological standards. A maximum and a minimum value have been given for each quality. Table 7 shows the analytical results of physical and chemical parameters of spring water in the study area, which were compared with the Jordanian standards, specifications, and values as recommended by the Ministry of Water and Irrigation (MWI) (2000, 2004) and the WHO for drinking and public health purposes. It appears that all the results fall within the permissible limits for using water for drinking and irrigation purposes. The analytical results of the physical parameters (TDS, pH, EC, and T) for Qunayya Springwater show that it follows the Jordanian and World Standards. Table 8 shows how to identify the taste of drinking water since there is a relationship between water quality and the total amount of dissolved solids (TDS) in the solution. The values of TDS were varied between 300–788 mg/l with an average of 383.4 mg/l, where the TDS concentration in 92.7 % of the samples was good while 7.3 % was acceptable. According to the Jordanian Standard (JS) and WHO guidelines, the range of eligible pH values of water specified for drinking purposes is between 6.5–9.2. The values of pH for the groundwater in the study area vary between 6.7 to 8.9 with a mean of 7.8 (Table 8).

Water type varies from one area to another and from time to time because of the geology of the aquifers and because of pollution sources (septic tanks, chemicals, and natural fertilizers…etc). Looking at the chemical analysis results along different periods, there are not any significant differences in the water quality. The hardness of water depends mainly upon the amounts of divalent cations, especially Ca^{2+} and Mg^{2+} which are the more abundant in groundwater. The acceptable limit of TH for drinking water is $\leq$ 300 mg/l as per WHO guidelines. Through the TH values of the groundwater samples in the study area, about 55.56 % of the total samples were classified under the category of very hard water, and they are not suitable for drinking (Table 4). Excess concentration of TH in water affects the formation of gallstones and bladder stones (Abboud, 2008), as well as affects the water's taste for drinking and the use of household items.

The most important ions that are used to determine the water suitability for drinking or irrigation are K^{+}, Na^{+}, Ca^{2+}, Mg^{+2}, HCO_3^{-}, Cl^{-}, SO_4^{2-}, NO_3^{-}, and PO_4^{-3}. So, any increase or decrease in the concentrations of these ions is attributed to several factors; lithology, structural setting, aquifer type, water flow, land uses, and human pollution. The concentrations of the ions of K^{+}, Mg^{+2}, and HCO_3^{-} are determined by the aquifer type and temperature (Gibbs, 1972). So, the concentrations of these ions will be increased through limestone or dolostone aquifers (Table 7). The analytical results of these ions in the groundwater

of the study area fall within the allowed limits according to Jordanian and international standards (Table 7). The relative increase in the concentrations of some of these ions in the groundwater may result from an increase in dissolution rate caused by an increase in the temperature in summer and the passage of water in the carbonate rocks.

Table 7. Specifications of Qunayya water depending on Jordanian Standard (JS), EPA, and WHO guidelines.

Variable (mg/l)	Spring rate	JS	WHO	EPA	Cause/Origin
pH	7.8	6.5 – 9	6.5-8.5	-	Acids, decrease CO_2 Pressure, bicarbonates increase pH
TDS	383.4	500-1500	500-1500	-	Dissolving rocks and soil, wastewater
TH	234–294	300–500	500	-	Calcium and Magnesium concentration total
Na^+	30–45	200–400	200	-	Dissolving all rocks and soil, connection with seawater and wastewater
K^+	4–6	12	12	-	Sediment rocks, man and cattle remnants
Ca^{2+}	43–65	75–200	75	-	Dissolving limestones and soil
Mg^{2+}	43–58	50–150	< 125	-	Dissolving all rocks and soil, connection with seawater and wastewater
Cl^-	65–83	200–500	250	250	Dissolving some rocks and soil, connection with seawater and wastewater
HCO_3^-	190–256	100–500	125–350	-	In all water types
CO_3^{2-}	0	-	-	-	Limestones and soil
SO_4^{2-}	12–42	200–500	250	250	Dissolving rocks and soil that contains sulfide and sulfates
NO_3^-	10–73	50–70	50	10	Dissolving the organic substances, wastewater, and fertilizers leftovers
PO_4^{3-}	0.01–3.5	0.2	0.2	-	Organic and chemical fertilizers, penetration of house wastewater, phosphate rocks

The decrease of Na^+, NO_3^-, and PO_4^{-3}concentration in the groundwater during the summer months (Table 7), may be the result of an increase in temperature which works to decrease the dissolution rate of the ions, which causes the decline in precipitation of ions to the aquifer. The water of Qunayya Spring that is pumped to the houses, has a decrease of K^+rate in the summer months (Table 7). That may be caused by the lack of water discharge in the aquifer. Moreover, The dissolution rate of K^+ becomes less during the winter months. Excessive sodium may lead to high blood pressure, heart disease, and kidney infection. Potassium is also important for maintaining fluid balance in the human body. While, the remarkable increase in the concentration of NO_3^- in the spring water over the allowed level may be caused by several reasons (Table 7), such as the use of natural and chemical fertilizers near the source of water, wastes which comes from the poultry farms and the cattle barns, wastes of olive mills, and finally, distribution of a large number of septic tanks in the area. Finally, the concentration of Ca^{2+} in the spring water has been higher than the permissible level according to the drinking water guidelines in the WHO, where it varies between 47 to 270 mg/l. Calcium and magnesium are two major components for building and healthy bones for a human and they are also essential in the metabolism process. Calcium is essential for preventing heart problems, while a deficiency of magnesium leads to protein deficiency and malnutrition (WHO, 2011). While the concentration means of Cl^-, NO_3^-, and SO_4^{2-} were within the permissible limit according to WHO (1998), and the water of Qunayya Spring was classified as being calcium bicarbonate water (alkaline water).

Table 8. Water classification depending on TDS in groundwater of Qunayya Spring (after WHO guidelines, 2004).

Type	TDS mg/l	% of samples
Very good	<300	-
Good	300 – 600	92.7 %
Acceptable	600 – 900	7.3 %
poor	900 – 1200	-
Unacceptable	>1200	-

4.6. Quality of Irrigation Water

4.6.1. Sodium percentage (Na%) and SAR Analyses

The suitability of water for irrigation was determined by the total amount of salt present and by the kind of salt and minerals in water (Wilcox, 1948; Todd, 1980). Increasing the total level of salts content in agricultural soil leads to the emergence of new problems in the growth and quality of different crops, so there may be an urgent need to impose special administrative and legal practices to maintain acceptable crop yields. The most important salts in this context are sodium, calcium, and magnesium concerning other cations and anions (Todd, 1980; Hem, 1991). The most harmful effects of water are the excessive accumulation of dissolvable salts and the concentration of sodium in the soil, which makes it difficult for plants to absorb water. Soils containing a high content of sodium with dominant carbonate anion are named alkaline soils; otherwise, if predominant of chloride or sulfate anion it develops to saline soil (Hem, 1991). Finally, the soil enriched in sodium will not support plant growth (Todd, 1980). The water at the study area was titrated and evaluated by studying values of $\%Na^+$, TDS, EC, and SAR, where the irrigation water has been

divided into groups to be compared with the international standards (Tables 9, 10, 11). Salinity is the total of inorganic solid material dissolved in water, and water salinization assigns to an increase of TDS and total chemical content of water (Ritcher and Kreitler, 1993). The percentage of sodium ($\%Na^+$) was measured related to the sodium hazard for judging the quality of water for irrigation, taking the ionic concentrations in meq/l. The content of sodium is commonly obvious in terms of sodium percent as summarized in Equation 2.

Table 9. Results of sodium ratio (Na%) analysis of Qunayya water.

Sample	December-2005	March-2006	May-2006	June-2006	July-2006	August-2006	Mean
Springhead	20.6	21.9	21.0	16.6	15.9	17.8	18.97
Chlorination	20.9	22.9	22.4	18.1	16.8	18.9	20.00
Bump water	21.9	24.1	22.7	18.7	17.6	19.5	20.75
House water1	21.8	24.4	23.3	19.0	18.1	19.5	21.02
House water2	-	-	18.9	19.1	18.1	19.7	18.95
C1-500 m	21.0	23.1	18.9	16.7	16.6	18.4	19.12
C1-tank	-	23.1	18.6	17.3	16.8	18.9	18.94
C2	-	22.3	17.6	16.9	16.3	18.6	18.34
C2-500 m	21.5	23.5	22.4	17.1	16.6	19.2	20.05
C2-1000 m	22.1	23.6	18.5	18.0	17.6	19.5	19.88
C2-1500 m	22.2	24.2	19.2	17.7	18.3	19.7	20.22
C2-tank	-	24.1	19.4	18.8	18.1	20.2	20.12
Mean	21.5	23.4	20.2	17.8	17.2	19.2	19.70

Table 10. Classification of irrigation water depending on sodium content (Na%) (after Glover, 1996).

Type	Na%	EC µS/cm
Excellent	20>	250>
Good	20 – 40	250 – 750
Acceptable	40 – 60	759 – 2000
Bad	60 - 80	2000 – 3000
Unacceptable	80<	3000<

Table 11. Results of sodium adsorption ratio (SAR) for Qunayya Springwater (meq/l).

Samples	December-2005	March-2006	May-2006	June-2006	July-2006	August-2006	Mean
Springhead	0.01	0.011	0.011	0.007	0.008	0.008	0.0092
Chlorination	0.01	0.011	0.011	0.008	0.008	0.009	0.0095
Bump water	0.011	0.012	0.011	0.008	0.008	0.009	0.0098
House water1	0.011	0.012	0.011	0.008	0.008	0.009	0.0098
House water2	-	-	0.008	0.008	0.008	0.009	0.0083
C1-500 m	0.01	0.012	0.008	0.008	0.008	0.008	0.0090
C1-tank	-	0.012	0.008	0.008	0.008	0.009	0.0090
C2	-	0.012	0.008	0.008	0.008	0.008	0.0088
C2-500 m	0.011	0.012	0.011	0.008	0.008	0.009	0.0098
C2-1000 m	0.011	0.012	0.008	0.008	0.008	0.009	0.0093
C2-1500 m	0.011	0.012	0.009	0.008	0.008	0.009	0.0095
C2-tank	-	0.012	0.009	0.008	0.008	0.009	0.0092
Mean	0.011	0.019	0.0094	0.008	0.008	0.0088	0.0093

The results of the percentage of sodium ($\%Na^+$) at Qunayya Springwater over 6 months are shown in table 9, where the increase in the percentage of sodium in the water harms the type of water and its suitability in agriculture or its usefulness for crops. Also, saline water, which contains high levels of sodium, reduces the permeability of agricultural soil due to the ion exchange processes between it and different soil ions such as calcium, potassium, and magnesium. The water classification in the study area in which the $\%Na^+$ varied between 15.9 to 24.4 with a mean of 19.7 (Table 9), came under an excellent classification in December, March, and May, while in the summer months, water was good and the classification varied between good to excellent (Table 10). The values of EC varied have between 446–943µS/cm (Table 3), and all samples were classified as good and acceptable (Table 10). Thus, the groundwater quality is suitable for irrigation. Sodium is adsorbed on clay surfaces by substitution of alkaline earth that destroys the soil structure

(Todd, 1980). The ion exchange process at the soil zone is commonly expressed in sodium adsorption ratio (SAR), the sodium hazard of water is mostly described by the SAR. The concentration of ions is taking in milliequivalents per liter (meq/l). This is computed by Equation 3. The effect of EC and (SAR) on water quality is shown graphically by the United States Salinity Laboratory (USSL: Richards, 1954). Table 11 shows the results of sodium adsorption ratio (SAR), which was determined from a chemical equation that relates the dissolved sodium concentration with the double valency cations dissolved in water. By using the results we can predict the rate of sodium between water and the soil which is saturated with the other double ions to make a balance. Thus, we can determine the water type to be used for irrigation and agriculture. The SAR values computed from the groundwater of the study area are in between 0.007 – 0.011 meq/l with a mean of 0.0093 meq/l, (Table 11).

Classification of groundwater quality for irrigation purposes depends on SAR versus EC (after Richards 1954). Therefore, we notice that the types of irrigation water in the study area based on that classification were concentrated in the medium (C2) and the high (C3) classifications (Richards, 1954; WHO, 1998), where the values of TDS ranged between 300–788 mg/l, and this indicates that the quality of the water of Qunnaya Spring for agriculture uses is threatened by salinity and not suitable for irrigation. This places the spring water in the medium salinity range that can be used in the medium sediment soil for irrigating plants without any special efforts for controlling salinity. According to the Wilcox salinity diagram (Figure 5) for the classification of sodium hazard, the zones of groundwater samples fall in two classes of water types; i.e., C2-S1 (57%) and C3-S1 (43%) which has medium to high salinity hazards and low sodium hazard. Besides, the zone of C2-S1 comes under the good water quality category, the zone of C3-S1 comes under the moderate water quality category for irrigation, with increasing salinity hazard from C1 to C4 and sodium hazard from S1 to S4 for irrigation processes (Figure 5). Finally, the distribution of Qunayya Springwater samples on Wilcox'ssalinity diagram by drawing the relationship between SAR and EC shows that the spring water is a low soda and medium salinity water. As spring water quality and its suitability for agriculture is a concern, it appears that the sodium concentration, which varies between 30–40 mg/l (Table 10) is within the permissible limit for agriculture. Whereas, the water is considered good according to the Todd classification (Todd, 1980).

4.6.2. Water Quality for Poultry and Cattle Uses

The high rates of ions in water may cause health problems and the death of animals. The high salinity of water used for poultry may harm the animals and cause them to die. The water type in the study area was evaluated for poultry and cattle based on issues of the National Academy for Science, 1972 (NRC, 1974). Comparing the results it appears that, the total dissolving salts (TDS) values vary between 300–788 mg/l (Table 3), and thus did not exceed the 1000 mg/l (Table 8) limit set by the recommendations of the National Academy for Science, 1972 (NRC, 1974). Hence, Qunayya Spring water is suitable for all purposes (drinking, agriculture, industry, poultry, and livestock).

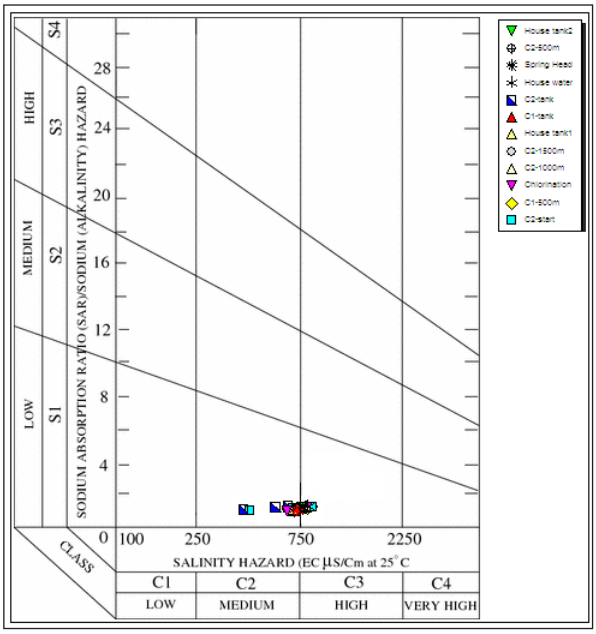

Figure 5. Classification of groundwater quality for irrigation purposes depends on SAR versus EC (after Richards, 1954).

4.6.3. Microbiological Water Quality

Qunayya Spring water has been used for drinking because of its high quality, since 1960 (WAJ, 2004). Recently different pollution cases have been reported as a result of the increase in bacillus coliforms above the permissible limits in the Jordanian Standards 286/2001 (WAJ, 2001). This has been attributed to leaking from septic tanks and the use of natural fertilizers in nearby farms (WAJ, 2004; MM, 2003). The existence of cattle and poultry farms at the northeast and northwest of the spring head is the main threat to the Quanyya spring water. The use of natural and chemical fertilizers in the surrounding farms and the existence of olive mills at the high areas northeast of the spring cause the residual of chemicals and olives oil leftovers to leak into the spring source. The burial of the poultry consumed cars, and detergent remnants in the spring water zone can pollutethe groundwater, especially when the water moves through it. Moreover, the overpumping of the groundwater and leakage of the wastewater from the septic tanks in the area lead to pollution of groundwater of Qunayya Spring.

The results of the bacterial analyses show the degree of water pollution by total coliform and faecal coliform bacillus. Table 12 shows the microbiological specifications for the water samples where the most probable number (MPN) of the bacterial colonies are less than one for every 100 ml of the sample is drinkable water, while the samples where the most probable number of the bacterial colonies are more than one is polluted water and not suitable for drink according to the Jordanian Standards Specifications (286/2001). Most of the results show that Qunayya Spring water is polluted in colon bacillus where the MPN for every 100 ml of total coliform vary between (15–100 MPN/100 ml), i.e it is undrinkable water except for the samples taken in March where the bacterial analysis results have been good and the water has not been polluted. But the faecal coliform bacteria' most probable number for every 100 ml varied between (10-35 MPN/100 ml). As a final result

of microbiological contamination in the study area; The results of faecal coliform culture indicate the risks of water pollution in the area of Qunayya Spring due to the spread of septic tanks in the area, in addition to the extensive use of chemical and natural fertilizers in agriculture. Therefore, the Ministry of Water and Irrigation (MWI) reported the pollution caused by organic substances in the Qunayya Spring waters in the period between 1980-1996, and it did not report the inorganic pollution present in the water. Thus, constant analyses in addition to the regular and periodical analyses for water quality before and after treatment of the spring is highly recommended.

Table 11. Results of microbiology analysis for Qunayya water during 6 months.

Sample	Decem.-2005		June-2006		March-2006		July-2006		May-2006		August-2006	
	F.CMPN/100ml	T.C MPN/100ml	F.C MPN/100ml	T.C MPN/100ml	F.C MPN/100ml	T.C MPN/100ml	F.C MPN/100ml	T.C MPN/100ml	F.C MPN/100ml	T.C MPN/100ml	F.C MPN/100ml	T.C MPN/100ml
Spring head	20	42	35	100	1>	1>	16	17	10	50	14	15
Chlorination	1>	42	60	84	1>	1>	19	33	14	40	1>	1>
Bump water	1>	1>	1>	1>	1>	1>	1>	1>	1>	1>	1>	1>
House water1	1>	3	1>	1>	1>	1>	1>	1>	1>	1>	1>	1>
House water2	1>	1>	1>	1>	1>	1>	21	31	1>	1>	1>	1>
C1-500 m	17	41	21	33	1>	17	-	-	5	22	5	7
C1-tank	-	-	25	50	1>	1>	1>	22	23	44	1>	1>
C2	-	-	9	11	1>	3	10	43	3	5	25	27
C2-500 m	67	79	24	30	1>	16	20	35	1>	12	19	30
C2-1000 m	2	52	1>	1>	1>	2	26	51	1>	2>	22	33
C2-1500 m	17	31	1>	1>	1>	16	9	17	1>	8	24	35
C2-tank	-	-	1>	1>	1>	1>	1>	3	1>	1>	1>	1>

5. Conclusions

This study has highlighted the hydrochemical regime of the Qunayya Springwater as well as identified the quality of the water in the Amman-Zarqa Basin. So, the rainfall amount at the study area along 22 years ranged between 100-355 mm, and during this period the total discharge in the catchment area was about 4.3 MCM/year. The quality of groundwater in the study area was characterized by moderately high to high pH and TH because of the high concentrations of carbonates. The TH is in between 176 and 412 mg/l and classified as hard to very hard categories. The major cations in the groundwater were arranged as follows Ca^{2+}> Mg^{2+}> Na^{+}> K^{+}, while the anions are also arranged as HCO_3^-> Cl^-> NO_3^-> SO_4^{2-}> PO_4^{3-}. Based on dominant cations and anions in the groundwater of Qunayya Spring, the main types of hydrochemical facies were found for the water samples are Ca^{2+}–HCO_3^-, Ca^{2+}–Mg^{2+}–HCO_3^-, and Ca^{2+}–Mg^{2+}–Cl^-. The facies also propose that the ion exchange and evaporation factors are the secondary processes for higher concentrations of Na^+ and Cl^- ions. The influences of country rocks, weathering process, dissolution of salts stocked in soil, irrigation practice, natural and chemical fertilizers, solid wastes, and anthropogenic actions are the other reasons for increasing Mg^{2+}, Na^+, Cl^-, SO_4^{2-}, NO_3^-, and PO_4^{3-} ions in the groundwater. Thus, the results of groundwater quality plotted on Piper's diagram, the geochemical classification of groundwater chemistry indicates that the origin of dissolved solids in the groundwater came of during infiltration of recharge water which loaded of the influences of anthropogenic sources. The distribution of groundwater samples on Wilcox's salinity diagram shows that the spring water is low soda and medium salinity water. The salinity hazard is considered as low to medium, which that the sodium concentration is between 30–40 mg/l, is within the permissible limit for agriculture. The groundwater quality is characterized by carbonate hardness exceeds 50%, and also suitable for drinking. The major element concentrations of all samples have lower content than the acceptable limits for drinking water. Finally, the reason for microbiological pollution hazards of water at Qunayya Spring area refers to the existence of leakage of the septic tanks in homes, and the use of chemical and natural fertilizers by farmers.

Acknowledgment

I would like to thank the Jordan Journal of Earth and Environmental Sciences (JJEES) represented by the Editor-in-Chief for its relentless and continuous endeavor to carefully and thoroughly review the manuscript to make it in its final form ready for publication. I would also like to thank the reviewers who made the great effort to audit and review the manuscript, and in particular, I would like to thank reviewer No. 3 who gave a clear and great effort in reviewing the manuscript and made accurate and valuable notes that raised the level of effort to produce the manuscript in its current form.

References

Abboud, I.A. (2008). Mineralogy and chemistry of urinary stones, patients from North Jordan. Environmental Geochemistry and Health 30(5):445-463. DOI: 10.1007/s10653-007-9128-7.

Abboud, I.A. (2014). Describe and statistical evaluation of hydrochemical data of karst phenomena in Jordan: Al-Dhaher Cave Karst Spring. Journal of Applied Geology and Geophysics 2(3):23–42.

Abboud, I.A. (2018a). Geochemistry and quality of groundwater of the Yarmouk basin aquifer, north Jordan. Environmental Geochemistry and Health (2018) 40:1405–1435. DOI: 10.1007/s10653-017-0064-x.

Abboud, I.A. (2018b). Statistical analysis of the hydro-geochemical evolution of groundwater in the aquifers of the Yarmouk basin, North Jordan. Arabian Journal of Geosciences 11: 111. DOI: 10.1007/s12517-018-3448-z.

Abed, A.A. (1982). Geology of Jordan. Publications of Islamic Progress Library, Amman-Jordan (in Arabic).

Abed, A.A. (2000). Geology of Jordan, environment and water. Jordan Geological Association, 571 pp. (in Arabic).

Abed, A., Sadaqa, R., Al Kuisi, M. (2008). Uranium and Potentially Toxic Metals during the Mining, Beneficiation, and Processing of Phosphorite and Their Effects on Ground Water in Jordan. Mine Water and the Environment 27: 171-182. DOI: 10.1007/s10230-008-0039-3.

Al Kuisi, M., Abed, A., Mashal, K., Saffarini, G. (2015). Hydrogeochemistry of groundwater from karstic limestone aquifer highlighting arsenic contamination: a case study from Jordan.

Arabian Journal of Geosciences (2015) 8:9699–9720. DOI: 10.1007/s12517-015-1919-z.

Al Kuisi, M., Al-Qinna, M., Margane, A., Aljazzar, T. (2009). Spatial assessment of salinity and nitrate pollution in Amman Zarqa Basin: a case study. Environmental Earth Sciences 59(1):117-129. DOI: 10.1007/s12665-009-0010-z.

Al Kuisi, M., Mashal, K., Al-Qinna, M., Abu Hamad, A., Margane, A. (2014). Groundwater Vulnerability and Hazard Mapping in an Arid Region: Case Study, Amman-Zarqa Basin (AZB)-Jordan. Journal of Water Resource and Protection. 6(4):297-318. DOI:10.4236/jwarp.2014.64033.

APHA (1998). Analytical methods for determining chlorine dioxide and chlorite in environmental samples by American Public Health Association. In Hofmann et al.

Berner, E.K., and Berner, R.A. (1987). The global water cycle, geochemistry and environment. Prentice-Hall, New Jersey.

Bhatt, K.S., and Saklani, S. (1996). Hydrogeochemistry of the Upper Ganges River. Journal of The Geological Society of India 48:171-182.

Brunke, H.P. (1997).Groundwater resources of northern Jordan. V5 Part 1: Three-dimensional groundwater flow model of northern Jordan. Unpublished report prepared by Federal Institute of Geosciences and Natural Resources (BGR) and Water Authority of Jordan (WAJ). Technical cooperation project "Groundwater resources of northern Jordan". BGR archive No 118705: Amman and Hannover.

CDM, Camp Dresser and McKee International Inc. (2002). Jordan Water Quality Management Program: Compilation of technical Memoranda. USAID Report, December 2002.

Cushing, E.M., Kantrowitz, I.H., Taylor, K.R. (1973). Water resources of the Delmarva Peninsular. US Geological Survey Professional, Paper 822, Washington DC.

Elemat, M. (2012). Climate in Jordan, Jordan Meteorological Department. Third MEDARE Workshop On Building Mediterranean Long-Term And Homogenized Climate Datasets. Istanbul, Turkey, 27-28 September 2012.

Eraifej, N., and Abu-Jaber, N. (1999). Geochemistry and pollution of shallow aquifers in the Mafraq area, North Jordan. Environmental Geology 37(1-2): 162-170.

Gibbs, R.J. (1972). Mechanism of trace metal transportation rivers. Science 180:71-73.

Glover, C.R. (1996). Irrigation Water Classification Systems. Cooperative Extension Service College of Agriculture and Home Economics. Guide A-116, 4p.

Hem, J.D. (1970). Study and interpretation of the chemical characteristics of natural water. 2nd, US Geological Survey Water-Supply Paper 1483, p 269.

Hem, J.D. (1991). Study and interpretation of the chemical characteristics of natural water: USGS Professional Paper Book 2254. 3rd edn. Scientific Publishers, Jodhpur.

Jacks, G. (1973). Chemistry of groundwater in a district in southern India Journal of Hydrology 18:185–200.

John, R., and Holum (1986). Fundamentals of general organic and biological chemistry, 3rd edition.

(JS) Jordanian Standards (1997). Jordanian Drinking Water Standards. JS 286/1997.

Karanth, K.P. (1991). Impact of human activities on hydrogeological environment. Journal of the Geological Society of India 38:195-206.

Karanth, K.P. (1997). Groundwater assessment, development and management.Tata McGraw-Hill Publisher, New Delhi.

Margane, A., and Almomani, M. (1995). Groundwater resources of northern Jordan, V2 Part 1: Groundwater abstraction in northern Jordan. Unpublished report prepared by Federal Institute for Geosciences and Natural Resources (BGR) and Water Authority of Jordan, (WAJ), Technical cooperation project 'Groundwater Resources of Northern Jordan', BGR-archive No. 118702; Amman and Hannover.

MM (2003). Ministry of Municipal: Village and environment affairs, Qunayya village organization plan–capital governorate (in Arabic).

MWI (2000). Ministry of Water and Irrigation (MWI), Central Laboratories for Water Type, Amman, Bayadir Wadi Al-Seer, Jordan (in Arabic).

MWI (2004). Ministry of Water and Irrigation (MWI) and German Technical Cooperation (GTZ); National water master plan. German Technical Cooperation, Amman.

MWI (2010). Ministry of Water and Irrigation (MWI), Water Information System. Hydrological, Geological and Hydrogeological Data Bank. MWI, Water Resources and Planning Directorate, Amman, Jordan.

NRA Natural Resources Authority, Geology Directorate, (2004). Geology Map of Amman Zarqa Basin. Scale 1:50,000. Natural Resources Authority Geology Directorate, Amman.

NRC National Research Council (1974). Nutrients and toxic substances in water for livestock and poultry. National academy of Sciences, Washington, Dc.

Pazand, K., Hezarkhani, A., Ghanbari, Y., Aghavali, N. (2012). Groundwater geochemistry in the Meshkinshahr basin Ardabil province in Iran. Environmental Earth Science 65:871-879. DOI: 10.1007/s12665-011-1131-8.

Piper, A.M. (1944). A graphic procedure in the geochemical interpretation of water analyses. American Geophysical Union Transactions 25:914–923.

Quennel, A. (1951). The Geology and Mineral Resources of Trans-Jordan. Colonial Geology and Mineral Resources 2: 85-115.

Rao, N.S. (2002). Geochemistry of groundwater in parts of Guntur district, Andhra Pradesh, India. Environmental Geolology 41:552-562. DOI: 10.1007/s002540100431.

Rao, N.S., Subrahmanyam, A., Ravi,S.K., Srinivasulu, N., Babu, G.R., Surya, P.R., Venkatram, G.R.(2012). Geochemistry and quality of groundwater of Gummanampadu sub- basin, Guntur District, Andhra Pradesh, India. Environmental Earth Sciences 67(5):1451- 1471. DOI: 10.1007/s12665-012-1590-6.

Richards, L.A. (1954).Diagnosis and improvement of saline and alkalis soils. US Department of Agriculture Handbook 60, ed. Washington; United States Salinity Laboratory Staff, 159p.

Rimawi, O. (1985). Hydrochemistry and isotope hydrology of groundwater and surface water in the northeast of Mafraq, Dhuleil, Hallabat, Azraq Basin. PhD dissertation, Technical University of Munich.

Ritcher, B.C., and Kreitler, W.C.(1993). Geochemical techniques for identifying sources of groundwater salinization. CRC, New York. ISBN 1-56670-000-0.

Ritzi, R.W., Wright, S.L., Mann, B., Chen, M. (1993). Analysis of temporal variability in hydrogeochemical data used for multivariate analyses. Ground Water 31:221–229.

Salameh, E. (1996). Water quality degradation in Jordan, Amman. The Higher Council of Science and Technology, Ebert, Fredrich.

Sawyer, G.N., and McCarty, D.L. (1967). Chemistry of sanitary engineers, 2nd edn, McGraw Hill, New York, 518 pp.

Stallard, R.E., and Edmond, J.M. (1983). Geochemistry of Amazon River: the influence of the geology and weathering environment on the dissolved load. Journal of geophysical research 88:9671–9688.

Stumm, W., and Morgan, J.J. (1996). Aquatic chemistry. Wiley-Interscience, New York.

Tabieh, M.A.S. and Al-Horani, A. (2010). An Economic Analysis of Water Status in Jordan. Journal of Applied Sciences 10(16): 1695-1704.

Todd, D.K. (1980). Groundwater hydrology. 2nd edition. John Willey and Sons, New York.

Todd, D.K., and Mays, L.W. (2005). Groundwater Hydrology, third Edition, 2005. Larry W. Mays (Author). Publisher NG.

UNESCO (2012). Managing Water under Uncertainty and Risk. The United Nations World Water Development, Report 4, Chapter 39.

WAJ (1995).Water Authority of Jordan.Groundwater resources of northern Jordan. Project No. 89.2105.8. V2 Groundwater abstraction groundwater monitoring. Part 1, report and appendix 1-4, Amman, Jordan.

WAJ (1996).Water Authority of Jordan. Groundwater resources of northern Jordan. Project No. 89.2105.8. V1 Rainfall, Spring discharge and baseflow. Part 2, report and appendix 1-4, Amman, Jordan.

WAJ (2001).Water Authority of Jordan, Jordanian standards. Guidelines for drinking water.

WAJ (2004).Water Authority of Jordan. Hannover and Natural Resources (BGR) and Water Authority of Jordan (WAJ), Technical cooperation project 'Groundwater Resources of Southern Jordan', Report No. 108652 and 107375; Southern Jordan, V1-5, Unpublished report prepared by Federal Institute for Geosciences.

Wardam, B. (2004). More politics than water: Water rights in Jordan. Global Issue Papers (11). Published by the Heinrich Böll Foundation, © Heinrich Böll Foundation: 60-107.

WHO (1998). World Health Organization. Guidelines for drinking water quality. V3, Drinking water quality control in small community supplies, Geneva.

WHO (2004). World Health Organization. Guidelines for drinking water quality, Geneva.

WHO (2011). World Health Organization. Guidelines for drinking water quality, Geneva.

Wilcox, L.V. (1948). Water quality for agriculture, Annex I Water analyses of 250 selected irrigation supplies from various locations in the world, FAO Irrigation and drainage paper 29 Rev., 1, Reprinted 1989, 1994, California, USA.

JJEES

JJEES (2021) 12 (3): 269-274
ISSN 1995-6681

Jordan Journal of Earth and Environmental Sciences

Soil phosphorus availability indices and saturation ratio as an index of environmental risk assessment

Jamiu Azeez[1*], Adeoba Aghorunse[1], Ganiyu Bankole[1], Melvis Anamezeonye[1], Timothy Adegbite[1], Saidat AbdulAzeez[2]

1Department of Soil Science and Land Management, Federal University of Agriculture Abeokuta, Nigeria
2Agricultural Technology Department, Yaba College of Technology, Epe Campus, Lagos

Received 7 December 2020; Accepted 15 March 2021

Abstract

The use of phosphorus saturation ratio (PSR) as the index for soil pollution potential in some animal waste dump sites of southwest Nigeria was evaluated. Surface and sub-surface soil samples were taken from 20 animal waste dump sites. Soil chemical properties, phosphorus availability indices and PSR were determined and analyzed. Results indicated that the unregulated dumping of manures in soils resulted in high phosphorus availability with a higher concentration in the top 20 cm of the soils. The PSR of the soils (0.42, topsoil and 0.32, subsoil) are more than the threshold values of 0.10-0.15, indicating soil P pollution of the environment. Some P availability indices could be used as a proxy for estimating soil PSR and hence soil P pollution potential. The soil P load is more than the amount that could be sorbed by the soil clay but has a strong correlation with soil organic matter. It was concluded that there is potential pollution of surface and groundwater in the vicinities of the dumpsites with possible attendant health hazards. Hence, the need to exploit alternative soluble P management options like precipitating the soluble P in the manure by applying materials rich in Al, Fe and Ca.

Keywords: Phosphorus saturation ratio; animal waste; dumpsites; phosphorus availability indices

1. Introduction

Across the globe, in the 1990s, the quantities of poultry meat and eggs from the developing countries was more than that of developed countries (Windhorst, 2006). Globally, data in 2005, showed that the contribution of the developing countries was 67 % in egg production (Windhorst, 2006), and was adjudged low. This is largely due to the proportion of these products dedicated to local consumption, and for use as raw materials in local food industries.

Recent agricultural policy of both state and federal government in Nigeria and other sub-Saharan African countries are geared towards increasing the production of poultry products. Primarily to meet up with global expectation and increase of balance of trade, and curb protein malnutrition. These have resulted in the increased production and consumption of livestock meat and meat products. Recently, the numbers of livestock producers have increased tremendously, particularly poultry farmers. Perhaps, due to the short gestation period of the venture (broiler production). The lucrative nature of these production ventures has attracted many unemployed people into the business.

Intensive livestock production entails the use of highly nutritious feed ingredients and additives. However, only a fraction of the ingredients and additives are utilized by the animals while some percentage of it is excreted. The disposal and management of the animal waste generated from the livestock industry are of great environmental concern, the drudgery and the high volume to nutrient content ratio have made the use of these resources limited in Sub-Saharan Africa. This has led to the accumulation of a huge mass of livestock wastes at dumpsites with the attendant pollution of the soil with heavy metals (Azeez et al., 2009).

Though, the land application of wastes from confined animal pens and cages is an effective disposal system, because it supplies nutrients to crops and pasture land (Soupir et al., 2005). However, the runoff from such land is a potential source of fecal contamination in water (Crowther et al., 2002; Gerba and Smith, 2005; Tian et al., 2002).

Animal wastes are rich in nutrients. Typically, poultry litter contains 8 to 25.8 g P kg^{-1} dry weight, with about 4.9 g P kg^{-1} being water-soluble reactive P. This is because P is added to chicken (Gallus gallus) diets to ensure rapid growth (Codling et al., 2000; Edwards and Daniel, 1992). The application of excess P through the deliberate deposition of the animal waste could results in environmental disaster (Sauer et al., 1999). In crop husbandry, excessive and unsynchronized application of excessive amounts of inorganic or organic P fertilizers is not desirable. Doing this will lead to loss of phosphorus to nearby water bodies, through runoff and subsurface losses (Nair, 2014; Hooda et al., 2000; Sharpley and Tunney, 2000). The consequent loss of P to soil and water bodies has an adverse impact on water quality. This eventually affects human and animals' health, ecological diversity, the cycling of nutrients and the proper functioning of the ecosystems (Nair, 2014).

Eutrophication and environmental degradation are some

* Corresponding author e-mail: azeez2001ng@yahoo.com

of the problems emanating from P loss to the environment (Liao et al., 2015). Unfortunately, there are many such dumpsites scattered across livestock farms with little or no regards for the consequences of such unregulated and improperly managed disposal systems, particularly in sub-Saharan Africa. Hence, to enhance the economic and ecological sustainability of these livestock production ventures, it is imperative to document the soil P status. Also, there is the need to evaluate the potential risk assessments, because, it was reported that non-point pollution from agricultural ventures is major causes of degradation to water bodies (USEPA, 2002 and 2003).

Iron and aluminum oxides play a substantial role in determining the soil P status (Azeez and Van Averbeke, 2010) and the amount of P loss to the environment. Hence, the direct measurement of P loading in agricultural systems without the concurrent measure of the Fe and Al in the soil could be challenging (Nair, 2014). This has led to the development of 'phosphorus saturation ratio' (PSR) with threshold values indicating risk assessment in land-use systems. Extensive use of the ratio has been reported in the literature for Europe and America (Breeuwsma and Silva, 1992; Nair et al., 2004; Sharpley et al., 2013), to predict environmental limits for soil P in soils. However, no documented information on its use in Africa and other less developed countries.

The P saturation ratio (PSR) was calculated as the molar ratio of Mehlich-1 P (P_{M1}) to Mehlich-1 Fe and Al (Fe_{M1} and Al_{M1}). The ratio was reported by Breeuwsma and Silva (1992) and Nair et al., (2004) to be related to soil solution P concentration. It computes threshold values that correspond to a set critical solution concentration.

Mathematically, it is expressed as:

$$PSR_{M1} = (P_{M1}/31) / [(Fe_{M1}/56) + (Al_{M1}/27)].$$

The use of this index for the evaluation of the soil of animal dumpsites will thus provide information for environmentalists and policymakers on the impact of dumping animal wastes on soils. It will also provide information on the status of the soils and the possible management options that could be adopted to make the practice ecologically sustainable. Consequent to above, the objectives of this study were to characterize soil P availability on manure impacted soils; evaluate the risk of P loss to the environment and determine the relationship between P availability indices, some soil properties and the P risk assessment index (PSR).

2. Materials and methods

2.1. Site Characterization

Representative samples were taken from twenty (20) different locations of animal waste dumpsites within Ogun and Oyo States, Nigeria. Ten of the locations were poultry waste dumpsite and the other ten locations were either cattle or goat or pig waste dumpsites. The Soil samples were collected at 1 meter away from the respective dumpsites at depths of 0-20 cm and 20-60cm, the coordinates of the sampling site were taken with the aid of Hand-Held Garmin (GPS) while data on the history of the sites were also taken. Details of the history and coordinates of the sites are shown in Table 1.

Table 1. Soil history and the GPS coordinate of the sampling sites.

Soil	Years	Location (Abeokuta)	Soil	Years	Location (Ibadan)
A1	>10	University farm (cattle)	B1	> 10	Eleyele (Poultry)
A2	> 10	University farm (pig)	B2	> 10	Mokola (Poultry)
A3	> 10	University farm (Goat)	B3	12	Egbeda (Poultry)
A4	> 10	University farm (sheep)	B4	> 15	Ring Road (Poultry)
A5	> 10	University farm (goat)	B5	8	Agugu (cattle)
A6	0.7	Kihinleyin, Camp (poultry)	B6	> 30	Oranyan Market Ibadan (Goat)
A7	2	Apakila, Abeokuta (poultry).	B7	3	Lagos-Ibadan expressway (cattle)
A8	5	Osiele, Abeokuta (poultry)	B8	>10	Alapafon Airport (Poultry)
A9	> 10	University Project Farm (poultry)	B9	> 30	Central Abattior (cattle)
A10	3	University farm (Poultry)	B10	> 20	Bodija (cattle)

2.2. Soil Determinations

The soil samples were air-dried, pulverized and screened with a 2mm sieve. The samples were analyzed for the particle size distribution using the hydrometer method (Bouyoucos, 1965). Soil pH was determined using the pH meter by preparing soil and water mixture of (1:2) solution after shaking using a mechanical shaker (Mclean, 1982). The organic matter content of the samples was determined by the dichromate acid oxidation method (Nelson and Sommer, 1982).

In triplicates, phosphorus availability indices were evaluated by determining the soil P content by colour formation using an ascorbic acid solution, potassium antinomy tartrate, sulfuric acid, and molybdate solution. The P was read on the spectrophotometer at a wavelength of 882 nm (Murphy and Riley, 1962). The P determinations were done after extraction with the following chemicals used as indices of P availability:

1. Distilled water extractants: Distilled H2O (Nair, 2004).
2. Mehlich 1, double acid extractant; 0.1 M sulfuric acid (H2SO4) + 0.1 M HCl (Mehlich, 1953).
3. Bray 1 extractant; 0.03 M NH4F + 0.025 M HCl (Bray and Kurtz 1945).53).
4. Olsen extractant; 0.5 M NaHCO3 and pH adjusted to 8.5 (Watanabe and Olsen 1965).ch, 1953).

From the supernatant of the Mehlich + soil solution mixture, extractable Fe was determined colorimetrically using the orthophenanthroline method at 510 nm. Aluminum

was determined colorimetrically by the xylenol orange method at 550 nm, both using a spectrophotometer. Phosphorus saturation ratio (PSR) was estimated as described earlier above.

2.3. Data Analyses

Data obtained were subjected to analysis of variance (ANOVA), and treatment means were separated using the Duncan's multiple range test at the 5% probability level using a statistical analysis system (SAS, 1990). Correlation and regression analyses were done to estimate relationships and their magnitude among the soil P availability indices, PSR and other soil properties.

3. Results and Discussion

3.1. Site Characteristics

In Table 1, it is obvious that the history of the dumpsites varies widely. Animal wastes have been dumped on the farm for as small as two years to more than 30 years, expectedly, the impact of these contrasting years is expected to vary. Sites in Ibadan also had more years of deposition of the waste compared with the sites in Abeokuta. The pictorial representation of the study sites is shown in Figure 1.

3.2. Effect of the Soil depth on P availability indices, PSR and soil properties

The effect of the soil sampling depths on the PSR, soil P availability indices and some soil properties is shown in Table 2. The four availability indices (water-extractable P, Olsen P, Mehlich P and Bray-1 P) were significantly higher in the topsoil (0-20 cm) compared with the subsoil. The high P values in this depth explain why many plants (arable and surface feeders) could not survive on the sites, probably due to P toxicities. The few higher plants (trees and shrubs) that survive are deep feeders that could tolerate the relatively lower nutrients at the subsoil. The environmental implication of this was that water that flows on the soil surface, even at 60 cm soil depth, as runoff or lateral flows stands the chance of exporting a large amount of P to the receiving water bodies. This could cause eutrophication and environmental degradation; such water will not be portable for human use. Mehlich extractable Fe was concentrated in the 0-20 cm depth while Al was higher at 20-60 cm depth. Generally, the PSR at both soil depths is higher than the threshold of 0.1-0.15 suggested by Nair, (2004) and Dari et al. (2018). This implies potential pollution of the soil with phosphorus. However, the tendency to pollute was higher at the 0-20 cm depth. The soil pH and dissolved salt are expectedly higher at the topsoil. The differences in value were only significant in the soil pH.

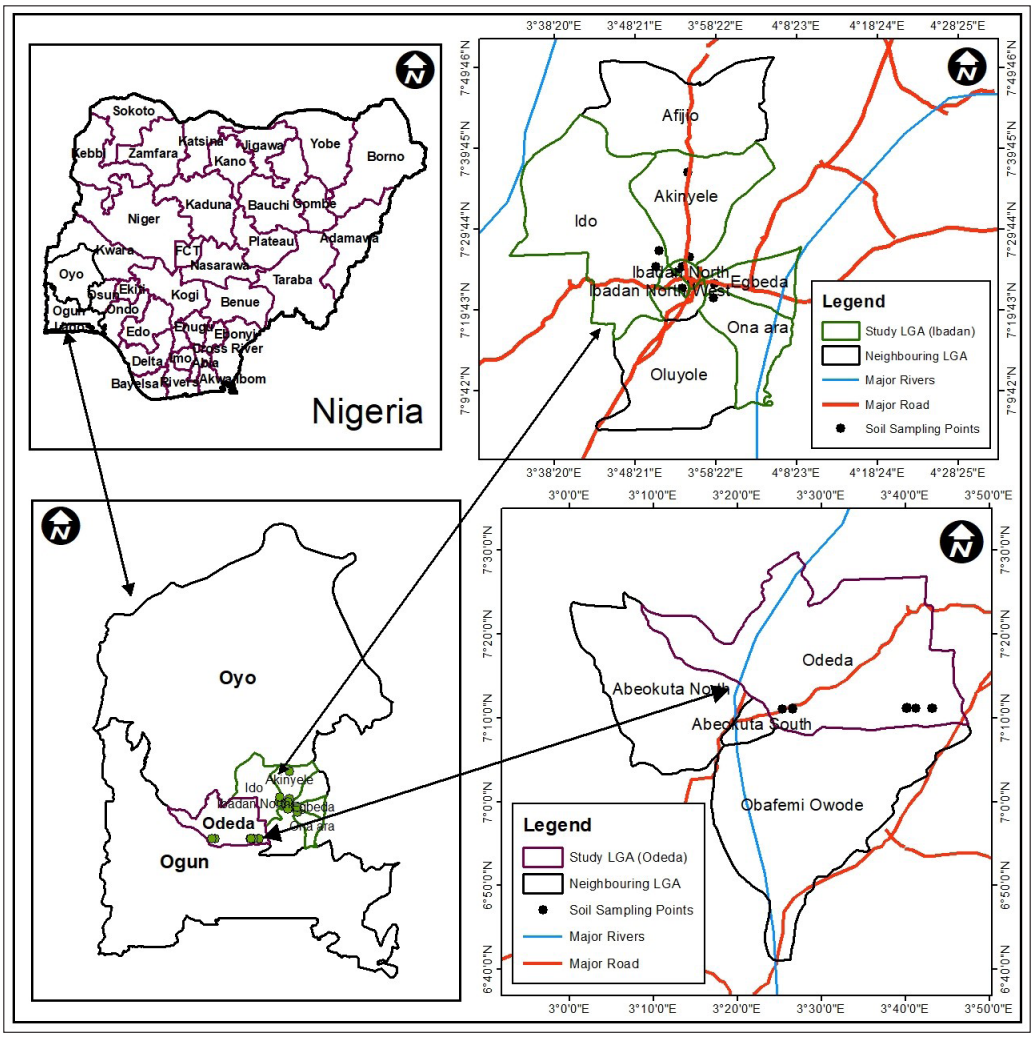

Figure 1. Map showing the study area.

Table 2. Effect of soil depth on PSR, P amounts and some soil chemical properties.

Depth (cm)	Water soluble	Olsen	Mehlich-1	Bray-1	M-Al	M-Fe	PSR	pH	EC
	mg kg^{-1}								µS cm^{-1}
0-20	278.16 ± 5.89 a	359.35 ± 15.27 a	426.24 ± 11.25 a	385.64 ± 12.69 a	527.32 ± 27.95 b	1174.3 ± 158.47a	0.42 ± 0.02 a	8.34 ± 0.05 a	872.30 ± 131.50 a
20-60	256.15 ± 3.36 b	305.59 ± 12.61 b	386.35 ± 15.03 b	378.10 ± 15.91 a	809.60 ± 48.39 a	760.80 ± 62.88 b	0.32 ± 0.02 b	7.33 ± 0.07 b	664.30 ± 133. 79 a

M-Al - Mehlich attractable aluminum *PSR – Phosphorus saturation ratio*
M-Fe - Mehlich attractable iron *EC – Electrical conductivity ± Standard error of mean*

3.3. Relationship between phosphorus saturation ratio availability indices and their implications

Figure 2, shows that the relationship between soil PSR and water-extractable P is positive and significant. The figure indicates that all the sites had PSR values higher than the threshold value of 0.10-0.15. It implies that the soils are all polluted with P from the accumulation of animal wastes. Water-soluble P (WSP) is an index of P pollution/availability and the strong relationship ($p < 0.01$) between the PSR and WSP shows that PSR is a valid tool that could be used in determining soil P pollution potential. Other researchers have also reported high PSR value in manure impacted soil with a strong relationship with WSP (Nair 2004; Liao et al., 2015).

Other soil P availability indices showed in Figures 3 and 4 show the same trend. Phosphorus extracted with acids (HCl in Bray 1; and HCl and H_2SO_4 in Mehlich), had all the P amounts higher than the threshold values. With acid extraction, the amount of P extracted is expected to be higher than the WSP. The significant relationship between the PSR and the P amounts by these extractants shows they could be used to predict the PSR. Bray-1 P and Mehlich-P are routinely determined in soil laboratories and hence could be used in the estimation of PSR values of soils. Other earlier researchers have reported that the potential loss of P from soils can be assessed using soil test phosphorus (STP). Extractants like Olsen, Mehlich-3, and acetic acid have been recommended by Miller et al. (1993), though were originally designed to estimate plant-available P. They also reported a certain degree of relationship between STP and the loss of P in runoff in soils of the same type (Hooda et al., 1999)

The effect of the soil organic matter on the PSR is shown in Figure 5. It was observed that the increase in soil organic matter as a result of the deposition of the manures had a significant and positive relationship with the PSR. Hence the more the increase in soil organic matter as a result of manure deposition, the more the soil PSR. It could then be concluded that the soil P pollution as measured by the PSR was caused by the manure deposition. Humus is the product of the decomposition of soil organic matter and it has been reported to be responsible for the sorption of nutrients like phosphate (Azeez and Van Averbeke, 2010). The contribution of the inorganic colloids (clay) to the PSR was estimated as shown in Figure 6. It was revealed that the relationship was negative and significant. This implies that the clay content of the soil had no positive effect on the P saturation of the soil. Hitherto, clay was presumed to be one of the soil components that adsorb phosphate in the soil, but this study shows that the heavy amount of phosphate in the soil is independent of the soil clay amounts. The heavy deposition of the manures could have impacted such a huge effect, over the soil clay P sorption capacity. Hence, for soil near manure dump sites, the soil colloidal ability to sorb P is usually exceeded particularly if such period of dumping is in excess of 10 years as seen in this study.

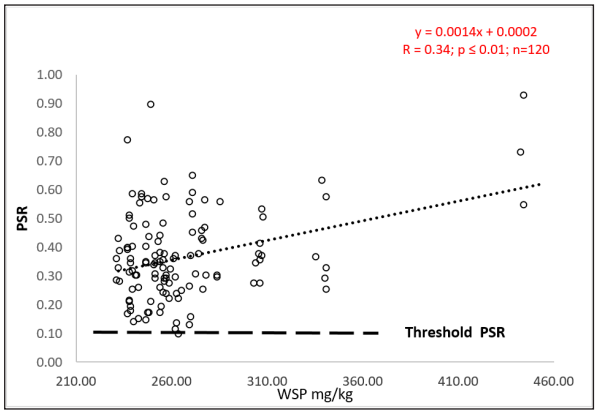

Figure 2. Relationship between P saturation ratio and water-soluble P (WSP).

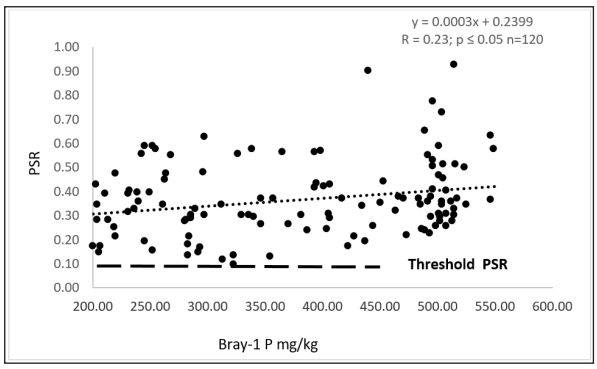

Figure 3. Relationship between P saturation ratio and Bray-1P.

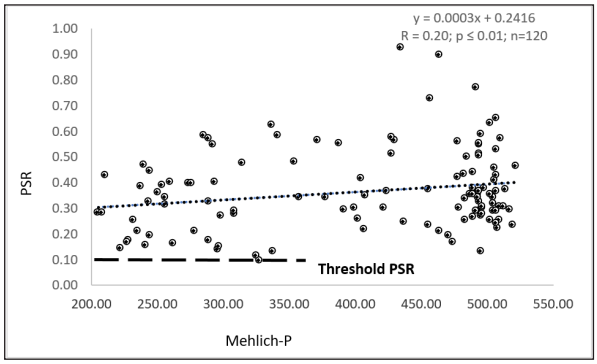

Figure 4. Relationship between P saturation ratio and Mehlich-P.

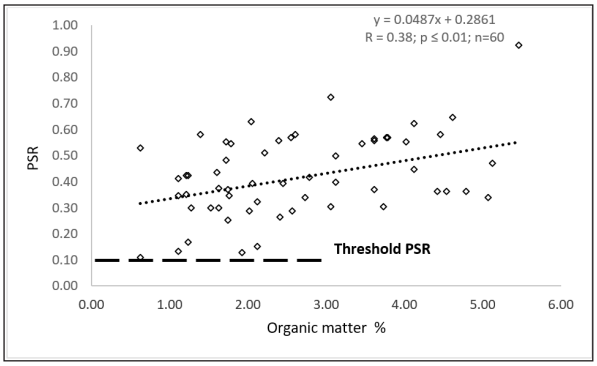

Figure 5. Relationship between P saturation ratio and organic matter.

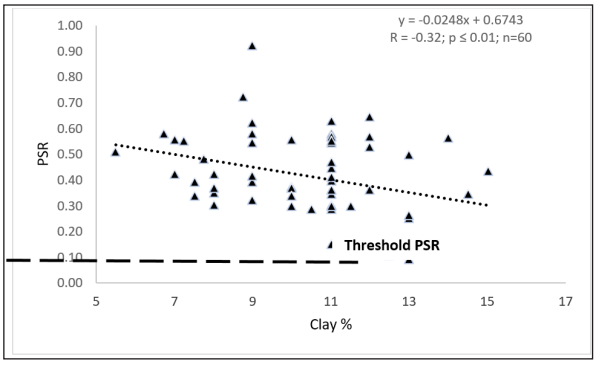

Figure 6. Relationship between P saturation ratio and clay percentage.

The correlation (Table 3) shows that the relationships between the soil P availability indices were positive and significant. This shows the validity in the use of any of the extractant in estimating soil P. The soil PSR had a negative but not significant relationship with Olsen extractable P while the relationship between the soil dissolved salts as measured by the soil electrical conductivity and the soil P availability indices were all positive and significant. It implies that the phosphate salts are among the dominant salts from the manures dumped on the sites. This was also confirmed by the PSR values. The soil clay has a significant correlation with Olsen extractable-P, and Mehlich extractable Fe.

Table 3. Correlation matrix of the Extractants, PSR and other Physico-chemical parameters (n=120).

	Water Soluble mg kg^{-1}	Olsen mg kg^{-1}	Mehlich-1 mg kg^{-1}	Bray-1 mg kg^{-1}	M-Al mg kg^{-1}	M-Fe mg kg^{-1}	PSR	pH	EC (ds/m)	OM§ %
Olsen	0.29**									
Mehlich-1	0.45**	0.64**								
Bray-1	0.50**	0.52**	0.87**							
M-Al	0.03 ns	0.16 ns	0.26**	0.24**						
M-Fe	-0.02 ns	0.31**	0.18 ns	0.09 ns	-0.11 ns					
PSR	0.34**	-0.03 ns	0.20*	0.23*	-0.50**	-0.50**				
pH	0.02 ns	0.14 ns	0.13 ns	-0.02 ns	-0.47**	0.34**	0.16 ns			
EC	0.21*	0.50**	0.32**	0.40**	0.02 ns	0.04 ns	0.11 ns	-0.16 ns		
OM§	0.16 ns	-0.07 ns	-0.05 ns	0.04 ns	-0.18 ns	-0.24 ns	0.38**	-0.32 ns	0.24 ns	
Clay§	-0.13ns	0.34**	0.07 ns	0.13 ns	0.21 ns	0.34**	-0.32*	0.02 ns	0.01 ns	0.03 ns

*** Significant at P0.01; * significant at P0.05; § n=60*
M-Al - Mehlich extractable aluminum M-Fe - Mehlich extractable iron PSR – Phosphorus saturation ratio
OM – Organic Matter EC – Electrical conductivity

5. Conclusions

From the study, it could be concluded that:

1. Unregulated and prolonged dumping of manures in soils led to the excess accumulation of phosphorus in the soil environment.
2. Some of the soil P availability indices could be used as a proxy for estimating soil PSR and hence soil P pollution potential.
3. The soil organic matter is a stronger determinant of soil P pollution than clay for soils of manure dump sites.
4. There is potential pollution of surface and groundwater in the vicinities of the dumpsites with the attendant health hazards.

Acknowledgment

The authors wish to acknowledge the assistance of Mr. Anthony Tobore in the graphics.

Declaration of Competing Interest

The authors declare that they have no known competing financial interests or personal relationships that could have appeared to influence the work reported in this paper.

References

Azeez, J.O., and Van Averbeke, W. (2010). Fate of manure phosphorus in a weathered sandy clayloam soil amended with three animal manures. Bioresource Technology 101: 6584–6588.

Azeez, J. O., Adekunle, I.O., Atiku, O.O., Akande, K.B., Jamiu-Azeez, S.O. (2009). Effect ofnine years of animal waste deposition on profile distribution of heavy metals in Abeokuta, south-western Nigeria and its implication for environmental quality. Waste Management 29: 2582–2586.

Bouyoucos, G.H. (1965). A calibration of the hydrometer method for testing mechanical analysisof soils. Agronomy Journal 43: 434–438.

Bray, R. H., and Kurtz, L. T. (1945). Determination of total, organic, and available form ofphosphorus in soils. Soil Science Society of America Journal 59: 39–45.

Breeuwsma, A., and Silva, S. (1992). "Phosphorus fertilization and environmental effects in the Netherlands and the PoRegion (Italy),"in Report57. Agricultural Research Department (Wageningen: The Win and Staring Centre for Integrated Land, Soil, and Water Research).

Codling, E. E., Chaney, R. L., Mulchi, C. L. (2000). Use of aluminum and iron rich residues to immobilize phosphorus in poultry litter and litter-amended soils. Journal of Environmental

Quality 29: 1924-1931.

Crowther, J., Kay, D., Wyer, M.D. (2002). 'Faecal-indicator concentrations in waters draining lowland pastoral catchments in the UK: Relationships with land use and farming practices', Water Research 36(7): 1725–1734.

Dari, B., Nair, V.D., Sharpley, A.N., Kleinman, P., Franklin, D., Harris, W.G. (2018). Consistency of the Threshold Phosphorus Saturation Ratio across a Wide Geographic Range of Acid Soils. Agrosystems Geoscience Environment. 1:180028. DOI:10.2134/age2018.08.0028.

Edwards, D.R., and Daniel, T.C. (1992). Environmental impacts of on farm poultry waste disposal- A review. Bioresource Technology 41: 9-33.

Gerba, C.P., and Smith, J.E. (2005). Sources of pathogenic microorganisms and their fate during land application of wastes. Journal of Environmental Quality 34: 42–48.

Hooda, P.S., Rendell, A.R., Edwards, A.C., Withers, P.J.A., Aitken, M.N., Truesdale, V.W. (2000). Relating soil phosphorus indices to potential phosphorus release to water. Journal of Environmental Quality 29:1166–1171. DOI: 10.2134/jeq2000.00472425002900040018x

Hooda, P.S., Moynagh, M., Svoboda, I.F., Thurlow, M., Stewart, M., Anderson, H.A., Sym, G. (1999). Phosphorus loss in drain flow from intensively managed grassland soils. Journal of Environmental Quality 28: 1235-1242.

Liao, X., Liu, G., Hogue, B., Li, Y. (2015). Phosphorus availability and environmental risks in potato fields in North Florida. Soil Use and Management 31: 308–312.

Mclean, E.O. (1982). Soil pH and lime requirement. In: Page A.L. (Ed.), Methods of Soil Analysis. Part 2: Chemical and Microbiological properties, 9.2.2 Second edition. American Society of Agronomy, Inc., Soil Science Society of America, Inc. Agronomy Monographs. DOI: 10.2134/agronmonogr9.2.2ed.c12.

Mehlich, A. (1953). Determination of P, K, Na, Mg, and NH4. Soil Testing Division Publication No. 1–53. North Carolina Department of Agriculture, Agronomic Division. Raleigh, NC.

Murphy, J., and Riley, J.P. (1962). A modified single solution method for the determination of phosphate in natural waters. Analytical Chemistry Acta 27: 31–36.

Miller, D.M., Moore, Jr., P.A., Edwards, D.R., Stephen, D.A., Gbur, E.E. (1993). Determination of water-soluble phosphorus in soil. Arkansas Farm Research 42: 10-11.

Nair, V.D. (2014). Soil phosphorus saturation ratio for risk assessment in land use systems. Frontiers in Environmental Science. Mini review 2 (6): 1-4. DOI: 10.3389/fenvs.2014.00006.

Nair, V.D., Portier, K.M., Graetz, D.A., Walker, M.L. (2004). An environmental threshold for degree of phosphorus saturation in sandy soils. Journal of Environmental Quality 33: 107–113. DOI:10.2134/jeq2004.1070.

Nelson, D.W., and Sommers, L.E. (1982). Total carbon, organic carbon and organic matter. In: Page A.L. (Ed.), Methods of Soil Analysis. Part 2: Chemical and Microbiological properties, 9.2.2 Second edition. American Society of Agronomy, Inc., Soil Science Society of America, Inc. Agronomy Monographs. DOI:10.2134/agronmonogr9.2.2ed.c29.

SAS Institute. (1990). SAS/STAT user's guide, release 6, 4th ed. Cary, N.C.: SAS Institute.

Sauer, T.J., Daniel, T.C. Moore, Jr. P.A., Coffey, K.P. Nichols, D.J., West, C.P. (1999). Poultry Litter and Grazing Animal Waste Effects on Runoff Water Journal of Environmental Quality 28: 860-865.

Sharpley, A., and Tunney, H. (2000). Phosphorus research strategies to meet agricultural and environmental challenges in the 21st century. Journal of Environmental Quality 29: 176–181. DOI:10.2134/jeq2000.00472425002900 010022x.

Sharpley, A., Jarvie, H.P., Buda, A., May, L., Spears, B., Kleinman, P. (2013). Phosphorus legacy: practices to mitigate future water quality impairment. Journal of Environmental Quality 42:1308– 1326. DOI:10.2134/jeq2013.03.0098.

Soupir, M.L., Mostaghimi, S., Yagow, E. R., Hagedorn, C., Vaughan, D.H. (2006).Transport of fecal bacteria from poultry litter and cattle manures applied to pastureland. Water, Air, and Soil Pollution 169: 125–136.

Tian, Y.Q., Gong, P., Radke, J.D., Scarborough, J. (2002). Spatial and temporal modeling of microbial contaminants on grazing farmlands. Journal of Environmental Quality 31(3): 860–869.

United States Environmental Protection Agency (USEPA) (2002). Environmental Indicators of Water Quality in the United States. EPA841-R-02-001. Washington, DC: USEPA Office of Water Quality.

United States Environmental Protection Agency (USEPA) (2003). 'National pollutant discharge elimination system permit regulation and effluent limitation guidelines and standards for concentrated animal feeding operations (CAFOs); final rule', Federal Register 68(29): 7176–7274.

Watanabe, F.S., and Olsen, S.R. (1965). Test of an ascorbic acid method for determining phosphorus in water and NaHCO3 extracts from soil. Soil Science Society of America Proceedings 29: 677–678.

Windhorst, H.W. (2006). Changes in poultry production and trade Worldwide. World's Poultry Science Journal 62: 585-602.

المملكة الأردنية الهاشمية

صندوق دعم البحث العلمي

الجامعة الهاشمية

المجلة الأردنية
لعلوم الأرض والبيئة

JJEES

مجلة علمية عالمية محكمة

المجلد (١٢) العدد (٣)

http:// jjees.hu.edu.jo/

ISSN 1995-6681

المجلة الأردنية لعلوم الأرض والبيئة

مجلة علمية عالمية محكمة

المجلة الأردنية لعلوم الأرض والبيئة: مجلة علمية عالمية محكمة ومفهرسة ومصنفة، تصدر عن عمادة البحث العلمي في الجامعة الهاشمية وبدعم من صندوق البحث العلمي - وزارة التعليم العالي والبحث العلمي، الأردن.

ترسل البحوث إلكترونيا إلى البريد الإلكتروني التالي:

رئيس تحرير المجلة الأردنية لعلوم الأرض والبيئة

jjees@hu.edu.jo

لمزيد من المعلومات والأعداد السابقة يرجى زيارة موقع المجلة على شبكة الانترنت على الرابط التالي:

www.jjees.hu.edu.jo

المملكة الأردنية الهاشمية صندوق دعم البحث العلمي الجامعة الهاشمية

JJEES

المجلة الأردنية لعلوم الأرض والبيئة

المجلد (١٢) العدد (٣)

مجلة علمية عالمية محكمة تصدر بدعم من صندوق دعم البحث العلمي

ISSN 1995-6681 jjees.hu.edu.jo أيلول ٢٠٢١